FLOWABLE AND STABLE CONCRETE

DESIGN, CHARACTERIZATION AND PERFORMANCE EVALUATION

Von der Fakultät für Bauingenieurwesen und Geodäsie
der Gottfried Wilhelm Leibniz Universität Hannover

zur

Erlangung des Grades Doktor-Ingenieur
[Dr.-Ing.]

genehmigte Dissertation

von

Yared Assefa Abebe, M.Sc.

Hannover 2017

Prüfungsausschuss

Referent:	Univ.-Prof. Dr.-Ing. Ludger Lohaus Leibniz Universität Hannover
Korreferent:	Univ.-Prof. Dr.-Ing. Viktor Mechtcherine Technische Universität Dresden
Prüfungsmitglied:	Univ.-Prof. Dr.-Ing. Katharina Klemt-Albert Leibniz Universität Hannover
Vorsitz:	Univ.-Prof. Dr.-Ing. Martin Achmus Leibniz Universität Hannover
Tag der Prüfung:	31.01.2017

Impressum

Autor:	Yared Assefa Abebe, M.Sc.
Titel:	Flowable and Stable Concrete: Design, Characterization and Performance Evaluation
Schriftenreihe:	Berichte aus dem Institut für Baustoffe, Heft 14
Herausgeber:	Univ.-Prof. Dr.-Ing. Ludger Lohaus
	Institute für Baustoffe Leibniz Universität Hannover Appelstraße 9A 30167 Hannover Tel.: 0511 / 762-3722 Fax: 0511 / 762-4736 http://www.baustoff.uni-hannover.de
ISBN	978-3-936634-16-7

FLOWABLE AND STABLE CONCRETE

DESIGN, CHARACTERIZATION AND PERFORMANCE EVALUATION

by

Yared Assefa Abebe, M.Sc.

Dissertation

Presented to the Faculty of Civil Engineering and Geodetic Science of
The Gottfried Wilhelm Leibniz Universität Hannover
in Partial Fulfillment of the Requirements for the Degree of Doctor of Engineering
[Dr.-Ing.]

Hannover 2017

Doctoral committee

Supervisor:	Univ.-Prof. Dr.-Ing. Ludger Lohaus Leibniz Universität Hannover
Co-supervisor:	Univ.-Prof. Dr.-Ing. Viktor Mechtcherine Technische Universität Dresden
Member:	Univ.-Prof. Dr.-Ing. Katharina Klemt-Albert Leibniz Universität Hannover
Chairmanship:	Univ.-Prof. Dr.-Ing. Martin Achmus Leibniz Universität Hannover
Date of Defense:	January 31, 2017

Imprint

Author:	Yared Assefa Abebe, M.Sc.
Title:	Flowable and Stable Concrete: Design, Characterization and Performance Evaluation
Publication series:	Berichte aus dem Institut für Baustoffe, Heft 14
Editor:	Univ.-Prof. Dr.-Ing. Ludger Lohaus Institute für Baustoffe Leibniz Universität Hannover Appelstraße 9A 30167 Hannover Tel.: 0511 / 762-3722 Fax: 0511 / 762-4736 http://www.baustoff.uni-hannover.de
ISBN	978-3-936634-16-7

Dedication

I dedicate this dissertation work to Birhan Jada, Meseret Alemu, Kidus Yared and Lukas Yared.

Acknowledgements

This dissertation is the final product of my engagement as a research assistant and doctoral candidate at the Institute of Building Materials Science of the Leibniz Universität Hannover. The time that I spent at the institute was, for the most part, filled with a lot of excitement and fun. The availability of adequate financial and material resources along with the freedom to try out new ideas made my stay at the institute a wonderful experience. Of course, like any other engagements, there were some challenges along the way. But, I can confidently assert that I have achieved a great deal in the process in terms of personal development and professional competence that the positive aspects significantly outweigh the hiccups. All these achievements were possible thanks to the love and support that I got from my family, friends and colleagues.

First and foremost, I would like to extend my sincere gratitude to Prof. Ludger Lohaus not only for giving me the chance to start this journey at the institute, but also for his tireless counseling and guidance along the way, as well as for working as a main supervisor of my dissertation. I would also like to express my appreciation to Prof. Viktor Mechtcherine for his willingness to take the time and effort to work as a co-supervisor of my dissertation. My thanks also extend to Prof. Martin Achmus for his chairmanship of the exam committee and Prof. Katharina Klemt-Albert for working as a member of the committee.

I am thankful to my colleagues for making me feel like part of the team from the beginning, for their productive cooperation, and also for the fun times. My appreciation also extends to the laboratory personal for putting the efforts in realizing the numerous experimental works. The credit also goes to “my students” that I had the privilege to supervise their thesis works.

My gratefulness to my family and friends for the love and support that I have received over the years goes without saying. Very special thanks to Bire for making me into the person that I am, to Mesi for having my back, to Kido and Luki for bringing joy into my life and to my siblings for all the fun. Love you all!

Yared A. Abebe

Abstract

Flowable concretes, while possessing remarkable workability properties, are inherently susceptible to sedimentation and segregation, especially under the influence of external stress such as vibration and pumping pressure. This situation is further aggravated by the fact that the concrete production, transportation and casting processes are liable to fluctuations in the quality of the raw materials and the environmental conditions. Consequently, their application in the concrete construction sector is currently very limited. However, when the geometrical complexity, reinforcement density and dimensional enormity of today's modern structures are considered, there remains no plausible option other than to use flowable concretes. Hence, dealing with the bottlenecks beforehand is of paramount importance for a reliable application of such concretes. Within the scope of this dissertation, three main aspects with regard to flowable and stable concrete are addressed: mix-design, characterization and performance evaluation.

The newly developed Water Balance Mix-Design method (WBMD) guarantees not only the flowability and pumpability but also stability (under vibration and pressure) and robustness of concrete. This is achieved through a systematic design strategy which includes optimization of the aggregate compositions to enhance the lattice effect, determination of the minimum paste demand of the aggregates and quantifying the effective water demand of fines compositions by integrating the effects of superplasticizers (SP). The water balanced concretes (WBC) were composed by making use of different paste and aggregate compositions. Moreover, extra water was added to the mixtures in order to evaluate their robustness.

The characterization of the fresh concrete properties was carried out using standard and new investigation methods. The flowability was investigated using slump flow tests (with and without tapping). The stability under vibration was evaluated using a modified wash-out test (WT), sedimentation - sieve - test (SST) and visual assessment of the sedimentation behavior on hardened concrete specimen. The pumpability and pump-stability were quantified by means of a pumping resistance simulator (PuReSi) and high pressure filter press (HPFP). Moreover, rheological characterization of the concretes was conducted using a rotational rheometer Viskomat XL while the extracted mortar and paste compositions were tested using Viskomat NT. A high level of shear loading was applied for the rheological investigations to reproduce the structural breakdown process that takes place when concretes are exposed to external stress.

Based on the results of the investigations, a detailed analysis is presented with regard to the effects of the different constituent materials and design parameters on

the fresh concrete as well as the rheological properties. Moreover, through a systematic assessment of the rheological properties of the subsequent phases of paste, mortar and concrete, a multiscale rheological model is developed for quantifying the structural breakdown process. The rheological studies are also applied for the characterization of the sedimentation behavior during the structural breakdown process and the quantification of the pumpability and pump-stability properties.

Furthermore, new performance evaluation criteria are defined for flowable concretes on the basis of the results of the stability, rheological and flowability investigations, especially with regard to the stability properties under vibration and pressure. To this end, the rheological performance criteria as applied to the paste, mortar and concrete phases are integrated with the performance criteria derived from the stability and flowability investigations to produce a multiscale performance evaluation strategy. A combined analysis of the water balance criteria (WB) with the performance evaluation criteria has confirmed the adequacy of the WBMD for designing flowable concretes of reliable stability. Finally, a comprehensive model for flowable and stable concrete comprising micro, meso and macro scales is presented that encompasses the WBMD, the relevant characterization methods and the corresponding performance evaluation criteria.

Keywords:

Water Balance Mix-Design, Flowability, Sedimentation under Vibration, Pump-stability, Pumpability, Performance Evaluation Criteria, Structural Breakdown, Multiscale Rheological Model

Kurzfassung

Trotz ihrer günstigen Verarbeitungseigenschaften zeigen fließfähige Betone eine große Anfälligkeit für Entmischung, insbesondere unter dem Einfluss von Rütteln und Pumpendruck. Die Entmischungsgefahr wird durch Schwankungen in der Gleichmäßigkeit der Ausgangsstoffe und der Umgebungsbedingungen verstärkt, welche üblicherweise bei Betonherstellungs-, Transport- und Anwendungsprozessen auftreten. Aus diesem Grund ist die Anwendung von fließfähigen Betonen derzeit stark eingeschränkt. Die heutigen modernen Bauwerke, die sich u.a. durch komplexe Bauteilgeometrie, hohe Bewehrungsgrade und große Dimensionen auszeichnen, fordern jedoch genau diese Art von Betonen. Daher ist der Umgang mit Engpässen, insbesondere hinsichtlich der Entmischungsproblematik sehr entscheidend, um solche Betone zuverlässig anwenden zu können. Im Rahmen dieser Dissertation werden drei Hauptaspekte behandelt: Der Mischungsentwurf, die Charakterisierung der Frischbetoneigenschaften und die Beurteilung der Leistungsfähigkeit von fließfähigen und gleichzeitig stabilen Betonen.

Die neu entwickelte „Water Balance Mix-Design Method“ (WBMD) garantiert nicht nur die Fließfähigkeit und die Pumpbarkeit, sondern auch die Stabilität (unter Rüttel- und Druckeinwirkungen) sowie eine gewisse Robustheit der so entworfenen Betone. Die WBMD verfolgt systematische Entwurfsstrategien: Optimierung der Kornzusammensetzung in Bezug auf die Steigerung des Netzeffekts, Bestimmung des minimal erforderlichen Leimbedarfs der optimierten Kornzusammensetzung und Quantifizierung des effektiven Wasserbedarfs des Mehlkorns durch Betrachtung der Auswirkungen der zugegebenen Fließmittel. Im Rahmen der experimentellen Untersuchungen wurden die wasserbilanzierten Betone (WBC) durch Kombination von verschiedenen Leim- und Kornzusammensetzungen zusammengesetzt, um ihren Einfluss auf die o.g. Frischbetoneigenschaften beurteilen zu können. Außerdem wurde eine Wasserüberdosierung angesetzt, um die Robustheit der Betone zu untersuchen.

Die Charakterisierung der Frischbetoneigenschaften erfolgte durch den Einsatz von Standardprüfverfahren, aber auch durch neue Prüfverfahren. Die Fließfähigkeit wurde mithilfe von Ausbreitmaß und Ausbreitfließmaß (mit und ohne Klopfen) untersucht. Zur Beurteilung der Rüttelstabilität kamen ein modifizierter Auswaschversuch (WT), ein Sedimentation – Sieb – Versuch (SST) und die visuelle Beurteilung der Sedimentation am Festbeton zum Einsatz. Die Pumpbarkeit und die Pumpstabilität wurden mittels eines „Pump Resistance Simulator“ (PuReSi) und einer Hochdruck-Filterpresse (HPFP) quantifiziert. Zur Charakterisierung der rheologischen Eigenschaften der Betone wurde ein Rheometer von Typ Viskomat XL angewendet. Ebenso wurden die rheologischen Eigenschaften der Mörtel- und

Leimzusammensetzungen, die aus dem Beton extrahiert wurden, mithilfe eines Rheometers von Typ Viskomat NT untersucht. Dabei wurde eine hohe Scherrate gewählt, um die rheologischen Eigenschaften während des Strukturbruchprozesses unter extremen Scherbelastungen, wie sie z.B. während des Rüttelns aufhalten, abbilden zu können.

Basierend auf den Versuchsergebnissen wurde eine detaillierte Analyse hinsichtlich der Auswirkungen der verschiedenen Ausgangsstoffe und betontechnologischen Parameter auf die Frischbeton- sowie rheologische Eigenschaften vorgelegt. Darüber hinaus wurde durch Anwendung einer systematischen Bewertungsmethodik ein Multiskalenmodell für die rheologischen Eigenschaften der aufeinander aufbauenden Phasen von Leim, Mörtel und Beton entwickelt. Dieses Modell ermöglicht die zusammenhängende Beschreibung und Quantifizierung der relevanten rheologischen Parameter während des Strukturbruchs. Die Stabilitätseigenschaften während des Strukturbruchs sowie der Pump- und Pumpstabilitätseigenschaften können ebenso im Zusammenhang mit den rheologischen Eigenschaften beschrieben und quantifiziert werden.

Darüber hinaus wurden anhand der Ergebnisse der Stabilitäts- und Fließfähigkeitsuntersuchungen sowie der rheologischen Messungen neue multiskalige Performancekriterien definiert, welche die Beurteilung der Stabilitätseigenschaften fließfähiger Betone unter Rüttel- und Druckeinwirkungen ermöglichen. Eine kombinierte Betrachtung der Wasserbilanzkriterien mit den Performancekriterien hat die Eignung der WBMD zur Herstellung fließfähiger und stabile Betone bestätigt. Anschließend wurde ein ganzheitliches Modell vorgestellt, welches die fließfähigen und stabilen Betone jeweils in der Mikro-, Meso- und Makroskala betrachtet und in dem das WBMD, die relevanten Charakterisierungsmethoden und die entsprechenden Performancekriterien enthalten sind.

Stichworte:

Water Balance Mix-Design, Fließfähigkeit, Rüttelstabilität, Pumpstabilität, Pumpfähigkeit, Performancebeurteilungskriterien, Strukturbruch, rheologisches Multiskalenmodell

Table of Contents

List of Symbols

Latin Notation

a	[cm^2/g]	Specific surface area
A_S	[N·m/s]	Interparticle structural strength of concrete
b_P	[bar·s/m]	Pressure gradient
D	[m]	Diameter
D_{50}	[m]	Median grain size
M	[Kg]	Mass
M_W	[Kg]	Mass of water
P	[bar]	Pressure
$P_{0,P}$	[bar]	Reference pressure
q	[-]	Gradation exponent
Q	[m^3/s]	Flow or discharge Rate
t	[s]	Time
V	[m^3]	Volume / Volume of concrete
V_A	[m^3]	Volume of air voids
V_G	[m^3]	Volume of aggregate
V_C	[m^3]	Volume of cement
V_{MA}	[m^3]	Volume of mineral admixtures
V_{MA}/V_F	[-]	Mineral admixtures – Fines ratio (volumetric)
V_G	[m^3]	Volume of aggregate
v_i	[m/s]	Falling speed
V_P	[m^3]	Paste demand
$V_{P,S}$	[m^3]	Surface paste demand
$V_{P,V}$	[m^3]	Voids paste demand
V_W	[m^3]	Volume of water
V_W/V_F	[-]	Water – Fines ratio (volumetric)
$V_{W,S}$	[m^3]	Surface water demand
w/c	[-]	Water – Cement ratio (mass)

Greek Notations

τ	[Pa]	Shear stress
τ_r	[N·m]	Relative yield Stress
τ_s	[Pa]	Static shear stress
τ_o	[Pa]	Yield Stress
$\dot{\gamma}$	[1/s]	Shear rate
μ	[Pa·s]	Plastic viscosity
η	[Pa·s]	Dynamic viscosity
η_r	[N·m·s]	Relative dynamic viscosity
$\eta_{r,C}$	[N·m·s]	Relative dynamic viscosity of concrete
$\eta_{r,M}$	[N·m·s]	Relative dynamic viscosity of mortar
$\eta_{r,P}$	[N·m·s]	Relative dynamic viscosity of paste
ρ	[Kg/m^3]	Density or specific gravity
ϕ	[-]	Solid fraction / Packing density
ϕ_{Max}	[-]	Max. solid fraction / Max. packing density
β_P	[-]	Basic water demand
β_E	[-]	Effective water demand
Δ	[-]	Difference or deviation

Abbreviations

AEA	[-]	Air entraining agent
BFP	[-]	Bauer filter press
CC	[-]	Conventional concrete
CEM	[-]	Cement
CG	[-]	Crushed gravel
FA	[-]	Fly ash
FG	[-]	Flaky gravel
FT	[s]	Flow time

HPFP	[-]	High pressure filter press
HPC	[-]	High performance concrete
HRWRA	[-]	High range water reducing admixture
LS	[-]	Limestone powder
MA	[-]	Mineral admixture
MFT	[-]	Flow time of mini V-funnel
NS	[-]	Natural Sand
OPC	[-]	Ordinary portland cement
PCE	[-]	Poly Carboxylic Ether Superplasticizer
PDT	[-]	Packing density test
PFT	[-]	Paste film thickness
PMS	[-]	Poly-melamine sulphonates
PNS	[-]	Poly-naphthalene sulphonates
PSI	[%]	Pump-stability Index
PuReSi	[-]	Pump resistance simulator
RG	[-]	River gravel
SCC	[-]	Self-compacting concrete
SF	[-]	Silica fume
SI	[%]	Stability Index
SLIPER	[%]	Sliding pipe rheometer
SSI	[%]	Sedimentation – Sieve – Index
SP	[-]	Superplasticizer
SST	[%]	Sedimentation – Sieve – Test
TR	[-]	Trass powder
VMA	[-]	Viscosity modifying agent
WT	[-]	Wash-out Test
WB	[dm^3]	Water balance
WBC	[-]	Water balanced concrete
WBMD	[-]	Water balanced mix-design method
WFT	[-]	Water film thickness

WRA	[-]	Water reducing admixture

Indices and Other Symbols

$\overline{M}$	[Kg]	Average mass
$\overrightarrow{N_c}$	[-]	Collison flux
$\overrightarrow{N_\eta}$	[-]	Viscosity flux

Chapter 1
Introduction

1.1 Background information

The immense dimensions and geometrical complexity of today's modern structures require a highly workable concrete that is pumpable over long distances, flowable enough to fill up formworks and passable through very tight spacing of reinforcements. To this end, appreciable progress has been made in the last few decades, especially following the introduction of self-compacting concrete (SCC). Thanks to its very high flowability and relatively higher viscosity, SCC can fulfill these workability requirements without the need to apply external compaction efforts. This fact is witnessed on a number of construction projects including the Phaeno Science Centre in Wolfsburg, which was designed by the renowned architect Zaha Hadid, where SCC was used on a large scale for the first time in Germany. Parts of this complex building were built to such a high standard, signifying the enormous advantages of SCC in realizing challenging concrete works; see Figure 1.1.

Figure 1.1: Complex structural geometries

Nevertheless, despite its tremendous advantages, the market share of SCC in concrete construction is significantly low. Even in the ready-mixed concrete industry where the quality assurance system functions much better than an in-situ concrete application, SCC makes up a meager 2% of the total ready-mixed concrete [1]. The relatively higher cost, the lack of robustness and to some extent the lack of guidelines and norms are mentioned as potential reasons for the lagging market

share of SCC [2]. Focusing on the robustness aspect, SCC by virtue of its meticulous design reacts very sensitively to changes in the component materials or to variations in external conditions such as the ambient temperature [3]. Such a problem was also encountered during the execution of the Phaeno Science Centre in terms of maintaining the required consistency of the SCC in the wake of the seasonal changes in temperature [4]. This highlights the intrinsic poor robustness of SCC against unforeseen changes even when rigorous quality control measures are put in place. Taking the fact into consideration that such fluctuations are inevitable in in-situ construction conditions, the application of SCC does not always guarantee the best result and in some cases could entail a consequential loss in the quality of construction, especially if problems arise with regard to the stability properties.

As a consequence of its poor flowability and deformability properties, the application of conventional concrete (CC) in structural elements with complex geometries and dense reinforcements is not a plausible option. Moreover, taking into account that some norms and guidelines prohibit touching the reinforcements during vibration or discourage the distribution of concrete with the help of vibration pokers, the practical application of CC in such construction works could be very challenging [5] [6]. This might even end up in sections of buildings with no concrete cover or cause a poor bondage between the reinforcements and the concrete, compromising the structural integrity of the whole system; see Figure 1.2.

Figure 1.2: Pitfalls of conventional concrete with dense reinforcements [7]

Pumpability is another aspect that has relevance to both SCC and CC. A properly composed SCC exhibits good pumpability properties, because it can easily build a lubrication layer due to the relatively high amount of paste. However, this might also increase the risk for the occurrence of “forward segregation” where the separation of the water or paste from the bulk concrete occurs under the action of pressure. This is especially critical if an unanticipated water overdosage occurs, e.g. due to rest water in mixers or fluctuating moisture content of aggregates. In contrast, CC contains a

relatively small amount of paste and the inevitable loss of some of it to form a lubrication layer could be detrimental to the pumpability. In both cases, the chance for the formation of a zonal aggregate cluster or interlocking increases thereby leading to a drastic increase in pumping pressure. A complete blockage of the pumping lines could be the ultimate consequence if the maximum capacity of the pump is exceeded. Such a phenomenon was observed on a concrete composition of consistency class F4 during a field investigation within the scope a cooperative research project between the Technische Universität Dresden (TUD) and Leibniz Universität Hannover (LUH), where different types of concrete mixtures were pumped using a 150 m long pumping line.

Figure 1.3: Blockage of pumping line (Research project: TUD and LUH)

The ideal solution for these application problems is the usage of highly flowable concrete that has the attributes of SCC in terms of the workability and pumpability properties and CC with regard to the stability under the application of external stress such as vibration. Such a concrete should also be robust enough in terms of maintaining the desired fresh concrete properties when changes in the component materials or external conditions occur. However, there are some hurdles that have to be overcome if this noble idea is to be realized.

First, there are no adequate mix-design methods that are specifically developed for flowable concretes which are exposed to extreme vibration or pumping pressure. While the different mix-design approaches developed for SCC might give some hints as to the guiding principles for attaining the desired high flowability, they specifically apply to the conditions under which a SCC is casted, namely without the application of vibration. In fact, the application of vibration as a compaction method is not recommended for flowable concrete of the consistency classes of F5 and above, pertaining to the high risk of sedimentation and segregation [8]. Thus, a whole new mix-design approach has to be developed for flowable concrete in which the stability under vibration and pressure take center stage.

Second, the fundamental behaviors of flowable concrete during exposure to external stress such as vibration and pressure are not yet thoroughly studied, especially with regard to the stability and the rheological properties. This is for the most part due to the lack of proper investigation and evaluation methods. There are, of course, some standardized investigation methods developed for characterizing the flowability and the stability properties of SCC. But these methods are conceived to function without the application of external stress. Thus, either the existing investigation methods have to be modified or new ones have to be developed for the characterization of flowable concretes under the actions of vibration. Likewise, in light of the effects these external stresses on flowable concretes, new rheological investigation methods have to be developed giving special emphasis to the structural breakdown process. This is yet again in stark contrast to SCC where the primary focus is on the structure build-up process at rest. Furthermore, adequate test methods have to be applied for quantifying the pumpability and pump-stability properties of such concretes.

Third, there are neither concrete technological nor rheological performance evaluation criteria upon which the quality of flowable concretes could be assessed, especially in terms of guaranteeing the stability under the influence of external stresses. Here too, the lack of adequate investigation methods and evaluation techniques is surely a contributing factor. Hence, the prospects for adopting the same approach as that of SCC with regard to e.g. definition of stability criteria or delineating workability zones have to be explored for these types of concretes.

1.2 Objective

The exemplary problems highlighted as part of the background information illustrate the challenges that are still persistent in concrete construction, despite the fact that tremendous progress has been made in the field of concrete technology. Thanks to the numerous research activities of the last few decades, there is a much better understanding as to the effects of most of the basic component materials and design parameters on the fresh concrete properties. However, combining these “individualistic” insights into an “integrated” solution for addressing the usually conflicting requirements of fresh concrete still remains a difficult undertaking.

For instance, a high level of flowability could be attained by increasing the paste content, the water – fines ratio (V_W/V_F) or the superplasticizer content. However, such adjustments or the combination thereof should not affect the other relevant requirements including the stability and robustness in the fresh state as well as the strength and durability in the hardened state. Economic and environmental considerations are also aspects that play an important role in choosing the optimal solution. Hence, the following questions take center stage in relation to the

production of flowable and pumpable concretes that show reliable stability and robustness under the effects of vibration and pumping.

- How can such concretes be composed so that the incompatible performance requirements of flowability and pumpability on the one hand and stability and robustness on the other are simultaneously guaranteed?
- What are the main concrete technological and rheological features that govern the properties of such concretes?
- What are the relevant performance evaluation criteria that ensure the quality conformance of such concretes?

The objective of this dissertation is, thus, providing the important theoretical and experimental methodologies that are specifically envisaged to address these questions so that the tremendous advantages of flowable concrete could be harnessed in realizing today's challenging construction works. In doing so, the following four main objective points shall be dealt with in great detail.

I. Introduction of a comprehensive mix-design method for flowable, pumpable, stable (under vibration and pressure) and robust concrete mixtures.
II. Characterization of the flowability, pumpability, stability (under vibration and pressure) and robustness properties of flowable concrete.
III. Characterization of the rheological properties of concrete, mortar and paste and development of a multiscale rheological model for the structural breakdown.
IV. Definition of adequate concrete technological and rheological performance evaluation criteria for flowable concrete.

A detailed explanation of each objective point is presented as follows.

I. Introduction of a comprehensive mix-design method for concretes that are flowable, pumpable, stable and robust

Currently, there is no adequate mix design method that addresses the contradictory requirements of flowability and pumpability on the one hand and stability and robustness on the other. To this end, a new systematic and tailored mix-design approach, which is referred to as the "Water Balance Mix-Design Method" (WBMD), is developed. The WBMD integrates the effects of the component materials as well as the chosen design parameters in such a way that the flowability, pumpability, stability and robustness requirements are addressed simultaneously.

II. Characterization of the flowability, pumpability, stability (under vibration and pressure) and robustness properties

There is only limited know-how with regard to the fresh concrete properties under the influence of external stresses, especially the stability (under vibration and pressure) and the robustness. One of the reasons for this is, of course, the lack of adequate investigation and evaluation methods. Hence, some of the existing test methods are modified and new ones are developed for the characterization of these properties. The investigations were conducted on several concrete mixtures by altering the composition and amount of the paste and aggregates.

III. Characterization of the rheological properties of concrete, mortar and paste and development of a multiscale model for the structural breakdown

While there is a relatively good understanding of the rheological properties of paste and mortar compositions, the question as to whether this suffices for describing the rheological properties of concrete is not yet adequately addressed. Information as related to the rheological properties of concrete under the action of external shear loading is in particular very scarce. To this end, new investigation and evaluation techniques are developed that help quantify the relevant rheological parameters of the subsequent paste, mortar and concrete phases during the structural breakdown process. Consequently, a multiscale rheological model is proposed which considers the concrete, mortar and paste compositions as macro, meso and micro scales respectively. The model incorporates the interdependence between the subsequent scales in such a way that estimation of the relevant rheological parameters based on the chosen mix-design parameters is possible.

IV. Definition of adequate concrete technological and rheological performance evaluation criteria for flowable concrete

Unlike SCC, there are no adequate performance evaluation criteria for flowable concrete exposed to external stresses, especially in relation with the stability. Therefore, by making use of a combined assessment of the fresh concrete properties and the rheological characteristics, new concrete technological and rheological performance criteria are introduced that guarantee the stability of flowable concrete exposed to vibration and pumping pressure. The rheological performance criteria are defined based on the scale at hand, e.g. rheology of concrete $\leftrightarrow$ stability of concrete, or the subsequent scales, e.g. rheology of mortar $\leftrightarrow$ stability of concrete.

Ultimately, a comprehensive overview of the main findings of the dissertation is provided which encompasses the WBMD, the relevant characterization methods and the corresponding performance evaluation criteria at each scale.

1.3 Outline of the work

The dissertation comprises ten chapters which are structured more or less in line with the main objective points of the dissertation. The **first chapter** lays out the background information and objective of the dissertation.

The **second chapter** provides a detailed literature review with regard to the relevant fresh concrete properties including the flowability, pumpability and stability. Here, special focus is given to the mechanisms and influencing factors that determine these properties. Moreover, a detailed review is presented on the subjects of rheology and packing density as applied to the fresh concrete properties.

The **third chapter** introduces the new Water Balance Mix-Design method (WBMD). First, different hypotheses as related to the flowability, pumpability, stability and robustness of concrete are presented. Afterwards, a detailed explanation of the design methodology is illustrated. This is then summed up in a mix-design model for water balanced concrete mixtures (WBC).

The **fourth chapter** presents the experimental conception as to the composition of the mixtures as well as the applied investigation methods and evaluation techniques. The approach with regard to the application of the characteristic parameters of the component materials as input parameters for designing a WBC is exemplified. Moreover, the results of the experimental investigations including the flowability, pumpability, stability (under vibration and pressure) and robustness are presented. The results of the rheological investigations conducted on the concrete mixtures as well as the extracted mortar and paste compositions are also illustrated. The experimental results are always accompanied by detailed analysis as to the effects of the component materials and the design parameters on the observed fresh concrete and rheological properties.

The **fifth chapter** deals with the rheological characterization and modeling of the structural breakdown process on a multiscale basis considering the subsequent paste, mortar and concrete phases as micro, meso, and macro scales. In addition to identifying the rheological parameters with relevance to the structural breakdown, mathematical relationships are established that help quantify these parameters at each scale on the basis of the chosen mix-design parameters. Moreover, the interdependence between the rheological and the stability phenomena during the structural breakdown is discussed in great detail.

The **sixth chapter** introduces new performance evaluation criteria for flowable concretes exposed to vibration. These criteria are defined on the basis of the rheological, stability and flowability parameters. A preliminary performance criterion is

also introduced for ensuring the stability under pressure. An overview of the sequential performance evaluation that integrates the rheological performance criteria of the subsequent phases with the stability and flowability performance criteria of concrete and mortar is also illustrated.

The **seventh chapter** illustrates a general approach with regard to the characterization of the pumpability and pump-stability in relation to the rheological properties of the paste and concrete. A brief discussion regarding the interdependence between the pumpability and pump-stability is also presented.

The **eighth chapter** presents a detailed study regarding the effect of the water balance in concrete on the rheological, stability (under vibration and pressure) and pumpability properties. Moreover, an assessment of the adequacy of the water balance criteria (WB) as a performance evaluation criteria is made by making comparisons with the performance criteria that are defined on the basis of the rheological and stability parameters.

The **ninth chapter** discusses the essence of the dissertation by recapitulating the main aspects of the design, characterization and performance evaluation of flowable and stable concrete. To this end, an overview incorporating the WBMD, the relevant characterization methods for concrete, mortar and paste and the corresponding performance evaluation criteria is presented.

The **tenth chapter** completes the dissertation with a summary of the most important findings of the work and recommendations as to the potential areas of further research on subjects that are not dealt herein.

Chapter 2
Literature Review

2.1 Short introduction

A detailed literature review with regard to the relevant fresh concrete properties including the flowability, pumpability and stability is presented in this chapter. Here, the main focus lies in determining the mechanisms and influencing factors that determine these fresh concrete properties. The subjects of rheology and packing density as related to the fresh concrete properties are also dealt with in great depth.

2.2 Flowability of concrete

Almost all the individual component materials in the concrete and their interaction directly affect the flowability characteristics. Generally, a concrete can be considered to be composed of the paste as a medium in which the fine-coarse aggregate composition is suspended. The correlation between paste composition and flowability is relatively very complex, pertaining to the fact that the desired properties of the paste could be regulated in many different ways. The composition of fines (cement and additions), which determines the resulting packing density and the water demand as well as the addition of chemical admixtures, especially HRWRA and VMA, directly influence the flowability characteristics.

2.2.1 Definition

There are different terminologies and definitions used to describe the flowability of concrete. Usually the term consistency, which is determined on the basis of the slump [9] or slump flow [10] is used to describe the flowability properties; see Table 2.1. But, these classifications give information only regarding the extent of the flow, i.e. they answer the question “how far does the concrete flow?”. Workability is another term that is customarily used to describe the flowability property of concrete in connection with the placing process. Tattersall has defined the term workability in a more exact way by differentiating the qualitative and the quantitative aspects [11]. The qualitative descriptions of the concrete could be its workability, compactability, stability, pumpability etc. The quantitative descriptions are categorized in simple

empirical terms such as slump, flow spread or flow time as well as in more fundamental rheological terms such as yield stress and viscosity. The workability of fresh concrete could also be described in terms of its passing ability, filling ability and segregation resistance.

Table 2.1: Consistency classes (EN 206-1)

Classification	**Slump flow [mm]**	**Description**
F1	≤ 340	Stiff
F2	350 - 410	Plastic
F3	420 - 480	Soft
F4	490 - 550	Very soft
F5	560 - 620	Flowable
F6	≥ 630	Highly flowable

A self-compacting concrete (SCC) could also be considered as a highly flowable concrete with a unique design and application techniques. However, in case of SCC, in addition to the slump flow, the viscosity is also determined with the help of the V-funnel test or the t-500, which measures the time required to reach a flow diameter of 500 mm, thereby delivering crucial information with regard to flow time and answering the question “how fast does the concrete flow?”. The consistency and viscosity classes of SCC in accordance with [12] are summarized in Table 2.2.

Table 2.2: Consistence and viscosity classes of SCC (EN 206-9)

Consistency class	**Slump flow [mm]**	**Viscosity class**	**V-funnel time [s]**	**Viscosity class**	**t-500 time [s]**
SF1	550 - 650	VF1	< 9	VS1	≤ 2
SF2	660 - 750	VF2	9 - 25	VS2	3 - 6
SF3	760 - 850	VF3	> 25	VS3	> 6

2.2.2 Factors affecting the flowability of concrete

I. Paste volume

A minimum amount of paste is required in order to transform the aggregate cluster into a concrete suspension. This minimum amount of paste depends on the degree

of packing and the specific surface area of the chosen aggregate compositions. For a certain mode of packing, the degree of packing of the aggregates mainly depends on the gradation and the geometrical characteristics of the aggregates, such as shape, angularity and roughness. The amount of paste required to fill the voids between the aggregates is equivalent to the minimum voids content corresponding to the maximum packing density. Moreover, a minimum paste thickness is required for the separation of the aggregates, depending on the geometrical characteristics, especially the specific surface area of the aggregates. This minimum paste thickness is necessary in order to reduce the friction between the aggregates and to initiate flow.

One of the first works regarding the required amount of paste in a concrete was from Kennedy who coined the term “excess paste theory”, which suggests the need for a certain paste thickness around the aggregates to initiate flow [13]. Powers also advocated the importance of an excess paste for the formation of a lubricating layer so that flowability of concrete can be achieved [14]. A study by Li and Kwan has shown that the paste film thickness (PFT) in combination with the water film thickness (WFT) significantly influences the flowability characteristics. As such, an increase in the paste volume could increase both the slump and the flow of the concrete as shown in Figure 2.1 [15].

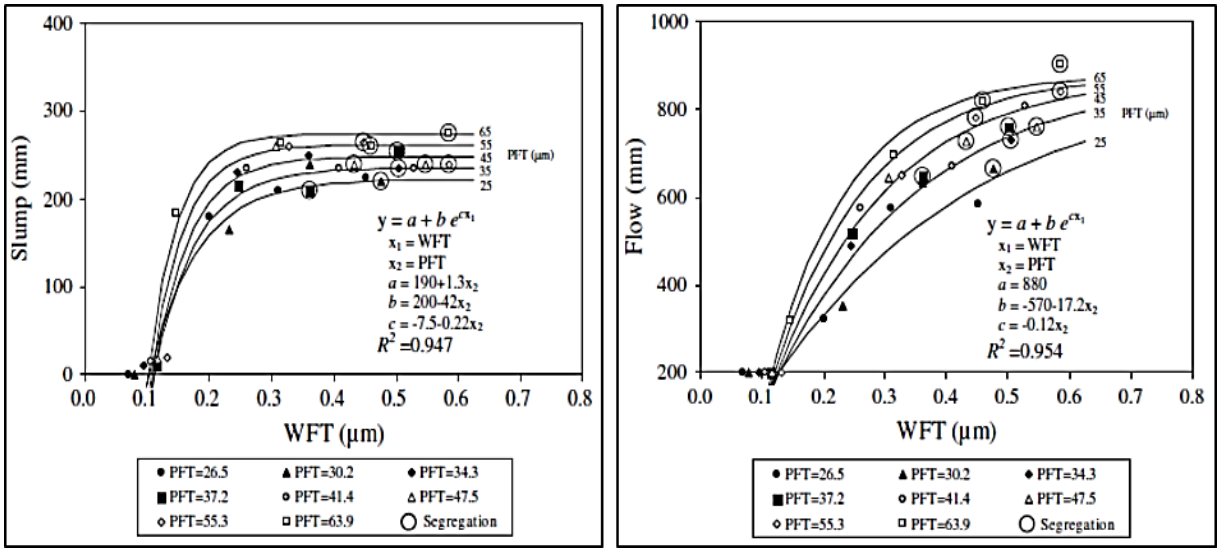

Figure 2.1: Effects of water film thickness (WFT) and paste film thickness (PFT) on slump (left) and flow (right) [15]

A study by Su and Miao has shown the need for a minimum amount of paste for the formation of a concrete suspension. The results of their investigation has shown a significant increase in slump flow from 300 mm to 600 mm as a result of a slight increase in paste content from 290 l/m^3 to 300 l/m^3 [16]. The same observation was

made by Neumann while investigating the effect of paste volume on pumping pressure. Here, despite the addition of superplasticizer above the saturation point, the target consistence class of F4 (slump flow = 490 – 550 mm) could not be reached, since the minimum paste content was not fulfilled [17]. The minimum paste content is also dependent upon the specific workability requirements such as passing ability and filling ability. Passing ability could be defined as the ability of the concrete to pass through possible hindrances, such as tight reinforcement spacing, without losing its homogeneity. Filling ability is the ability of the concrete to fill the formwork regardless of the geometrical complexity of the structural element [18]. The amount of paste required for filling ability and passing ability could differ, in which case, the larger of the two should be adopted [19].

II. Packing density of fines

The packing density of fines and the resulting voids ratio play a decisive role in determining the amount of water required to form a paste suspension. The packing density primarily depends on the composition of the fines, assuming that the same method of compaction is applied. For a certain paste composition, an increase in packing density means minimizing the available void spaces between the fines either through reorientation of the existing particles or the filling effect of finer particles. This sets the constricted water between the voids free, which ultimately contributes to higher flowability. Accordingly, Kwan and Wong have shown that a partial substitution of ordinary portland cement (OPC) with either pulverized fuel ash (PFA) and / or condensed silica fume (CSF) could lead to an increase in the packing density as shown in Figure 2.2 [20].

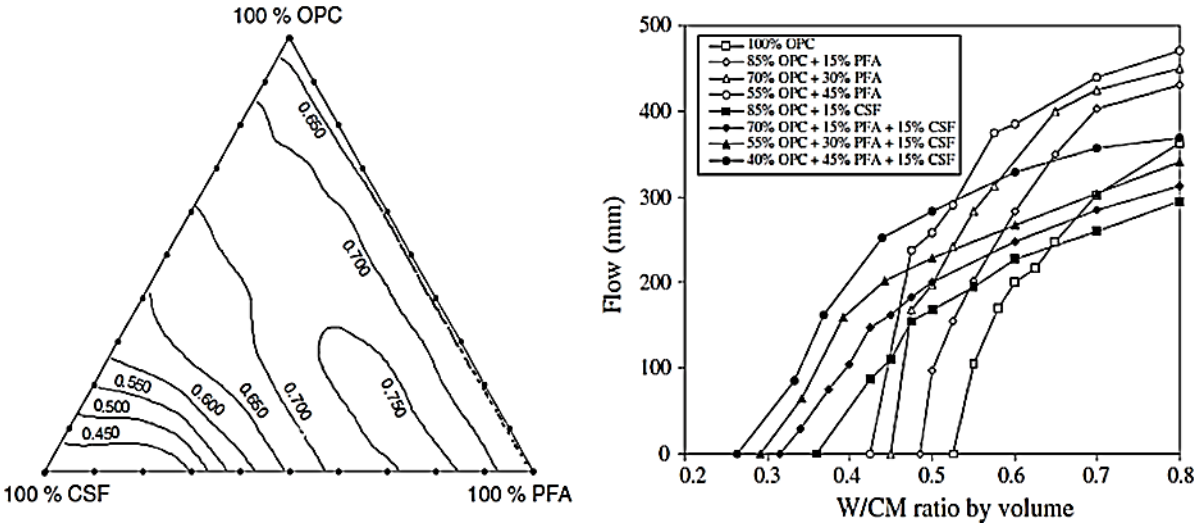

Figure 2.2: Variation of packing density of blended mixes (left) and flow of paste (right) [20]

The authors attributed the increment in the packing density to the filling effect of the PFA and the CSF, which is also helped by their spherical shape that ultimately reduces the voids between the OPC particles. Consequently, the “excess” water which is displaced by the smaller filling particles would act as a lubricating layer adding to the flowability of the paste. In other words, the W/CM values required for a certain constant slump-flow decrease with increased substitution of OPC with either PFA or CSF. A similar observation was made by Nanthagopalan et al. They observed a higher packing density and flowability with an increased substitution of OPC with Fly ash as shown in Figure 2.3. They also suggested that the packing density has a significant influence on the yield value and lesser influence on the plastic viskosity [21].

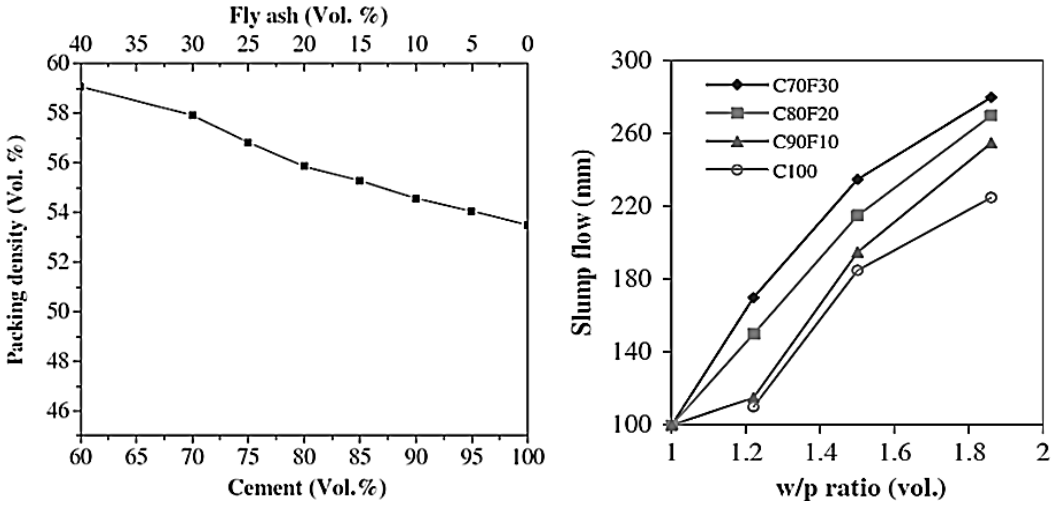

Figure 2.3: Packing density of binary blended mixes (left) and paste flow (right) [21]

III. Water demand of fines

The water demand of fines is another decisive factor, in combination with the packing density of fines, in determining the amount of water needed to achieve the desired flowability. Generally speaking, fines with larger surface area have higher water demand leading to a reduced flow at certain water content. This was observed by Artelt and Garcia who investigated the effects of ultra-fine powders such as silica fume (SF) on the flow properties of mortars. They observe a reduction in the slump flow and an increase in flow time due to the significantly higher surface area caused by the addition of the ultra-fine powders as shown in Figure 2.4 [22].

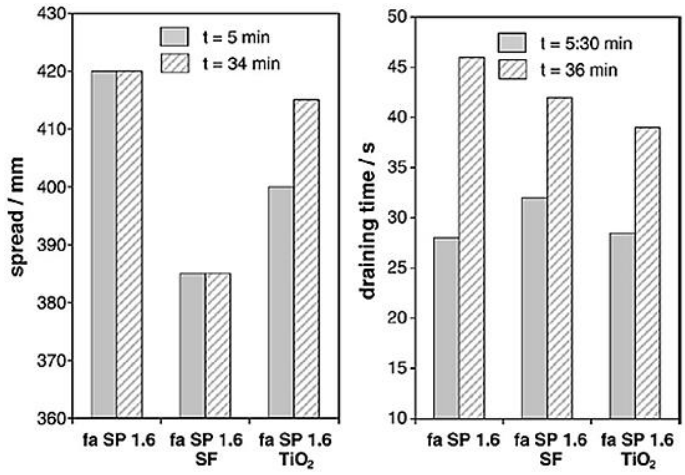

Figure 2.4: Slump and funnel flow test for fly ash mortars containing ultra-fine powder [22]

Papo et al. have investigated the rheological properties of cement pastes made of CEM 32.5 R and CEM 52.5 R with the same w/c ratio. They observed that the pastes with CEM 52.5 R were far more viscous in comparison to those with CEM 32.5 R. This could be attributed to the higher water demand of CEM 52.5 R which possesses a higher surface area of 1.82 m^2/g when compared to 1.38 m^2/g for CEM 32.5 R. Consequently, for a comparable flowability CEM 52.5 R and CEM 32.5 R require a w/c ratio 0.42 and 0.32 respectively, as shown in Figure 2.5 [23].

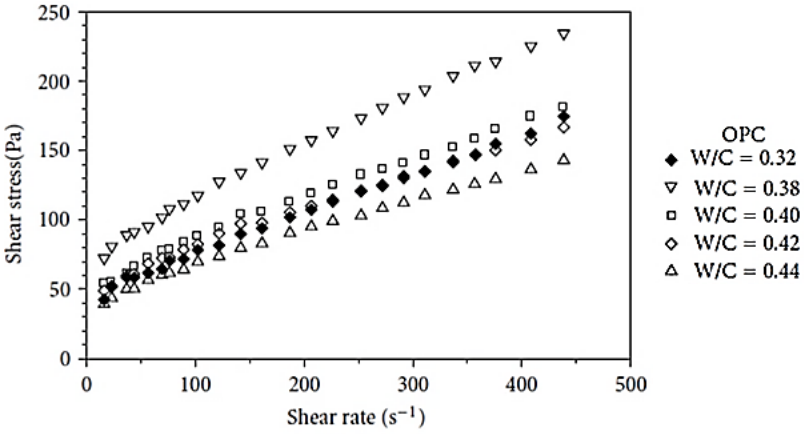

Figure 2.5: Shear stress v. shear rate flow curves [23]

The increased flowability that is gained through enhancing the packing density of the fines could be lost or starts to decline if the water demand of the fines that are used for the optimization is too high. Investigations by Ludger Lohaus and Thomas Gläser [24] on mortars has revealed that the flowability of mortar compositions could be enhanced by partial replacement of sand with a fly ash up to a certain peak point after which the flowability starts to decline, as shown in Figure 2.6. The enhanced flowability could be attributed to the increase in the packing density, while the

decrease after the peak is a consequence of the increment of the total surface area due to the fly ash.

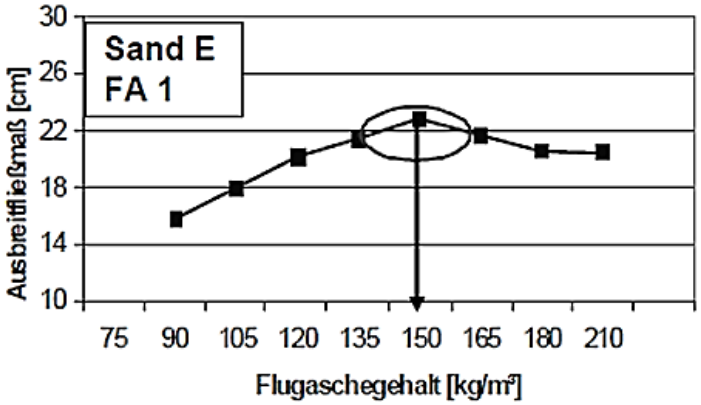

Figure 2.6: Effects of packing density and water demand on the flowability [24]

For a certain water content, the thickness of the lubricating water depends on the total surface area of the particles in a mixture. Kwan et al. designated the term water film thickness (WFT) which is the ratio of the excess water to solid surface area [25]. Based on the results of their investigations on mortar, the authors concluded that the WFT is the single most important parameter governing the flowability and rheological propertes as shown in Figure 2.7. There is a minimum WFT of about 0,05 µm that is required to achieve a reasonably good flowability. Higher values of WFT imply higher flowability, while a negative WFT implies insufficient amount of water to fill up the voids.

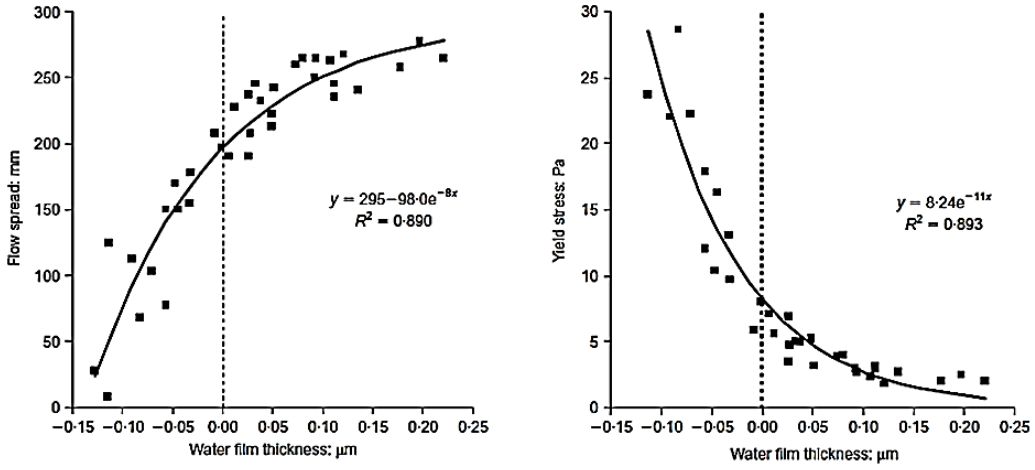

Figure 2.7: Effect of water film thickness on the flowability (left) and yield stress (right) [25]

IV. Chemical admixtures

The effect of chemical admixtures, especially superplasticizers and stabilizers, on the flowability of concrete was extensively investigated. It is well known that the usage of superplasticizers results in higher flowability of concrete. Moderately effective superplasticizers such as lignosulphonate (LS) and polycondensate resins including poly-naphthalene sulphonates (PNS) and poly-melamine sulphonates (PMS) exhibit short chains with high anionic charges that adsorb on the clinker and hydration phases. Consequently, the negatively charged cement particles get electrostatically repelled and dispersed resulting into an increased flowability of the mix [26]. On the other hand, the highly effective polycarboxylate (PC) superplasticizers disperse the particles mainly by virtue of steric repulsions through the usage of graft chains of keep the particles at a distance [27]. Based on the adsorption model developed by Yoshioka et al., the contribution of the electrostatic repulsions in PC polymers is negligible when compared to the effect of the steric hindrance caused by the graft chains, which makes PC based superplasticizers superior in enhancing the flowability of concrete mixtures [28]. The working mechanisms of the electrostatic and steric repulsions are illustrated in Figure 2.8 [29].

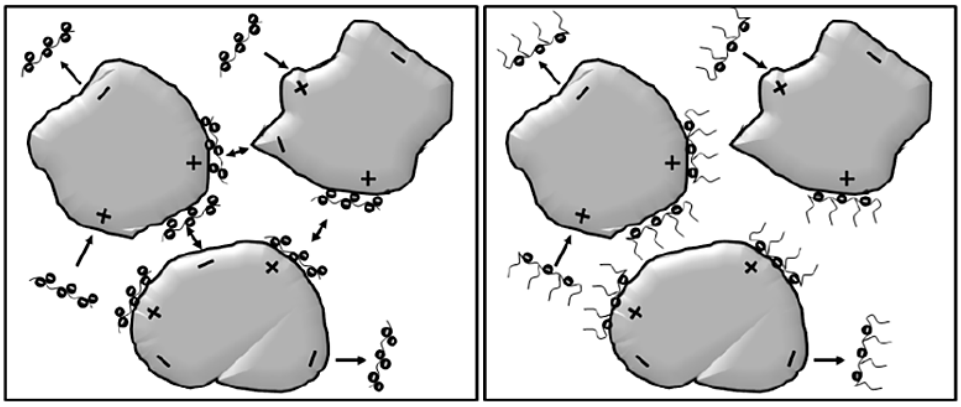

Figure 2.8: Electrostatic repulsion (left) and steric repulsion (right) [29]

Generally, addition of superplasticizers results into increased flowability. Flowability investigations by Schmidt on pastes using low charge (LC), medium charge (MC) and high charge (HC) superplasticizers at different time intervals has shown that the flowability increases regardless of the type of the superplasticizer used as shown in Figure 2.9. Moreover, an indication of a saturation point of superplasticizers after which no significant increment in the slump flow occurs and the pronounced effect of the HC superplasticizer on the flowability could also be noted [29]. This increment in flowability with the addition of superplasticizer is also confirmed by several researchers including, [30] [31] [32] [33].

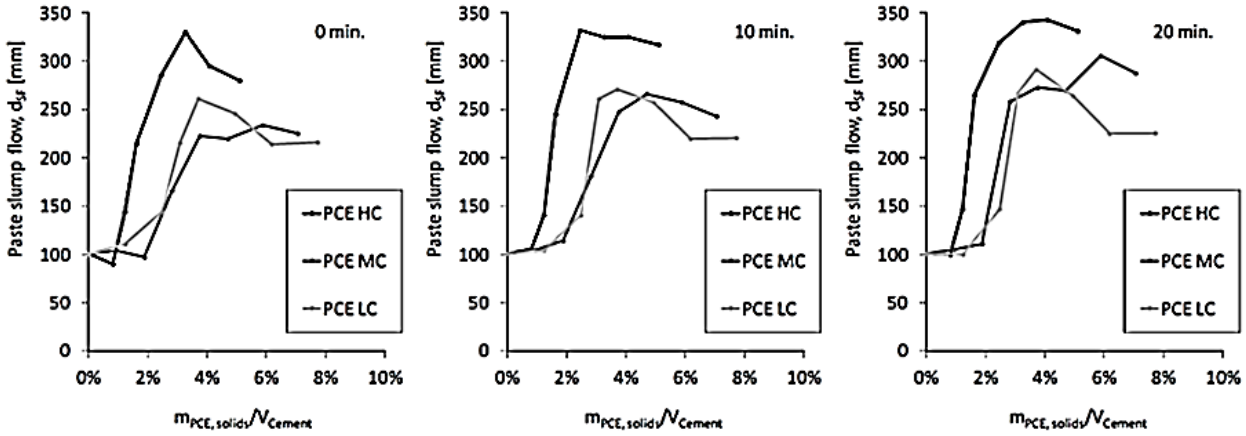

Figure 2.9: Effect of different superplasticizers on the flowability of paste [29]

Another chemical admixture that significantly influences the flowability of concrete is stabilizing agent which are also referred as or viscosity modifying agent (VMA). According to Khayat, there are basically three mode of operation of VMA. First, the VMA polymers swell on contact with water, thereby trapping some water molecules. Second, the polymers block the movement of water by forming a network built by the attractive forces. The third stabilization mechanism is through intertwining and entanglement of the polymer chains [34]. Overall, the addition of VMA leads to an increase in viscosity and a reduction in the flowability. Investigations by Leemann and Winnefeld on the effects of VMA on the flowability properties of mortar compositions has shown a decrease in the slump flow and an increase in flow time as a consequence of the addition of VMA of the type natural polysaccharide (PS) at different water to powder ratios as shown in Figure 2.10 [35]. Similar findings about the effects of VMA on the flowability properties are also reported by other authors including [36] [37] [38].

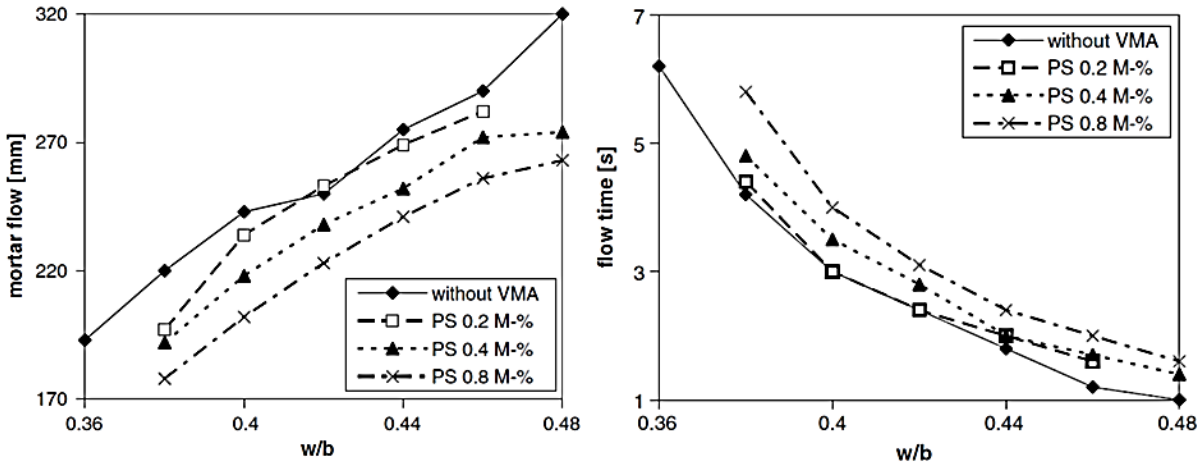

Figure 2.10: Effect of SA on the flow properties of mortar [35]

Lachemi et al. have compared the performance of four new types of polysaccharide-based VMA (simply denoted as A, B, C, D) with a commercially available VMA (denoted as COM), in combination with superplasticizer (SP). Whereas the COM type VMA also contains SP, the composition of the four new VMA is not described. Contrary to the general consensus as to the effects of VMA on the flowability, the authors observed an increase in the slump flow of mortar due to the addition of all types of VMA at a constant SP content. They also observed an increase in the slump flow with an increased content of VMA as shown in Figure 2.11 [39]. The authors did not give explanation as to the reason for this occurrence. However, according to Schmidt, such unexpected behaviors could occur depending on the solid concentration as well as the dosage and the mode of operation of the VMA in the presence of SP [29]. His investigation based on a diutan gum has shown that the yield stress of a cementitious system at a SP dosage of 0.3% does not significantly change up to a diutan gum concentration of 5.0%. However, he concluded that the yield stress and plastic viscosity could significantly be increased at higher dosages of diutan gum [40], which is generally contrary to the findings by Lachemi et al.

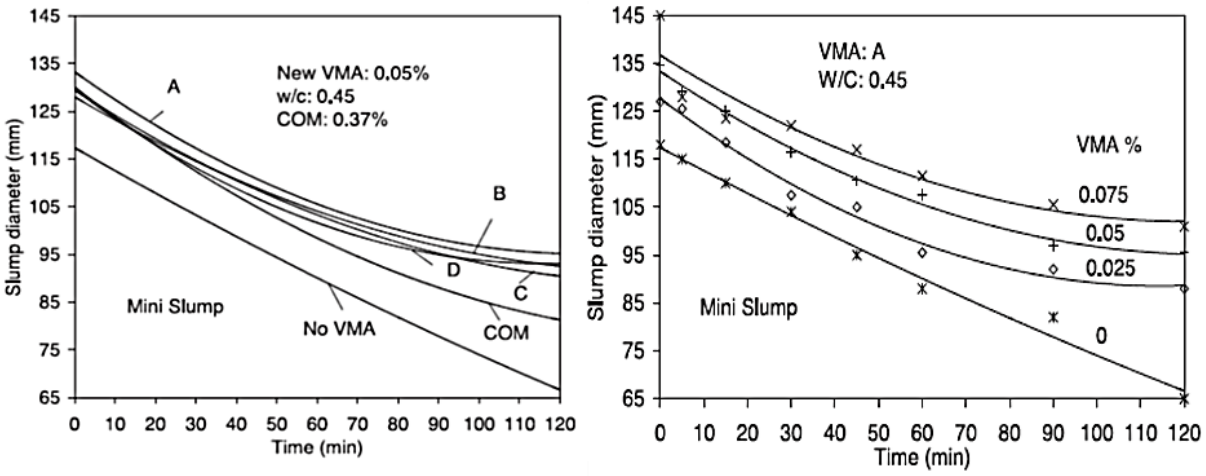

Figure 2.11: Effect of type and amount of VMA on the slump flow (SP = 0.25%) [39]

V. Aggregate properties and composition

The shape, size, surface texture and gradation of the aggregates significantly influence the flowability properties of the concrete. The effect of these different features in relation to the flowability properties is directly correlated with the total paste demand, which is composed of the amount of paste needed to fill up the voids between the aggregate and the additional amount of paste needed to coat the surface of the aggregates in order to achieve a certain level of flowability. The shape of an aggregate describes the sphericity, form and roundness of the particle [14] [41]. While sphericity describes the extent to which the three principal axes or dimensions of the particle are equivalent, the form is a measure of the relationship between the

three dimensions based on the ratios or proportions of the long, medium and short dimensions of the particle [42]. Angularity is another term that is describes the sharpness of the edges and corners of the particle [43]. Another term that is usually used to describe the geometrical properties of aggregates is surface texture or roughness. Evaluation of these geometric properties of aggregates mostly relies on visual assessment as shown in Figure 2.12 by [44] as mentioned in [45].

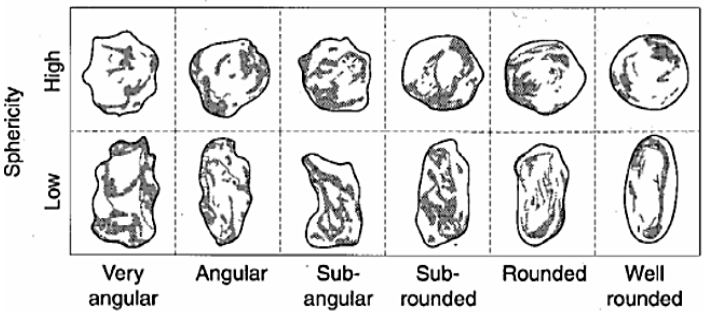

Figure 2.12: Visual assessment of the shape of aggregates [45]

Krumbelin and Sloss developed a method with which the geometrical properties of an aggregate could be quantified based on the roundness and sphericity [46]. Determination of these geometrical parameters using conventional methods is not only laborious but also highly susceptible to errors [47]. As a result, new modern digital processing techniques that make use of images and videos are increasingly being applied [43] [48] [49]. Other modern techniques involve 3D profiling of the aggregates using laser techniques [50] [51]. Some of the methods among these technologies are satisfactorily accurate and can deliver a significant amount of data regarding the geometrical properties of the aggregates in real-time. Tomographic techniques that make use of x-rays or gamma rays as well as magnetic or acoustic resonance technology were also applied for aggregate shape characterization [52].

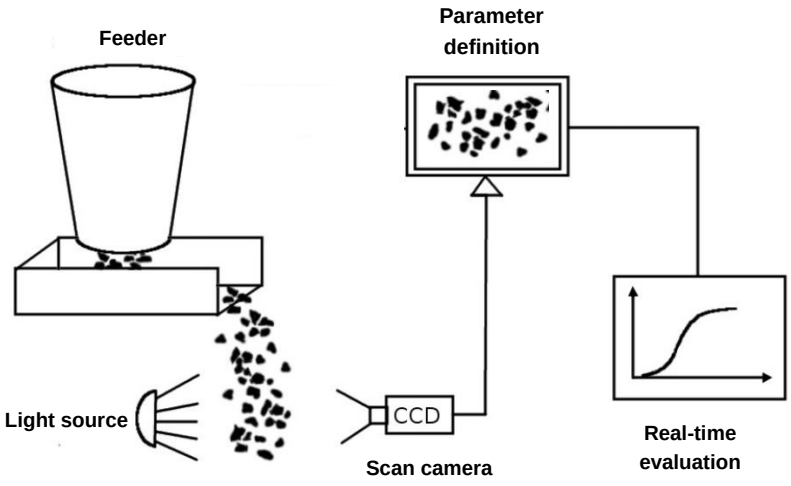

Figure 2.13: Computerized particle analysis system adopted from HAVER CPA [49]

For a certain aggregate composition, the effects of the geometrical characteristics of the aggregates on the concrete properties could be explained in terms of their influence on the packing density and the total surface area, which ultimately determines the total paste demand. Generally speaking, round or nearly spherical aggregates are preferable for concrete production since they are able to roll or slide over each other as a result of the ball-bearing effect resulting into a lesser void content. Moreover, for a given mass, spherical shaped particles have smaller surface area, which means a lesser paste demand for coating them. The combination of these two factors contributes to a good flowability and workability of the mix [11]. Flaky and irregular shaped aggregates affect the workability of concrete negatively and they also exhibit higher paste demand. Similarly, aggregates with rough surface textures may lead to poor workability and higher paste demand [53] [54] [55].

Kaplan's investigation using different natural and crushed aggregates has revealed that increased angularity and flakiness generally lead to a reduction in the workability of concrete. He also observed a reduction in the compaction factor with increased angularity and flakiness. This implies that the reduction in workability could be the result of the increased percentage of voids of the aggregates that need an additional amount of paste to be filled with. However, he found no significant correlations between the surface texture and the water adsorption properties of the aggregates and the workability of concrete [56].

Bloomer has conducted rheological investigations to quantify the effect of rounded gravel and crushed aggregates on the relative yield stress (g) and relative plastic viscosity (h). The content of the natural sand and cement remained constant. The results of the investigation have indicated that while the g-values remain comparable for mixes with both aggregates, the h-values were tendencially higher for the mixtures containing crushed aggregates [57].

Huss has combined different natural and crushed aggregates using different gradations of A16, AB16, ABB16 and B16 based on [10] in order to investigate the surface water demand. The results of his investigation show the lowest and highest surface water demand for the natural sand – gravel and crushed sand – crushed stone combinations respectively. This implies the existence of a direct relationship between the shape and surface texture of aggregates and the water demand as shown in Figure 2.14.

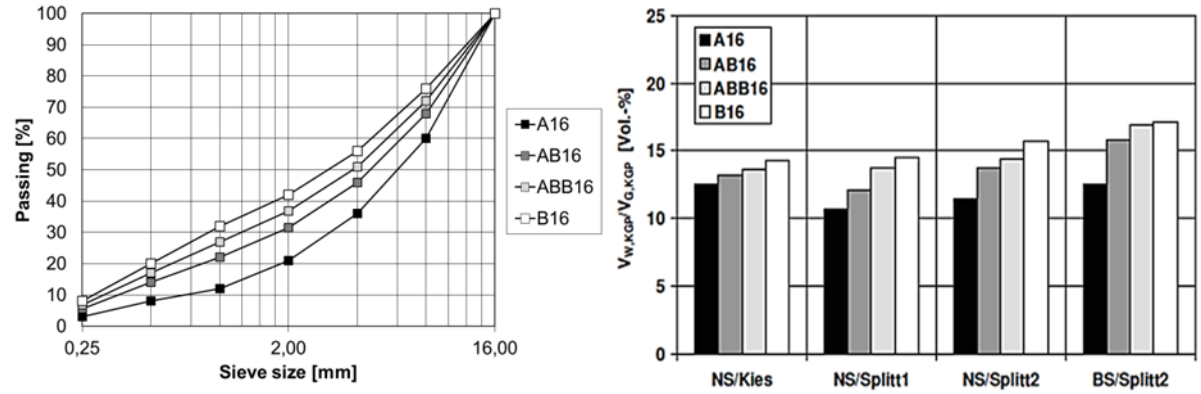

Figure 2.14: Gradation (left) and water demand for different natural and crushed aggregate compositions (right)* [49]

* NS/Kies = natural sand – gravel, NS/Splitt 1 = natural sand – crushed stone 1, = natural sand – crushed stone 2, BS/Splitt 2 = crushed sand – crushed stone 2

Aggregate gradation is another decisive factor that influences the flowability and workability of concrete. It is recommended to use the largest maximum size as much as possible since the total surface area and the void content of the aggregates decreases thereby reducing the required amount of paste. However, an excess amount of coarse aggregates could also lead to an increased void content and poor workability of the concrete [55] [58]. A mix lacking enough amounts of fine fractions will be harsh and lack cohesiveness potentially leading to segregation, inhomogeneity and poor finishability [11].

Hence, attaining the required fresh as well as hardened concrete properties usually require an optimization with respect to the fine - coarse aggregate compositions. Shilstone has stated that the relationship between the coarseness of two larger aggregate fractions and the fine fraction, the total amount of mortar and the aggregate particle distribution are the principal factors upon which mixture proportions can be optimized. Accordingly, the amount of sand needed to optimize a mixture is a function of the relationship between the larger aggregate fractions and the amount of cementitious materials in the mixture. If there is too much sand; the mixture gets "sticky," has a high water demand, requires more cementitious materials to produce a given strength, increases pump pressures, and creates finishing problems. If there is not enough sand, the mixture is "bony" and creates a different set of placing and finishing problems [54].

Huss has investigated different fine – coarse aggregate compositions as presented in Figure 2.15 for the gradation curves A16, AB16, ABB16 and B16 with the respective fine to coarse aggregate proportions of 21:79, 32:68, 37:63 and 42:58. The results of the investigation reveal an increase in surface paste demand with increasing fine -

coarse aggregate ratio, regardless of the type of aggregates combined. This could be attributed to the increase in surface area of the aggregate compositions due to the increased fine aggregate content. The surface paste demand represents the excess paste amount that is needed to coat the aggregates, so that flow can be initiated. Hence, an increase in surface water demand due to the shape, texture or composition of the aggregates results in an increased surface paste demand. The total paste demand of a concrete comprises of the paste amount required to coat the aggregates and to fill-up the voids between them. For a certain method of compaction, the void content depends on the type and composition of the aggregates. The investigation results from Huss have shown that, regardless of the aggregate composition, the void content decreases with an increasing fine – coarse aggregate ratio. In fact, an opposite trend could be observed when the paste demands for surface coating and void filling are compared across the different gradations between A16 and B16. On the other hand, for the same gradation, the paste demand for the surface coating and void filling tend to increase with the inclusion of crushed aggregates, the crushed stone – crushed sand (Q-BS) composition exhibiting the highest paste demand in both cases [49].

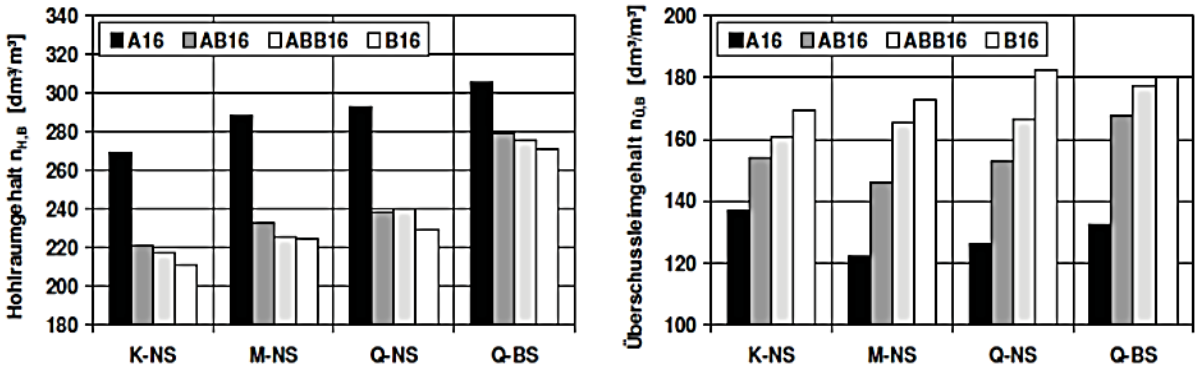

Figure 2.15: Paste demand for voids filling (left) and surface coating (right) of different natural and crushed aggregate compositions* [49]

* K-NS = gravel - natural sand, M-NS = crushed stone 1 - natural sand, Q-NS = crushed stone 2 - natural sand, Q-BS = crushed stone 2 - crushed sand

The total paste demand, which is the sum of the paste amount required for surface coating and void filling, generally increases with the inclusion of crushed aggregates and across the gradation lines, except for the gradation line A16 (see Figure 2.16). The reason for the higher total paste demand of A16 gradation might be due to the imbalance between the excessive voids created by the higher amount of coarse aggregates (Vol. ≅ 79%) that could not be filled with the relatively small amount of sand (Vol. ≅ 21%). This confirms the importance of aggregate optimization in relation to the reduction of the amount of paste in a concrete.

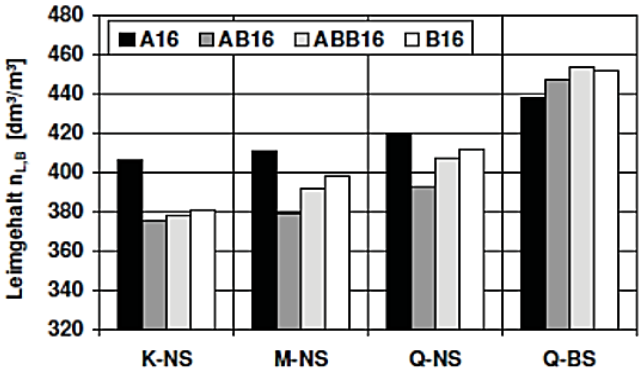

Figure 2.16: Total Paste demand for different natural and crushed aggregate compositions* [49]

* K-NS = gravel - natural sand, M-NS = crushed stone 1 - natural sand, Q-NS = crushed stone 2 - natural sand, Q-BS = crushed stone 2 - crushed sand

Thus, it could be concluded that for constant paste volume, aggregate compositions, which by virtue of their shape, texture or gradation require higher amount of paste, produce concretes with less flowability and poor workability properties.

2.2.3 Design aspects for flowable concrete

Regardless of the concrete type, the basic design requirements such as maximum water – cement ratio, minimum strength class, minimum cement content, maximum fines content and permissible amount of additives, which emanates from the exposure classes or other relevant specifications, remain benchmarks that have to be fulfilled in the design of flowable concrete [10]. Moreover, economy and sustainability are important factors that play a major role in concrete design. The fundamental difference between today´s concrete technology and the one before some decades is the existence of several possibilities to attain the desired concrete properties such as flowability. To this end, the introduction of poly-naphthalene sulphonates (PNS), lignosulphonates (LS) and poly-melamine sulphonates (PMS) in the 1930s through the 1960s as normal water reduction admixtures (WRA) had changed the landscape of concrete production in two major ways.

On the one hand, for the same water content, it was possible to produce highly flowable concrete without affecting the hardened concrete properties. On the other hand, it was possible to enhance the hardened concrete properties by reducing the water content without affecting the workability [59]. The later introduction of modern polycarboxylate based superplasticizers (SP) in the 1980s as high range water reducing admixtures (HRWRA) have taken these phenomena to the extreme that it is possible today to apply special concretes such as self-compacting concrete (SCC) and ultra-high strength concrete (UHPC).

The “excess paste theory” developed by Kennedy, which assumes an equivalent layer of excess paste for all particle sizes that is dependent upon a workability factor, is considered to be the first systematic design approach for flowable concrete [13]. This theory has later served as a basis upon which many researchers developed models for flowable concretes including SCC. Accordingly, Bui and Montgomery developed a model for SCC that considers the excess paste layer to be equivalent to the average spacing between the aggregate particles, assuming them to be spherical [60]. In the SCC-model from Oh et al., the thickness of the excess paste layer differs depending on the size of the aggregate particles [61]. The model by Wüstholz for SCC assumes an equivalent excess paste layer regardless of the particle size as illustrated in Figure 2.17 [62].

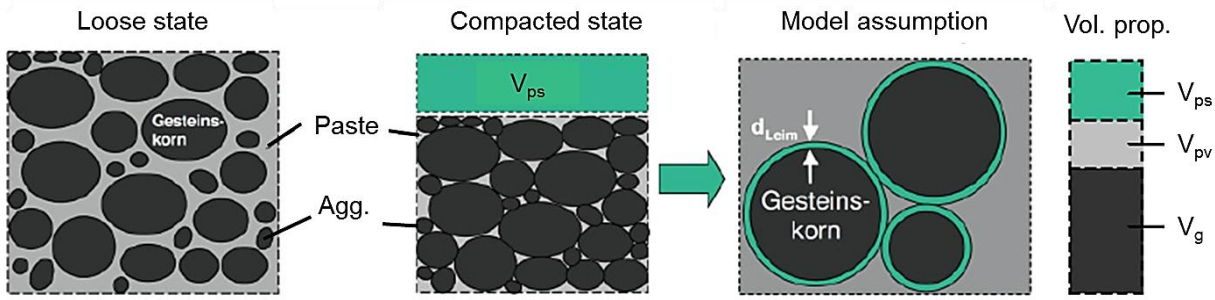

Figure 2.17: Excess paste theory as applied to SCC [62]

For a given paste volume in a concrete, the amount of the excess paste layer can be determined using Equation (2.1).

$$V_p = V_{ps} + V_{pv} \rightarrow V_{ps} = V_p - V_{pv} = V_p - V_g\left[\frac{1}{n_g} - 1\right] = V_p - \frac{m_g}{\rho_g}\left[\frac{\rho_g}{\rho_b} - 1\right] \qquad (2.1)$$

Where: V_p = total paste volume in concrete (dm^3/m^3), V_{ps} = excess paste volume for surface coating (dm^3/m^3), V_{pv} = excess paste volume for void filling (dm^3/m^3), V_g = absolute aggregate volume (dm^3/m^3), $n_g = V_g / V_b$ = loose solid concentration (-), V_b = bulk aggregate volume (dm^3/m^3), m_g = mass of aggregate (kg), ρ_g = specific gravity of aggregate (kg/dm^3) and ρ_b = loose bulk density of aggregate (kg/dm^3)

For a known total surface area of the aggregates, the excess paste layer thickness could also be determined using Equation (2.2).

$$d_{ps} = \frac{V_{ps}}{O_g} \qquad (2.2)$$

Where: d_{ps} = thickness of excess paste layer (dm), V_{ps} = excess paste volume for surface coating (dm^3/m^3) and O_g = total surface area of the aggregates (dm^2/m^3)

In order to determine the total surface area, the aggregate compositions could be classified into several size fractions ($n_{i)}$ with respective fictive radiuses (r_i).

$$O_g = 4\pi \cdot \sum n_i \, r_i{}^2, \text{where } r_i > 0.125 \text{ mm} \tag{2.3}$$

The results of the investigations on SCC that are made based on this model are presented in Figure 2.18. As can be seen from the diagrams, the slump flow increases and the funnel flow-time decreases with increasing layer thickness. However, the effect of the layer thickness seems to subside upon reaching approximately the 0.03 mm mark. This reveals the dominant role played by the particles-to-particle friction between the aggregates that are not yet fully coated by a paste layer. After reaching such a point, the flowability properties of the concrete will be dominated by the rheological characteristics of the paste composition.

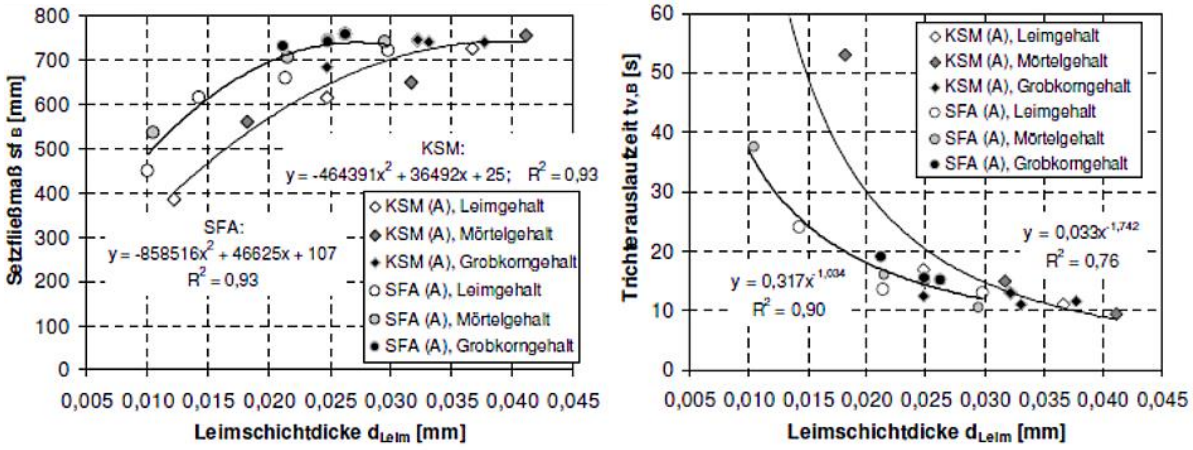

Figure 2.18: Influence of the thickness of excess paste layer on slump-flow (left) and funnel flow-time (right) of SCC [62]

Huss has adopted the model developed by Wüstholz and introduced a method with which the excess paste amount for SCC could be determined. To this end, he applied the so called Korn-Gemisch-Prüfung (KGP) investigation method, with which the packing density and the water demand of the aggregates could be determined. First, the water demand of the aggregates' surface (V_{ws}) is determined by pumping out the water between the voids of a completely saturated aggregate composition using a water-jet pump. Afterwards, a compaction method, which makes use of vibration and surcharge weight, is applied to determine the packing density.

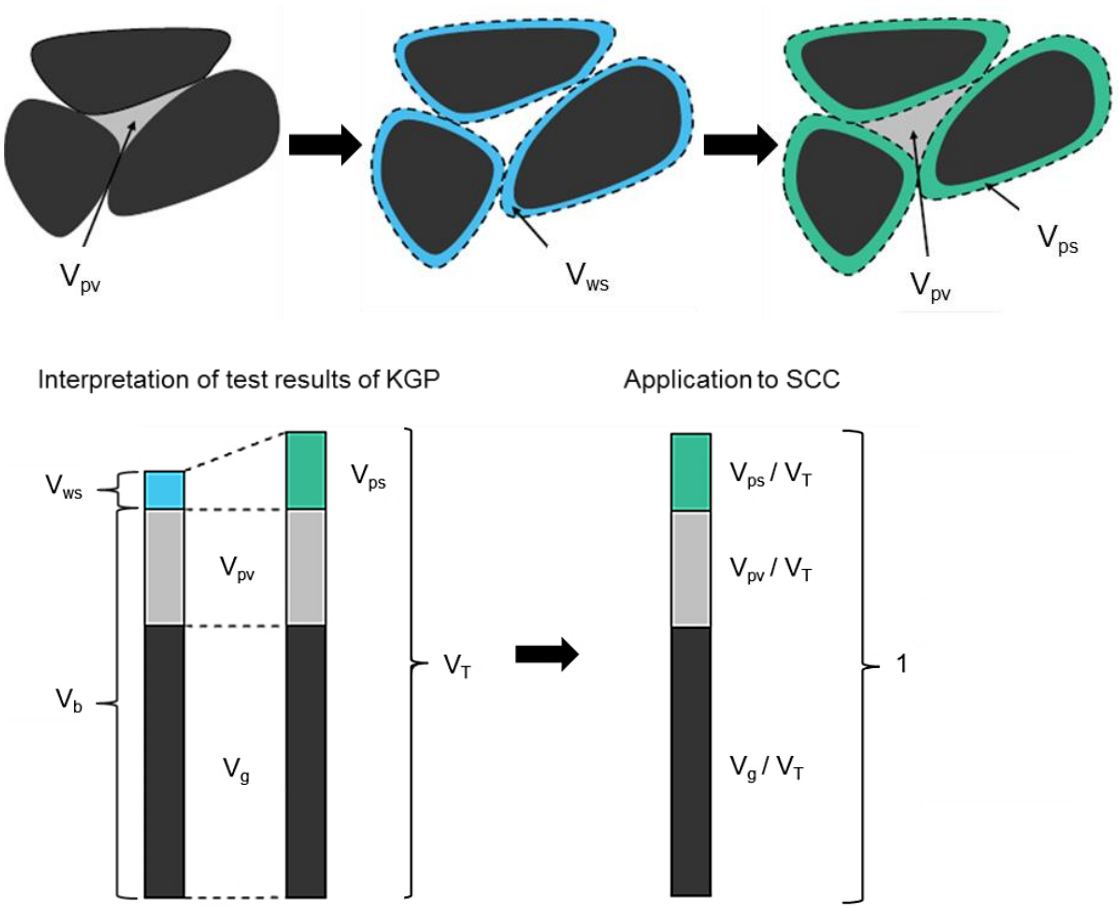

Figure 2.19: Determination of excess paste content based on the water demand and the packing density [49]

From the chosen water – fines ratio ($f = V_w/V_f$) for the design of SCC, the excess paste for surface coating could be calculated using Equation (2.4).

$$V_{ps} = V_{ws}\left(1 + \frac{1}{f}\right) \cdot \frac{1}{(1 - \varepsilon_{ap})} \tag{2.4}$$

Where: V_{ws} = water demand for surface coating from KGP (m^3), V_{pv} = excess paste volume for surface coating from KGP (m^3) and ε_{ap} = air content of the paste (assumed as 0.003)

The classic volumetric mix-design approach is then adopted to determine each component in the SCC.

$$\frac{V_p}{V_T} + \frac{V_g}{V_T} = 1 \tag{2.5}$$

$$\frac{V_p}{V_T} = (V_w + V_f) \cdot \frac{1}{1000\ dm^3} + \varepsilon_a \tag{2.6}$$

$$V_f = \frac{M_c}{\rho_c} + \frac{M_{g<0.125\,mm}}{\rho_g} + \frac{M_{ma}}{\rho_{ma}} \quad (2.7)$$

$$V_w = \frac{M_w}{1\ \frac{kg}{dm^3}} + \frac{M_{ca}}{\rho_{ca}} \quad (2.8)$$

$$\frac{V_g}{V_T} = \frac{V_{g\geq 0.125\,mm}}{1000\ dm^3} \quad (2.9)$$

$$V_g = \frac{M_{g\geq 0.125\,mm}}{\rho_g} \quad (2.10)$$

Where: V_p = total paste volume from KGP (dm^3), V_T = total volume from KGP (dm^3), V_g = aggregate volume from KGP (dm^3), $V_{g \geq 0,125\ mm}$ = aggregate volume ≥ 0,125 mm (dm^3), V_w = volume of water (dm^3), V_f = volume of fines (dm^3), M_c = mass of cement (kg), $M_{g < 0,125\ mm}$ = mass of aggregate < 0,125 mm (kg), $M_{g \geq 0,125\ mm}$ = mass of aggregate ≥ 0,125 mm (kg), M_{ma} = mass of mineral admixtures (kg), M_w = mass of water (kg), M_{ca} = mass of chemical admixtures (kg), ρ_c = specific gravity of cement (kg/dm^3), ρ_g = specific gravity of aggregates (kg/dm^3), ρ_{ma} = specific gravity of mineral admixtures (kg/dm^3) and ρ_{ca} = specific gravity of chemical admixtures (kg/dm^3)

Wong and Kwan suggested a three tier system design for high performance concrete (HPC) based on a wet packing method [63] [64]. In this approach, the concrete is assumed to be constituted of three phases.

- Paste phase: cementitious materials + water + any superplasticizer added
- Mortar phase: cement paste + aggregate particles smaller than 1.2 mm
- Concrete phase: mortar + aggregate particles larger than 1.2 mm

The packing density of the cementitious materials in the paste phase determines the water demand and the excess water, which is the dominant factor that determines the flowability properties of the cement paste. The packing density of the aggregates smaller than 1.2 mm determines the paste demand and the excess paste demand, which determines the flowability properties of the mortar. Similarly, the packing density of the aggregate particles larger than 1.2 mm would determine the mortar demand and the excess mortar, which is responsible for the workability of the concrete mix. The basis for the determination of the wet packing density is shown in Figure 2.20 [65].

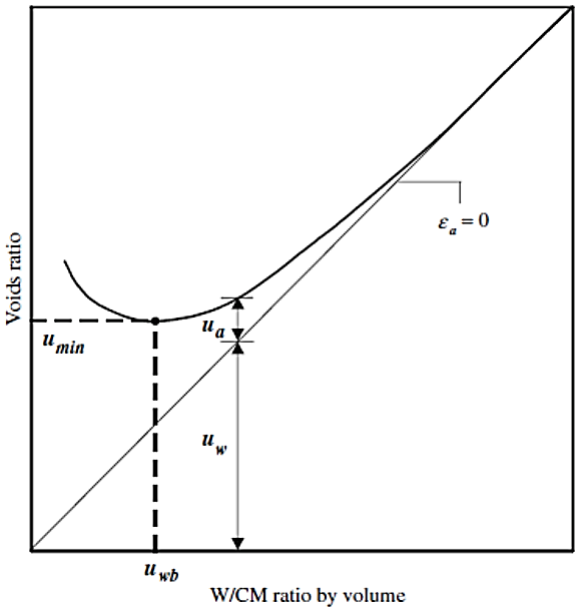

Figure 2.20: Determination of void ratio based on the wet packing method [65]

The voids between the solid particles could be filled with water, air or both. Based on the corresponding void ratio (u_i), which is the ratio of the volume of voids to the volume of solid particles, the void contents filled by water (ε_v) or air (ε_a) could be determined as follows.

$$\varepsilon_w = \frac{u_w}{1+u_w+u_a} \text{ and } \varepsilon_a = \frac{u_a}{1+u_w+u_a} \tag{2.11}$$

The solid concentration of the particles (ϕ), which is the ratio of the solid volume to the bulk volume of particles, could be determined using Equation (2.12) .

$$\phi = 1 - \varepsilon = \frac{1}{1+u} \tag{2.12}$$

Accordingly, the minimum voids ratio ($u_{s,min}$) can be determined based on the measurement of the maximum packing density of all the particles in the concrete ($\phi_{s,max}$) using Equation (2.13).

$$u_{s,min} = \frac{1-\phi_{s,max}}{\phi_{s,max}} \tag{2.13}$$

The excess water ratio (u_{we}), which is the ratio of the volume of excess water to the volume of solid particles, could then be determined using Equation (2.14)

$$u_{we} = u_w - u_{s,min} \tag{2.14}$$

On the basis of the particle size distribution, the specific surface area of the particles (A_S), which is the solid surface area per unit volume of particles could be determined. The water film thickness (WFT) is then calculated using Equation (2.15).

$$\mathrm{WFT} = \frac{u_{we}}{A_s} \tag{2.15}$$

The same methodic could be applied to determine the paste film thickness based on the minimum void ratio ($u_{a,min}$) of the aggregates larger than 75 μm, since the particles smaller than that belong to the paste phase. Accordingly, the excess paste ratio (u_{pe}), which is the ratio of the volume of excess paste to the solid volume of the aggregate particles > 75 μm, could be determined using Equation (2.16)

$$u_{pe} = u_p - u_{a,min} \tag{2.16}$$

Similarly, the paste film thickness (PFT) is calculated by considering the specific surface area (A_a) of the aggregates > 75 μm using Equation (2.17).

$$\mathrm{PFT} = \frac{u_{pe}}{A_a} \tag{2.17}$$

The mortar film thickness is determined based on the minimum void ratio ($u_{c,min}$) of the aggregates larger than 1.2 mm, since it was observed that even under segregation, the particles smaller than that tend to stay with the paste. Accordingly, the excess mortar ratio (u_{me}), which is the ratio of the volume of excess mortar to the solid volume of the aggregate particles > 1.2 mm, could be determined using Equation (2.18)

$$u_{me} = u_m - u_{c,min} \tag{2.18}$$

The mortar film thickness (MFT) is calculated by considering the specific surface area (A_c) of the aggregates > 1.2 mm using Equation (2.19).

$$\mathrm{MFT} = \frac{u_{me}}{A_c} \tag{2.19}$$

The authors conducted elaborate investigations with regard to the flowability, filling / passing ability and segregation properties on different concrete compositions to analyze the adaptability of the three tier design approach [64]. They suggested that the WFT has the most significant influence on the flowability properties. Generally, the mixtures didn't show any noticeable flowability when the WFT values were less than 0.14 μm. After exceeding this point, however, the flow spread increases drastically, regardless of the paste or mortar amount. The effect of the WFT on the flow spread starts to diminish as its values get much higher. The authors also observed the occurrence of serious segregation for WFT values higher than 0.4 μm. The reverse is true with regard to the flow time, which drastically increases at higher values of WFT. The paste and mortar film thicknesses (PFT and MFT) have also noticeable influence on the flow spread and the flow rate. However, after studying the

combined effects of the WFT, PFT and MFT using a multi-variable regression, the authors concluded that at a constant WFT, the PFT significantly influences the flow spread and the flow rate in comparison to the MFT. In fact, the flow rate decreased with increasing MFT; see Figure 2.21.

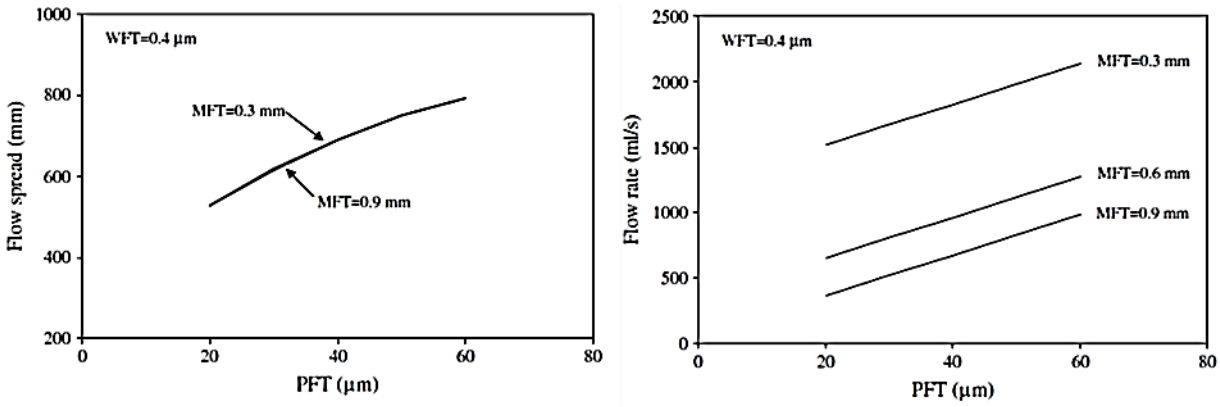

Figure 2.21: Combined effects of WFT, PFT and MFT on the flow spread (left) and flow rate (right) [64]

They also observed no noticeable filling height or passing ability for WFT less than 0.14 μm. Then with increasing WFT, the filling height also increases up to a certain WFT of ca. 0.3 – 0.4 μm. Further increase in the WFT beyond this point has negligible effect on the filling height. Generally, the sieve segregation index (SSI) increases with increasing WFT regardless of the PFT or the MFT. This increment becomes more drastic at higher WFT values, even exceeding the SSI limit of 20% beyond which the likelihood for the occurrence of segregation is much higher.

The combined effects of WFT, PFT and MFT on the filling ability and sieve segregation properties are illustrated in Figure 2.22.

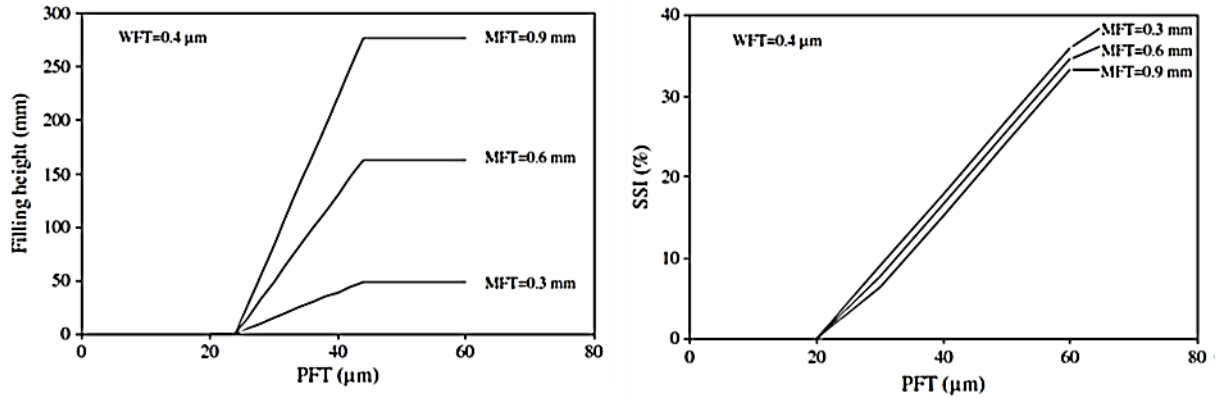

Figure 2.22: Combined effects of WFT, PFT and MFT on the filling height (left) and sieve segregation index (right) [64].

It was observed that for a WFT within the range of 0.3 μm to 0.6 μm, both the PFT and MFT have pronounced effects on the filling ability than the WFT, with the MFT having a greater role at higher PFT values. The SSI is more dependent on the PFT than the MFT for a constant WFT. For the design of HPC, the authors suggested a WFT within the range of 0.14 – 0.4 μm in order to guarantee good flowability and stability against segregation. They also advocated for choosing the highest water – cementitious materials ratio (w/cm) that fulfills the minimum strength requirement. The WFT could then be determined based on the chosen w/cm-ratio and the packing density of the cementitious materials. If the calculated WFT is less than 0.14 μm, then packing density of the cementitious materials need to be increased by optimizing the particle size distribution or even adding finer powders. If the calculated WFT is greater than 0.4 μm, then the w/cm value should be decreased. Moreover, a PFT within the range of 20 μm to 60 μm should be chosen in order to satisfy both the flowability and cohesiveness requirements. The influence of the MFT with regard to the flowability is considered to be negligible. The required PFT for a specific flow spread can also be determined based on the WFT as shown in Figure 2.21 (left). The SSI of the mixtures that designed on the basis of the WFT and PFT should be controlled in order to ensure sufficient cohesiveness. If need be the WFT and PFT have to be adjusted. Finally, the MFT should be chosen in such a way that its negative effect on the flow rate could be minimized while exploiting its positive effect on the filling height. If the HPC in question is a SCC, the authors suggest minimum values of MFT of 0.9 mm and PFT of 44 μm in order to satisfy the stringent requirements of the filling height. On the contrary, for a normal pumpable HPC, the flow rate is the decisive factor and hence the least possible MFT should be adopted. The PFT for the desired flow rate could then be determined based on the MFT as shown in Figure 2.22 (right).

Midorikawa et al. have determined the excess paste layer thickness based on a “water layer model”, which was applied in the investigation of a self-compacting. Depending on the sand and powder content in the mortar, the water and superplasticizer contents were adjusted, so that a relatively constant slump flow of 245 ± 10 mm could be attained. For a known excess paste volume, which was determined by subtracting the voids paste demand from the total paste volume in the mix, the thickness of the excess paste layer was determined using Equation (2.20).

$$V_{ps} = \sum_{i}^{n} \frac{1}{6} \pi \left\{ \left[D_i + 2t_{ps} \right]^3 \pm {D_i}^3 \right\} n_i \qquad (2.20)$$

Where: V_{ps} = excess paste volume, D_i = diameter of particle of size i (from sieves or laser diffraction), t_{ps} = thickness of excess paste and n_i = number of particle of size i

The results of his investigations have indicated that regardless of the type of sand (Ar, Br or Cr), with increasing sand content, both the water - powder ratio (V_w/V_p) and the superplasticizer content should be increased in order to attain the same slump flow. Moreover, the thickness of the excess paste depends on the aggregate size and the paste composition. The larger the aggregate size and the smaller the V_w/V_p ratio, the higher is the required paste film thickness of the mortar [66].

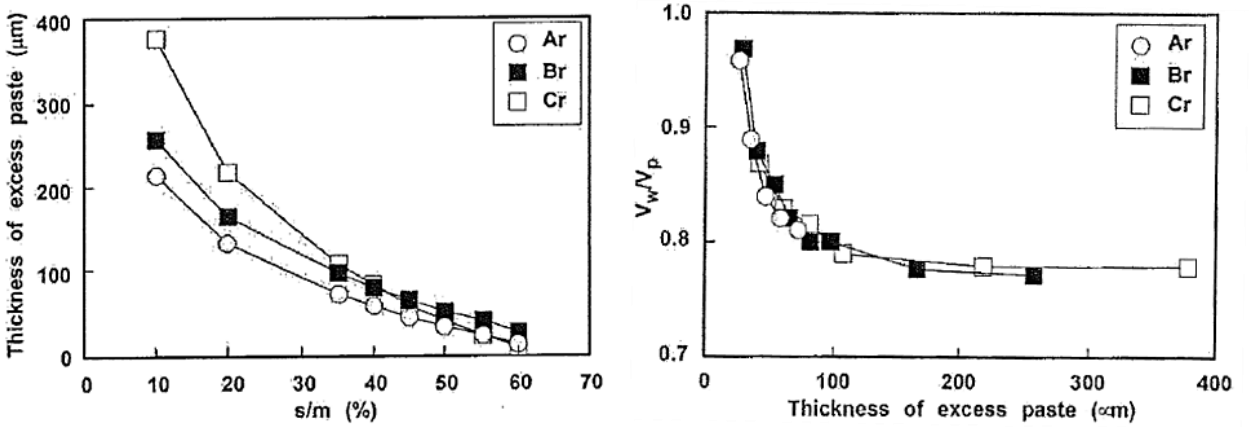

Figure 2.23: Influence of grain size (left) and water – powder ratio (right) on the layer thickness of the excess paste [66]

2.3 Stability of concrete

2.3.1 Definition

According to ACI, stability is the flow of fresh concrete without applied forces and is measured by bleeding and segregation characteristics. Bleeding is defined as the undesirable separation of water from an unstable mortar while segregation is the instability of the mixture caused by a weak matrix that is not capable of retaining the individual aggregate particles in a homogeneous dispersion. Wet segregation or sedimentation occurs when the paste is not capable of holding the aggregate particles in position. Dry segregation describes the crumbly nature of the mixture as a result of the lack of enough water or paste [67].

2.3.2 Bleeding

In principle, the aggregates in a concrete are dispersed by the paste while the fines in the paste are dispersed by water. As such, there is an inherent risk of settlement due to the difference in density between the suspending medium and the suspended particles. The settlement of the fines in the paste results in the accumulation of water at the top, which is usually referred to as bleeding. However, this bleeding process do not continue endlessly, since an equilibrium is reached at some point between the

combined forces of electrostatic repulsion and disjoining pressure of adsorbed water on the one hand and the unbuoyed weight of the particles on the other. This settlement can also come to an end when the dormant period is over at which point the hydration products are interconnected thereby blocking the downward movement of particles [14]. Accordingly, in a sufficiently deep sample of paste, three zones could be delineated in relation to the bleeding/settlement process.

- Zone I: a zone of clear water at the top.
- Zone II: a zone of uniformly density equal to the original density after mixing.
- Zone III: a compressed zone in with a gradient of density which increases towards the bottom.

The emergence of a clear water at the top, despite the high viscous drag on the finest particles, indicate that the finest particles remain attached to the coarser particles by interparticle forces and settle together with them. If the depth of the sample is not high enough, zone II converges with zone III and ultimately only zones I and III could be observed [44]. A conceptual model of such a zoning during the bleeding and settlement processes was also presented by Peng and Jacobsen who made use of hydrostatic pressure test in order to determine changes in the solid fraction (ϕ) over time and sample depth. The change in solid fraction could then be used as a basis to analyze the bleeding and settlement process [68].

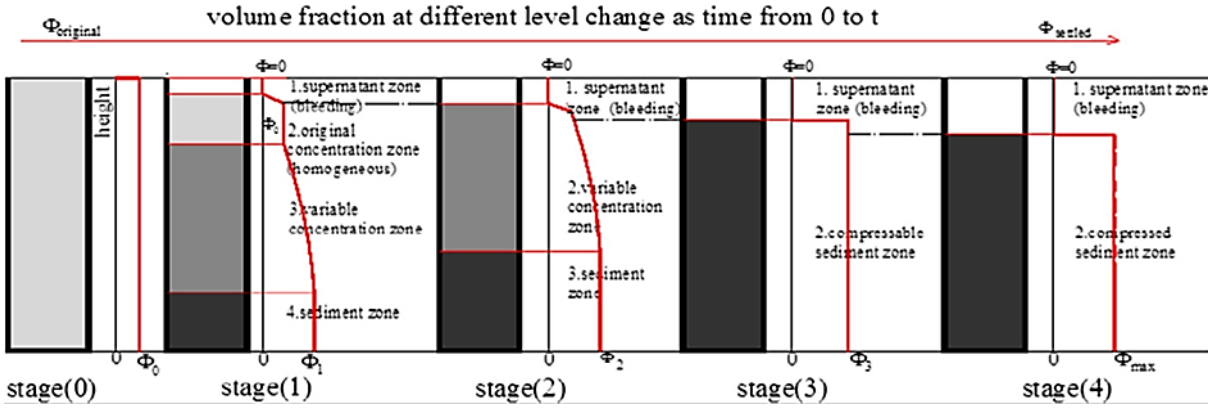

Figure 2.24: Conceptual model for sedimentation and bleeding [68]

Initially, the bleeding occurs at a constant rate and starts to decline as time goes on, see Figure 2.25, left [69]. There is also a critical sample height below which a direct proportionality exists between the rate of bleeding and the depth of the sample during the dormant period. Power's investigation on a paste composition with a w/c-ratio of 0.42 has shown that this is true for sample heights of up to ca. 12 cm. This direct proportionality, however, doesn't hold anymore for greater sample heights, since the time interval within which the constant rate of settlement occurs exceeds the dormant period and the stiffening process begins. The correlation between the total amount of

bleeding and the sample height is also dependent on the bleeding capacity of the mixture. Comparison by Schiessl and Schmidt on two mortar compositions with the same w/c-ratio and cement type but different types of sand indicated a direct correlation between the total bleeding and the sample height for the mixture with higher bleeding capacity, while no reliable trend could be observed for the mix with lower bleeding capacity [70].

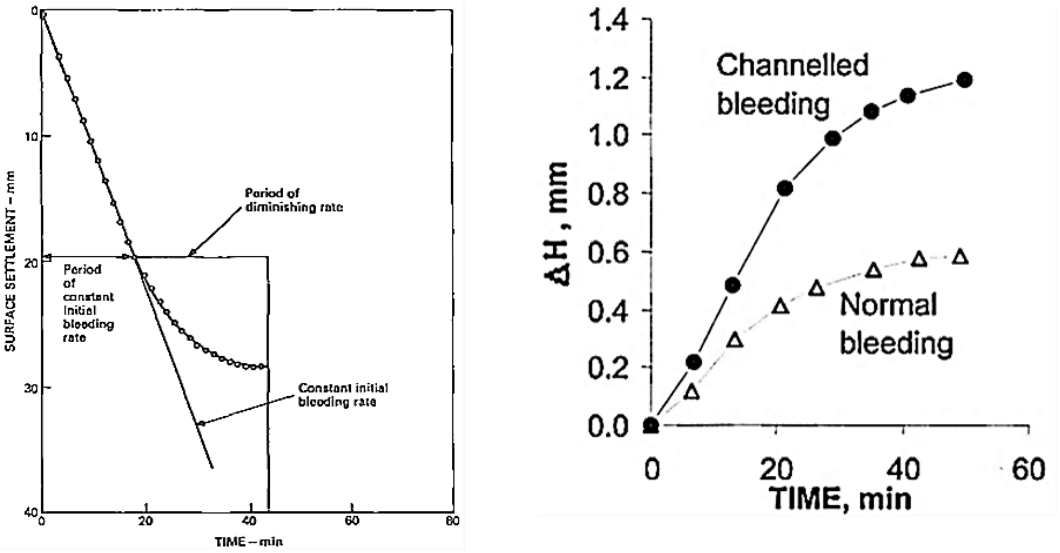

Figure 2.25: Bleeding curve (left) [69] and bleeding rate (right) [71]

Bleeding could occur in a form of uniform seepage over the whole surface of the concrete or through localized channels through which fine particles that are mixed with water could get transported to the top. The damaged caused by channel bleeding is reported to be more adverse in comparison to normal bleeding, see Figure 2.25, right [71].

According to Loh et al., channel bleeding is characterized by a distinct sudden increase in the rate of surface settlement, which he determined using the float method. Its occurrence is dependent upon the height, density and level of dilution of the sample. The results of his investigation have shown the occurrence of channel bleeding in paste compositions with volumetric w/c-ratios of 1.6, while the mixtures with w/c-ratios of 1.4 and 2.0 showed normal bleeding. As the density of the paste and the mortar samples increased, the critical height for the commencement of the channel bleeding also increased. This is contrary to the findings from other authors who reported the increasing chances for the creation of channeled bleeding with increasing w/c-ratios [72]. The authors also suggested that the mechanism through which channeled bleeding occurs in both paste and mortar compositions to be similar [73]. Tan et al. attributed normal bleeding and channel bleeding to consolidation and sedimentation processes respectively [74].

Power suggested that the bleeding rate of concrete depends on the coefficient of permeability of the paste it contains and on the paste content. Assuming that aggregates are added to the paste without changing the paste composition, one could expect reduction in the bleeding capacity just proportional to the volume of paste displaced by the aggregates, except perhaps the increment as a result of the weight of the aggregate. This theoretical assumption suggests that the bleeding capacity in a concrete (ΔH) should at least be equivalent to the bleeding capacity of the paste (ΔH_p); also $\Delta H / (P/V) \geq \Delta H_p$. However, the results of his investigation have not confirmed this assumption, except for concrete compositions that are rich in paste volume. This is an indirect proof regarding the effect of particle interference during the settlement process. The bleeding rate decreases when aggregates are added to the paste, since particle interference is imminent. However, for the same w/c-ratio, the velocity of water movement in the interstitial spaces in concrete are much greater than it would be in the paste alone, since the concrete has a higher hydraulic head in comparison to the pure paste by virtue of its greater unit weight [14]. To this end, investigations by Yim et al. have shown that concrete has a faster settlement as a result of its higher permeability, when compared to the mortar contained in it [75].

It should also be noted that the observance of no bleeding at the surface doesn't necessarily imply an inherent stability of the concrete. The microscopical investigation by Newmann on a concrete composition has revealed the accumulation of water under the aggregates, even though no noticeable surface bleeding was observed; see Figure 2.26 [17]. This phenomenon is referred to as "internal bleeding", which comes about when the bleeding water stays trapped under the aggregates. Internal bleeding could have adverse consequences with regard to the strength and durability properties of the hardened concrete.

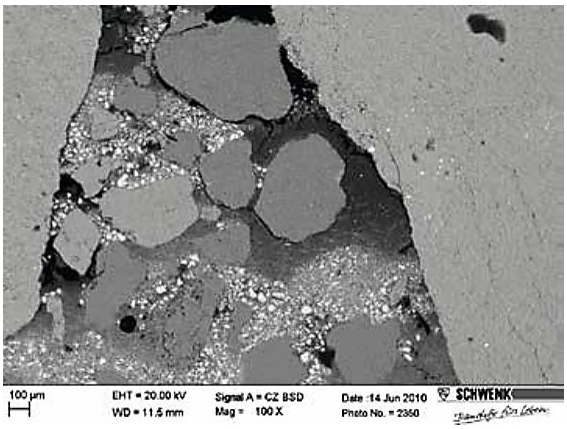

Figure 2.26: Internal bleeding of concrete [17]

The results of the investigations by Soshiroda showed a smaller tensile strength for concrete specimen that were recovered in the direction of casting (t_S) in comparison to those recovered perpendicular to the direction of casting (t_R), also $t_S < t_R$. He also compared the projected surface area of the aggregates from the fracture surfaces after the splitting tensile tests in order to compare the bond strength between the aggregates and the surrounding mortar. For the concrete specimen recovered perpendicular to the direction of casting, the projected surface areas of the aggregates had a 50% - 50% distribution for the upper and lower fractured faces. However, for the concrete specimen recovered in the direction of casting, there was 70% - 30% distribution of the projected surface areas of the aggregates for the upper and lower fractured surfaces. This implies the existence of a weaker bond under the aggregates which is caused by the internal bleeding in the direction of casting. This was proven by the investigation results which showed a decreasing t_S / t_R ratio with increasing bleeding capacity of mortar [76].

2.3.3 Factor affecting the bleeding of concrete

For a certain cement paste composition, the bleeding rate and capacity is directly related to the water content and the specific surface area of the cements. The investigations conducted by Powers on cement pastes had shown that for a constant w/c-ratio, the rate of bleeding increases with decreasing specific surface area of the cement particles. Moreover, for the same particle size, the rate of bleeding increased with increasing w/c-ratio by virtue of the increased distance between the particles and the reduced cohesiveness [14]. Similar findings are also reported in the AiF research report which dealt with different concrete technological aspects that influence the quality of concrete floors for industrial and open space applications [77]. Steinour has reported that the rate and capacity of bleeding is lower for cements exhibiting faster initial chemical reactivity, since such cements are able to produce a larger amount of calcium sulphoaluminate (CSA) that ultimately produces ettringite. Generally, cements containing higher amount of tricalcium aluminate (C_3A) tend to show relatively low rates and amount of bleeding [78]. Concretes made of portland composite cements (CEM II) and blast furnace cements (CEM III), by virtue of their fineness, exhibit lower bleeding tendency in comparison with those made with portland cement (CEM I). Similarly, the bleeding capacity decreases with an increasing strength class of a cement, which can also be attributed to the increased fineness of the cement particles [77].

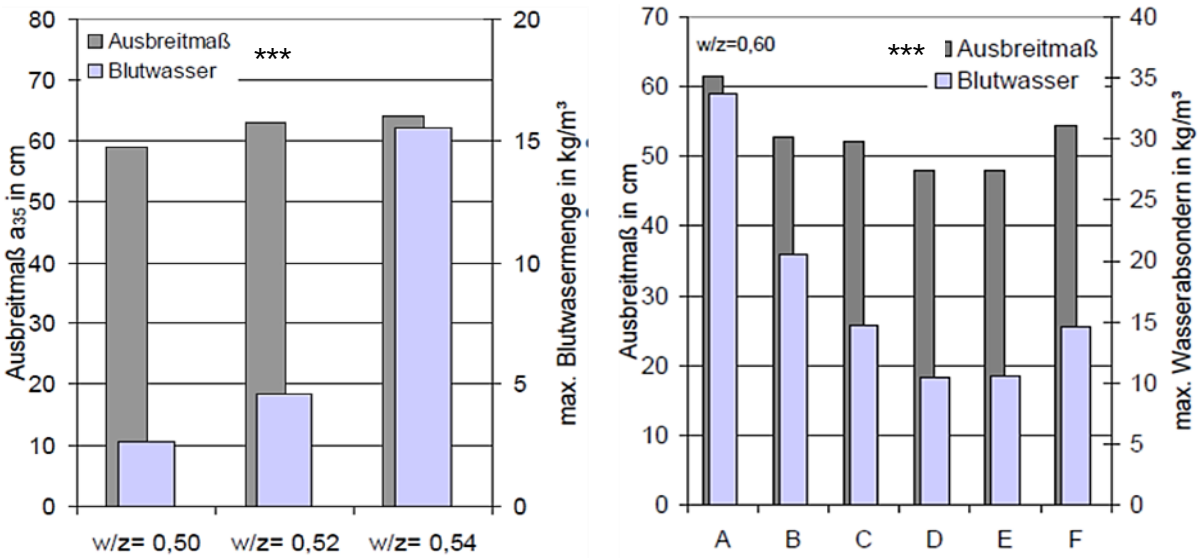

Figure 2.27: Effects of w/c-ratio (left)* and different cement types (right)** on bleeding [77]

* cement = 340 kg/m³; CEM II/A-LL 32.5 R; agg. gradation A16/B16; SP: MNS 1.4 M.-% of cement

** A: CEM I 32.5 R; B: CEM I 32.5 R; C: CEM II/A-LL 32.5 R; D: CEM II/B-S 42.5 N; E: CEM II/B-M (S-LL) 32.5 R; F: CEM III/A 42.5 (cement = 340 kg/m³; w/c = 0.60; agg. gradation A16/B16)

*** Ausbreitmaß = slump flow (cm) and Blutwasser = bleeding capacity (kg/m^3)

The paste content also has a direct influence on the bleeding properties of concrete. This fact is stated in the project report by Siewert et al. regarding the concrete technological aspects that were addressed during the construction of the Lobdeburg tunnel construction in Germany. Here, the effect of the paste content on the bleeding capacity was investigated using 16 concrete compositions, all having a w/c-ratio of 0.5, that were made of 4 types cement (all having strength class of 32.5 R) each composed at 4 different levels of paste content (267, 295, 323 and 351 l/m^3). The results of their investigation revealed that regardless of the type of cement, the bleeding capacity increased with increasing paste content. Moreover, the smaller the specific surface area of the cement, the higher was the measure bleeding capacity, regardless of the paste content, confirming the observation by Powers [79]. Spanka et al. reported the results of their investigations with regard to the effect of naphthalene sulphonates based SP on the bleeding capacity of cement pastes. They observed the separation of pure water from the paste mixtures even with lower SP contents of up to 0.5%, which lies under the SP saturation point. However, for a SP content of 1.5 %, which is beyond the SP saturation point, very fine particles were suspended in the bleeding water indicating the complete dispersion of the fines in the mix. Moreover, the dried specimen of the mixtures made with only water as well as a

SP contents below the saturation point showed a homogeneous distribution of the solid particles. On the contrary, the dried specimen of the mixtures with SP contents beyond the saturation point showed a clear distinction between the upper and lower part. It should be noted that the definitions of saturation point of SP in this investigation is somewhat ambiguous. It was assumed that the upper white zone, which made up ca. 20% vol. of the specimen, is composed of very light fine particles that took longer time to settle while the lower dark zone was made of the heavier particles which settled much faster. Moreover, the authors asserted that the upper white zone do not have any appreciable strength which they attributed to the lack of a proper hydration process, the minimal strength being a mere product of the surface forces [80].

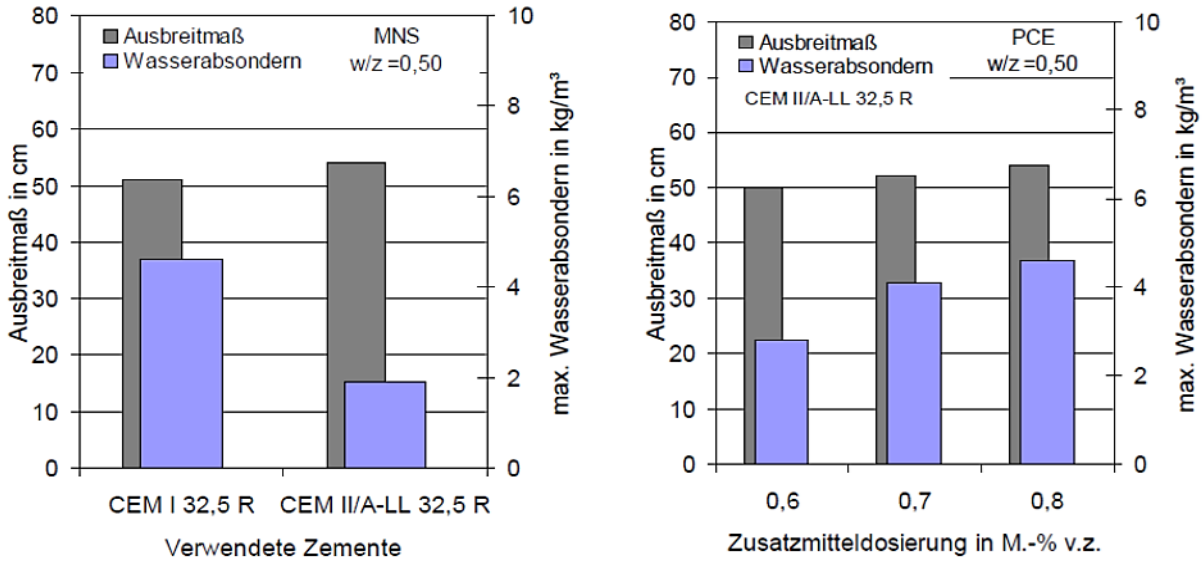

Figure 2.28: Effects of SP type* and content** on bleeding [77]

* SP type: MNS (left) and PCE (right)

** SP content: 0.6, 0.7 and 0.8 M.-% of cement

***cement = 340 kg/m³; w/c = 0.5; agg. gradation A16/B16, total fines content = 340 kg/m^3

The effects of the type and content of SP on the bleeding capacity is also reported in [77] and [81]. A repeated dosage of superplasticizers that aims to control the loss of slump and overdosage of superplasticizers could also result into bleeding and segregation of the mix [82].

The hydrostatic pressure based investigation by Peng and Jacobsen on limestone slurries and cement pastes with and without SP revealed that even at a relatively low concentration of 0.3%, the SP could significantly prolong the sedimentation process, by virtue of the dispersion of the finest particles. The sedimentation process took even longer time when the SP content was increased from 0.3% to 1.2%. Moreover,

the total amount of bleeding measured after 4 h increased from 3 mm to 11 mm as a result of the addition of 0.6% of SP to the reference paste. A diluted layer of water containing fines could also be observed at the top when only SP was added to the reference mixture, as observe by Spanka et al. On the contrary, a pure water layer was observed when SP and VMA were added together as shown in Figure 2.29 [68].

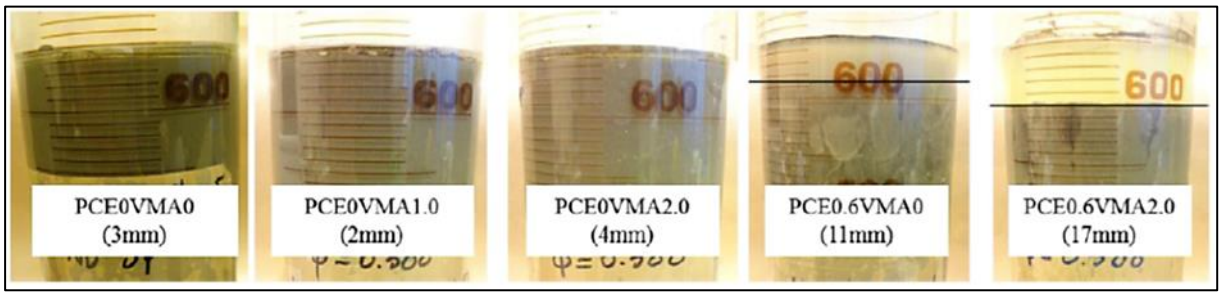

Figure 2.29: Bleeding of paste at 4h (ϕ = 0.388) with SP and VMA combinations [68]

Viscosity modifying agents (VMA) have generally a positive influence with regard to reducing the bleeding and segregation in concrete [83]. To this end, Khayat and Guizani conducted experimental investigation with regard to the effect of VMA on the stability of concrete. The investigation with regard to the bleeding and settlement was conducted using concrete columns with a height of 70 cm by altering the dosage of the VMA, w/c-ratio ranging from 0.5 to 0.7 and slump values of 140 mm – 220 mm. They also investigated the effects of sample depth on the bleeding and settlement by using concrete columns with a height of 50-, 70- and 110 cm. They observed that the addition of VMA has enhanced the resistance to bleeding, settlement and segregation regardless of the w/c-ratio, the slump, casting height and mode of consolidation [84]. A reduction in the bleeding capacity as a result of the addition of VMA is also reported in [70]. However, the positive effects of VMA on the stability depend on its type and dosage. The investigations by Lachemia et al. with regard to the effect of different VMAs on the resistance to loss of material in a wash-out test had given mixed results. While the noble polysaccharide-based VMAs he used for his investigations generally improved the resistance to washing, the one which was commercially available (with unknown compositions) was found to be ineffective or gave results that were even worse than the reference mixtures [39]. Vahdani et al. also reported an increase in bleeding as a result of the usage of VMA [85]. Peng and Jacobsen also got unexpected results in which the total bleeding increased with the addition of VMA. This increment was also much pronounced when the VMA was used in combination with SP; see Figure 2.29 [68].

Another chemical admixture that has influence on the bleeding capacity is air entraining agent (AEA). The addition of AEA stabilizes the air bubbles in a concrete which are created during the mixing process by the formation of vortex and the three

dimensional screen effects of the aggregates which traps the air bubbles. The air bubbles make the concrete more cohesive and create a quasi-structure with the solids through the process of adsorption. They also have a buoyancy effect which acts against the settlement of the solid particles and a surface area which binds the water molecules. Since the air bubbles occupy a relatively larger volume in the paste, the air-water interface formed by them could also hinder the flow of water. The combination of these effects results in the reduction of the bleeding rate and capacity when AEA is added to a concrete [14] [86].

With regard to the effects of aggregates on bleeding, Powers reported that the aggregate grading do not have any significant effect on the rate of bleeding, even with a discrepancy in the specific surface area of about 45% which resulted from the change in aggregate gradation. This might be due to the significantly smaller contribution of the aggregates in comparison to the fines in terms of the total specific surface area of the solids in a concrete [14]. However, the aggregate type seems to have an influence on bleeding. The investigations by Yim et al. in which they replaced natural coarse aggregates with glass beads, while maintaining the other components in the concrete the same, has revealed an increase in the external bleeding and a reduction in the internal bleeding. This might be attributed to the spherical shape of the beads and the resulting small specific surface area, which generally lead to increased bleeding capacity [75].

In the AiF study, the gradation and the fines content were altered in order to investigate their effect on the bleeding capacity and sedimentation. As can be seen in Figure 2.30, increasing the fines content just by an amount of 10 – 20 kg/m^3 resulted in a significant reduction of the bleeding capacity (compare S3 and S5 as well as S9 and S7). Moreover, for the same fines content, the increment in the 0 / 2 mm size fraction from ca. 32% (S3) to ca. 39% (S4) has led to a reduction in the bleeding capacity (compare S3 and S4 both with MNS content of 2.4%). However, the same cannot be said for the S7 and S4 mixtures where the 0/2 mm fraction increased from ca. 26% to ca. 39% respectively. The results of the two S4 mixes with the respective SP contents of 2.1% and 2.4% confirms the fact that an increase in the SP content could lead to an increased bleeding capacity. In fact, the comparison between the S4 and S8 mixtures reveals the decisive role the SP plays with regard to the stability of concrete. Here, the S8 mixture (SP = 1.8%) while having lesser fines content of 10 kg/m^3 still shows a higher resistance against bleeding in comparison to the S4 mixture (SP = 2.1%), the reason being the lesser amount of SP in the S8 mixture. Besides, concretes with smaller maximum size show lesser tendency to bleed [77].

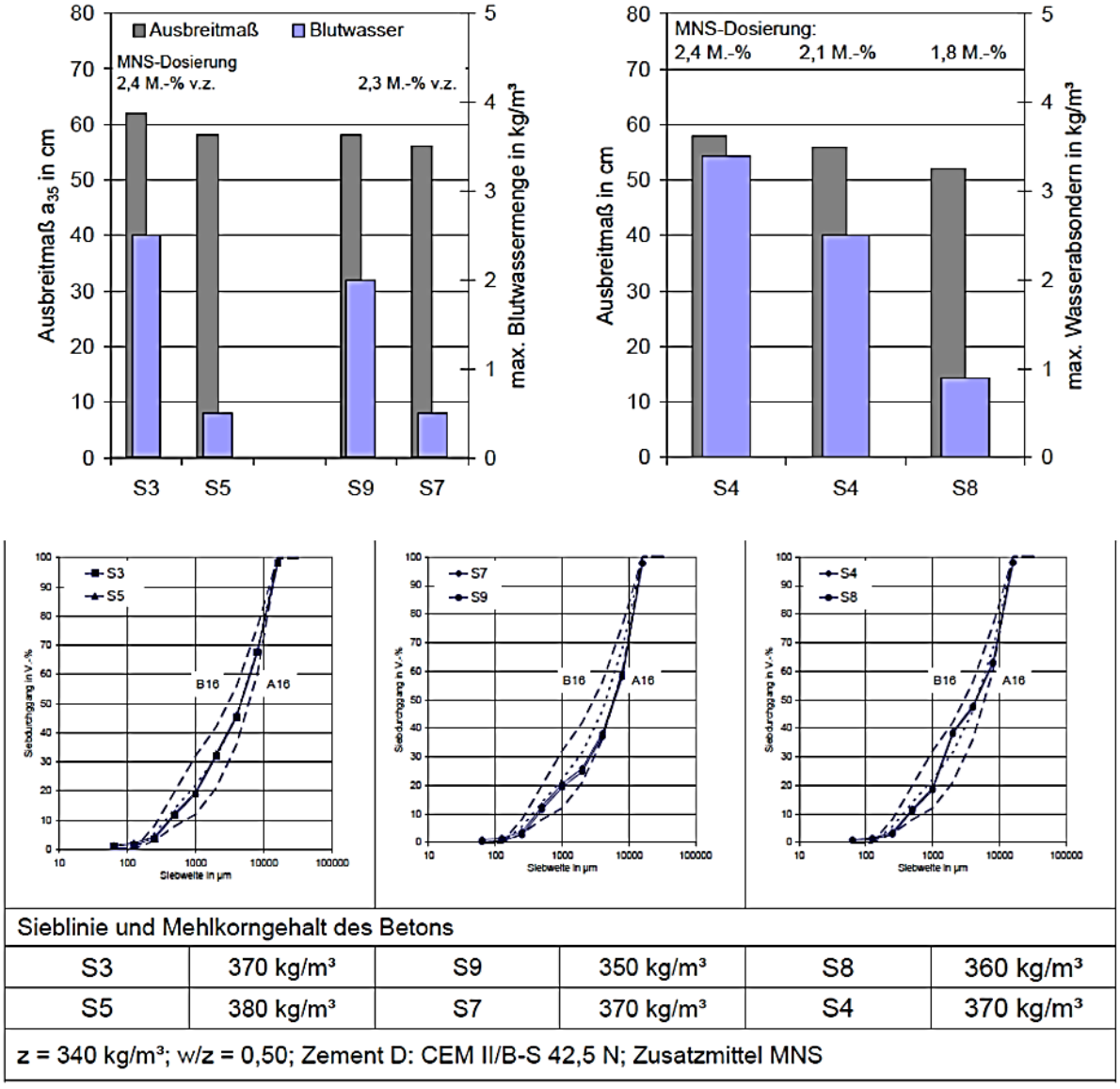

Sieblinie und Mehlkorngehalt des Betons					
S3	370 kg/m³	S9	350 kg/m³	S8	360 kg/m³
S5	380 kg/m³	S7	370 kg/m³	S4	370 kg/m³
z = 340 kg/m³; w/z = 0,50; Zement D: CEM II/B-S 42,5 N; Zusatzmittel MNS					

Figure 2.30: Effects of aggregate gradation and fines content on bleeding [77]

The addition of mineral admixtures generally improves the resistance against bleeding [87] [88]. The substitution of cement by finely pulverized natural pozzolans results in the reduction of the bleeding capacity, which is caused by the interference of the flow channels by the pulverized particles and the formation of microporous structures by the pozzolanic materials. However, it should be noted that the natural pozzolans generally do have a higher water demand when compared to industrial pozzolanic by-products such as fly ash [89]. The usage of fly ash in concrete could also be seen as beneficial in reducing bleeding as long as the concrete is proportioned properly [90] [91]. Usually, fly ash has a lower water demand when compared to cement and as a result a simple substitution of cement with fly ash, while maintaining a constant volume of water, could potentially lead to an increased bleeding [92]. Thus, pertaining to the facts that fly ash has a relatively spherical

shape and smooth surface as well as good filling ability by virtue of the improved grading and the higher volume it occupies when compared to the same mass of cement, a concrete containing fly ash require lesser amount of water for the same flowability [93]. Blast furnace slag and condensed silica fume are usually ground to a higher fineness when compared to cement and thus, a lower bleeding capacity could be expected due to their higher specific surface area and the blocking of the pores in fresh concrete [94] [95] [96] [97].

2.3.4 Segregation

The other phenomenon which designates the instability in concrete, in addition to bleeding, is the occurrence of separation of the liquid and solid phases or segregation of the large particles. If the segregation takes place when the concrete is at rest, it is referred to as static segregation. The segregation which is caused by external forces such as vibration energy or pumping pressure is referred to as dynamic segregation. Regardless of the type of segregation, it could be stated that any concrete technological factor that could potentially weaken the overall resistance of a concrete increase the risk of segregation. On the other hand, concrete technological factors that could potentially enhance the loading side would also increase the risk of segregation. This is mainly manifested by the size or weight of the aggregates that should be kept in position.

2.3.5 Static segregation of concrete

Detail studies of static segregation in concrete were conducted in relation to the application of self-compacting concrete (SCC). This is because SCC, unlike conventional concrete, is not exposed to vibration after being casted and as such, the segregation process, especially the sedimentation of the coarse aggregates, could be treated as a quasi-static segregation phenomenon.

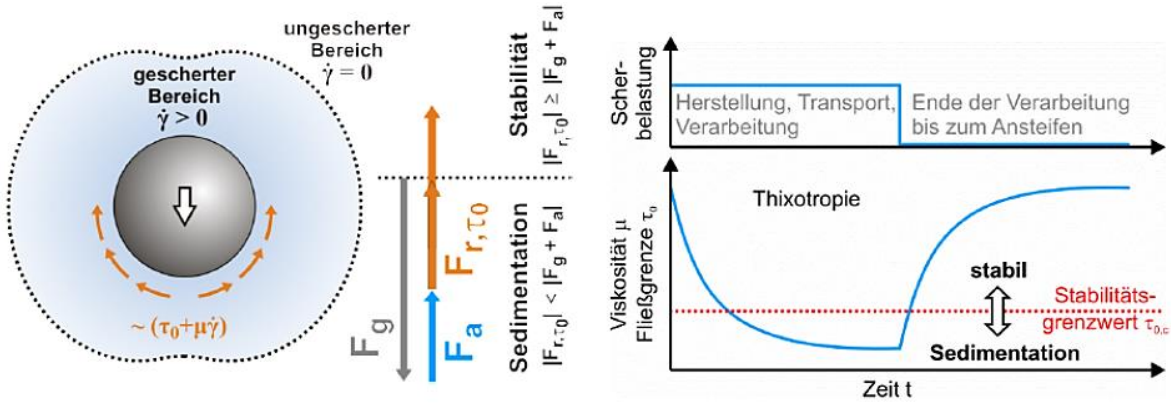

Figure 2.31: Equilibrium of forces during particle sedimentation (left) and changes in rheological properties in concrete processing (right) [98]

When an ideal solid sphere undergoes a quasi-static segregation in a suspending medium, a small envelope of fluid whose shape depends on the yield stress of the medium is formed around the sphere [99]. The movement of the aggregate caused by its self-weight is counter balanced by the buoyancy and friction along its surface. The friction in a non-Newtonian fluid is composed of the static yield stress and the dynamic plastic viscosity. As such, the stability of the aggregate in a SCC at rest basically depends on the yield stress of the suspending medium. The viscosity, on the other hand, determines the settlement velocity of the aggregate [98] [100] [101].

Based on the Navier-Stoke function, the drag force (F_R) acting on the particle can be determined using Equation (2.21).

$$F_R = 3\pi \cdot d \cdot v_s \cdot \eta \tag{2.21}$$

Where: F_r = drag force; d = diameter of the particle; v_s = settlement velocity and η = dynamic viscosity

Assuming that the fluid layer in the immediate vicinity of the sphere, which is sheared as a result of the downward movement of the sphere, has a thickness of d, the shear rate ($\dot{\gamma}$) could be determined using Equation (2.22).

$$\dot{\gamma} = \frac{v_s}{d} \tag{2.22}$$

For a non-Newtonian fluid, the apparent viscosity (η) of the fluid after its yield stress (τ_0) is exceeded could be calculated by considering the plastic viscosity (μ) as shown in Equation (2.23).

$$\eta = \frac{\tau}{\dot{\gamma}} = \frac{\tau_0}{\dot{\gamma}} + \mu \tag{2.23}$$

By substituting Equations (2.22) and (2.23) into Equation (2.21), one gets Equation (2.24).

$$F_R = 3\pi \cdot d^2 \cdot (\tau_0 + \mu \cdot \dot{\gamma}) = 3\pi \cdot d^2 \cdot \tau_0 + 3\pi \cdot d \cdot \mu \cdot v_s \tag{2.24}$$

At equilibrium, the net driving force ($F_N = F_G + F_B$), which is a combination of the gravitational force (F_G) and buoyant force (F_B), should be equivalent to the drag force (F_R).

$$F_N = \frac{\pi \cdot d^3}{6} \cdot (\rho_s - \rho_f)g \tag{2.25}$$

Where: ρ_s = specific gravity of sphere; ρ_f =specific gravity of suspending fluid and g = gravitational acceleration

By equating Equations (2.24) and (2.25), one can define a simplified stability criterion as depicted in Equation (2.27)

$$F_R = F_N \Rightarrow 3\pi \cdot d^2 \cdot \tau_0 + 3\pi \cdot d \cdot \mu \cdot v_s = \frac{\pi \cdot d^3}{6} \cdot (\rho_s - \rho_f)g \tag{2.26}$$

As long as the friction component is equal to or greater than the net bouncy component, the sphere remains in position ($v_s = 0$).

$$\tau_0 \geq \frac{d}{18} \cdot (\rho_s - \rho_f)g \tag{2.27}$$

By introducing a constant K which stands for the particle concentration and shape, the stability criterion could be generally defined as stated in Equation (2.28).

$$\tau_0 \geq \frac{d}{6K} \cdot (\rho_s - \rho_f)g \tag{2.28}$$

That means, for an ideal sphere suspended in a fluid satisfying the Stoke's law, K assumes the value of three (K = 3). This is also confirmed by experimental and numerical investigations [98] [101]. It could also be stipulated that for a given Bingham fluid with a yield stress τ_o, there is a critical particle diameter (d_c) below which the stability criterion is fulfilled and the sphere remains in position. Accordingly, particles with diameters greater than d_c would surely settle through the suspension.

$$d_c \leq \frac{6K \cdot \tau_0}{(\rho_s - \rho_f)g} \tag{2.29}$$

If a suspension contains more than one particle, there would be certain interference between the shear zones and the solid fraction of the particles starts to play a role on the stability properties, usually in a positive way. Bethmont et al. introduced an equivalent term $K_{lattice}$, which is higher than K stated in Equation (2.29) in case of a positive group effects of the particles in relation to the stability and vice versa. $K_{lattice}$ considers the interaction between the particles by adopting a supplementary dimensionless parameter which is the ratio of diameter to spacing of particles (d/a). In other words, $K_{lattice}$ considers the solid fraction (ϕ) in the suspending medium. Accordingly, considering the case of one particle remaining in position ($v_s = 0$) in a matrix with a solid fraction (ϕ), the drag force as stated in Equation (2.24) could be modified as in Equation (2.45) [102].

$$F_R = K_{lattice}(\phi) \cdot \pi \cdot d^2 \cdot \tau_0 \tag{2.30}$$

If a group of identical spheres are added to an infinite Newtonian fluid mass, they move at the same speed and the distance between them, which depends on the

particle concentration, remains constant. However, in a finite fluid mass restricted by the geometry of the container or formwork, the spheres stop moving and start to get accumulated after reaching a certain boundary. The concentration could assume a maximum value for a random loose packing of identical spheres of ϕ_{max} = 0.74. According to Yang et al., when two similar spheres of diameter (d) approach each other at speed (v_s) in a Newtonian fluid of viscosity (η) , the dynamic force (F_D) acting on one sphere when the gap between them (δ) is at its minimum, could be determined using Equation (2.31) [103].

$$F_D = \frac{3\pi \cdot d^2 \cdot v_s \cdot \eta}{4\delta} \tag{2.31}$$

The concentration of solids in a non-Newtonian fluid is, however, influenced by the rheological properties of the fluid, which usually limit the tendency for segregation. Thus, by substituting the apparent viscosity of a Bingham fluid in Equation (2.31), one gets Equation (2.32).

$$F_D = \frac{3\pi \cdot d^2 \cdot v_s \cdot \left(\frac{\tau_0}{\dot{\gamma}} + \mu\right)}{4\delta} = \frac{3\pi \cdot d^2 \cdot v_s \cdot \mu}{4\delta} + \frac{3\pi \cdot d^3 \cdot \tau_0}{4\delta} \tag{2.32}$$

The spheres stop moving towards one another (v_s = 0) when the net driving force (F_N = F_G + F_B) gets lower than a certain critical value (F_C), which could be determined using Equation (2.33)

$$F_C = \frac{3\pi \cdot d^3 \cdot \tau_0}{4\delta} \tag{2.33}$$

Just at stoppage, the net driving force (F_N) as stated in Equation (2.25) is equal to the critical force (F_C) from Equation (2.33) and by equating them, one could determine the minimum gap between the two particles as shown in Equation (2.34).

$$\delta = \frac{9\tau_0}{\pi(\rho_s - \rho_f)g} \tag{2.34}$$

A factor M could be introduced if the spheres are of different diameters. De Larrard has correlated the minimum gap (δ) between the spheres with the solid fraction (ϕ) and the maximum solid fraction (ϕ^*) of the spheres as shown in Equation (2.35).

$$\delta = d\left[\left(\frac{\phi}{\phi^*}\right)^{\frac{-1}{3}} - 1\right] \tag{2.35}$$

The stability criterion, which encompasses the yield stress, the particle size, the solid fraction and the density difference, could be deemed to be fulfilled based on the

derivation as stated in Equation (2.36), which is determined by combining Equation (2.34) with Equation (2.35).

$$\phi \geq \phi^{*}\left(\frac{9\tau_0}{\pi \cdot d \cdot (\rho_s - \rho_f)g} + 1\right)^{-3} \tag{2.36}$$

On the basis of such theoretical consideration, three cases of stability could be stipulated.

i. Particles having a diameter less than the critical diameter (d_c) → the particles do not settle, since the stress generated by the net force is not enough to overcome the yield stress of the suspending fluid.
ii. Particles have a diameter larger than the critical diameter (d_c) → the particles do not settle, since the final predicted solid fraction in the segregated zone is lesser than the solid fraction in the mix-design.
iii. Particles have a diameter larger than the critical diameter (d_c) → the particles do settle, since the final predicted solid fraction in the segregated zone is higher than the solid fraction in the mix-design.

Based on the two criteria stated in Equations (2.29) and (2.36), it could be concluded that the segregation tendency of a solid particle in a Bingham suspension depends on the yield stress of the suspending medium and not on the plastic viscosity. The plastic viscosity takes a role in determining the settlement velocity of the particles in case the yield stress is exceeded and the particles indeed start to settle [101].

Considering the group effect on the static segregation in SVB, the sedimentation of the larger particles is hindered by the lattice effect generated by the smaller particles that are stably suspended in the mortar or the paste phase as shown in Figure 2.32. However, if the smaller particles themselves undergo a settlement, they eventually contribute more to the instability rather than the stability of the system. As such, the lattice effect can act either on the side of loading as part of the driving force (F_N) or the resistive force (F_R) [98].

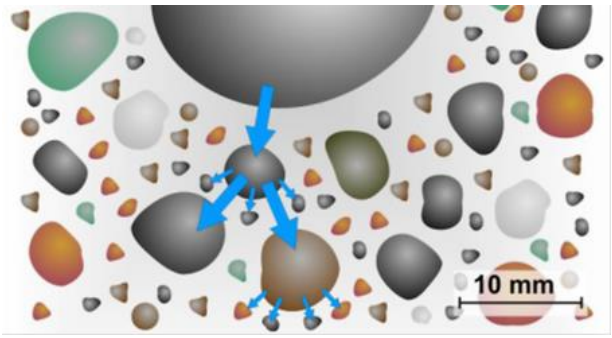

Figure 2.32: The lattice effect [98]

Accordingly, one can device coupled optimization strategies that aim at minimizing the risk of segregation by reducing the effects of the driving force (i and ii) and maximization of the resistance (iii).

i. Reduction of the maximum grain size (d_{max})
ii. Using aggregates with smaller specific gravity (ρ_s)
iii. Maximizing the density of the paste or mortar matrix (ρ_f)

Lowke suggested three cases of stability based on five scenarios (A – E) in which the static segregation of coarse particles in SVB could be correlated with the rheological properties of the suspending mortar, see Figure 2.33.

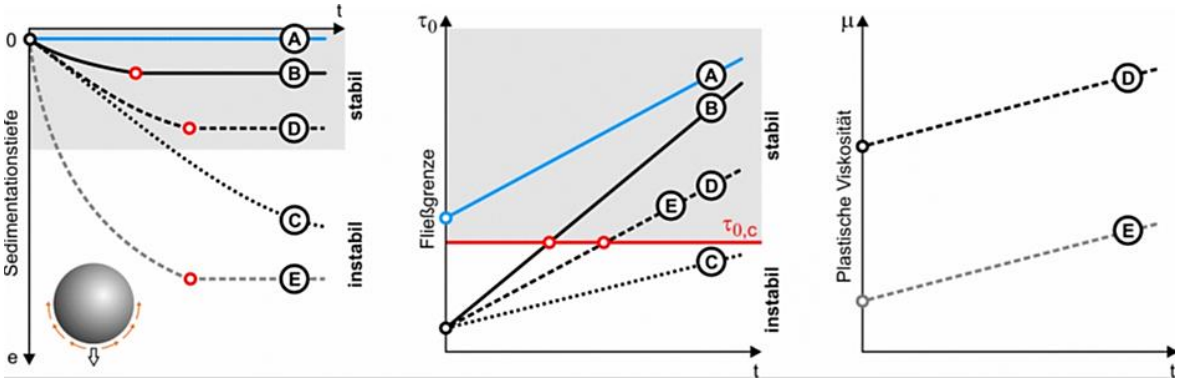

Figure 2.33: Scenarios between static segregation of coarse aggregates and rheological properties [98]

I. Stability based on yield stress: Case A

If the yield stress (τ_o) of the mortar is higher than the critical yield stress ($\tau_{o,c}$), there is no settlement of coarse aggregate.

II. Stability based on thixotropy: Cases B or C

If the yield stress (τ_o) is lower than the critical yield stress ($\tau_{o,c}$), the coarse aggregates begin to settle. However, as in case (B), if the mortar has a strong thixotropic behavior, the inter-particle structures could be built up instantly and the yield stress exceeds the critical yield stress in a relatively short time span, thereby limiting excessive aggregate settlement. On the contrary, if the mortar has a weak thixotropic behavior as in case C, the time span for the recovery would be too long and a substantial segregation would take place.

III. Stability based on thixotropy and Viscosity: Cases D or E

A higher viscosity would reduce the settlement velocity. Thus, during the time span when the yield stress (τ_o) remains lower than the critical yield stress ($\tau_{o,c}$), the extent of the settlement could be reduced which helps mixtures with a relatively weaker

thixotropic properties to remain stable as in case D. On the contrary, a mortar exhibiting a lower viscosity and a lower thixotropy would lead to significant sedimentation of coarse aggregates as in case E.

2.3.6 Dynamic segregation of concrete

Spangenberg et al. treated the dynamic segregation in concrete as a flow induced particle migration in which the mechanisms could be classified as shear induced, gravity induced and granular blocking processes [104]. The shear induced particle migration takes place when the particles migrate from zones of high shear rate, e.g. near the pipe wall during pumping, towards zones of lower shear rate, e.g. center of pipe during pumping. The migration of particles is the result of two fluxes induced by gradients of the collision rate and the viscosity. The collision flux $(\overrightarrow{N_c})$ describes the migration of particles from zones of high number of collisions to zones of lower number of collisions and it is dependent on the gradients in shear rate and in particle concentration. The viscosity flux $(\overrightarrow{N_\eta})$, which is caused by the existence of gradients in the particle concentration, describes the tendency to migrate from higher to lower viscous zones, since during collision; the particle displacement in the lower viscous zones is larger than in the higher ones. That means, the migration of particles caused by the collisions in the highly sheared and/or highly concentrated zones is counterbalanced by the local increase in the suspension viscosity as a consequence of the migration [105] [106] [107].

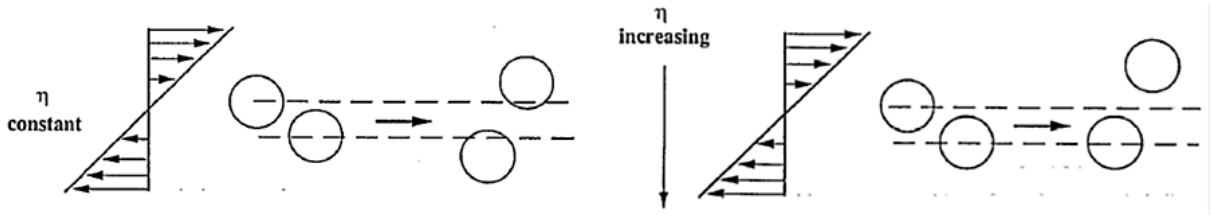

Figure 2.34: Schematic diagrams of two-body collisions with constant viscosity (left) and spatially variable viscosity (right) [106]

For a Couette device, for example, the values of $(\overrightarrow{N_c})$ and $(\overrightarrow{N_\eta})$ could be determined using Equations (2.37) and (2.38), see [106].

$$\overrightarrow{N_c} = -K_c \cdot a^2 \cdot (\phi^2 \cdot \nabla\dot{\gamma} + \phi \cdot \dot{\gamma} \cdot \nabla\phi) \tag{2.37}$$

$$\overrightarrow{N_\eta} = -K_\eta \cdot \frac{a^2 \cdot \dot{\gamma} \cdot \phi^2}{\eta} \cdot \frac{d\eta}{d\phi} \nabla\phi \tag{2.38}$$

Where: K_c and K_η = empirical parameters; a = the particle radius; $\dot{\gamma}$= the shear rate; ϕ = volume fraction of particles and η = viscosity

As can be seen from the Equations, $(\overrightarrow{N_c})$ and $(\overrightarrow{N_\eta})$, and thus the particle migration is highly dependent on the particle diameter, the solid concentration and the resulting viscosity. Thus, the aggregate size and the viscosity of the suspending medium are the most relevant factors governing the dynamic segregation and sedimentation processes, which occur during a high shear-related concrete handling processes such as vibration and pumping.

The characteristic time for the migration, which is the duration from flow start to stop in slump flow measurement for example or the time interval the concrete stays in the pipe during pumping, can be estimated using Equation (2.39), see [107].

$$\tau_c \sim \left(\frac{H}{a}\right)^2 \frac{1}{\dot{\gamma}} \tag{2.39}$$

Where: H = length scale of the flow, i.e., the smallest dimension of the element to be cast or the radius of the pipe for pumping

Spangenberg et al. suggested that the shear induced migration shall stop before the local particle volume fraction reaches the so called random loose packing (RLP), since the shear induced particle migration reaches a point of equilibrium as the viscosity of the adjacent zone increases. By taking the quotient of random loose packing (ϕ_L = 0.5) and random close packing (ϕ_C = 0.64) of mono sized spheres as reported in [108], i.e. (ϕ_L/ϕ_C = 0.8), they suggested that the highest variation in particle volume fraction due to shear induced particle migration after an infinite time to be lower than $\Delta\phi^{\mathrm{shear}}$ as determined using Equation (2.40).

$$\Delta\phi^{\mathrm{shear}} = \phi_0 \left(1 - \frac{\phi_0}{0.8\phi_C}\right) \tag{2.40}$$

Where: ϕ_0 = the mix design particle volume fraction and ϕ_C = particle volume fraction at random close packing

Moreover, on the basis of experimental results which showed that the particle volume fraction profile reaches a steady state after a certain critical deformation γ_c of the suspension, the characteristic time (T_c^{shear}) when the shear induced particle immigration reaches its full extent could be estimated using Equation (2.41).

$$T_c^{\mathrm{shear}} = \frac{H^2}{10 \cdot a^2 \cdot \phi^2 \cdot \dot{\gamma}} \tag{2.41}$$

Gravity induced particle migration is a case in which the particle migration occurs when a concrete, which is stable at rest, is flowing or being cast. The migration occurs when the stress caused by gravity is higher than the yield stress of the

material while it is flowing. In such cases, the additional stress caused by a density difference between an aggregate and the suspending medium, even when it is lower than the yield stress of the suspending medium, would cause a local flow around the aggregate. It can be assume that, similar to the shear induced particle migration, the gravity induced migration also comes to an end before the local particle volume fraction reaches a random loose packing state. Thus, the highest variation in particle volume fraction due to the gravity induced migration could also be estimated using Equation (2.40), see [104]. The characteristic time ($T_c^{gravity}$) associated with the gravity induced particle migration could be estimated by using Equation (2.42).

$$T_c^{\text{gravity}} \cong \frac{18 \cdot \mu_0 \, H}{g \cdot \Delta\rho \cdot a^2} \tag{2.42}$$

Where: μ_0 = the apparent viscosity of the suspending medium and $\Delta\rho$ = the density difference between the aggregates and the suspending medium

A granular blocking induced segregation is relevant only in cases where the coarsest particle sizes are not compatible with the cross sections through which they must pass, such as the gap between reinforcement bars or the diameter of the pipe. The chances for the occurrence of granular blocking generally increases with the number of particles crossing the hindrance, their volume fraction and the ratio between the size of the particles and the opening size of the hindrance. As such, the granular blocking segregation mainly depends on the geometrical conditions and not on the rheological properties of the suspending phase. When it occurs, however, the granular blocking segregation dominates both the shear induced and gravity induced segregations, since the particle concentration could reach and potentially exceed the random loose packing state around the vicinity of the hindrances. Another geometrically dependent segregation phenomenon is induced by the wall effect. Because of geometrical conditions, only the center of particles with diameters lesser than **a** could be found at a distance lesser than 0.5.**a** from the wall. This implies an inherent segregation where the coarse particles volume fraction increases from zero at the wall to the bulk volume fraction at a distance **a**. Assuming an average value of the bulk volume fraction in the depleted zone of $\phi_0/2$, the variation in coarse particle volume fraction due to the wall effect for a concrete flow with thickness H could be estimated using Equation (2.43), see [104].

$$\Delta\phi^{\text{wall effect}} \cong \frac{\phi_0 \cdot a}{2H} \tag{2.43}$$

By focusing on the migration process involving the coarse aggregate, Spangenberg et al. studied the induced segregation phenomena based on the following concrete casting or testing processes.

i. Slump test of conventional concrete
ii. Slump flow test for SCC
iii. Typical concrete rheometer test
iv. Typical casting and pumping processes

The authors suggested that while the shear induced and wall effect induced particle migrations are dominant during pumping process, the gravity induced particle migration governs the typical industrial casting process. Moreover, the slump flow was marginally affected by flow induced particle migration (shear and gravity induced), while the slump was not affected by it. The concrete rheometer was influenced by both the flow induced and the wall effect induced particle migrations. Moreover, the results of the model casting studies clearly showed the increased dynamic segregation potential with increasing particle size (7 mm > 5 mm > 2mm). However, the application of these findings to a real concrete is not trivial. Since the volume fraction of coarse aggregates in concrete is much higher than the 10% used in the study, the local rheological properties and thus the particle migration or settlement process are strongly affected by the local volume fraction of aggregates.

Table 2.3: Origins and magnitude of average particles volume fraction variations due to flow induced particles migration in typical concrete flows and in the model casting

Flow	**Shear induced heterogeneities**	**Gravity induced heterogeneities**	**Wall effect induced heterogeneities**
Slump	Negligible	Negligible	1–2%
Slump flow	of the order of 1%	of the order of 1%	3–5%
Rheometer	3–5%	1–2%	1–2%
Casting	Negligible	5–10%	of the order of 1%
Pumping	3–5%	Negligible	3–5%
Model casting (beads dia. = 2 mm)	Negligible	1%	Negligible
Model casting (beads dia. = 5 mm)	Negligible	5%	Negligible
Model casting (beads dia. = 7 mm)	Negligible	7%	of the order of 1%

Hence, in a follow-up study, Spangenberg et al. particularly investigated the patterns of gravity induced aggregate migration during casting of fluid concretes using two beams of length, width and height of 4 m x 0.2 m x 0.3 m, see Figure 2.35 – one for

concrete investigation in fresh state and one in a hardened state. The induced horizontal heterogeneity was determined by determining the aggregate contents belonging to the 6/11 mm and 11/16 mm size fractions after washing the mixture from the nine sub-sections along the beam. The vertical heterogeneity was determined by cutting the second beam and by applying image analysis of the relative concentration of 11/16 mm size fractions in the upper, middle and lower zones [109].

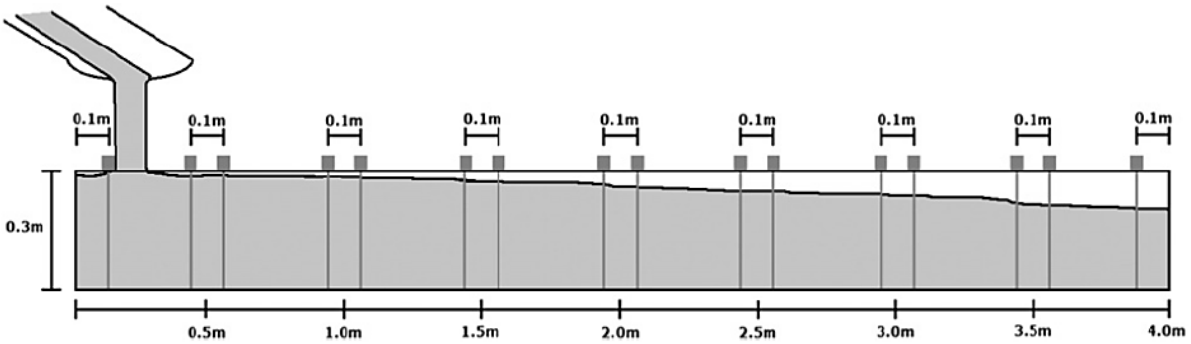

Figure 2.35: Beam geometry and casting [109]

The characteristic time for the shear induced particle migration determined using Equation (2.41) was found to be much higher than even the duration of casting and hence, the migration of the coarsest particles could not be shear induced. However, determination of the characteristic time for gravity induced particle immigration ($T_c^{gravity}$) using Equation (2.42) for the 6/11 mm and the 11/16 mm aggregate size fractions were found to be 200 s and 50 s respectively. These values were in compliance with the duration of the casting process. Moreover, the aggregate volume for the 6/11 mm and 11/16 mm aggregate size fractions decreased by 20% and 65% respectively revealing the effects of larger aggregate size on the sedimentation behavior. Thus, the authors concluded that the migration process is induced by gravity. However, it is to be noted that these determinations were made by assuming a complete shearing of the concrete and a constant apparent viscosity (μ_0) of 10 Pa.s, without any consideration for the non-Newtonian nature of concrete. In reality, only part of the concrete is sheared when it is being casted and there are zones where the stress is lower or higher than the yield stress. The casting process can be considered to be composed of two flow regimes, namely the transient flow regime in which the concrete propagates horizontally until it reaches the end of the formwork followed by a steady flow regime where the boundary conditions remain almost the same after the concrete has reached the end of the formwork, see Figure 2.36. In the transient flow regime, the particle concentration profile decreases with increasing distance from the point of casting. Moreover, the horizontal heterogeneity is affected by the completion between the casting velocity and the settlement velocity of the

aggregates. Increasing the casting velocity for shear thinning material such as concrete could lead to a reduced viscosity and shorter duration for particle migration, thereby minimizing the horizontal heterogeneity.

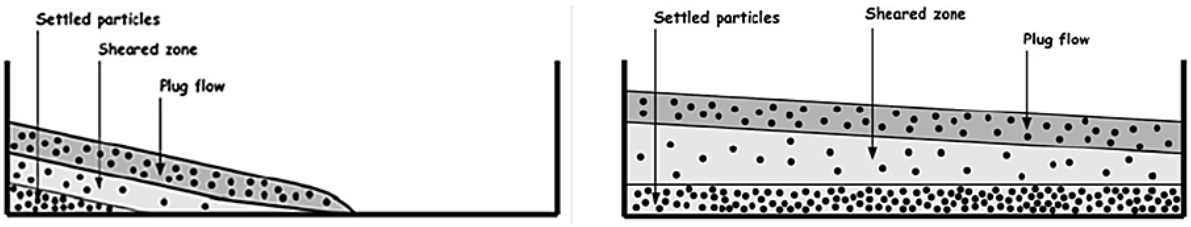

Figure 2.36: Multilayer structure in a transient (left) and steady (right) flow [109]

In the steady flow regime, the particle concentration profile could be assumed to be constant along the length of the beam and thus, only a gravity-induced vertical heterogeneity, which increases with time, could be observed. As such, for flowable concretes such as SCC and a limited beam length, the transient flow regime could be neglected and a constant particle concentration along the beam could be expected. This assumption was confirmed for two-third of the beam as shown in Figure 2.35. However, in the last third, a reduction in the aggregate concentration and the number of visible aggregates at the surface were observed. This was attributed to the change in the rheological properties of the concrete caused by the particle migration in which the zones from which the aggregates migrated became more fluid exhibiting lower yield stress and viscosity while the opposite holds true for the zones to which the aggregates migrated. Thus, the change in aggregate profile is a complex coupled effect of particle migration and local rheological properties.

In both regimes, the stress increases linearly from zero at the free surface to a maximum value at the bottom interface. However, since the stress equilibrium during the whole flow process should be maintained, there should be a zone just below the free surface where the material is not sheared and flows as a plug. In this zone, the stress caused by the flow is lower than the yield stress. If the material is stable at rest, no gravity induced segregation would take place. Hence, the aggregate volume fraction is the same as the one in the mix design. Under the top layer, there exists a zone where the concrete is sheared and the aggregates could settle at a certain velocity depending on the suspending medium viscosity, size of the particles and the density difference between the particle and the suspending medium. The volume fraction of the settled particles at the bottom of the formwork could get as high as the random loose packing state. It is the combination of these phenomena during the casting process that result in a vertical heterogeneity, i.e. a non-uniform aggregate distribution profile, which is usually observed in a hardened concrete.

Shen et al. has applied a flow trough with a width, height and length of 0.15 x 0.15 x 1.8 m in order to investigate the dynamic segregation of SCC during casting. By determining the aggregate content at the discharge point and at the end point of the flow trough (by washing out the mix on a 4.8 mm sieve), he calculated the dynamic segregation index (DSI) as shown in Equation (2.44) [110].

$$DSI = \frac{(CA1 - CA2)}{CA1} \tag{2.44}$$

Where: CA1 = weight of coarse aggregate at the discharge point and CA2 = weight of coarse aggregate at the end point

In order to avoid a severe dynamic segregation, the authors proposed limiting the concrete flow distance by introducing a quotient $DSI_{1.8}$ / DSI_{max}. $DSI_{1.8}$ designates the value for the dynamic segregation index at 1.8 m and DSI_{max} could be determined using Equation (2.45), see Figure 2.37.

$$\mathrm{DSI_{max}} = 1 - \frac{1000 - 10\mathrm{c} - \mathrm{b} \cdot \mathrm{e} - \frac{\mathrm{e}}{\mathrm{d}}}{1000 - 10\mathrm{c} - \mathrm{b} \cdot \mathrm{a} - \frac{\mathrm{a}}{\mathrm{d}}} \tag{2.45}$$

Where: a = mass of cementitious material (kg/m^3); b = w/cm ratio; c = air void (%); d = bulk density of cementitious material (g/cc) and e = max. allowable cement content (kg/m^3)

The results of the laboratory investigations had revealed that both the static segregation and the dynamic segregation increased with increasing slump flow. The slump flow was increased from 530 mm up to 790 mm by increasing the amount of SP. It is worth noting that the dynamic segregation occurred at a lower slump flow of 630 mm when compared to the static segregation which was first detected at a slump flow of 790 mm. This clearly indicates the usually neglected but the major role the dynamic segregation could play with in relation to the general stability of concrete.

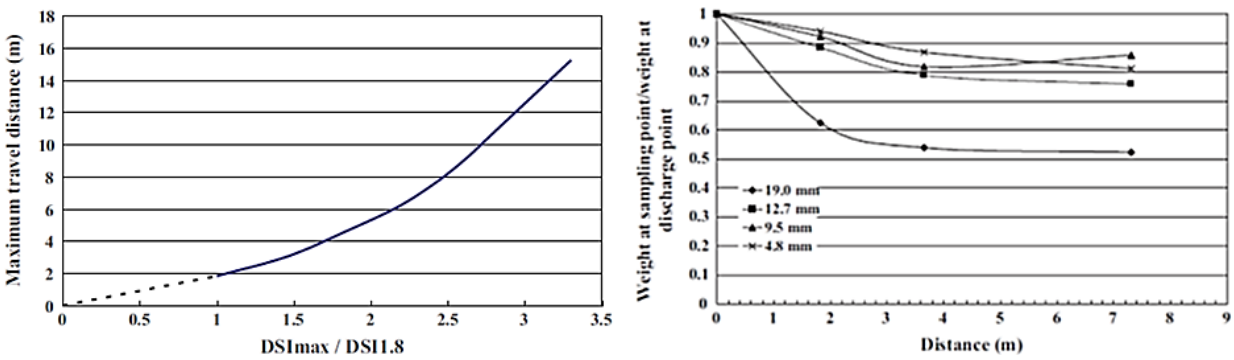

Figure 2.37: Maximum travel distance for SCC (left) and effect of size of coarse aggregate over the travel distance (right) [110]

In a field test during casting of a wall with a respective width, height and length of 1.3 m x 6 m x 9 m the authors observed a continuous reduction of the coarse aggregate content over the flow distance. This phenomenon was much more pronounced with increasing size of aggregates with the 19 mm aggregate, especially, showing a drastic decrement as shown in Figure 2.37 (right). A ca. 20% higher concentration of coarse aggregates in comparison to the one stipulated in the mix design was also observed at the discharge point which could be the result of immediate settlement of the coarse aggregates caused by the higher density and the inertia of flow [110].

Another critical element that has relevance to segregation of concrete is the application of vibration. The primary effects of vibration on concrete according to Bartos are:

i. The breaking-down of the flocculated cement paste by the oscillatory shear stress which turns the paste from a Bingham fluid into a Newtonian fluid of lower viscosity
ii. Motion of the aggregate particles

Accordingly, the combination of these two effects increases the workability or fluidity of the concrete to such an extent that the trapped air rises to the surface and the particles rearrange themselves through motions caused by their self-weight resulting into a higher compaction [111].

Tattersall and Baker applied two-point rheological measurements by simultaneously applying vibration to the concrete in order to study its effects on the rheological properties (flow curve). The flow curves of the unvibrated concrete took a linear form (Bingham law) with a substantial yield stress. The flow curve under the application of vibration, on the other hand, took a shear thinning form (Power law) with a yield stress approaching zero as shown in Figure 2.38, left. However, the authors suggested that at low shear rates such as when concrete flows under its own weight, the concrete behaves as a Newtonian fluid even under the application of vibration [112]. In a further study, the authors applied a vertical pipe apparatus connected to a vibrating table to investigate the effect of vibration on the workability of fresh concrete. They reported that the vibration velocity is the most decisive factor in determining the effectiveness of vibration. To this end, there is a minimum amplitude below which the vibration has no effect and also an upper limiting frequency above which the effectiveness of vibration could be neglected, see Figure 2.38, right [113].

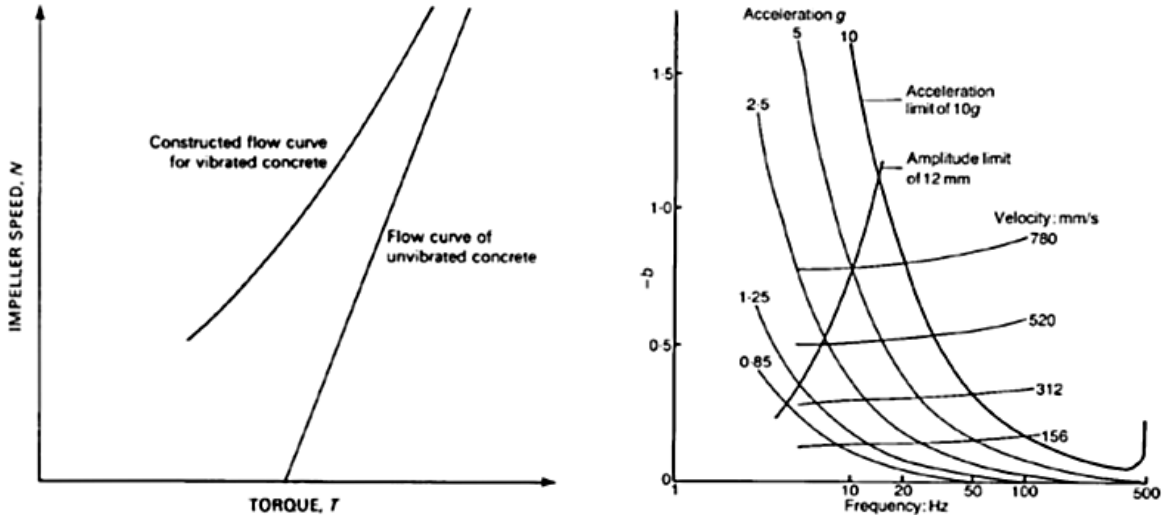

Figure 2.38: Flow curves of vibrated and unvibrated concrete (left) [112] and fluidity (b) as a function of frequency at constant values of acceleration and velocity (right) [113]

Banfill et al. postulated that the shear field generated by the vibration imparts kinetic energy which reduces the yield stress of the concrete to zero by breaking the links between cement particles and/or dispersing particles to such an extent that the interparticle forces become negligible and the concrete acts as a Newtonian liquid. As such, the flow of fresh concrete under vibration is mainly governed by the vibrational velocity and the rheological properties of the unvibrated fresh concrete. The viscosity of vibrated concrete could be assumed to be proportional to the plastic viscosity of the unvibrated concrete. Based on experimental investigations conducted with the help of a vertical pipe apparatus connected to a vibrating table, the authors suggested that the fluidity of concrete (b), i.e. the inverse of viscosity, increases linearly with increasing vibrational velocity (v) until a critical vibrational velocity is reached, beyond which no significant difference could be observed with regard to the fluidity, see Figure 2.39 (left) [114]. A further study with regard to the effectiveness, i.e. the radius of action of vibrators, in correlation with the rheological properties of the concrete has revealed that the radius of action increases with increasing plastic viscosity and with decreasing yield stress as can be seen in Figure 2.39 (right). That means, for practical applications, a concrete with low plastic viscosity required frequent poking with a vibrator, since the radius of action is lower. The radius of action generally increases with increasing vibrator diameter, increasing amplitude as well as increasing frequency. The influence of amplitude and frequency of vibration could also be expressed in terms of the vibrational velocity. At a constant acceleration, increasing the amplitude and decreasing the frequency results in increased vibrational velocity which leads to higher degree of compaction. Increasing the frequency and reducing the amplitude would have the opposite effect [115].

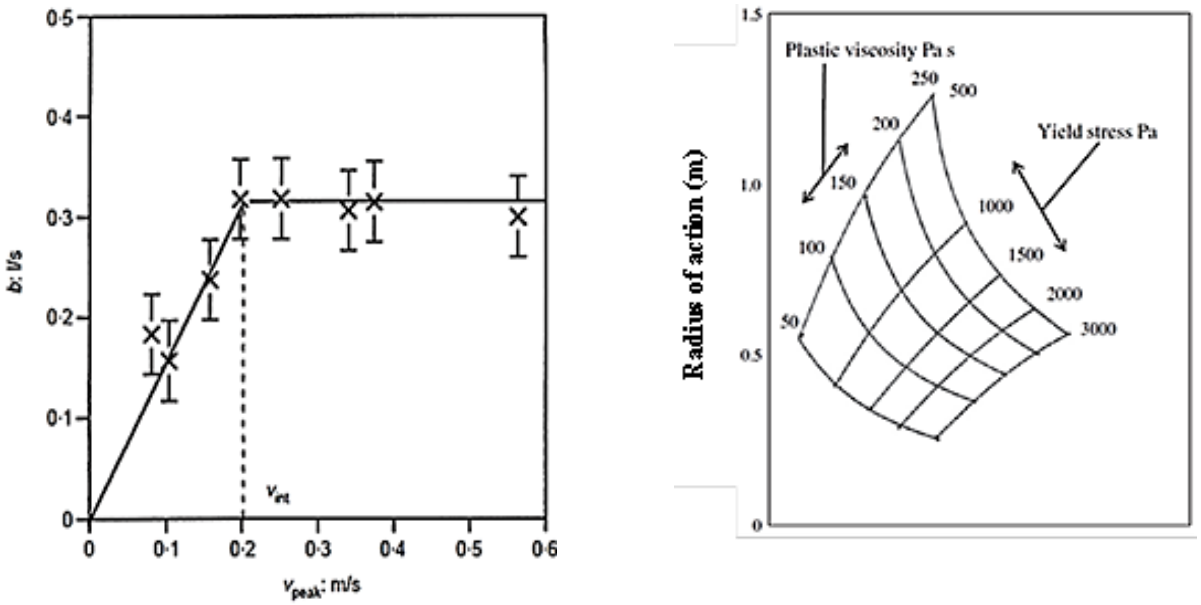

Figure 2.39: Relationship between vibrational velocity and fluidity (left) [114] and radius of action and rheological properties (right) [115]

Experimental investigation was also conducted by Petrou et al. that make use of a real-time imaging of the settlement of spheres made of aluminum (diameter = 22 mm, ρ = 2.7 kg/dm^3) and steel (diameter = 19 mm; ρ = 7.75 kg/dm^3) in a mortar and concrete. Prior to the application of vibration, all the balls remained in positions without any settlement. After the application of vibration, however, all the balls showed different degrees of settlement depending on their mass or position from the source of vibration. The steel ball showed the highest settlement both in mortar and concrete. The aluminum ball near the source of vibration settled to a higher degree in comparison with the aluminum ball that is positioned further away. The effect of the distance from the source is more pronounced in mortar than in concrete. Moreover, the settlement immediately came to a halt after the vibration was stopped. They attributed the occurrence of the settlement during vibration to the reduction in both yield stress and plastic viscosity [116].

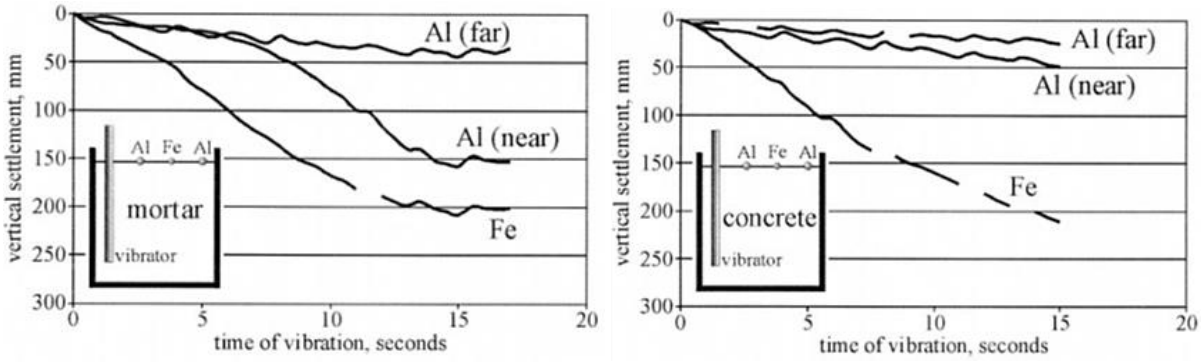

Figure 2.40: Aggregate settlement in mortar (left) and in concrete (right) [116]

Juradin and Krstulovic delivered somewhat a contrary argument in that vibration do not have any effect on the orientation of the fine materials (size < 0.25 mm) in concrete, since insignificant frictional forces would suffice to prevent the self-oscillation of such particles. They also suggested that the collision and rattling of aggregates, which take place immediately after the application of vibration, ceases once a quasi-Newtonian layer is formed around the aggregates. At this point, the aggregates could not come in contact anymore and the oscillation caused by vibration is transmitted to the aggregates only through the fluid phase. As a result, the deformation behavior of the concrete would be improved as the layer around the aggregates has a much lower resistance to movement than the whole mass making it possible for the aggregates to assume the most favourable position and thereby increasing the compaction. Moreover, the results of their investigation using a vibration rheometer have shown that the relative partial amplitude (A2), which represented the effect of vibration, is dependent upon the mass of the suspended particles (m) and the dynamic apparent viscosity of the material (b). To this end, the particles having higher masses than the one, which translates into an equivalence weight to the bouncy force, show a higher degree of oscillation with increasing amplitudes. On the contrary, those particles with lesser masses show negative amplitudes which implicitly prove the upward movement of entrapped air and lighter solids to the surface, see Figure 2.41 [117].

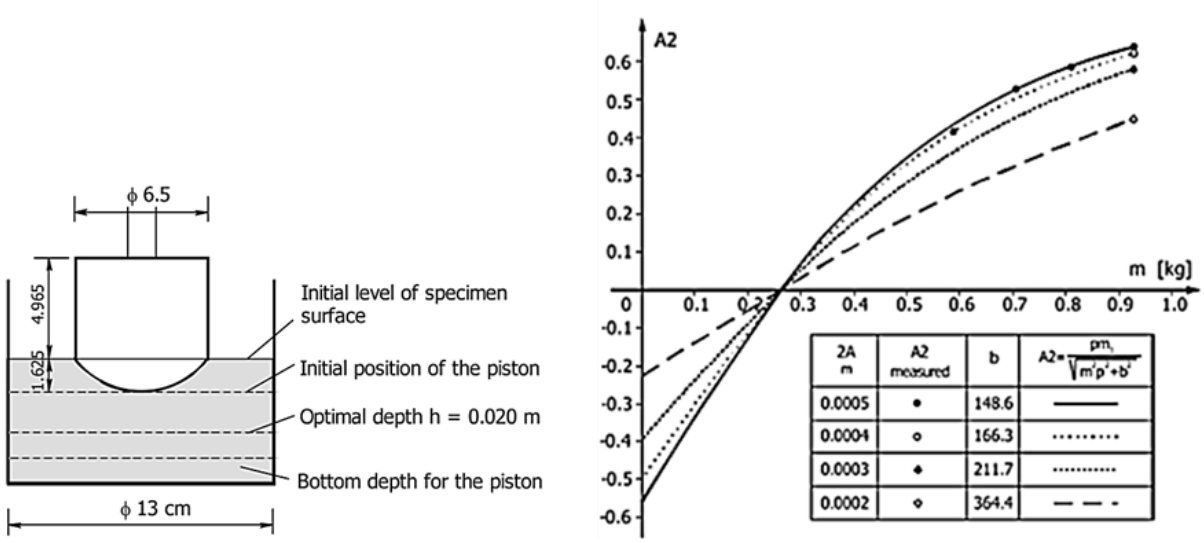

Figure 2.41: Test apparatus (left) and the relationship between mass, dynamic apparent viscosity and relative particle amplitude (right) [117]

Moreover, it was suggested that the actions of vibration on the concrete is a reversible process in that when the vibration stops, an immediate recovery in yield stress could take place and the settlement of the aggregates comes to an end [112].

Petrou et al. have conducted experiments using an irregular shaped stone (147 mm x 92 mm x 57 mm) having a mass of 0.95 kg in a mortar with a slump flow of 155 mm. At first, the stone did not settle when no vibration was applied. However, during the application of vibration, the stone continued to sink and when the vibration was stopped, the stone came immediately to a halt. This was attributed to the immediate recovery of the yield stress after the vibration was stopped [100].

The working mechanisms of vibrators in concrete were the subject study of many researchers. A vibrator transmits its energy to the concrete in the form of waves [118]. The attenuation of vibration, which could be expressed in acceleration, amplitude, radius of action, etc., is very high in the immediate vicinity of the vibrator and decreases very rapidly as the distance from the vibration point increases. An example of the reduction of amplitude [119] and frequency [120] with increasing distance from the source of vibration are shown in Figure 2.42.

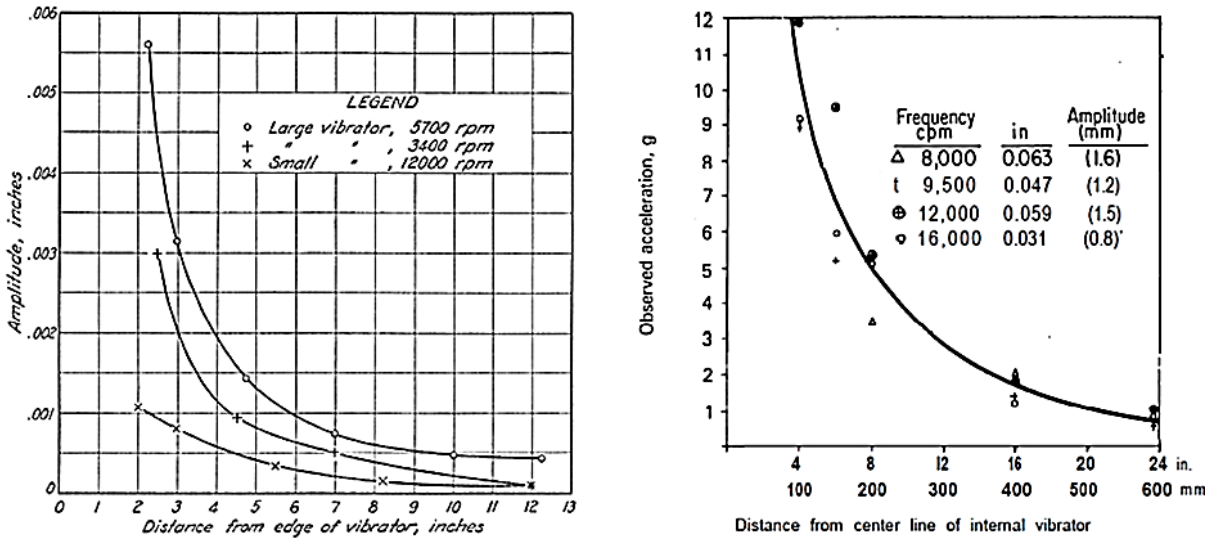

Figure 2.42: Variation of amplitude (left) [119] and acceleration (right) [120] with distance from vibrator

This reduction in vibration attenuation, which generally takes an exponential decay formation, is assumed to be the result of a reduction in energy flux density due to the outward propagation of the waves and the absorption of energy by the concrete. In doing so, the vibration causes first a rapid subsidence of the uncompacted mixture and liquefaction of the mass. This is then followed by de-aeration in which the entrapped air bubbles are forced out and the voids in the concrete substantially decrease. Additional vibration is usually accompanied by further compaction of the mass and escaping of the remaining small bubbles [121]. However, if the duration of vibration is excessively prolonged, it could potentially lead to segregation [67] [118] [122].

Safawi et al. have conducted investigations with regard to the effects of vibration on the segregation potential of flowable concretes having different viscosities as determined by flow time (C-2 > C-3 > C-1) and yield stresses as measured by slump flow (C-3 > C-2 > C-1). While no noticeable settlement could be observed in all mixtures with no vibration, just a 10 s vibration has led to a drastic increment in the aggregates settlement. The segregation coefficient even got almost doubled when the duration of vibration was further increased by 10 s; see Figure 2.43 [123]. Olbert and Moses also made a similar observation with regard to the effect of duration of vibration on aggregate settlement [124].

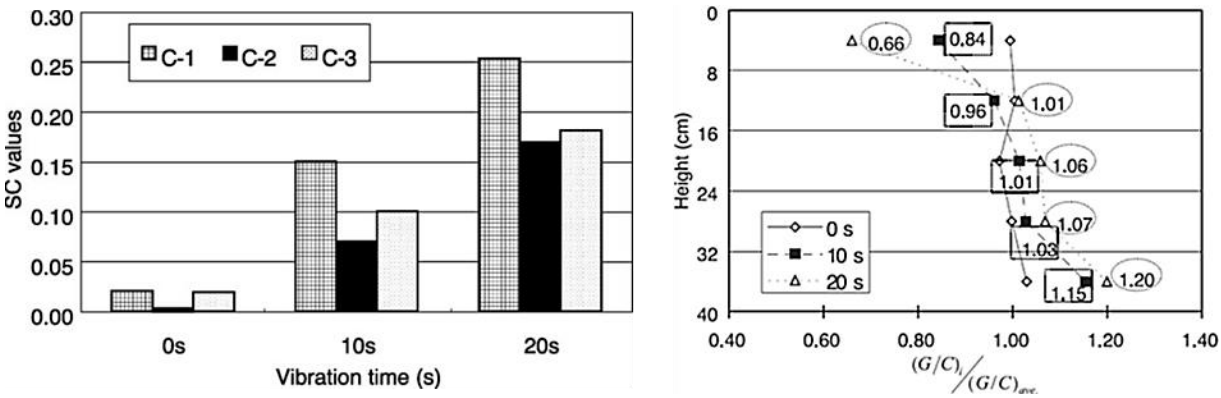

Figure 2.43: Effect of vibration duration on the segregation coefficient (SC) values (left) and aggregate segregation profile for the mix C-3 (right) [100]

This risk for segregation due to vibration is further aggravated with increasing size of aggregates as can be seen from the segregation profiles for 13/20 mm and 5/13 mm size fractions of aggregates in Figure 2.44. The 5/13 mm size fraction is more or less uniformly distributed while the 13/20 mm size fraction shows great discrepancy along the height of the concrete specimen after being vibrated for 20 s. The reason that the smaller sizes remained relatively in position while the larger sizes settled could be attributed to the rheological properties of the suspending mediums.

The yield stress of the concrete is mostly exceeded by the stress caused by vibration and as a result the concrete transforms from a classic Bingham material into a fluidized state. Hence, the only rheological component that contributes to the stability would be the viscosity. This is confirmed by the test results in which an increase in segregation (SC-values) was registered with decreasing flow time while there were no reliable correlation between slump flow and SC-values could be determined. As such, flowable concretes possessing a V-flow time of 10 s or less are were found to be very susceptible to segregation [123].

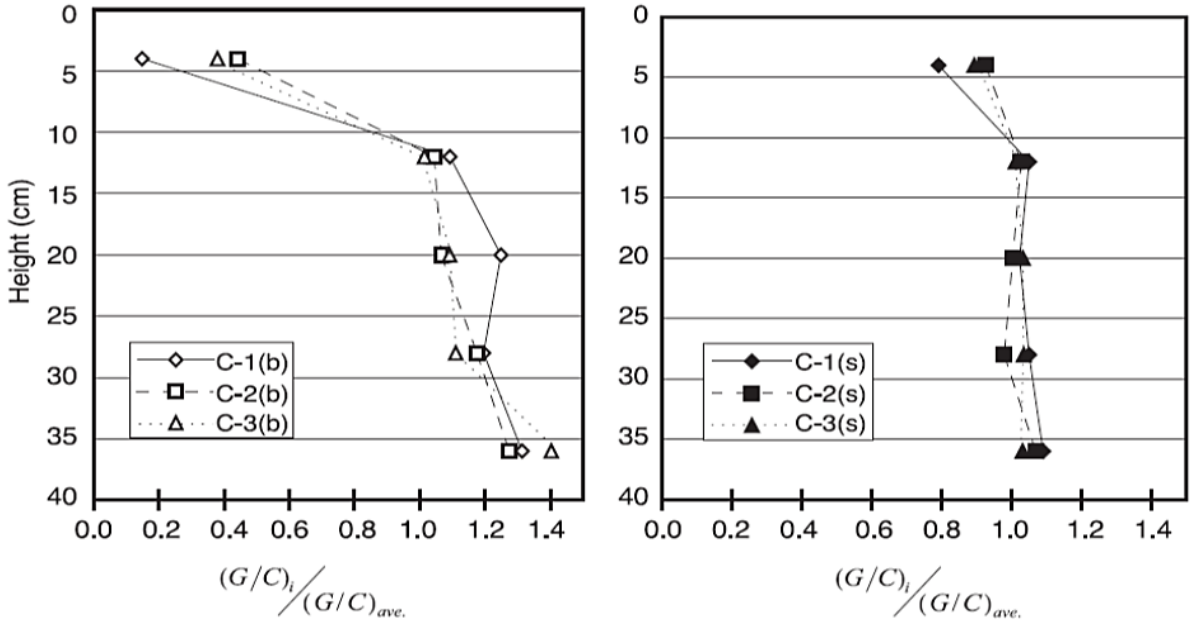

Figure 2.44: Segregation profiles for 13/20 mm (left) and 5/13 mm (right) aggregates [100]

2.4 Pumpability of concrete

Pumping is one of the most effective methods for conveying a large volume of concrete in a relatively short period of time, provided that the concrete exhibits good pumpability properties. These properties could be characterized on the basis of technical features such as lower pumping pressure and higher output as well as relevant concrete technological features such as maintaining the required fresh concrete properties before and after pumping.

2.4.1 Definition

According to ACI, pumped concrete is defined as a concrete that is transported through hose or pipe by means of a pump [125]. Pumpability of concrete could also be defined as the ability of concrete to flow in pipes under the application of pressure without changing its properties [126].

2.4.2 Behavior of concrete in a pipe

A concrete flowing in a pipe shows basically a laminar flow behavior with the exception that the velocity profile remains constant along its cross section [127] [128] [129]. During the pumping process, the concrete is exposed to different levels of shear stress along its cross section with the stress reaching its maximum value at the pipe wall and progressively decreasing towards the center.

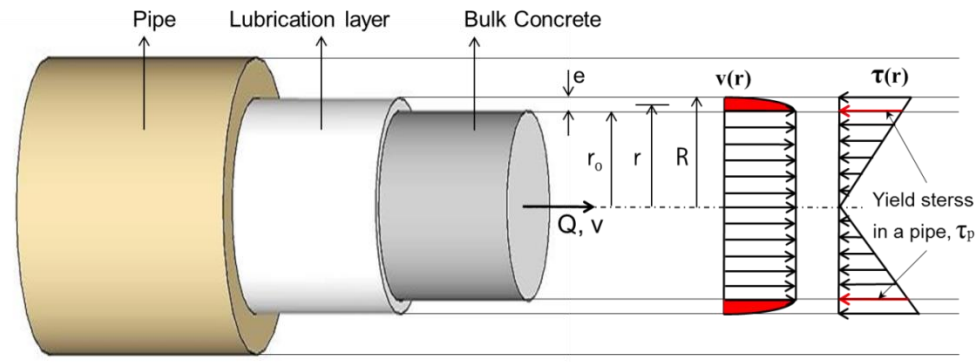

Figure 2.45: Behavior of concrete in a pipe [7] [130]

Based on the theoretical model as suggested by Kaplan, which is illustrated in Figure 2.45, the following zonal classifications based on the shear $\tau(r)$ and the flow velocity v(r) could be made [130].

i. Zone of bulk concrete: $r \leq r_o \Rightarrow v(r) = \text{constant}$; $\tau(r) \leq \tau_p$
ii. Zone of lubrication layer: $r_o < r \leq R \Rightarrow v(r) = \text{variable}$; $\tau(r) > \tau_p$

Adopting the classical rheological model from Bingham and applying it to the shearing phenomena in the pipe by taking the pumping relevant rheological parameters, the following correlation could be established.

$$\tau = \tau_0 + \mu \cdot \dot{\gamma} \Rightarrow \tau(r) = \tau_P + \mu \cdot \frac{v(r)}{e} \tag{2.46}$$

Taking an infinitesimal element of concrete and the forces acting on it, one gets the following relationship.

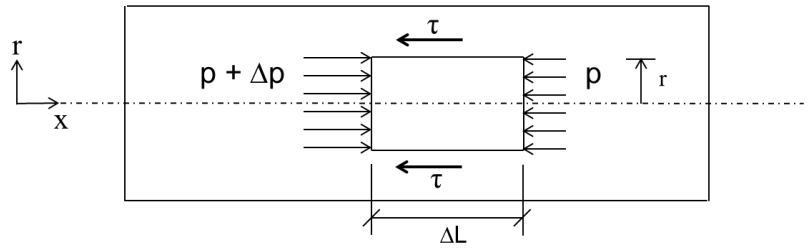

Figure 2.46: Equilibrium of forces on an infinitesimal element of concrete [131]

$$\sum F = 0 \Rightarrow 2\pi r \cdot \Delta L \cdot \tau(r) - \pi r^2 \cdot \Delta p(x) = 0 \Rightarrow \tau(r) = \frac{r}{2} \cdot \frac{\Delta p}{\Delta L} = \frac{r}{2} \cdot \frac{dp}{dx} \tag{2.47}$$

The pressure required to initiate flow in the pipe can be determined by combining Equations (2.46) and (2.47).

$$\tau(r) = \tau_P + \mu \cdot \frac{v(r)}{e} = \frac{r}{2} \cdot \frac{\Delta p}{\Delta L} \Rightarrow \frac{P}{L} = \frac{2}{r}\left[\tau_P + \mu \cdot \frac{v(r)}{e}\right] \Rightarrow P = \tau_P \cdot \frac{2L}{r} + \frac{\mu}{e} \cdot \frac{2L \cdot v(r)}{r} \tag{2.48}$$

Considering the case where a concrete is pumped in the vertical direction using a pipe with a height of H, the required pumping pressure which consists of the yield stress, viscosity and gravitational components could be determined by replacing the flow velocity with the discharge and considering the gravitational force acting on the concrete as shown in Equation (2.49).

$$P = \tau_P \cdot \frac{2L}{r} + \frac{\mu}{e} \cdot \frac{2 \cdot L}{r} \cdot \frac{Q}{\pi r^2} + \rho \cdot g \cdot H \tag{2.49}$$

Where: P = required pumping pressure; L = length of the pipe, r = pipe radius; Q = flow rate of concrete; τ_p = shear stress at the pipe wall; μ = plastic viscosity of the lubrication layer; e = thickness of the lubrication layer; ρ = density of concrete; g = gravitation constant; H = height of pumping

This reveals that the pumpability of concrete depends on concrete technological factors such as the yield stress, viscosity and the adequacy of the paste amount in the concrete to form a lubrication layer as well as the pumping constellation including the height, length and diameter of the pipe. The extent of the shearing process and its effect on the formation of the lubrication layer depends on the shear resistance of the concrete. In case of conventional concretes, the shear resistance of the concrete is usually higher than the acting shear stress and as a result only the lubrication layer get sheared allowing the bulk concrete to flow as a plug. On the contrary, flowable concretes such as SCC do exhibit a lower shear resistance and as such under the action of shear stress, the thickness of the sheared layer could propagate towards the bulk concrete. The same could also apply for conventional concrete when the pressure is increased drastically as illustrated in Figure 2.47.

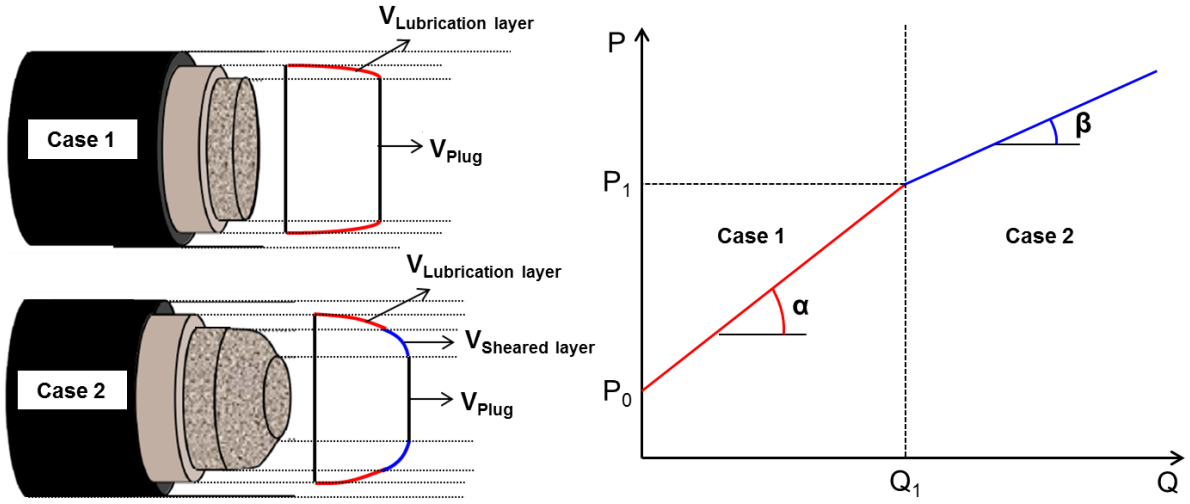

Figure 2.47: Shearing phenomena in a pipe depending on concrete type and level of shear stress [7] [130]

Accordingly, based on the Kaplan's model, the pressure loss (ΔP) for the two cases could be quantified as follows [130].

Case 1: The yield stress of the concrete is greater than the shear stress at the wall ($\tau_0 > \tau_p$) $\Rightarrow$ only the lubrication layer gets sheared

$$\Delta P = \frac{2L}{r}\left[\frac{Q}{3600 \cdot \pi r^2 \cdot k_r} \cdot \eta_{LL} + \tau_{0,LL}\right] \tag{2.50}$$

Case 2: The yield stress of the concrete is smaller than the shear stress at the wall ($\tau_0 < \tau_p$) $\Rightarrow$ both the lubrication layer and the bulk concrete get sheared

$$\Delta P = \frac{2L}{r}\left[\frac{\frac{Q}{3600 \cdot \pi r^2 \cdot k_r} - \frac{r}{4 \cdot \mu_p} \cdot \tau_{0,LL} + \frac{r}{3 \cdot \mu_p} \cdot \tau_0}{1 + \frac{r}{4 \cdot \mu_p} \cdot \eta_{LL}} \cdot \eta_{LL} + \tau_{0,LL}\right] \tag{2.51}$$

Where: ΔP = pressure loss over the length of the pipe; L = length of the pipe; r = pipe radius; Q = flow rate of concrete; k_r = filling coefficient of the pumping cylinders; η_{LL} = viscous constant of the lubrication layer representing the viscosity of lubrication layer divided by its thickness (μ/e); $\tau_{0,LL}$ = yield stress of the lubrication layer, τ_0 = the yield stress of the bulk concrete; μ_p = plastic viscosity of the bulk concrete

However, Feys et al. have found out that the assumption with regard to the shearing of only the lubrication layer in conventional concrete holds true only at lower flow rates. At higher flow rates, the bulk concrete could also get sheared depending on the pumping characteristics, the pipe diameter and the rheological and tribological properties of the concrete [132].

2.4.3 Factors affecting the pumpability of concrete

The pumpability of concrete depends on the interaction between the concrete technological aspects and the applied pumping technique. Depending on the type of concrete, completely different pumpability properties could be observed in a pipe as explained in section 2.4.2. Conventional concrete tend to form a plug flow where a relatively thin lubrication layer, which is composed of paste or fine mortar, is formed at the pipe wall. To this end, the availability of an adequate amount of paste is a pre requisite for the formation of the lubrication layer [133] [134]. When there is enough amount of paste, the concrete could be considered to be in a saturated state, where the pumping pressure is transferred to the concrete through the liquid phase or the paste. In such cases, the pressure decreases linearly with the length of the pipe. On the other hand, in an unsaturated state where aggregate contact is unavoidable, the required pumping pressure increases exponentially due to the high friction between

the aggregates themselves and the pipe wall which results into a non-linear pressure loss along the pipe. However, even after being introduced to the pumping lines in a saturated state, some concrete compositions, especially those with low fines content, could rapidly transform into unsaturated state due to the occurrence of “dewatering” as illustrated in Figure 2.48. Such cases could similarly lead to the formation of aggregate clusters which ultimately increases the required pressure drastically. Pipe blockage would be the consequence if the capacity of the pump is exceeded by the frictional stress. Thus, the permeability of concrete should be as such that no “dewatering” could take place [135].

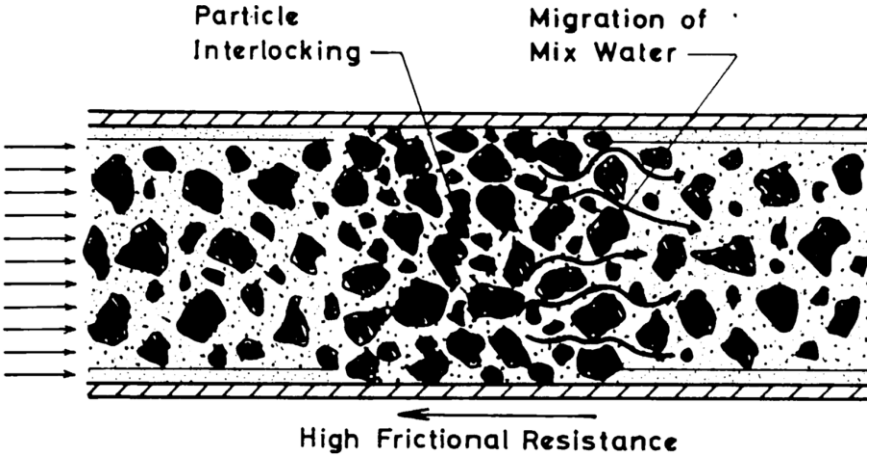

Figure 2.48: Forward segregation in a pipe line [135]

Kaplan et al. have conducted an in-situ pumping experiment using a 148 m long pumping circuit and identified four types of blockages that occur during priming, pumping, restarting and cleaning. The most frequent type of blockage happened during priming. They attributed this to the coarse aggregates flowing through the mortar, leaving the front of the concrete and being accumulated to form a plug. Blockage occurs once a critical concentration of the coarse aggregates is reached. During the priming process, the whole pumping apparatus is lubricated with paste or mortar. However, in practical applications, the concrete is added directly to the hopper while there is still some lubricating material inside it. This causes an intermingling of the concrete with the lubricating material, thereby changing the original concrete composition. The authors have observed that this procedure tendencially lead to blockage.

On the contrary, the risk for blockage during priming decreases when the concrete was added to the hopper after clearing the lubricating material. They encountered no significant blockage problem during the normal pumping phase. They also suggested that the tendency to segregate in a pipe line is correlated with the bleeding phenomena [136]. The chances for a concrete to cause blockage after passing the

first set of obstacles in a piston pump, namely undergoing a great deformation at high velocity while passing through the S-valve and being pressed out of the piston cylinders with larger cross section into the pumping lines with smaller diameters, is very small [134].

Investigations with regard to the influence of concrete compositions on the pumpability were conducted by Mechtcherine et al. by making use of a Sliding Pipe Rheometer (SLIPER), which helps quantify the pressure – discharge (P – Q) relationship. They found out that concrete compositions with higher water - binder ratio (w/b) require lower pumping pressure. Moreover, concrete mixtures with rounded aggregates were found to be favorable for pumping than those with crushed aggregates. This was attributed to the round aggregates encountering lower resistance from the mortar matrix during shear deformation. The addition of mineral admixtures such as silica fume and fly ash could also have a positive effect on the pumpability as long as the addition is done in such a way that the water demand of the mineral admixtures is also taken into consideration. No significant difference was observed as a result of altering the cement type from CEM II to CEM I. Generally, concrete compositions with flowable consistency required less pumping pressure when compared to those having stiffer consistency [137].

Investigations by Abebe and Lohaus with regard to the effects of different paste and aggregate compositions on the pumpability and pump stability of concrete have revealed the contradictory nature of the two properties. As such, concrete technological factors that enhance the pumpability as measured by a pumping resistance simulator such as higher water – binder ratio or lower amount of fine aggregates has led poor pump-stability as expressed in terms of the water retaining capacity of the concrete mixtures under high pressure [138].

Neumann and Lietzmann used a truck mounted concrete pump to investigate the effects of SP and paste content as well as the type and gradation of aggregates on the pumping of concrete. They observed the increment of the required pressure with decreasing amount of paste even though the consistency was maintained constant through the addition of SP. Moreover, there is a minimum paste volume under which an attempt to attain the desired slump flow through the addition of high amount of SP could potentially lead to blockage as a result of excessive segregation. The aggregates with higher water adsorption capacity led to an instantaneous blockage of the pumping lines. Moreover, for a constant amount of paste, aggregate compositions with a higher amount of sand have led to a drastic increase in pumping pressure. The type of SP or aggregate (natural or crushed) did not influence the pumpability significantly [139].

2.5 Rheology of concrete

Rheology is a subject area which deals with the flow or deformation behavior of materials under the application of loading. With regard to the deformation behavior of fluids, three main categories could be made – Newtonian, non-Newtonian and viscoelastic flow behaviors. As applied to concrete technology, the rheological properties determine not only the flow but also other important fresh concrete properties such as the stability as detailed in sections 2.3.5 and 2.3.6.

2.5.1 Rheological characteristics of fluids

I. Newtonian fluids

Newtonian fluids such as water and oil are described by the linear relationship between the applied stress and the deformation. Assuming a fluid of thickness of (h) with a surface area of (A) is sheared with a force (F), the shear stress (τ) and the shear rate ($\dot{\gamma}$) could be determined as shown in Equation (2.52).

$$\tau = \frac{F}{A} \text{ and } \dot{\gamma} = \frac{v}{h} \tag{2.52}$$

The shear stress (τ) and the shear rate ($\dot{\gamma}$) are correlated linearly by a constant - dynamic viscosity (η) as in Equation (2.53).

$$\tau = \eta \cdot \dot{\gamma} \tag{2.53}$$

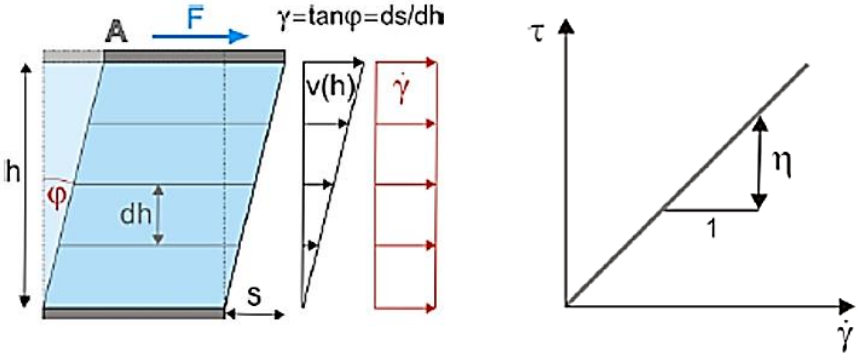

Figure 2.49: A fluid under shearing (left) and flow curve of Newtonian fluid (right) [98]

II. Non-Newtonian fluids

In case of non-Newtonian fluids, the relationship between the applied stress and the deformation is not linear. The relationship constant (dynamic viscosity) rather depends on the shear rate, the shear deformation and the duration of shearing, i.e. $\eta = f(\dot{\gamma}, \gamma, t)$. Non-Newtonian fluids exhibiting reversible time dependent shear stress and viscosity properties are categorized as thixotropic or rheopexic. In a thixotropic

fluid, the shear stress and the viscosity decrease over time under the action of a constant loading and increase after the loading is removed. The reverse effect is termed as rheopexy, see Figure 2.50, right.

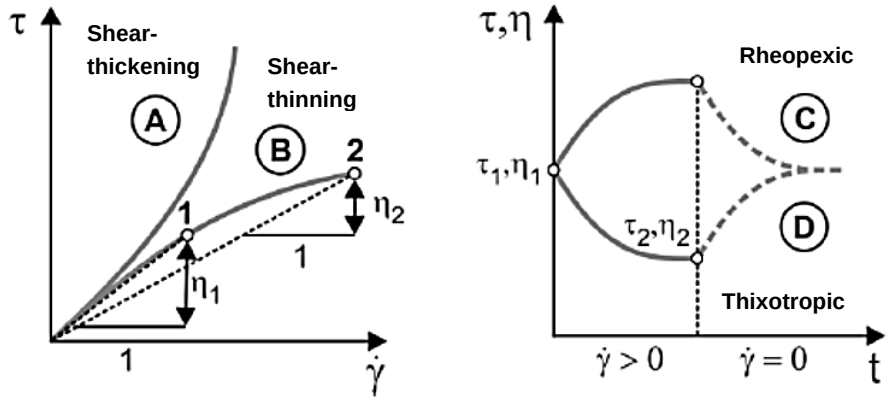

Figure 2.50: Non-Newtonian flow curves (left) and time and loading dependent flow behaviors (right) [98]

III. Viscoelastic fluids

If a non-Newtonian fluid has a yield stress (τ_o), it shows no deformation until the yield stress is exceeded by the applied stress (τ). That means as long as of $\tau < \tau_o$, the fluid assumes an elastic property. When $\tau > \tau_o$, the fluid starts to show a viscous flow property which depends on the magnitude of $\tau - \tau_o$.

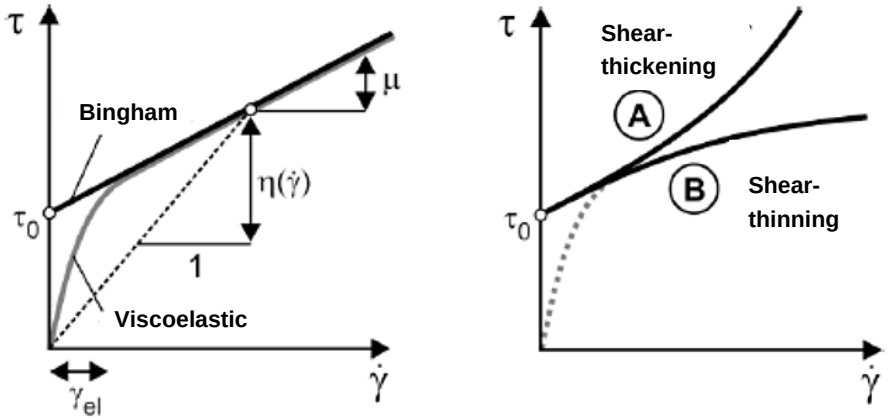

Figure 2.51: Bingham fluid (left) and non-Newtonian fluids with yield stress (right) [98]

By ignoring the elastic part in Figure 2.51, the flow curves could be mathematically explained by using the Bingham model, which stipulates a linear correlation with the constant (μ) between the shear stress and shear rate after initiation of flow ($\tau > \tau_o$).

$$\tau = \tau_0 + \mu \cdot \dot{\gamma} \qquad (2.54)$$

There are of course different mathematical models that could be applied to describe these complex flow curves of shear-thinning or shear-thickening fluids with yield stress. Among them is the Hershel-Bulkley Modell as shown in Equation (2.55), which usually represents such flow curves satisfactorily.

$$\tau = \tau_0 + k \cdot \dot{\gamma}^n \tag{2.55}$$

Where: k and n = dimensionless constants

A value of n > 1 indicates a shear-thickening behavior, n < 1 a shear-thinning behavior and n = 1 a classic Bingham function. The dynamic viscosity (η) of a Bingham fluid depends on the shear rate and can be estimated using Equation (2.56)

$$\eta = \frac{\tau(\dot{\gamma})}{\dot{\gamma}} + \mu = \frac{\tau_0}{\dot{\gamma}} + k \cdot \dot{\gamma}^{n-1} \tag{2.56}$$

2.5.2 Structural formations in concrete

Extensive studies with regard to the rheological properties of concrete has revealed that concrete is in fact a thixotropic material and undergoes a structural breakdown under the application of shear loading [140] [141] [142].

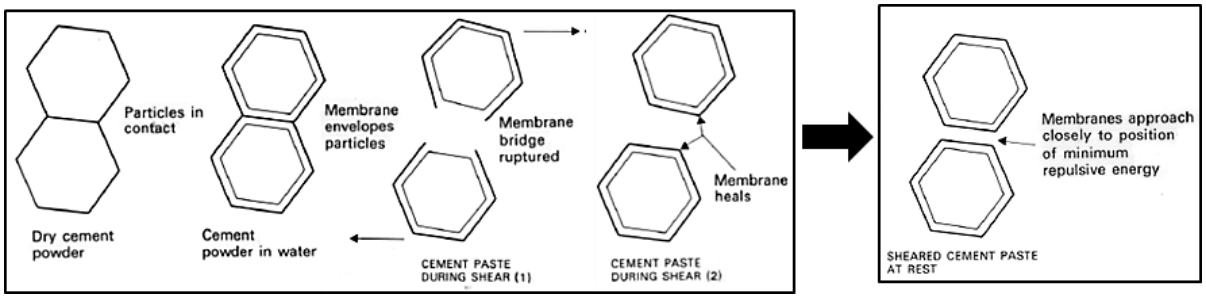

Figure 2.52: Structural formation in cement paste during shear (left) and at rest (right) [141]

The addition of water to the cement causes the formation of CSA membranes around the cement grains. Such a membrane is responsible for holding the cement grains together. However, when a shear force is applied to the cement paste, the bridging membranes get ruptured and the cement particles drift apart from one another. After some time, the membranes start to heal, but they won't be able to form a bridge due to the continued shearing, see Figure 2.52, left. After the shearing is stopped, the particles approach one another without coming in contact, since the small charged particles are subjected to the forces of attraction and repulsion. This irreversible structural breakdown differs from the reversible thixotropic behavior where the particles rebuilt a structure by coalescing after the shearing is stopped. [140].

According to Wallevik, the thixotropic behavior of a cement paste is directly related to the coagulation, dispersion and re-coagulation of the cement particles. The cement particles become glued as a result of the total potential energy interaction which constitutes of van der Waals attraction, electrostatic repulsion and steric hindrance. Two types of coagulation are discussed – reversible (designated by reversible junctions J_t) and permanent reversible (designated by permanent junctions J_t^P). A generalized illustration of the formation of reversible and irreversible structural breakdown processes in cement pastes is shown in Figure 2.53. The yield stress (τ_o) and the plastic viscosity (μ) increase with the order of A – B – C – D, where:

A. Fully dispersed cement particles.
B. Formation of hydrate membranes around particles leading to a large surface roughness and stronger grip.
C. Formation of permanent coagulation of some particles.
D. Growing connections due to reversible coagulation of some particles.

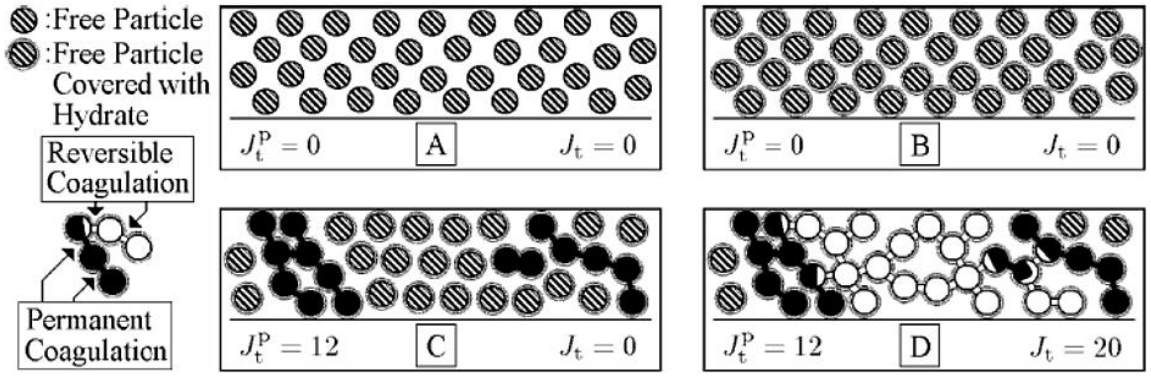

Figure 2.53: Demonstration of permanent and reversible coagulation [142]

According to Roussel et al., a fresh cement paste undergoes a short, medium and long term evolution process during the dormant period as explained below, see Figure 2.54.

a) Directly after mixing, the cement particles are fully dispersed.
b) After a couple of seconds, a flocculation process begins due to the colloidal attractive forces and a network of cement particles forms rendering the system a resistance to stress and elastic modulus.
c) Simultaneous to the flocculation process, a nucleation of CSH phase occurs at the pseudo contact points turning the soft colloidal forces into CSH bridges. Consequently, percolation of particles that are interacting purely through the CSH bridges forms leading to an increase in the elastic modulus.
d) As time goes by, the size and number of the CSH bridges increase and the elastic modulus also increases.

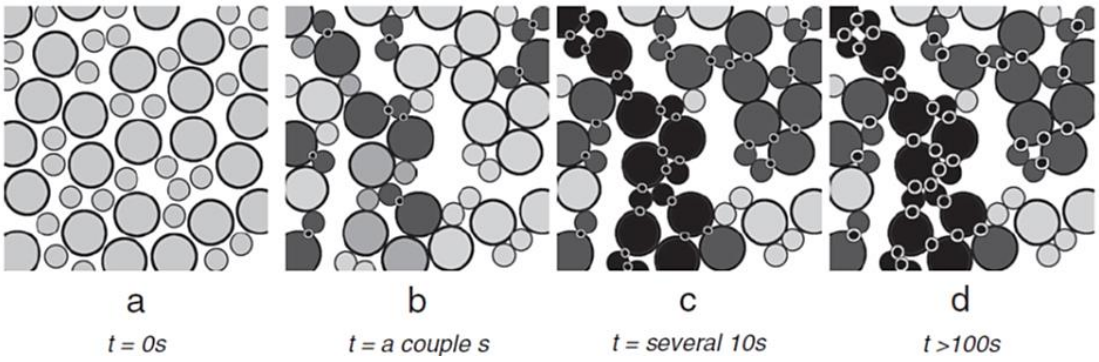

Figure 2.54: Evolution of the inter particle structure in cement pastes over time [143]

The common experimental methods based on stress and strain evolutions that are implemented to study thixotropic behaviors are very much dependent on the time at which the critical strain is determined. This critical strain corresponds to the peak stress (static yield stress) at which a rupture or breakdown of the interparticle structure occurs. The measured peak stress depends on the resting time. Experimental investigation by the authors on a cement paste with a w/c = 0.4 has shown that the measured peak stress for resting time less than 10 min corresponds to the colloidal critical strain. For longer resting times, the measured peak stress corresponds to the rigid critical strain. The stress level at the colloidal critical strain quantifies the interparticle structure formed by colloidal interactions between the cement particles. The stress level corresponding to the rigid critical strain quantifies the interparticle structural strength built by early hydrates formed at the contact points of the cement particles. It is worth noting that the colloidal interaction affects thixotropy for the first few seconds and as such the CSH nucleation could be considered as the main cause of thixotropy. In fact, for the purpose of determining thixotropy, the type of the interparticle structure, whether it is colloidal or rigid, is irrelevant as long as the applied shear energy is enough to break down the material to its initial state. Therefore, measures that accelerate the hydration process of concrete also enhance the thixotropic behavior [143].

The effect of the different production and application processes of SCC on the structural breakdown or the change in the thixotropic behavior and the corresponding the yield stress (τ_o) and the plastic viscosity (μ) as proposed by Lowke is presented in Figure 2.55. The intensive structure breakdown during the mixing, transport and casting processes leads to the rapid decrease in the yield stress and viscosity of SCC, thereby lending it a high flowability and good deaeration properties. After the casting process is finished, the concrete at rest starts to rebuild its structure and consequently the yield stress and viscosity increase over time. In fact, the rate at the yield stress and the viscosity are regenerated is the most decisive factor in relation to the segregation of the coarse aggregates in SCC [98].

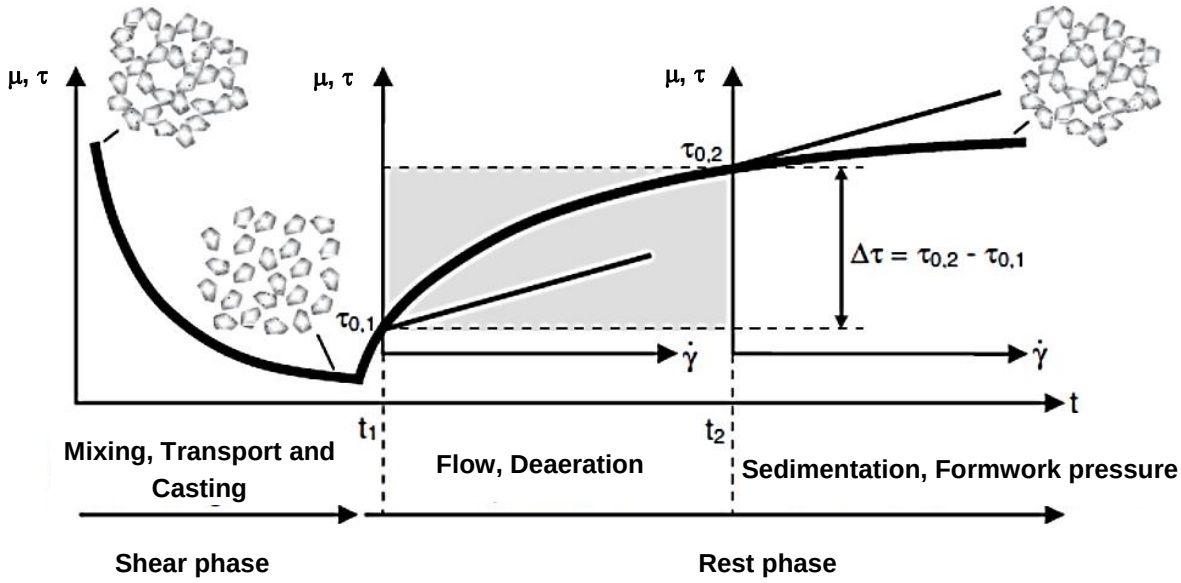

Figure 2.55: Effect of thixotropy on the yield stress and the viscosity of SCC [98]

2.5.3 Factors affecting the rheological properties of concrete

The rheological properties of concrete (yield stress, viscosity and thixotropy) are influenced by almost all the component materials and their composition. A concrete is a suspension constituting of materials of sizes from μm - cm scales (cements - coarse aggregates). If the classical definition of suspension is applied to concrete, then the water would be the suspending medium in which the solid particles are suspended. However, the system of suspension in concrete doesn't entirely work on a physical interaction basis as a consequence of the immediate chemical reaction taking place between the cement and the water leading to the formation of hydrates. For this reason, usually the paste and sometimes the mortar are treated as the suspending medium in concrete. These mediums, however, show entirely different rheological properties in comparison to concrete; see Table 2.4 [141].

Table 2.4: Rheology of cement paste, mortar and concrete [141].

Material	Cement paste	Mortar	Flowable concrete	SCC	CC
Yield stress (N/m^2)	10−100	80−400	400	50−200	500−2000
Plastic viscosity ($N.s/m^2$)	0.01−1	1−3	20	20−100	50−100
Structural breakdown	significant	slight	none	none	none

Rheological investigations by Toutou and Roussel on multi scale basis - Nano silica suspension, cement paste, mortar and concrete – have revealed that the nano silica scale and the cement paste scale could be considered as a colloidal system in which

the interaction between the particles have significant influence on the yield stress. On the contrary, the mortar and concrete could be considered as non-colloidal systems in which the yield stress depends on the solid fraction of the sand or aggregates. As such, an increased sand/aggregate content above a certain solid fraction results in a drastic increase in yield stress [144].

Rheological measurements generally indicate that the cement paste is affected to a higher degree than the concrete by changes in the constituent materials. This could be attributed to the more pronounced effects of the structural breakdown (dispersion) or the thixotropic behavior (coagulation) in cement pastes when compared to the concrete. In the presence of aggregates, however, this effects are somewhat weakened because the aggregates are capable of withstanding the applied stress without deformation [141]. When a concrete proportioned at 50% - 50% by volume of aggregate and paste is exposed to a shear rate of ($\dot{\gamma}$), the actual shear rate in the paste could get as high as 5.$\dot{\gamma}$ while it is equal to zero for the aggregates. Accordingly, a comparison is shown in Figure 2.56, left, illustrating the effects of superplasticizer (SP) on the rheological properties of the different phases (water, cement paste and mortar) of a reference concrete. Here, the SP has affected both the yield stress (τ_o) and the plastic viscosity (μ) of the paste while only the yield stress (τ_o) is affected in the concrete, confirming the higher sensitivity of the paste to changes in concrete composition [145] [146].

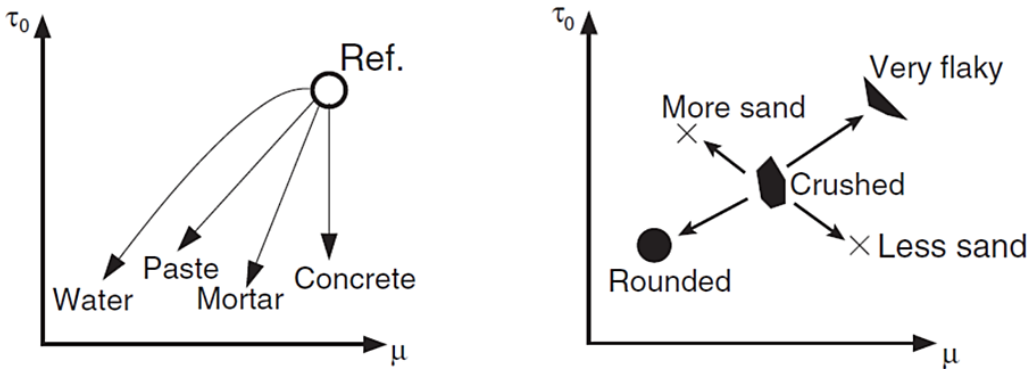

Figure 2.56: Effect of SP on the rheological properties of paste, mortar and concrete (left) and effect of aggregates on the rheological properties (right) [146]

With regard to the effects of aggregates on the rheological properties, generally concretes with rounded aggregates have slightly lower yield stress (τ_o) and significantly lower plastic viscosity (μ) when compared to those made of crushed coarse aggregates. Moreover, replacing crushed coarse aggregates with sand results into an increased yield stress (τ_o) and significantly lower plastic viscosity (μ).

Concretes containing flaky aggregates are characterized by high yield stress (τ_o) and high plastic viscosity (μ), see Figure 2.56, right.

The effects of increasing the contents of different constituent materials on the rheological properties of a reference concrete are illustrated in Figure 2.57 [146] . On the one hand, the addition of water, fly ash and superplasticizer result in a substantial reduction of the yield stress (τ_o). The addition of air and silica fume up to a limited content doesn't seem to have a significant influence on the yield stress (τ_o). However, the yield stress (τ_o) decreases with an excessive amount of air while it considerably increases with higher amount of micro silica.

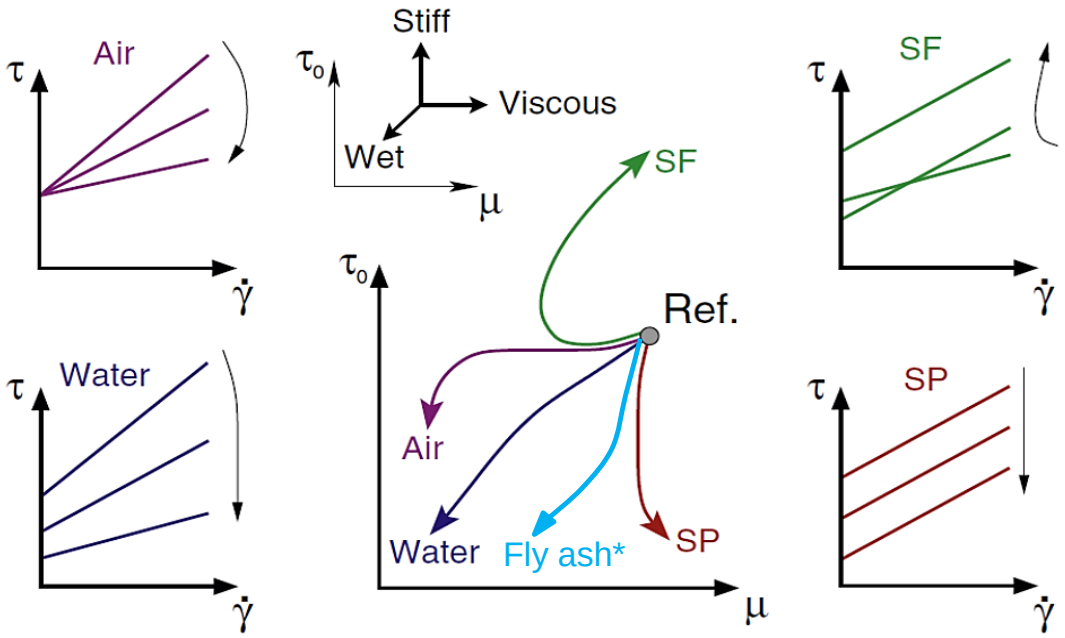

Figure 2.57: Effect of different constituent materials on the rheological properties [146] (* adopted from [147])

Considering a constant paste volume, the addition of water decreases the solid fraction (ϕ), thereby increasing the distance between the individual particles and reducing the contact points [148]. Consequently, the formation of colloidal or CSH based interparticle structures as explained in [143] gets weaker making the mix less resistant to the action of shear force. This leads to a better deformability of the mix which is manifested by the reduction in yield stress (τ_o), plastic viscosity (μ) as well as thixotropy [140] [149] [150]. Investigations conducted by Billberg on micro-mortar phase extracted from different SCC mixtures have shown that an increase in the solid volume fraction enhances the structure build-up, which he quantified in terms of the static yield stress (measured peak stress at the beginning of structural breakdown). The increase in the structural build-up would consequently lead to an increase in the yield stress, plastic viscosity and thixotropy as explained in section

2.5.2. The micro-mortars designated as Mix 1, 2 and 3 contained a coarser lime stone powder (LP1) with a median size of 40 µm. In contrast, Mix 4, 5 and 6 constituted LP2 with a median size of 25 µm. The pair Mix 1 & 4, Mix 2 & 5 and Mix 3 & 6 had respective water to powder (w/p) ratio of 0.344, 0.329 and 0.315. All mixtures had a w/c-ratio of 0.58. As can be seen in Figure 2.58, the structural build up and inherently the yield stress, plastic viscosity and thixotropy increase with increasing solid fraction (ϕ) (Mix 1 > Mix 2 > Mix 3 and Mix 4 > Mix 5 > Mix 6). Furthermore, the finer the solid particles, the higher is the rate of structure build-up and thus the rheological parameters (LP1 > LP2) [150].

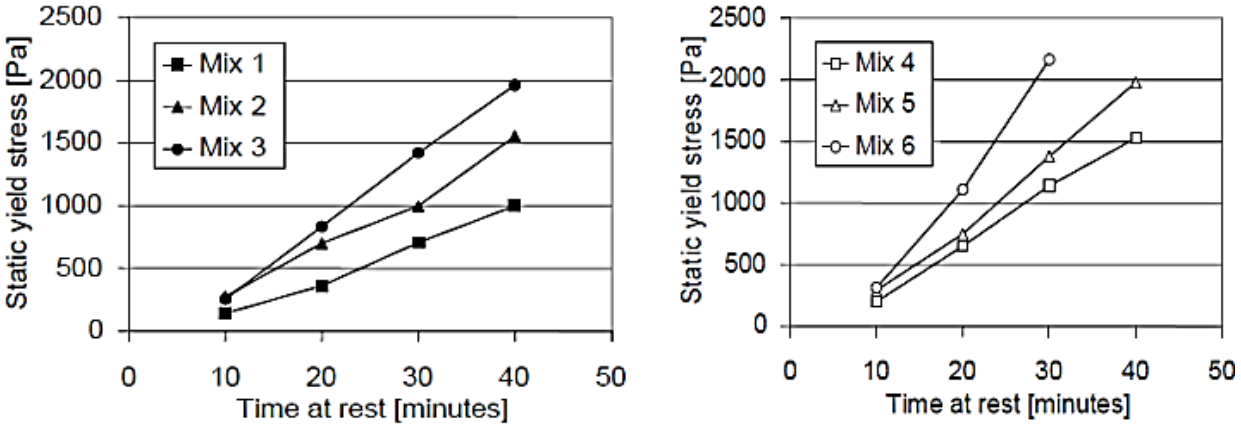

Figure 2.58: The effect of solid volume fraction on the structural build-up with coarser fines LP1 (left) and finer fines LP2 (right) [150]

Regardless of the mode of operation of superplasticizers (SP), whether electrostatic or steric, their main function is to repel or disperse the cement or other fine particles, onto which they get absorbed, from one another. In doing so, the resistance against flow that would have occurred due to the coming-together of the particles could be hindered or delayed thereby leading to a reduction in the yield stress (τ_o), plastic viscosity (μ) and thixotropy [23] [82] [151] [152] [153]. However, Banfill noted that a decrease in plastic viscosity (μ) in cement paste due to the addition of SP doesn't necessarily lead to a decrease in plastic viscosity (μ) of concrete. He reasoned that the dispersion of the fine particles caused by the SP eases the coagulation of the aggregates which otherwise would have been limited when the fine particles form agglomerates. As a result, by virtue of the higher friction between the aggregates, the resistance to flow (viscosity) of the concrete could possibly increase [140] [145]. Investigation by Ferron et al. on paste compositions of comparable flowability has revealed that the rate of structure rebuilding or thixotropy is higher for the paste compositions with lower w/c containing SP in comparison with those with higher w/c ratio having no SP [154].

The rheological properties of cement based systems are also influenced by viscosity modifying agents (VMA). Mineral based VMA modifies the rheological properties through the additional surface area and modification of the particle size distribution. In contrast, polymer based VMA basically bind the water rendering it a more viscous nature and sometime causing an intertwining effect, especially at higher content. To this end, starch based VMA mainly affects the yield stress by filling the space between particles while products such as diutan gum or welan gum affect both the yield stress and viscosity through binding high amount of water [29]. The usage or an increased dosage of VMA generally results into an increase in the plastic viscosity (μ) and yield stress (τ_o) [35] [37] [40] [155] [153] as well as thixotropy [150] [156] [157].

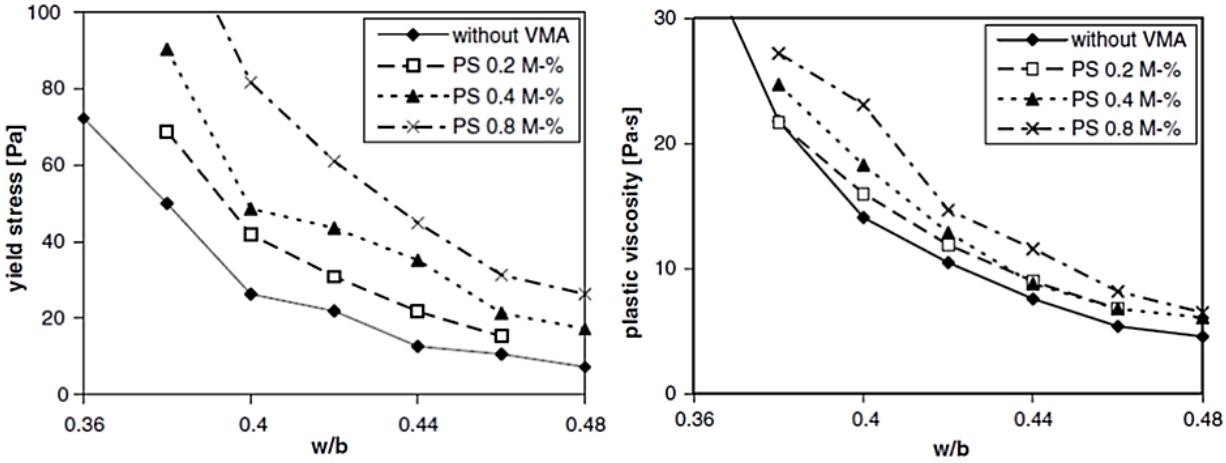

Figure 2.59: Effect of VMA on the rheological properties [35]

Air entertaining admixtures decrease both the yield stress (τ_o) and the plastic viscosity (μ), with the reduction in μ being highly pronounced. This is due to the "ball bearing" effect of the bubbles which makes it easier for the aggregate particles to move past each other. Moreover, the bubbles interrupt the formation of a continuous interparticle structure between the cement particles, thereby decreasing the yield stress [140].

The substitution of cement with finer supplementary cementitious materials (SCM) leads to a reduction in the void volume in concrete while releasing the trapped water, thereby increasing the flowability of the mix [158]. Khayat et al. have reported that the effect of SCM on the rheological properties is very much dependent on the content and composition of the SCM as well as the state of dispersion of the solid particles. Generally, up to a certain level of substitution, SCM improve the rheological properties of the mix by decreasing yield stress (τ_o) and by increasing the plastic viscosity (μ), especially in well dispersed system. This could be beneficial for the production of flowable and stable mixtures such as SCC. The authors observed an increase in plastic viscosity (μ) due to the partial substitution of cement with fly ash

(FA), silica fume (SF) and slag (SG) regardless of the SP content. Moreover, the yield stress generally decreased in a well dispersed system when a SP amount beyond the saturation point was used. In contrast, the yield stress (τ_o) increased for SP content below the saturation point; see Figure 2.60, left. Usually, the SCM have smaller particle sizes when compared to the cement and thus their water demand is higher; see Figure 2.60, right [88]. Consequently, the total number of contact points between the particles would also increase when cement is replaced with SCM. As such, if the system is not well dispersed, the SCM, instead of filling up the voids between the cements and improving the flowability, would add to the agglomeration process, thereby increasing the yield stress.

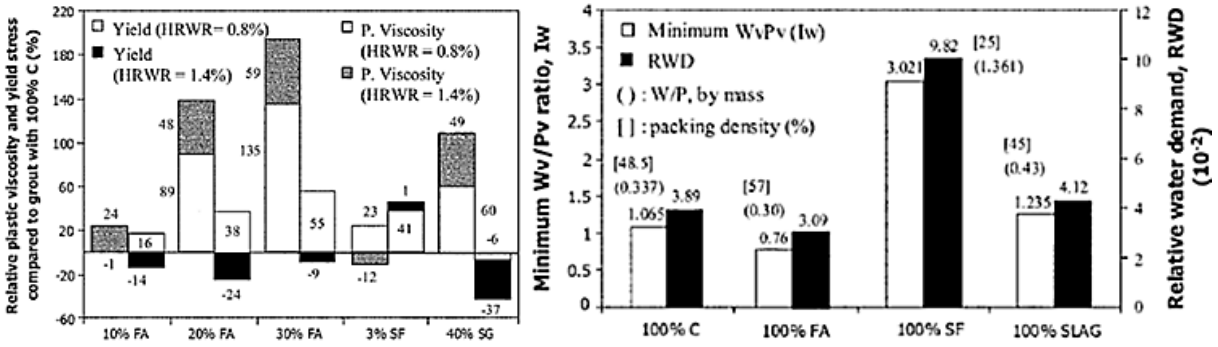

Figure 2.60: Effect of SCM substitution on the rheological properties (left) and water demand of the fines (right) [88]

Billberg observed no significant changes in yield stress (τ_o) and plastic viscosity (μ) due to the substitution of cement by slag at contents of 100 kg, 150 kg and 200 kg, regardless of the type of SP used in the investigation. Here, it should be noted that the total specific surface area and the solid volume fraction has increased as a result of the substitution. Thus, one can expect the yield stress (τ_o) and plastic viscosity (μ) to increase. He attributed the indifference in the rheological properties to the glassy nature of the surface of the slag particles and the higher negative zeta-potential they possess which is generally favourable for dispersion of the particles [151].

2.6 Packing density

There is a general consensuses among researchers engaged in the field of concrete technology that the packing density of the solid materials is one of the most important factors that influences the fresh and hardened concrete properties. Hence, different experimental and mathematical approaches or a combination of both were devised in order to attain the maximum possible packing density. When it comes to concrete technology, the wide ranging type and sizes of materials makes it really difficult to choose the proper experimental or theoretical method for the determination of the

packing density. The main objective of maximizing the packing density, however, is the respective minimization of the required water or paste demand for filling up the voids between the fines or aggregates.

2.6.1 Packing density of fines

One decisive factor that influences the packing density of fines is the applied method of compaction which could take place in dry or wet conditions as well as in compacted or non-compacted states. Wong and Kwan have observed a significant increase in the packing density when wet packing method was used instead of a dry packing method in accordance with the [159]. In the dry packing method the formation of serious agglomeration due to colloidal surface interactions has strongly undermined the packing density of the fines. They also investigated the effects of the addition of SP on the packing degree of fines and found out that the voids ratio decreases significantly, which could be attributed to the dispersing effects of the SP, thereby avoiding agglomeration. However, the addition of superplasticizer after the saturation point here designated as 1x SP, did not have any noticeable effect on the packing density. The packing density of fines also depends on the fines composition. The same authors found out that the CSF, which has a mean particle size 10 times smaller than that of PFA, is more effective in improving the packing density than the PFA, because of its higher fineness [160]. Based on their investigation, the authors concluded that the addition of a supplementary cementitious material finer than OPC would broaden the range of particle size distribution thereby increasing the packing density. In this respect, a supplementary cementitious material with a higher fineness would be more effective, since it effectively broaden the range of the particle size distribution [161].

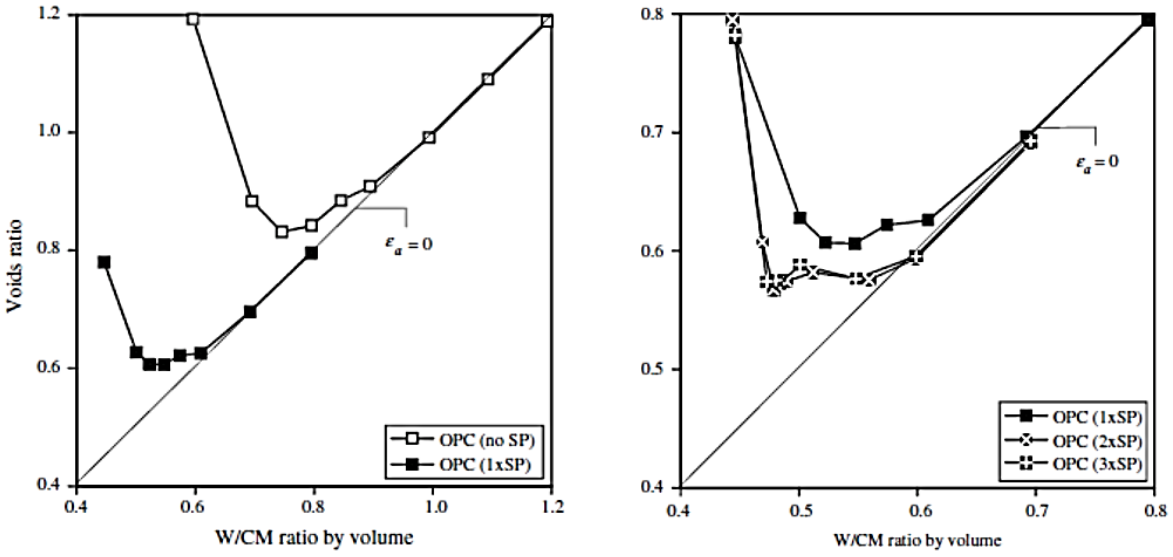

Figure 2.61: Void ratios of OPC with and without SP and the effect of dosage [160]

Chen and Kwan also conducted a similar investigation using superfine cement (SFC) as a substitute material for OPC and observed an increment in the packing density of about 6.6% and a decrease in the voids ratio of about 17.0% [162]. Detailed explanation with regard to the effects of packing density of fines on the fresh concrete properties could be found in section 2.2.2.

2.6.2 Packing density of aggregates

The packing density of aggregates also depends on whether an external energy is applied in some form during the compaction process. This is considered in the compressive packing model (CPM) developed by De Larrard. The parameters needed for this model are the packing density of monosize classes, the size distribution of the mix and the applied compaction energy. The compaction index (K) designates the extent to which the actual packing density gets closer to the virtual one. In other words, K depicts the effectiveness of the applied compaction energy - loose packing ($K \approx 4.1$), pocking ($K \approx 4.5$), vibration without loading ($K \approx 4.75$) and vibration with loading ($K \approx 9.0$) [163]. Regarding the influence of aggregates on the packing density, Hummel has shown that for the same aggregate composition, regardless of the method of packing, round aggregates do show higher packing density in comparison to angular aggregates as shown in Figure 2.62 [164].

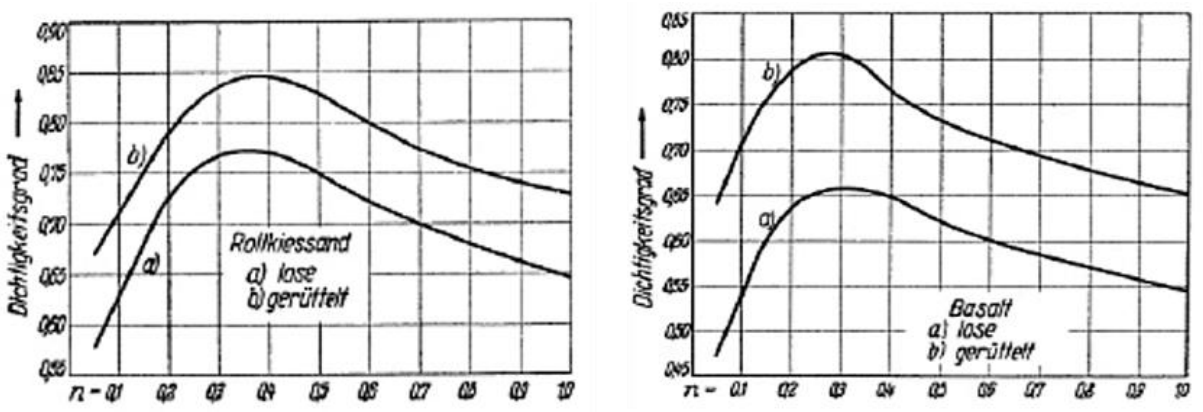

Figure 2.62: Packing density for round (left) and angular (right) aggregates without vibration (a) and with vibration (b) [164]

The investigation results from Huss using different aggregate compositions of natural sand - gravel, natural sand - crushed stone and crushed sand - crushed stone - have shown that, regardless of the aggregate composition, the packing density increases with increasing ratio of fine – coarse aggregate [49]. This is contrary to the findings of Hummel or Abebe and Lohaus, where the packing density starts to fall after a certain fine aggregate content is exceeded; see [164] [165].

2.7 Short summary

I. Flowability of concrete:
   - Flowability could be defined in terms of consistency classes or workability properties of concrete.
   - The flowability of concrete depends on the paste amount, the size, gradation, specific surface area, shape and textural features of the solid particles and the resulting packing density and water demand as well as the type of chemical admixtures, especially SP and VMA.
   - The excess paste theory or the subsequent paste – mortar – concrete phased design concepts could be devised to produce flowable concretes.

II. Stability of concrete:
   - Bleeding, segregation and sedimentation are the main phenomena that are associated with the instability of concrete.
   - There are three main modes of bleeding. Normal bleeding occurs due to the settlement of particles as a consequence of the density difference between the suspending medium (water) and the suspended particles (fines). Channeled bleeding is a form of uniform seepage of water intermingled with some fines over the whole surface of the concrete or through localized channels. Internal bleeding designates the accumulation of water under the aggregates.
   - The bleeding of concrete depends on the specific surface area of fines, the water content, the paste content, the type of chemical admixtures, especially SP, VMA and AEA as well as the type and gradation of the aggregates.
   - The segregation of concrete is strongly affected by the application of external loading such as vibration. Static segregation represents the sedimentation and bleeding without the application of external loading, e.g. in SCC. Dynamic segregation depicts the sedimentation and bleeding under external loading, e.g. in vibrated conventional concrete.
   - The static stability of aggregates in SCC at rest mainly depends on the yield stress of the mortar. No settlement of coarse aggregate would take place if the yield stress (τ_o) of the suspending medium (mortar) is higher than a critical yield stress ($\tau_{o,c}$). If that is not the case, settlement of the coarse aggregates would be inevitable. However, the extent of the settlement of the coarse aggregates depend on the dynamic viscosity (η), which determines the settlement velocity of the aggregates, and the thixotropic behavior, which designates the rate at which the inter-particle structure is built up until the critical yield stress is exceeded.

- The dynamic stability of concrete during casting / flow could be described as a particle migration process which is induced by shear loading, gravitational force or geometrical hindrances such as granular blocking and the wall effect.
- Usually, the dynamic segregation occurs prior to the static segregation, e.g. during concrete casting. Thus, a concrete that show reliable dynamic stability could be expected to possess sufficient static stability.
- Particle migration is depends on the particle size, the solid concentration and the resulting viscosity as well as the density difference between the aggregates and the suspending medium.
- The type of particle migration also depends on the concreting process. To this end, concrete pumping is governed by the shear and wall effect induced particle migrations while concrete casting is mainly dominated by gravity induced particle migration.
- The primary effects of vibration in concrete are the breaking-down of a flocculated cement paste, which turns it from a Bingham fluid into a Newtonian fluid, and the movement of the aggregate particles. Consequently, the trapped air rises to the surface and the aggregate particles rearrange themselves resulting into a higher compaction.
- The dynamic stability of concretes during vibration depends on the vibration intensity (frequency and amplitude), the duration of vibration, the size of the suspended particles (coarse aggregates) and the rheological properties of the suspending medium (mortar).
- The yield stress of the concrete is often exceeded by the shear stress caused by vibration. Consequently, the concrete transforms from a classic Bingham material into a fluidized (Newtonian) state. Hence, the viscosity is considered to be the only rheological component that contributes to the stability under vibration.

III. Pumpability and pump-stability of concrete:

- Pumpability could be characterized in terms of technical features such as lower pumping pressure and higher output or on the basis of relevant concrete technological features such as maintaining the required fresh concrete properties before and after pumping.
- The Pumpability of concrete depends on concrete technological factors such as the yield stress, viscosity and the adequacy of the paste amount in the concrete to form a lubrication layer as well as the pumping constellation including the height, length and diameter of the pipe.
- The shear resistance of conventional concretes is usually higher than the shear stress at the wall and thus only the lubrication layer get sheared

allowing the bulk concrete to flow as a plug. On the contrary, flowable concretes such as SCC possess a lower shear resistance and as such the thickness of the sheared layer could propagate inwards to the bulk concrete due to the action of the shear loading at the wall.

- A concrete could be assumed to be in a saturated state provided that there is enough amount of paste which guarantees the direct transfer of the pumping pressure to the concrete through the liquid phase or the paste. In such cases, the pressure decreases linearly with the length of the pipe.
- In an unsaturated state, the required pumping pressure increases exponentially due to the high friction between the aggregates themselves and between the aggregates and the pipe wall. In such cases, the pressure loss along the pipe is non-linear.
- At times, concrete compositions that are introduced to the pumping lines in a saturated state could rapidly transform into an unsaturated state due to the occurrence of dewatering or forced bleeding. This could potentially lead to the formation of aggregate clusters thereby drastically increasing the required pressure or in extreme cases causing a pipe blockage.
- The most frequent type of blockage happens during priming, especially when the concrete gets intermingled with the lubricating material inside the pumping lines. Here, the risk for the coarse aggregates to flow through the mortar and get accumulated in front of the concrete is much higher.
- The pumpability of concrete depend on the paste amount, the water - binder ratio, the type of mineral admixtures, the type and size distribution of the aggregates as well as the SP content.

IV. Rheology and structural formations in concrete:

- Concrete is basically a viscoelastic fluid which shows no deformation or an elastic behavior until a certain yield stress (τ_o) is exceeded by the applied shear stress (τ). When the yield stress is exceeded ($\tau > \tau_o$), the concrete exhibit a viscous flow property which depends on the magnitude of $\tau - \tau_o$.
- Different mathematical models are suggested to quantify the complex rheological properties of concrete including the widely used models from Bingham and Hershel-Bulkley. The Bingham model stipulates a linear correlation between the shear stress and shear rate after initiation of flow. The Hershel-Bulkley model is able to quantify the shear-thinning or shear-thickening behavior considering a non-linear correlation between the shear stress and shear rate.
- Concrete is a thixotropic material that undergoes a structural breakdown under the application of shear loading. At the cement paste level, a shear

loading causes rupturing of the bridging membranes between the cement particles forcing them to drift apart from one another (dispersion).

- After the shearing is stopped, a flocculation process due to the colloidal attractive forces between the particles is followed by the formation of stronger CSH bridges as a consequence of the nucleation of CSH phases rendering the mixture an increased resistance to shear stress over time (thixotropy).
- The intensive structure breakdown that take place during the mixing, transport and casting processes leads to a rapid reduction in the yield stress and viscosity.
- After the casting process, the concrete at rest starts to rebuild its structure thereby increasing its yield stress and viscosity over time. In SCC, the rate at the yield stress and the viscosity are regenerated is the most decisive factor governing the segregation of the coarse aggregates.
- The cement paste could be considered as a colloidal system in which the interaction between the particles has significant influence on the rheological properties. On the contrary, the mortar and concrete could be considered as non-colloidal systems in which the rheological properties depend on the solid fraction of the sand or aggregates.
- Cement paste is affected to a higher degree by changes in the constituent materials or shear loading in comparison with mortars and concretes. This could be attributed to the more pronounced effects of the structural breakdown (dispersion) or the thixotropic behavior (coagulation) in cement pastes. These effects are weakened in mortar and concrete due to the ability of the aggregates to withstand the shear stress without deformation.
- Almost all the fresh concrete properties are governed by the rheological properties. The rheological properties of concrete are in turn governed by the type, composition and amount of each constituent material including the aggregates, cement, mineral admixtures, chemical admixtures, water and air content.

V. Packing density of fines and aggregates:

- Maximizing the packing density is crucial for minimizing the required water or paste demand for filling up the voids between the fines or aggregates.
- Wet packing method with the addition of SP for fines and a combined application of vibration and loading for aggregates results into a higher and realistic packing density determination.
- Generally, the packing density mainly depends on the type and size distribution of the fines or aggregates.

Chapter 3
Water Balance Mix-Design

3.1 Short introduction

The newly developed Water Balance Mix-Design method (WBMD) is presented in this chapter. First, different hypotheses as related to the flowability, pumpability, stability and robustness properties of concrete are put forward. Afterwards, the design methodologies applied in the WBMD are illustrated in a great detail. This is then summed up in a conceptual model for the WBMD.

3.2 Hypotheses

As explained in section 1.2, the water balance-mix design method (WBMD) integrates the effects of the component materials as well as the chosen design parameters in such a way that the flowability, pumpability, stability (under vibration and pressure) and robustness requirements are addressed simultaneously. The WBMD was devised based on the following sets of hypotheses in relation to the flowability and stability of concrete.

3.2.1 Flowability

The following hypotheses form the basis for ensuring the flowability of concrete.

I. Maximizing the lattice effect in aggregate compositions ensures a homogenous flow.
II. A minimum amount of paste, which is dependent on the aggregate and the paste composition, is required for initiation of flow.
III. A certain amount of water reducing admixtures such as superplasticizer (SP) is required to ensure good flowability, even with an enough amount of paste.
IV. The effect of the SP on the flowability could be directly equated to the amount of water that is set free due to the dispersion of fines.
V. There is a saturation point of SP beyond which further dosage does not contribute to the flowability.

3.2.2 Stability

The following hypotheses are suggested for ensuring the stability of concrete.

I. Maximizing the lattice effect in aggregate compositions contributes a great deal to the static and dynamic stability of concrete.
II. Unbound water in concrete, which is triggered by excessive water or SP addition, is the main reason for the static as well as dynamic instability.
III. The paste compositions in flowable concrete could be assumed to be stable as long as there is no unbound water in the system.
IV. The effect of the SP on the stability could be directly equated to the amount of water which is set free due to the dispersion of fines.
V. Further addition of SP beyond the saturation point only leads to instability of concrete.

3.2.3 Robustness

The following hypotheses are suggested for ensuring the robustness of concrete.

I. Maximizing the lattice effect of aggregates enhances the robustness of concrete.
II. Robustness requires deviation from the optimum. As such, aggregate or fines compositions that result into a maximum packing density and a respective minimum paste or water demand does not necessarily produce a robust mix.
III. While maintaining the original properties in the face of changes in component materials or outside influences is a good virtue, the ultimate evaluation criteria for robustness should be the fulfillment of the stipulated performance requirements.

3.2.4 Pumpability

The following hypotheses are proposed with regard to the pumpability of concrete.

I. Maximizing the lattice effect in aggregate compositions enhances the homogeneity of concrete in pumping lines.
II. A minimum amount of paste is required for the formation of lubricating layer and separation of aggregates so that the friction in the pipe could be kept at a minimum.
III. The pumpability is directly dependent upon the pump-stability.

3.3 Methodology

The WBMD consists of the four main components as depicted in Figure 3.1. The aim is to combine these main components in such a way that the flowability and stability as well as the robustness and pumpability of concrete could be guaranteed.

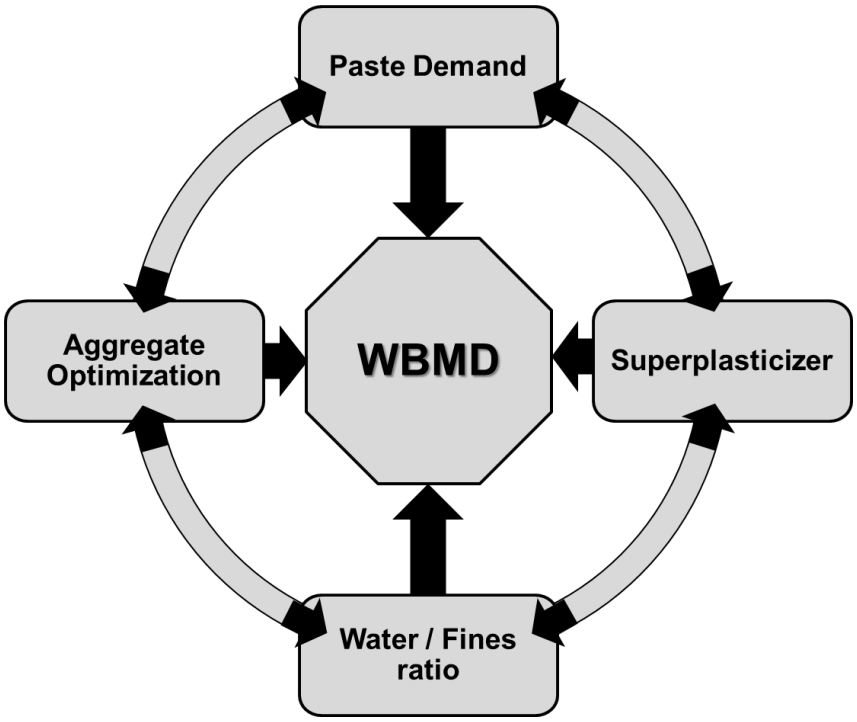

Figure 3.1: Main components of the WBMD

The procedures used in the WBMD are explained as follows.

3.3.1 Aggregate Optimization

The main objective of the aggregate optimization in the WBMD is maximization of the lattice effect, which is advantageous in promoting both the flowability and stability properties of concrete. As to the choice of the proper method with which the aggregate optimization could be conducted, different models and normative regulations and recommendations were considered. There are basically three approaches that are widely used for composing aggregates in concrete – the original Fuller and Thompson function (F&T) [166], the original Andreasen and Andersen function (A&A) [167] and the modified Andreasen and Andersen function by Funk and Dinger (F&D) [168]. The F&T function was developed for dense packing of aggregates in concrete based on the packing of polydispersions of discrete sizes. On the contrary, the A&A as well as F&D function are developed on the basis of packing models with a continuous distribution, considering the fact that all particle sizes exist in most cases, including concrete.

The ideal Fuller and Thompson (F&T) gradation function is shown in Equation (3.1).

$$P_i = \left[\frac{d_i}{d_{max}}\right]^{0.5} \tag{3.1}$$

Where: P_i = percent passing i^{th} sieve; d_i = opening size of i^{th} sieve; d_{max} = maximum particle size

The original Andreasen and Andersen (A&A) function is shown in Equation (3.2).

$$P_i = \left[\frac{d}{d_{max}}\right]^{q} \tag{3.2}$$

Where: P_i and d_{max} = as explained in Equation 3.1; d = particle size being considered; q = gradation exponent

The gradation exponent **q** could assume the values between 0 and 1. However, based on experimental investigations, the authors suggested values of **q** between 0.33 and 0.5 for optimal packing [167]. Note that F&T and A&A are similar for q = 0.5. While the F&T as well as the A&A functions result into gradation curves extending up to an unrealistic particle size of zero, the F&D function gives a gradation line that starts at the minimum particle size. Based on numerous 3-D modeling, the authors suggested that an optimum packing of continuous distribution of spheres occurs at q ≈ 0.37 [168]. The Funk and Dinger (F&D) function is shown in Equation (3.3).

$$P_i = \frac{d^q - d_{min}^q}{d_{max}^q - d_{min}^q} \tag{3.3}$$

Where: P_i, d, d_{max} and q = as explained in Equation 3.2; d_{min} = minimum particle size

Moreover, there are standard gradation lines that are prescribed in the norms and favorable zones where the gradation line should lie into – most of the time between the standard gradation lines A and B as shown in Figure 3.2. Hence, the aggregate optimization based on the ideal particle size distribution functions (Equation 3.1 – 3.3) should be done in such a way that the gradation curves fall within the favorable zone. Depending on the chosen function, the sieve size parameters d_{max}, d_i or d_{min} could be used to generate the data for the ideal curves $P_{i,(Ideal)}$. Assuming an aggregate composition consisting of **x, y** and **z** percent of 0/2, 2/8 and 8/16 fractions respectively, the percentage passing each sieve size ($P_{i,(Real)}$) can be determined as:

$$P_{i,(Real)} = x \cdot pi\,(0/2) + y \cdot pi\,(2/8) + z \cdot pi\,(8/16) \tag{3.4}$$

Where: $P_{i,(Real)}$ = total percentage passing i^{th} sieve; p_i (0/2), p_i (2/8), p_i (8/16) = particle sizes passing i^{th} sieve from 0/2, 2/8 and 6/8 fractions respectively

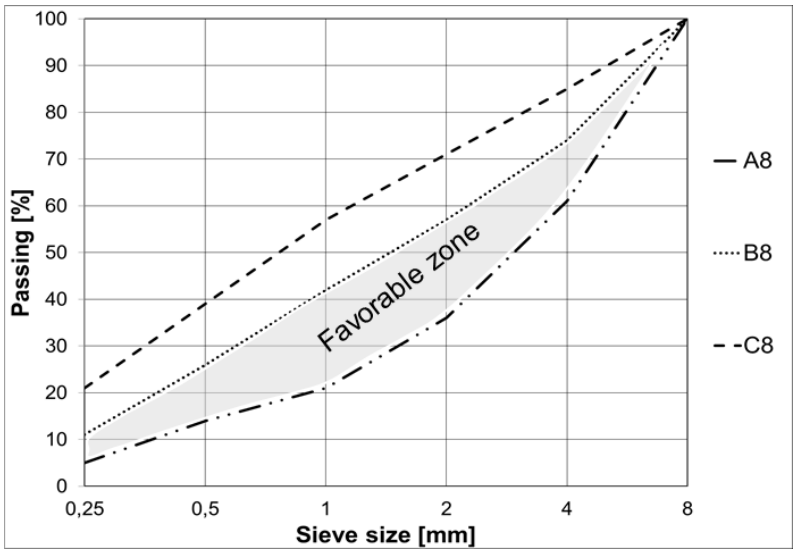

Figure 3.2: Standard gradation lines and preferable gradation zones (DIN 1045)

The values of the optimized aggregate gradation $P_{i,(Opt)}$ could then be determined using the generalized reduced gradient (GRG2) non-linear algorithm in excel which considers **x**, **y** and **z** as adjustable cells, the values of $P_{i,(Ideal)}$ as observed data points and the values of $P_{i,(Real)}$ as fitted data points. A zero percentage passing the sieve pan is the only constraint cell. The sum of the squares to be minimized could be calculated as:

$$S = \sum_{i=1}^{n} \left[P_{i(Ideal)} - P_{i,(Real)} \right]^2 \tag{3.5}$$

The optimum aggregate gradation for the chosen ideal distribution function and values of **q** could then be determined on the basis of the adjusted values of **x**, **y** and **z** which results into the least value of the sum of the squares (S).

Figure 3.3 shows the integration of the ideal gradation curves based on A&A / F&T and F&D with q = 0.5 in the standard gradation curves according to DIN 1045-2: 2008 for a maximum aggregate sizes of 8 mm and 16 mm considering a minimum cement particle size of 1 µm. It could be clearly seen that for particle sizes greater than 0.5 mm, the ideal gradation curves lie in the favorable zone. It is also worth noting that the ideal gradations curves based on the A&A/F&T and F&D functions are essentially the same. The optimized aggregate compositions for the 8 mm and 16 mm maximum sizes based on the A&A/F&T and F&D functions as depicted by the blue and red lines respectively remain well within the favorable zone. Both gradation lines also overlap to a higher degree revealing the adequacy of all three functions for this set of boundary conditions.

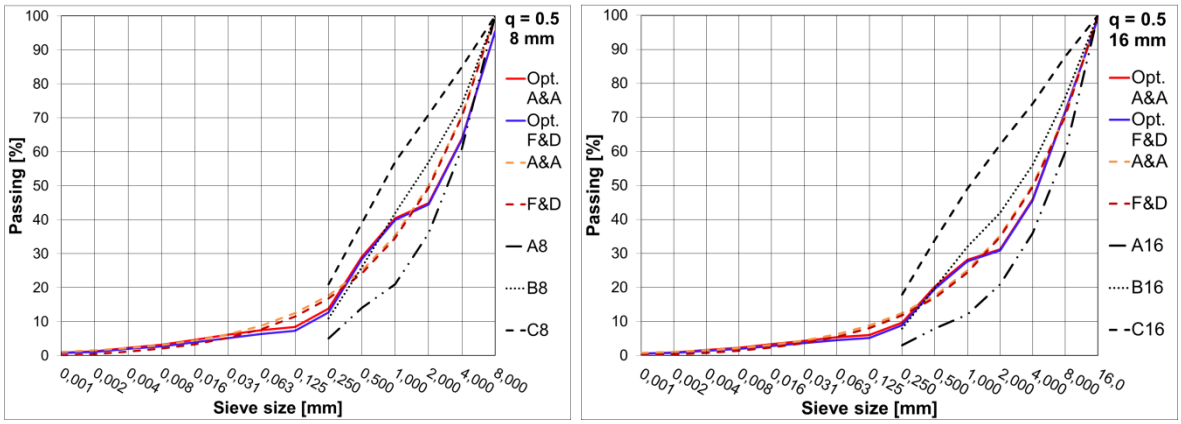

Figure 3.3: Integration of ideal particle distribution curves for q = 0.5 in the standard gradation curve

For q = 0.37 as suggested by F&D, both the ideal curves based on the A&A and F&D functions as well as the corresponding optimized gradation lines lie partly outside the favorable zone, especially for sieve sizes less than 2 mm. Thus, optimization of the aggregates based on these ideal curves is not recommended. In fact, the F&D model was developed for applications in ceramics, where much finer and arguably roundly-shaped materials are used and as a result its application to concrete requires modification the gradation exponent **q**.

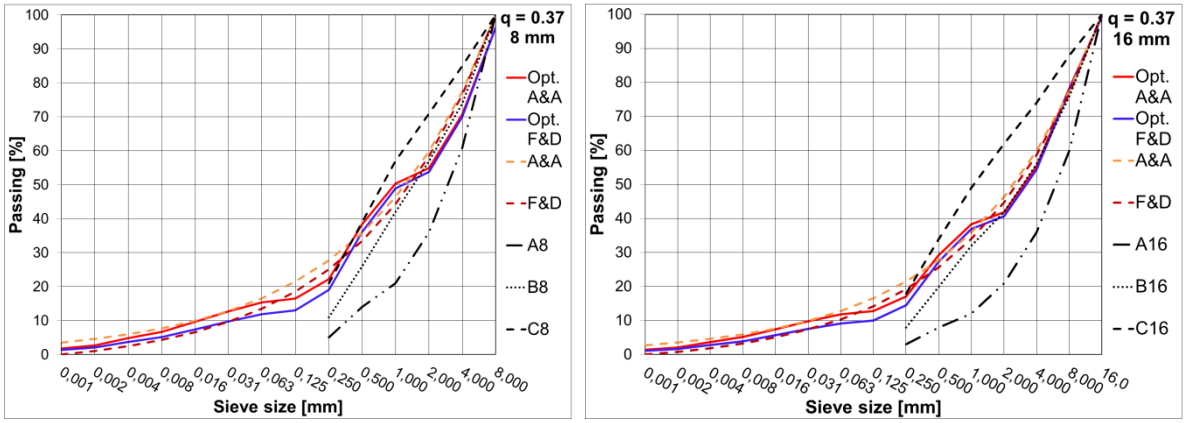

Figure 3.4: Integration of ideal particle distribution curves for q = 0.37 in the standard gradation curves

For q > 0.5, there is no difference between the ideal gradation curves based on the A&A and F&D functions as illustrated in Figure 3.5. Aggregate optimization based on such ideal curves, however, could result into a mix with relatively high amount of coarse aggregates as depicted by the blue and red lines which ultimately renders the concrete poor workability and potentially make it prone to segregation. Values of q > 0.75 also result into ideal gradation curves that lie outside the favorable zone below the standard gradation line A.

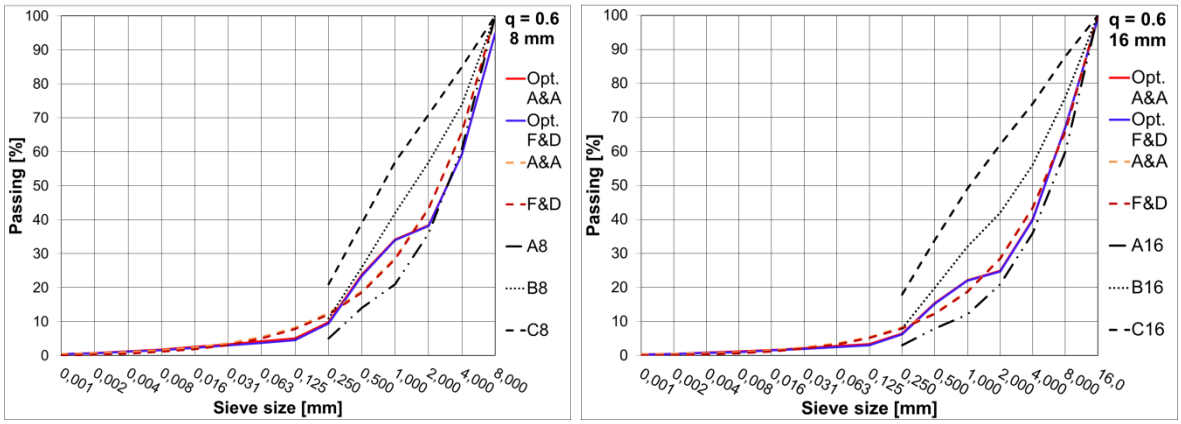

Figure 3.5: Integration of ideal particle distribution curves for q = 0.6 in the standard gradation curve

Thus, regardless of the type of functions used for establishing ideal gradation curves, **q** values of about 0.5 seem to be adequate for maintaining the optimized aggregate gradation lines within the favorable zone as long as the optimization is conducted in consideration of the whole particle size spectrum in concrete (µm – mm).

However, in practical mix-design, aggregate optimization is carried out by considering only the sand and coarse aggregate fractions and not the whole particle size spectrum. Nonetheless, the same approach could be applied for the aggregate optimization by considering the minimum particle size of the sand. Here, unlike the case of the whole particle size spectrum, the ideal gradation curves based on the A&A and F&D functions differ for q = 0.5. As a consequence, the optimized gradation lines also differ depending on the function as shown in Figure 3.6.

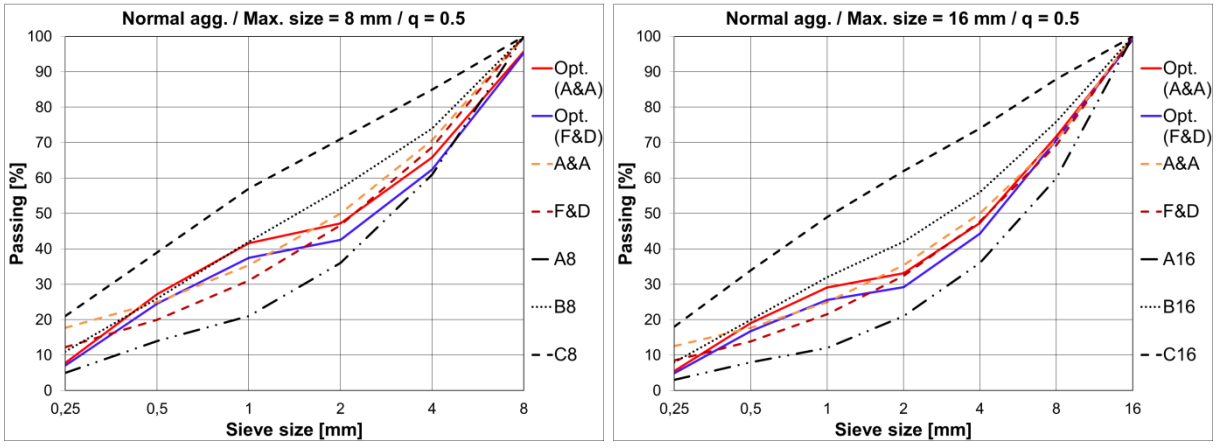

Figure 3.6: Effect of the optimization function on the aggregate gradation for different types of aggregates

For the same value of q = 0.5, the red gradation lines optimized based on the A&A function result in a higher amount of the whole size fractions in comparison with the

blue gradation lines which were optimized using the F&D function. They also run much closer to the standard gradation curve B which in general is considered to be positive in terms of maximizing the lattice effect. The difference between the two ideal curves disappears for q > 0.75. However, the application of the F&D function for aggregate optimization on the basis of the results of sieve test is somewhat dubious since the minimum particle size in aggregates is not determined as a standard procedure. Consequently, the A&A function, with the gradation exponent q = 0.5, could effectively be used for aggregate optimization making use of only the results of sieve tests as input parameter. The adequacy of this optimization technique is also confirmed using flaky and crushed aggregate compositions; see appendix A-1.

3.3.2 Determination of paste demand

The second step in the WBMD after the optimization of the aggregates is determining the required paste demand. The paste demand of flowable concrete consists of the amount of paste that is required to fill up the voids between the aggregates and to coat the aggregates' surface, so that they are separated from one another. These voids' and surface's paste demands are directly correlated with the packing density and the water demand of the aggregates respectively, which in turn are dependent upon the shape, roughness, size and grain size distribution of the aggregates.

Rounded aggregates are generally associated with good workability, since they are able to easily roll or slide over one another, thereby maximizing the packing density and minimizing the voids' paste demand. Particles with flaky shapes and rough-surfaced textures, on the other hand, are characterized by higher voids ratio and larger surface area, resulting into a higher paste demand [164] [54] [53]. Aggregates with larger maximum sizes require lower amount of paste by virtue of their smaller specific surface area. However, an excess amount of coarse aggregates could also lead to an increased void content, thereby leading to a higher paste demand [58].

Of all the parameters, the grain size distribution or the gradation is the most important one since both the packing density and the surface paste demand directly depend on it [169] [49] [165]. For a given maximum grain size and aggregate type, there is an optimum gradation where the finer particles subsequently fill up the voids between the larger ones, thereby reducing the voids between the aggregates and consequently the paste amount for void filling. However, it should be noted that aggregate compositions which lead to minimum voids do not always produce the most stable or robust concrete in terms of the sedimentation or segregation behavior as shall be explained in section 4.8.

3.3.3 Determination of packing density and void's paste demand

The packing density (ϕ) was determined using a dry-layered compaction method by applying vibration and additional loading simultaneously. Preliminary investigations were carried out first in order to optimize the necessary boundary conditions such as vibration time, surcharge weight as well as the aggregate handling and filling processes, so that the maximum packing density (ϕ_{Max}) could be achieved, see Figure 3.7. The vibration table used for the investigation has a constant frequency and amplitude of 50 Hz and 1 mm respectively.

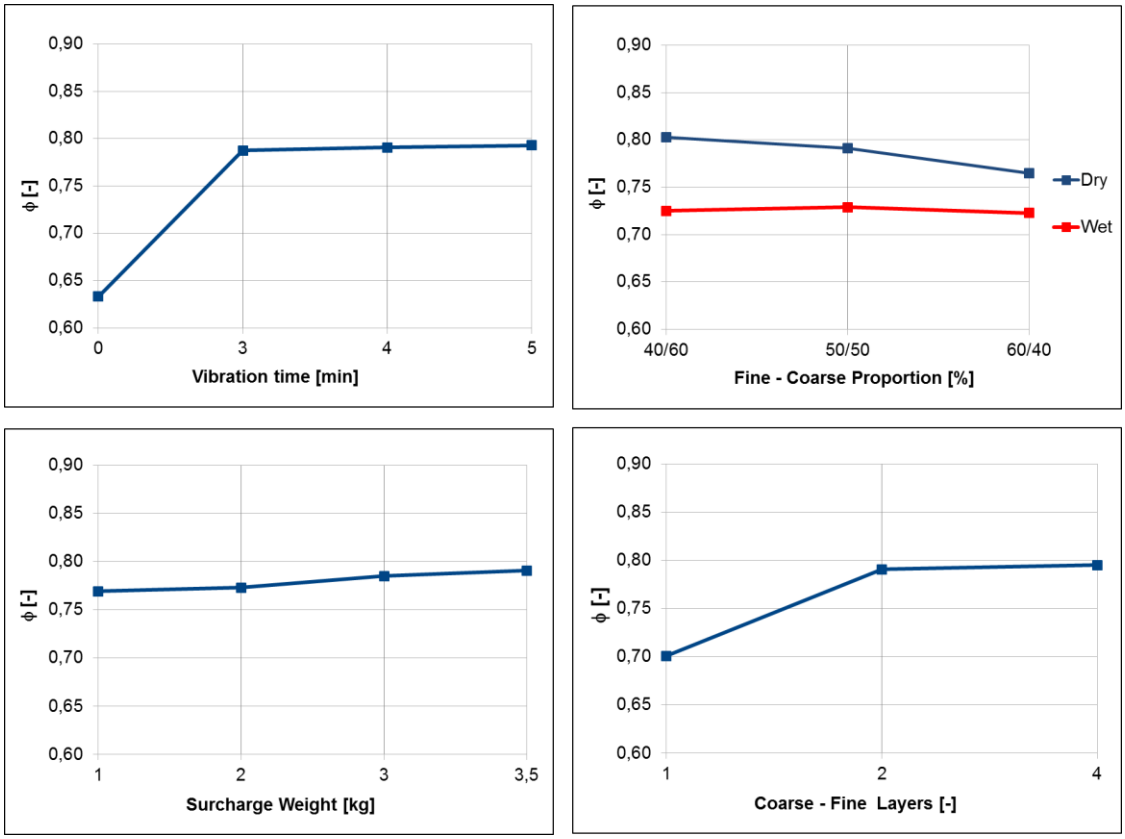

Figure 3.7: Optimization of the packing process

As can be seen from the diagrams in Figure 3.7, the ϕ_{Max} was achieved for a vibration time of 3 minutes and a surcharge weight of 3 kg under similar boundary conditions of fine (0/2 mm) – coarse aggregate (2/8 mm) combination of 50% - 50% using dry packing method. Moreover, under similar boundary conditions, the dry-layered packing method has resulted into a higher packing density when compared to a wet packing method, where the aggregates are first soaked in water before the test was conducted. In the wet packing method, the adhesion of the particles caused by the water on the surface could possibly hinder their movement and consequently the void filling process. In the dry-layered compaction method, each aggregate fraction is equally divided and placed successively with the coarsest at the bottom and the

finest at the top. Based on the results of the preliminary investigations, the boundary conditions as shown in Table 3.1 were applied for the main investigation. The reliability of the test results during the main investigation was guaranteed by conducting three tests per aggregate composition and taking the average values.

Table 3.1: Boundary conditions for determining the packing density

Vibration Frequency	Vibration Amplitude	Vibration time	Surcharge weight	Aggregate Mass	Mode of preparation	Filling
s^{-1}	mm	min.	kg	kg	-	-
50	1	5	3.5	1.8	dry	2 x coarse - fine layers

If a concrete is assumed to be a system in which the aggregates form a solid-phase skeleton, filling up of the voids with a paste would be a prerequisite for the formation of a suspension. For a certain aggregate composition, the voids' paste demand is at its minimum when the packing density is at its maximum. The minimum paste amount needed to fill the voids ($V_{P,V}$) could be assumed to be equivalent to the void volume (V_V) which is determined by subtracting the absolute volume of the aggregate (V_G) from the bulk volume (V_B).

$$V_{P,V} = V_V = V_B - V_G \tag{3.6}$$

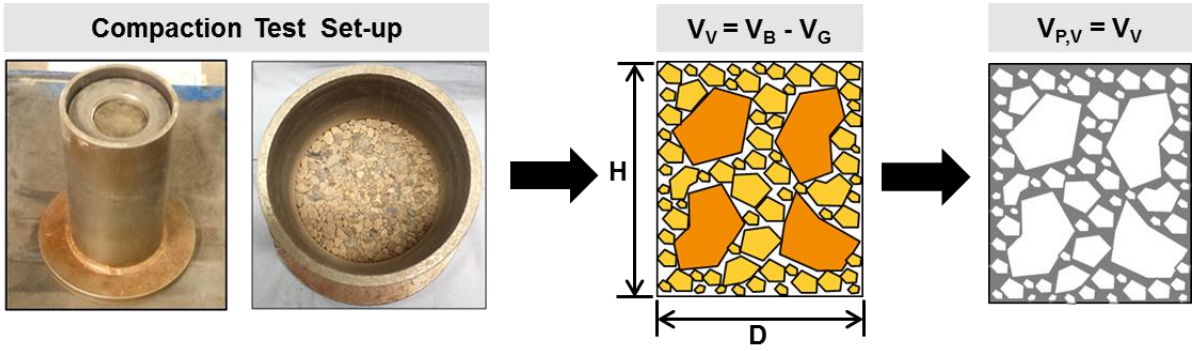

Figure 3.8: Determination of packing density and void's paste demand

The bulk volume (V_B) and the absolute volume (V_G) of the aggregates could be determined using Equation (3.7).

$$V_B = \pi \cdot \frac{D^2}{4} \cdot H \text{ and } V_G = \sum_{i=1}^{n} \frac{M_{Gi}}{\rho_{Gi}} \tag{3.7}$$

Where, D = diameter of container (100 mm); H = height of the bulk aggregate in container after compaction; M_{Gi} = mass of each aggregate; ρ_{Gi} = density of aggregate

However, this amount of paste is not yet enough to initiate flow, since the interlocking between the aggregates and the resulting friction remains very high. Hence, additional amount of paste is required to coat and separate the aggregates from one another. In addition, the packing density (ϕ) and the void ratio (ε) could also be determined using Equation (3.8).

$$\phi = \frac{V_G}{V_B} \text{ and } \varepsilon_{min} = \frac{V_V}{V_B} = 1 - \phi \tag{3.8}$$

3.3.4 Determination of water demand and surface paste demand

For the determination of the water demand of the aggregates, the approach developed by Huss [49] was modified through the application of filter press. First, the dry aggregate with a known mass (M_D) is filled in the container and water is added until the aggregates are completely saturated. Such a saturation state ensures a complete filling of the voids and coating of the surface of the aggregates. Afterwards, the water in the voids shall be pressed out using a filter press (Bauer Spezialtiefbau GmbH) which makes use of air pressure. A complete draining out of any remaining free-water is ensured by applying a water jet pump. In the end, only a mass of wet aggregates (M_W) whose surface is completely coated with water remains in the cylinder. Three tests were performed per aggregate type and the average value was taken.

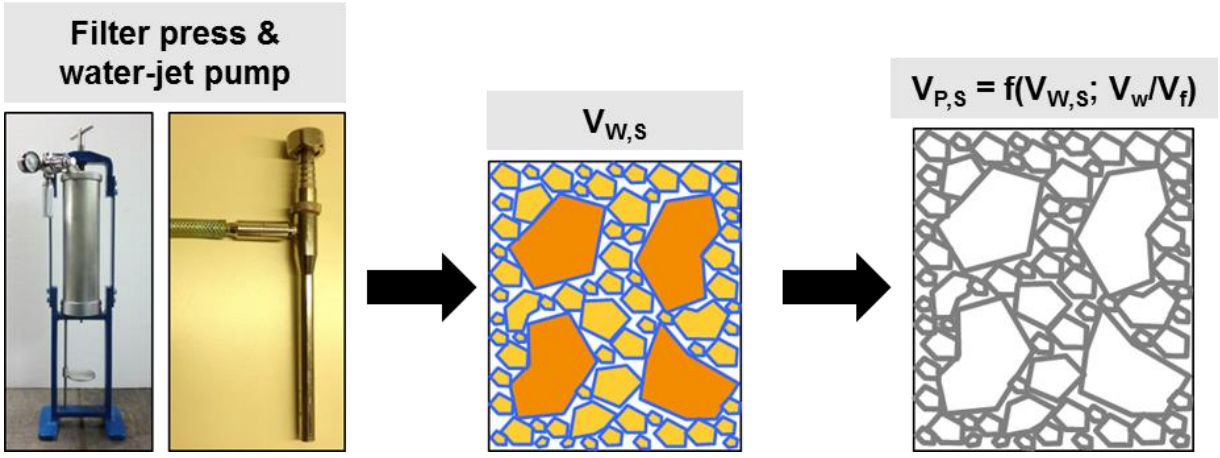

Figure 3.9: Determination of water demand and surface's paste demand

The sum of the mass difference between the wet aggregates (M_{Wi}) and the dry aggregates (M_{Di}), determined for each size fraction in a certain aggregate composition, gives the total water demand required to coat the aggregate surface area ($M_{W,S}$).

$$V_{W,S} = M_{W,S} = \sum_{i=1}^{n} (M_{Wi} - M_{Di}) \tag{3.9}$$

The paste amount required to coat the aggregate can be directly derived from the total water demand of the aggregate surface by considering the chosen water – fines ratio (V_W/V_F) of the mix-design. It could be assumed that a concrete composition is comprised of three phases - aggregates, paste and air voids. Accordingly, the paste could be assumed to be composed of water (V_W) and fines (V_F).

$$V_P = V_W + V_F \tag{3.10}$$

Hence, using the chosen water – fines ratio ($f = V_W/V_F$) from the mix design and the determined water demand of the aggregates ($V_{W,S}$) from Equation (3.9), a correlation could be established to determine the amount of paste needed to coat the aggregates' surface ($V_{P,S}$).

$$V_{P,S} = V_{W,S} + V_{F,S} = V_{W,S} + \frac{V_{W,S}}{f} = V_{W,S}\left[1 + \frac{1}{f}\right] \tag{3.11}$$

The total paste demand for the optimized aggregate is determined by adding the paste amount required to fill the voids between the aggregates ($V_{P,V}$) at ϕ_{Max} and to coat their surface ($V_{P,S}$) as determined from Equation (3.6) and (3.11) respectively.

$$V_P = V_{P,V} + V_{P,S} \tag{3.12}$$

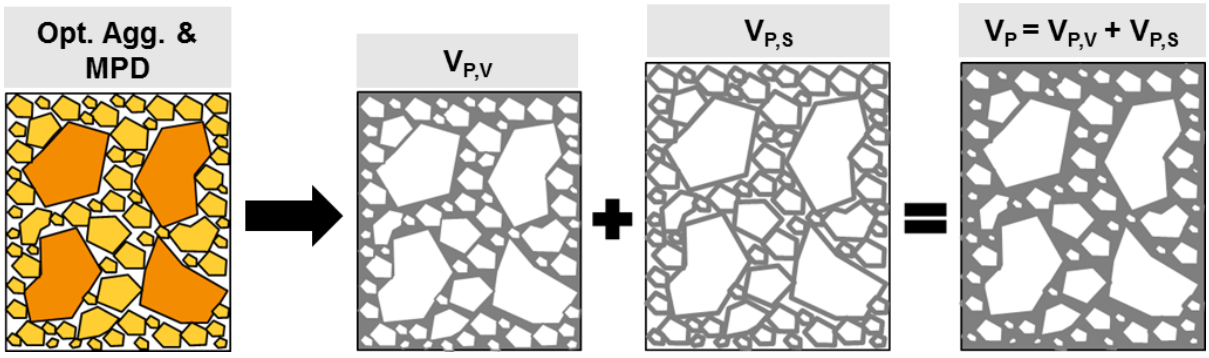

Figure 3.10: Determination of the total paste demand of optimized aggregate composition

3.3.5 Determination of the basic components in a concrete

The air voids in a conventional concrete, which usually occupy about 1.5% of the total volume, could be assumed to be found distributed among the paste phase. Thus, the total volume of air void (V_A) in the packing density experimental procedure could be determined using Equation (3.13).

$$V_A = 1.5\% \cdot V_B \tag{3.13}$$

This total volume of air void could then be distributed proportionally among the paste amount for voids' filling ($V_{A,V}$) and surface coating ($V_{A,S}$).

$$V_{A,V} = V_A \cdot \frac{V_{P,V}}{V_P} \text{ and } V_{A,S} = V_A \cdot \frac{V_{P,S}}{V_P} \tag{3.14}$$

With the assumption that the concrete is composed of aggregates and a paste containing air voids, the amount each basic component – aggregate ($V_{G,C}$), paste ($V_{P,V}$) and air voids ($V_{A,C}$) – in a 1 m^3 of concrete could be determined as follows.

$$V_{G,C} = \frac{V_G}{V_B} \cdot 1000;\ V_{P,C} = \frac{V_P - V_A}{V_B} \cdot 1000;\ V_{A,C} = \frac{V_A}{V_B} \cdot 1000 \tag{3.15}$$

$$V = V_{G,C} + V_{P,C} + V_{A,C} = 1 m^3 \tag{3.16}$$

The practical application of these methods are illustrated in Figure 3.11 based on a theoretical determination of the total paste demand at different V_W/V_F ratios for 0/8 mm and 0/16 mm aggregate compositions. It could be observed that the 0/8 mm aggregate composition requires ca. 40 lit more paste in comparison with the 0/16 mm composition. This is in large part due to the higher total specific surface area of the 0/8 mm aggregate composition and to some extent due to its higher void ratio. The paste demand also seems to increase drastically with decreasing V_W/V_F ratios. Reducing the V_W/V_F value from 1.0 to 0.8 results into an increase in paste demand of ca. 20 lit while increasing it to 1.2 brings about only a 10 lit reduction in paste volume.

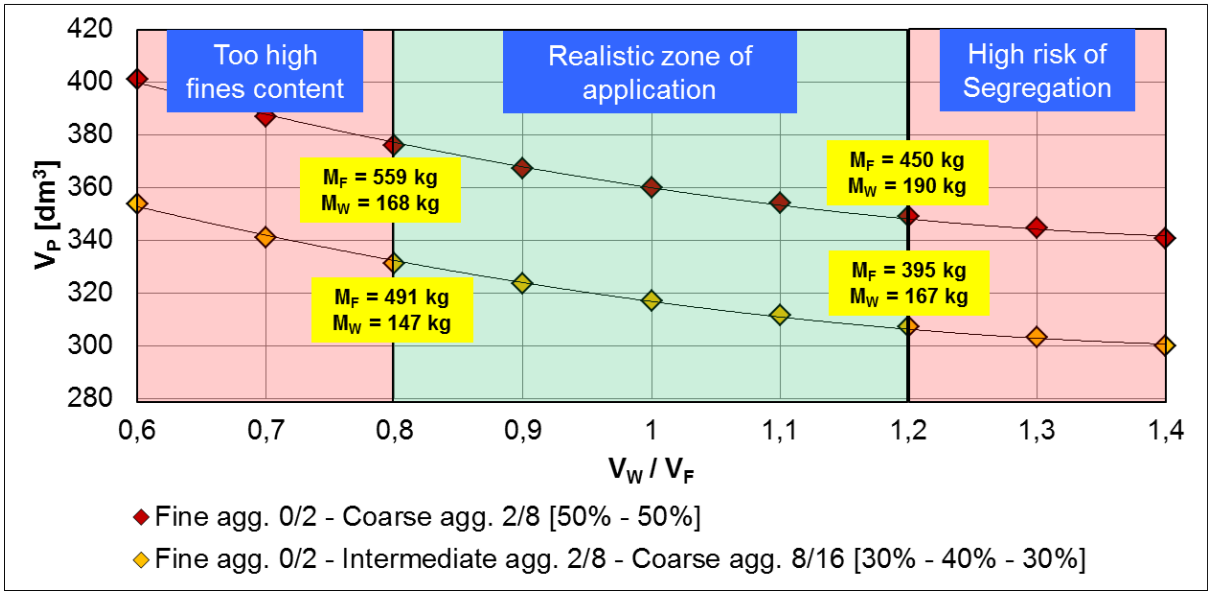

Figure 3.11: Relationship between V_G, V_W/V_F and V_P

3.3.6 Effective water demand of fines

The amount of water in a concrete composition is among the most decisive factors that affect the stability and flowability properties. In general, flowable concretes are produced using high-range water reducing admixtures (HRWRA), usually of PCE types. In fact according to EN 206-1; concretes with a consistency class of F4 and above have to be produced using HRWRA [10]. In most practical applications, PCE is added to the concrete with the aim of achieving the required consistency, without any regard to its effect on the stability. However, exceeding the “right” amount of HRWRA could also have an adverse effect on the stability by creating or increasing the amount of unbound water in a concrete as illustrated in Figure 3.12.

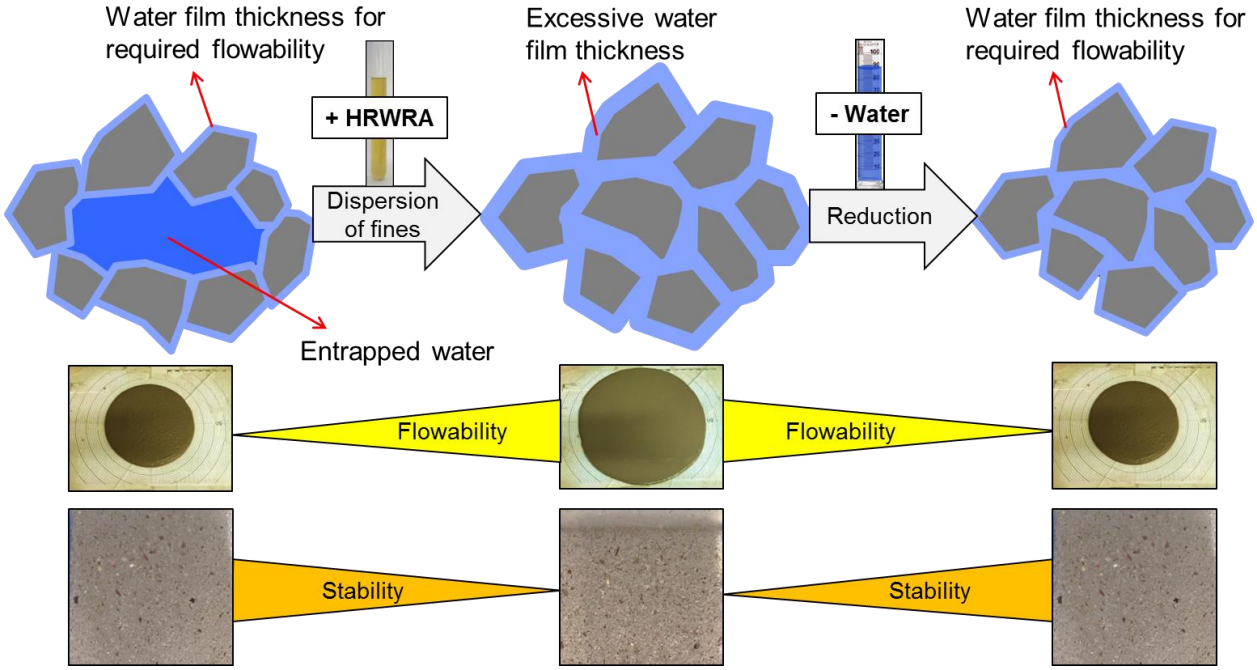

Figure 3.12: Effect of HRWRA on the flowability and stability

Considering the paste phase, when fines are mixed only with water, they form a flocculent-structure within which part of the water gets entrapped. This entrapped water does not readily contribute to the flowability of the paste. However, the addition of HRWRA causes electrostatic and / or steric repulsions, thereby dispersing the individual fine particles [170]. This action sets the water entrapped within the agglomerates free. As a result, the water film thickness around the particles increases ultimately resulting into increased flowability. However, a simultaneous reduction in stability is also to be expected as a consequence of the destruction of the interparticle structure of the flocs and the potential reduction in the viscosity and yield stress of the mix by virtue of the existence of more unbound water in the paste. Hence, if the aim is to achieve a good flowability while maintaining good stability, the

addition of HRWRA paves the way for the reduction of a certain amount of water that would otherwise lead to segregation or sedimentation of the paste while leaving enough of it to form the required film thickness and achieve the desired flowability. However, one should also consider the water demand of the aggregates which is directly correlated with the paste demand required for coating and separation of the aggregates as explained in section 3.3.4. As such, the extra potentially "harmful" water in the paste which comes into being as a result of the addition of HRWRA is not necessarily harmful to the concrete as long as this extra water is bound by the aggregates. In fact, on the basis of the three phase consideration consisting of aggregates, paste and air void phases, the paste composition in a flowable concrete is almost always unstable since the water that is normally bound by the aggregates is accounted for as part of the paste phase. Nonetheless, avoiding any unbound water in the concrete is of paramount importance in order to guarantee its stability. This requires, determining the right Water – HRWRA combinations by considering the water demand of the whole solid particles in a concrete from micro fines up to the maximum aggregate size. The aim of the design concept is, thus, maintaining a zero water-balance in the concrete by comparing the amount of free-water in the paste phase ($V_{W,P}$) with the water demand of the aggregates' surface ($V_{W,S}$). The free-water volume ($V_{W,P}$) is the amount of water which is effectively saved due to the addition of HRWRA to a reference paste composition while maintaining a constant mini-slump flow. This is determined by experimental investigation of the effective water demand of the fines in accordance with the method developed by Okamura [171].

- According to Okamura, the water demand of the fines depends on the amount (V_F) and composition (V_{Fi}/V_F) of the fines; [$\beta_P = V_W/V_F = f(V_F, V_{Fi}/V_F)$]
- According to WBMD, the water demand of the fines depends on the amount (V_F) and composition (V_{Fi}/V_F) of the fines as well as the amount and type of HRWRA (V_{SP}) used; [$\beta_E = V_W/V_F = f(V_F, V_{Fi}/V_F, V_{SP})$]

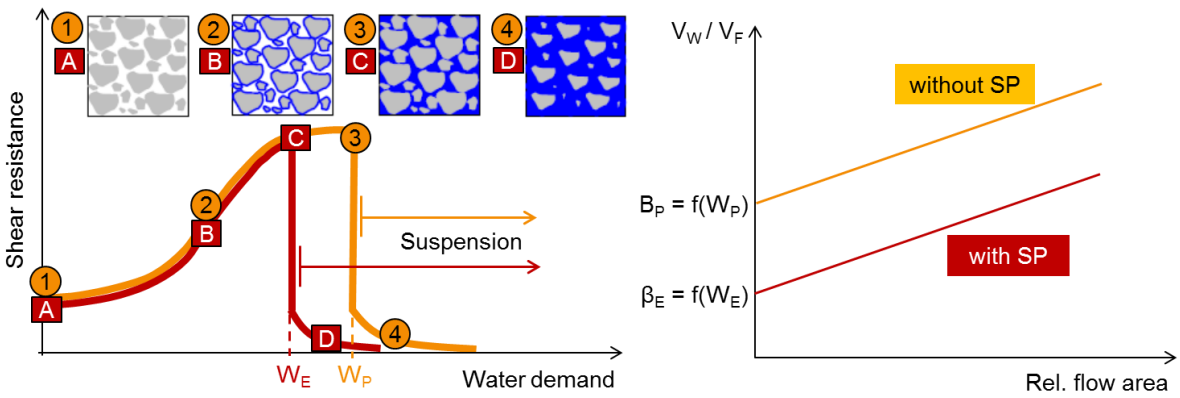

Figure 3.13: Basic water demand (β_P) and effective water demand (β_E) of fines for the formation of suspension

On the basis of the description by Kordts and Grube with regard to the formation of a suspension composed of only water and fines [172], the following postulations as illustrated in Figure 3.13 are proposed for the WBMD considering the role a HRWRA plays in the process. The formation of a flowable suspension requires a complete saturation state at which enough water is available for covering the surface of the fines and for filling the void spaces between them. In the dry state (1 & A) and even when water film is formed around the particles as a result of the increase in water content (2 & B), the shear resistance could be expected to remain relatively the same whether HRWRA is added or not. This is due to the fact that without enough water in the system, the dispersion of the particles due to the addition of HRWRA would not materialize and the system remains in a flocculated state. However, the shear resistance increases with increasing water content since the mixture becomes more cohesive. Further increase in the water content would then lead to an abrupt fall in the shear resistance which designates the saturation state. The addition of HRWRA would bring about a significant difference in this regard. Because of the dispersion effect of the HRWRA, the water could be used more effectively for filling the voids and coating the surface of the particles. Thus, the water demand for the formation of a suspension or reaching the saturation state generally decreases when HRWRA is use as depicted by point C and point 3 for paste suspensions with and without HRWRA respectively. For convenience, the water demand with HRWRA is called here as effective water demand, β_E. The procedure for determining β_E is similar to the classical Okamura method with the only difference being that the average slump flow diameter and not the relative flow area is considered for the calculation.

$$D_0 = D_1 + D_2 \tag{3.17}$$

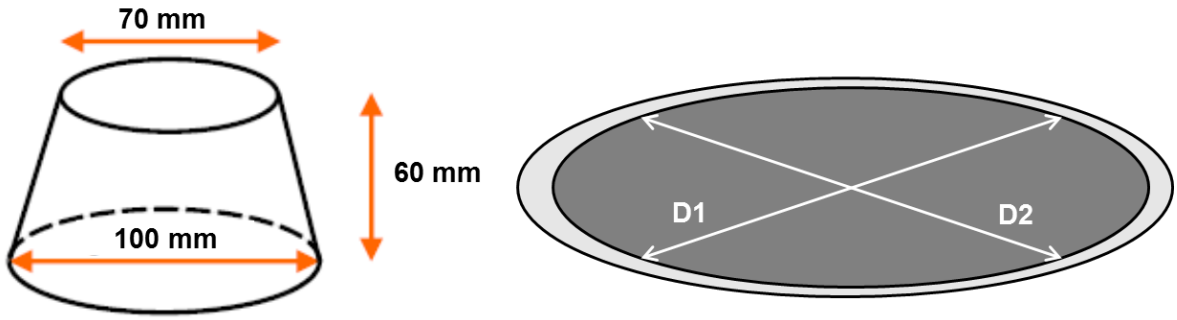

Figure 3.14: Determination of the slump flow of pastes using the mini slump cone

The effect of SP on the slump flow of the paste is as such that at the beginning it increases almost linearly with the SP content. This is followed by a transition zone where the increment in the slump flow starts to decrease until the saturation point is reached. No significant increment in slump flow would be observed after the saturation point is reached [173] [33]. For the determination of β_E at different contents

of SP, a linear regression is formulated in the first linear increment zone using three or more points. The V_W/V_F value, which is determined by extrapolating the regression line up to the 10 cm slump flow, could be considered as the effective water demand β_E. This represents theoretically the state at which the slump cone, which also has a bottom diameter of 10 cm, is filled with a paste that is just completely saturated but has not yet started to flow.

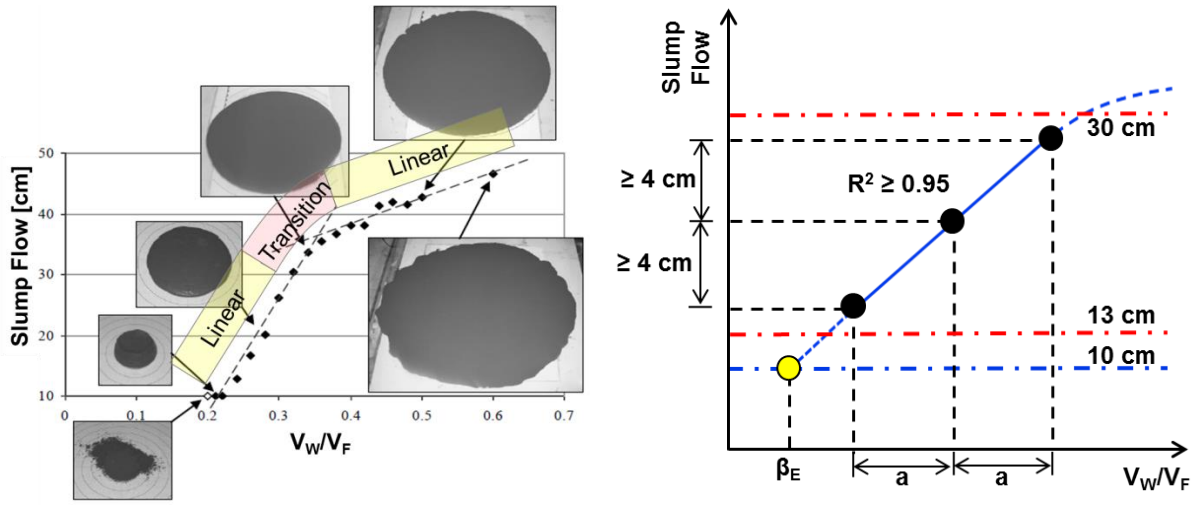

Figure 3.15: Determination of the effective water demand of fines

In order to attain reliable test results, a set of limitations are defined for the determination of the slump flow as shown in Figure 3.15 .

- The slump flow values should fall in the range between 13 cm and 30 cm.
- For a constant SP content, the V_W/V_F values have to be chosen with equal interval (a) and the corresponding points should fall within the 13 cm – 30 cm range.
- A slump flow difference of ≥ 4 cm between each point is desirable. A fourth point is recommended if the difference is less than 4 cm. In either case, the correlation of determination $R^2 \geq 0.95$ should be fulfilled.
- The effective water demand β_E is determined by extrapolating the linear regression line up to the 10 cm slump flow line.
- The β_E function is formulated by increasing the SP content at equal interval and afterwards this shall be integrated in the WBMD.

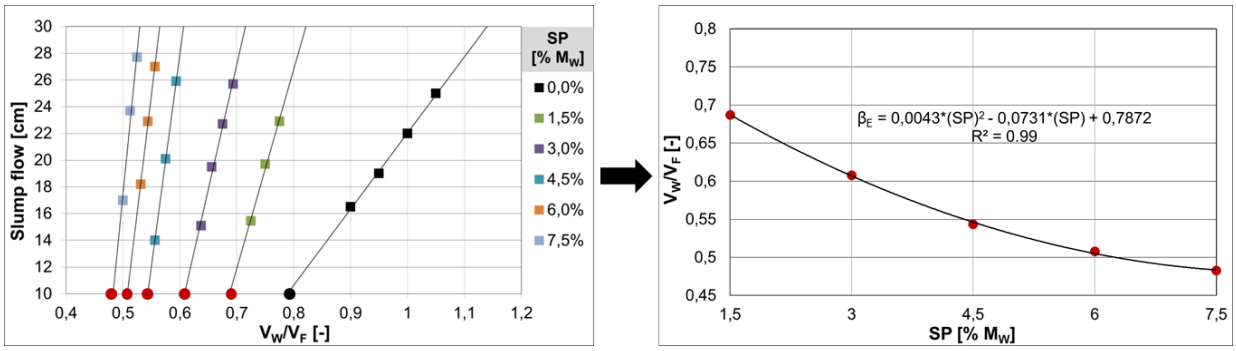

Figure 3.16: Mathematical formulation of the effective water demand of fines

By making use of the β_E function, it is possible to determine the effective water demand of the fines for an arbitrary SP content in the mix. Moreover, the theoretical saturation point of the SP could be estimated by determining the minimum value of the polynomial function. Generally, the β_E function is determined by maintaining the required w/c-ratio, which is often determined beforehand based on the hardened concrete requirements.

In the WBMD, the paste (V_P) is considered to be composed of water (V_W) and fines (V_F).

$$V_P = V_W + V_F \tag{3.18}$$

For an arbitrarily chosen $\mathbf{V_W / V_F = f}$, the amount of fines and water in the paste could be determined as follows.

$$V_P = V_W + V_F \Rightarrow V_P = V_W + \frac{V_W}{f} \Rightarrow V_P = V_W \cdot \left[1 + \frac{1}{f}\right] \tag{3.19}$$

By solving Equation (3.19) for V_W and V_F, one gets:

$$V_W = \frac{V_P}{1 + \frac{1}{f}} \text{ and } V_F = \frac{V_P}{1+f} \tag{3.20}$$

The fines are usually composed of cement (V_C) and mineral admixtures (V_{MA}). By assigning the ratio between the mineral admixture and the cement, $\mathbf{V_{MA} / V_C = x}$, one gets the following correlation:

$$V_F = V_C + V_{MA}\ ;\ x = \frac{V_{MA}}{V_C} \Rightarrow V_C = V_F - x \cdot V_C \Rightarrow V_C = \frac{V_F}{1+x}$$

$$\Rightarrow V_C = \frac{V_F}{1 + \frac{V_{MA}}{V_C}} \tag{3.21}$$

The water - cement ratio (w/c) could then be correlated with the water - fines ratio (V_W/V_F) as follows.

$$\frac{w}{c} = \frac{\rho_w \cdot V_w}{\rho_C \cdot V_C} = \frac{\rho_w \cdot V_w}{\rho_C \cdot \frac{V_F}{1+\frac{V_{MA}}{V_C}}}$$

$$\Rightarrow \frac{V_w}{V_F} = \frac{\frac{w}{c} \cdot \rho_C}{1+\frac{V_{MA}}{V_C}} \tag{3.22}$$

Even if the β_E function is formulated using a certain constant w/c-ratio, theoretically, one can also determine the effective water demand for other w/c-values by establishing a correlation between V_W/V_F and V_{MA}/V_F as shown in Equation (3.23).

$$\frac{V_w}{V_F} = \frac{\frac{w}{c} \cdot \rho_C}{1+\frac{V_{MA}}{V_C}} = \frac{\frac{w}{c} \cdot \rho_C}{1+\frac{V_{MA}}{V_F - V_{MA}}} \Rightarrow \frac{V_{MA}}{V_F - V_{MA}} = \frac{\frac{V_{MA}}{V_F}}{1 - \frac{V_{MA}}{V_F}} = \frac{\frac{w}{c} \cdot \rho_C}{\frac{V_W}{V_F}} - 1$$

$$\Rightarrow \frac{V_{MA}}{V_F} = 1 - \frac{1}{\left[\frac{\frac{w}{c} \cdot \rho_C}{\frac{V_W}{V_F}}\right]} \tag{3.23}$$

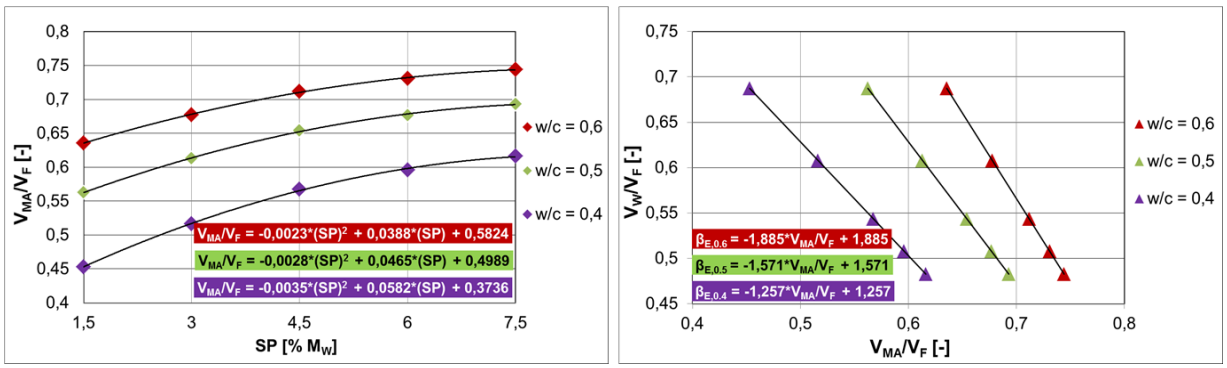

Figure 3.17: Extending the mathematical formulation for other design parameters

Illustrated in Figure 3.17 are the results of the experimental investigation for w/c = 0.6 and the extended mathematical formulations for w/c-ratios of 0.4 and 0.5. Accordingly, for any arbitrary constant w/c-ratio, the possible fines composition V_{MA}/V_F and the corresponding effective water demand (β_E) at a given SP content could be mathematically estimated. Thus, the approach provides good flexibility with regard to estimating the effective water demand (β_E) for a wider range of combinations of mix-design parameters based on the results of only one set of experimental investigations conducted using a certain w/c-ratio. In doing so, the

interactions between the individual components in a paste, namely the fines, water and SP, are also quantified indirectly through their effect on the effective water demand. The approach works satisfactorily for standard cements and the usual mineral admixtures such as fly ash and lime stone powder.

3.3.7 Checking for water balance

The integration of the β_E function in the WBMD works in such a way that first the water saved by the addition of SP is quantified and compared with the water demand of the aggregates. The amount of saved water is directly proportional to the difference between the basic and the effective water demand [$\Delta V_{W,\beta} \sim (\beta_P - \beta_E)$].

$$WB = \Delta V_{W,\beta} = (\beta_P - \beta_E) \cdot V_F \tag{3.24}$$

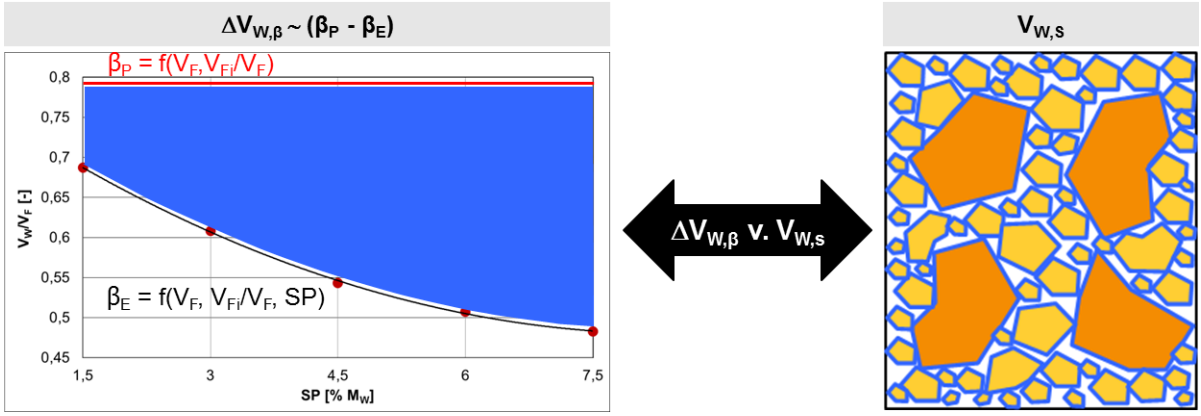

Figure 3.18: Checking the WB in a concrete

The water demand of the aggregates' surface ($V_{W,S}$) is determined using the method as explained in section 3.3.4. Reliable flowability and stability of concrete is then guaranteed when the unbound or saved water in the paste does not exceed the water demand of the aggregates, i.e. a **zero WB** ($\Delta V_{W,P} - V_{W,S} \leq 0$). A positive water-balance ($\Delta V_{W,P} - V_{W,S} > 0$) indicates excess water in the concrete which would increase the risk of bleeding, sedimentation and segregation. Now, based on Equation (3.24) and Equation (3.20), the following stability and flowability criteria could be defined.

1. $\Delta V_{W,\beta} = V_{W,S}$: Unbound water in the paste is equal to water demand of aggregates
   - No unbound water in the concrete and thus the stability is guaranteed.
   - The desired flowability could be achieved by increasing the SP content up to the saturation point, SP_{Max}.
   - The volume and composition of the optimized aggregates remains constant.

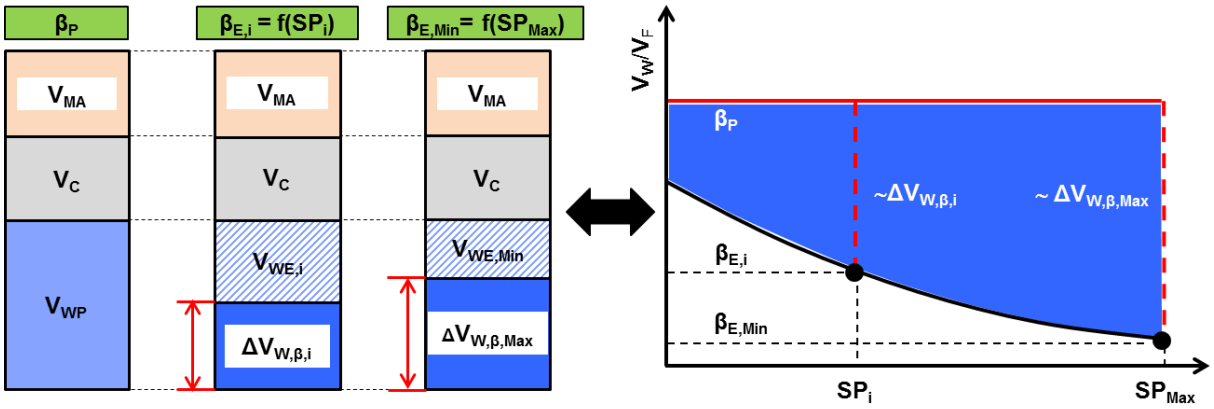

Figure 3.19: Case 1: Fulfilling the flowability and stability by adjusting the SP content to a zero WB.

It should be noted that, in most cases, the amount of water saved through the addition of SP even up to the saturation point ($\Delta V_{W,\beta,Max}$) is inadequate to cover the complete water demand of the aggregates ($V_{W,S}$). Thus, a very high amount of paste might be required to satisfy this requirement so that the amount of paste required for aggregate separation would be readily available. However, by virtue of the relatively small V_W/V_F ratio and the corresponding high amount of paste, a flowable concrete designed in such a way often contains very high amount of fines which renders it more or less the characteristics of a powder rich SCC. While this is advantageous in terms of the workability aspects, the economic viability and the robustness of the mixture would remain rather questionable.

2. $\Delta V_{W,\beta,Max} < V_{W,S}$: Unbound water in paste is less than water demand of aggregates
    - No unbound water in the concrete and thus the stability is guaranteed.
    - The desired high flowability might not be achieved even at the SP's saturation point, SP_{Max}.
    - A higher V_W/V_F ratio than the β_P should be chosen while maintaining the w/c-ratio constant.
    - The volume and composition of the optimized aggregates remain unchanged.

If the aim is to design a highly flowable concrete of consistency class of F5 / F6, it is recommended to adopt a realistic V_W/V_F value higher than β_P with a factor of 1.2 – 1.4 should be adopted; i.e. $V_W/V_F \approx 1.2 \times \beta_P - 1.4 \times \beta_P$ as a starting parameter for the WBMD. Higher values of V_W/V_F could potentially increase the risk of segregation and inhomogeneity of concrete especially if there is a slight discrepancy in the water or SP dosages.

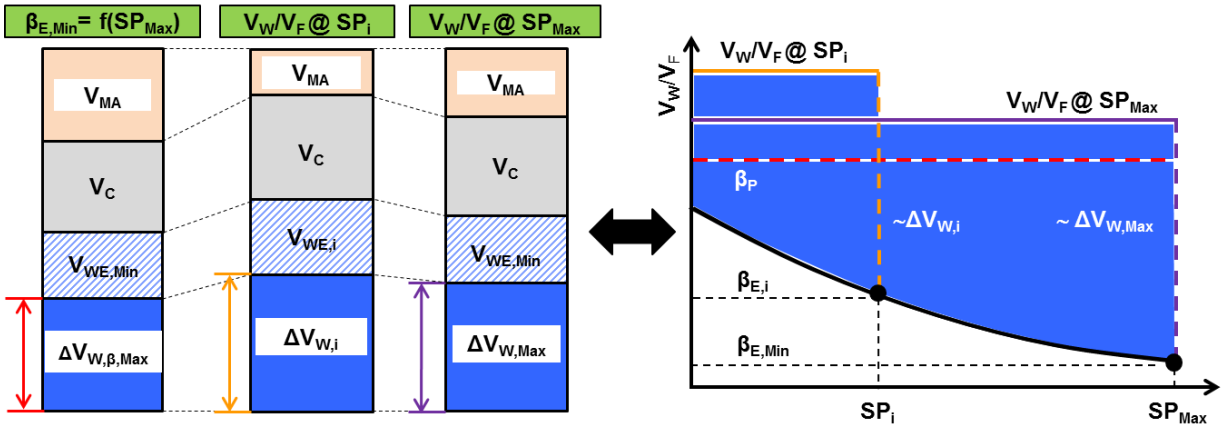

Figure 3.20: Case 2: Fulfilling the flowability and stability by adjusting the V_W/V_F ratio and the SP content to a zero WB.

This option is the more flexible and realistic in that the V_W/V_F ratios and the SP content could be adjusted in a combined manner until the flowability and stability requirements are met. In doing so, the hardened concrete requirements as stipulated in the specifications such as [10] could be addressed by maintaining the minimum w/c-ratio, the minimum cement content as well as the maximum fines content. Moreover, the economic aspects with regard to the amount of fines in the concrete could also be managed.

As far as the mix design of a flowable and stable concrete using the WBMD is concerned, the following strategical precedencies are to be preferred.

I. Aggregate optimization with the aim of maximizing the lattice effect and thereby the stability
II. Determining the right amount of paste for flowability.
III. Choosing a realistic V_W/V_F ratio > β_P so that the total amount of paste and the resulting fines content remains reasonable.
IV. Using SP up to the saturation point to achieve the required flowability while avoiding unbound water in concrete.

The conceptual Model of the WBMD including the methodologies applied at each relevant scale of phases is presented in Figure 3.21.

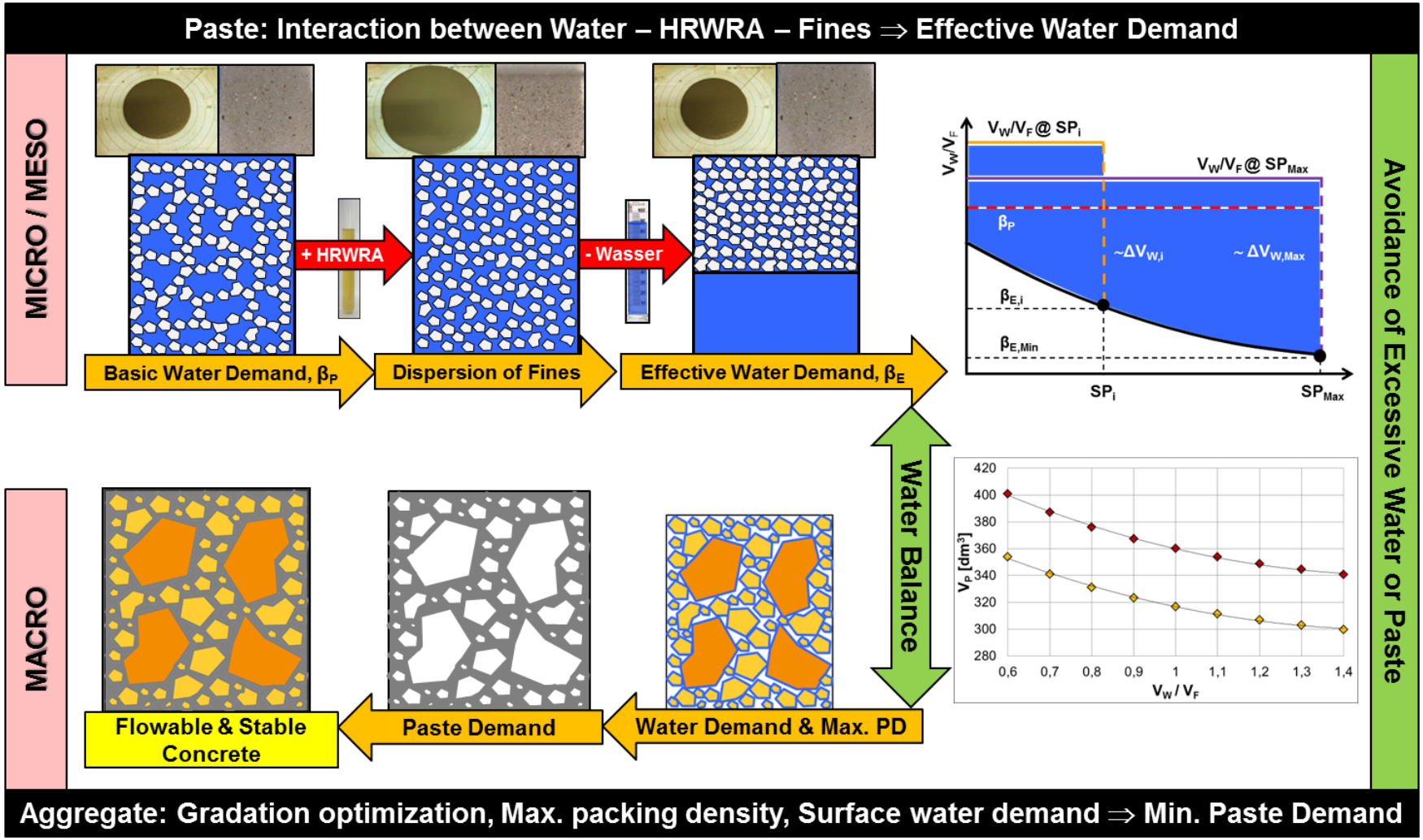

Figure 3.21: Conceptual Model of the WBMD

3.4 Short summary

I. The WBMD combines the main constituent materials of concrete compositions in such a way that the normally conflicting fresh concrete requirements – flowability and pumpability on the one hand, and stability and robustness on the other – could simultaneously be fulfilled. This is achieved through:
   - Aggregate optimization with the aim of maximizing the lattice effect and thereby the stability.
   - Determining the right amount of paste for the optimized aggregate composition.
   - Choosing a realistic V_W/V_F ratio > β_P so that the total amount of paste and the resulting fines content remains reasonable.
   - Using SP up to the saturation point to achieve the required flowability while avoiding unbound water in concrete.

II. The aggregate optimization could be done using a generalized reduced gradient (GRG2) non-linear algorithm on the basis of ideal particle distribution functions such as the one developed by Andreasen and Andersen. The optimized aggregate gradation curves should fall within the favorable zone between the standard gradation lines A and B, ideally between AB and B.

III. The total paste demand of the optimized aggregate is the sum of the paste amount required to fill the voids between the aggregates ($V_{P,V}$) and to coat their surface ($V_{P,S}$). $V_{P,V}$ is a function of the maximum packing density as determined using a compaction test set up applying vibration and loading. $V_{P,S}$ is derived from the water demand of the aggregates ($V_{W,S}$) as determined using the filter press and water-jet pump.

IV. The difference between the realistically chosen V_W/V_F ratio, which should be higher than the basic water demand (β_P), and the effective water demand of the fines (β_E) represents the free unbound water in the paste ($\Delta V_{W,P}$). For the realistic V_W/V_F ratio, the WBMD makes sure that the SP content is chosen in such a way that the unbound water in the paste ($\Delta V_{W,P}$) does not exceed the water demand of the aggregates ($V_{W,S}$). The flowability and stability are guaranteed simultaneously as long as $\Delta V_{W,P} - V_{W,S} \leq 0$.

V. The WBMD guarantees the stability and robustness of flowable and pumpable concretes through maximization of the lattice effect (aggregate optimization) and maintaining the right balance between the amount and composition of the paste. This ensures the avoidance of excessive paste, water or SP which would otherwise lead to concrete compositions possessing poor stability and robustness.

Chapter 4
Experimental Investigations

4.1 Short introduction

In this chapter, the experimental conception with regard to the mixture compositions as well as the applied investigation methods and evaluation techniques is presented. The approach as to the incorporation of the characteristic parameters of the component materials in designing the water balanced concretes (WBC) is explained. The results of the experimental investigations with respect to the fresh concrete properties including the flowability, pumpability, stability (under vibration and pressure) and robustness are illustrated. Similarly, the results of the rheological investigations on different types of concrete mixtures as well as the extracted mortar and paste compositions are presented. The experimental results are accompanied by detailed analysis as to the effects of the component materials and the chosen design parameters on the fresh concrete and rheological properties.

4.2 Materials

The following materials whose parameters and compositions are listed in Table 4.1 were used for the experimental investigations.

- Cements: CEM I 42.5 N and CEM III/A 42.5 N-NA
- Mineral admixtures: three types of fly ashes, limestone and trass powders
- Chemical admixtures: two types of SP
- Aggregates: natural sand 0/2 mm; normal natural gravels 2/8 mm and 8/16 mm; flaky natural gravel 2/8 mm and crushed aggregates 2/8 mm.

Table 4.1: Material properties and compositions

Cements			Parameters			Grain Sizes Distribution
Material Type	Id.	Foto	ρ g/cm³	D_{50} µm	Blaine cm²/g	
CEM I 42.5 N	CEM I		3.14	18.7	3100	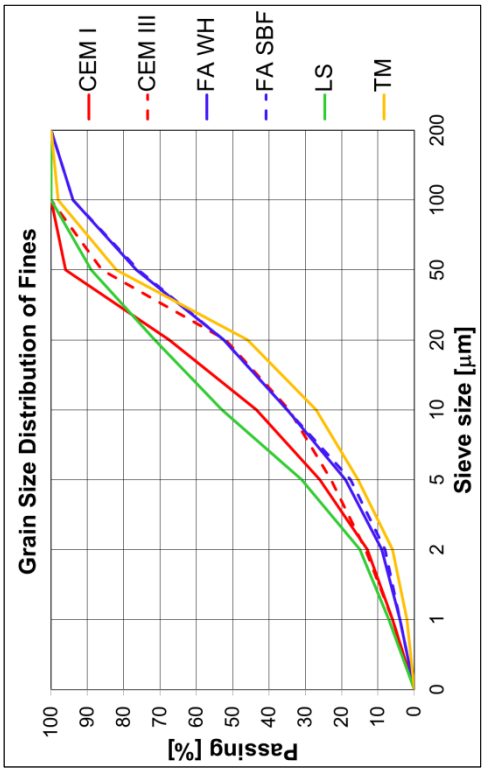
CEM III/A 42.5 N NA	CEM III		3.05	12.9	3880	
Mineral Admixtures			ρ g/cm³	D_{50} µm	Blaine cm²/g	
Fly ash EFA-Füller WH	FA WH		2.31	18.5	3120	
Fly ash EFA-Füller S-B/F	FA SBF		2.28	18.3	3190	
Limestone Powder KSM 60/3	LS		2.73	9.1	4140	
Fly ash EFA-Füller HP	FA HP		2.26	-	-	
Trass Powder Tubag	TR		2.52	23.2	5000-8000	
Chemical Admixtures			ρ g/cm³	Special features	Recommended consistence class	Dosage % M. of Cement
HRWRA Glenium Sky 594	GL 594	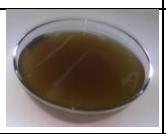	1.05	PCE based	F3 - F6	0.2 - 3.0
WRA Glenium SKY 188	GL 188		1.11	Lignosulfonate based	F2 - F5	0.2 - 1.5
Water			Tap water from the city of Hannover			

Table 4.1: Material properties and compositions (contd.)

Aggregates			ρ	Size range	Shape / Texture	Water Demand	Grain Sizes Distribution
Material	Id.	Foto	g/cm³	mm		% $V_{agg.}$	
Natural Sand	NS		2.66	0/2	Regular / Normal	22.5	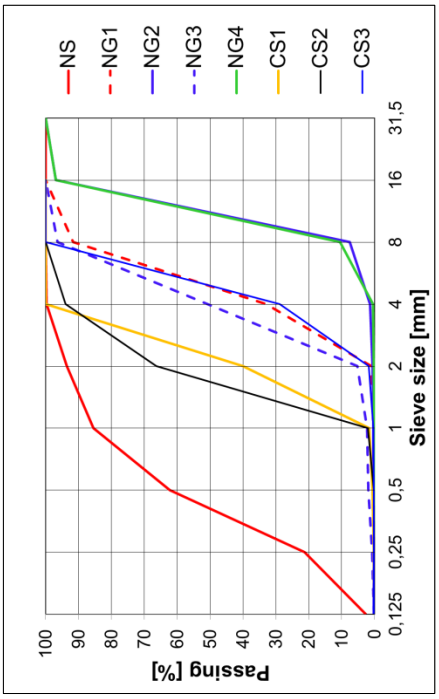
Round Natural Gravel	RG1		2.59	2/8	Regular / Normal	12.3	
Round Natural Gravel	RG2		2.60	8/16	Regular / Normal	6.5	
Flaky Natural Gravel	FG		2.63	2/8	Flaky / Normal	13.1	
Crushed Gravel	CG		2.67	2/8	Irregular / Rough	11.0	

4.3 Experimental conception

The experimental conception begins with characterization of the constituent materials for determining the input parameters for the water balance mix design (WBMD). This includes the determination of the basic (β_P) and effective water demand (β_E) of the fine compositions as well as the packing density and water demand of the aggregates, which later are used for the determination of the minimum paste demand (V_P) of the aggregates. These input parameters are used to produce different water balanced concrete (WBC) composed of different paste and aggregate compositions.

These WBC are then characterized for their flowability, pumpability, stability (under vibration and pressure) and robustness. In addition, extensive rheological investigations are conducted on the concrete mixtures as well as the extracted paste and mortar compositions. The experimental conception describing the stepwise approach is schematically illustrated in Figure 4.1.

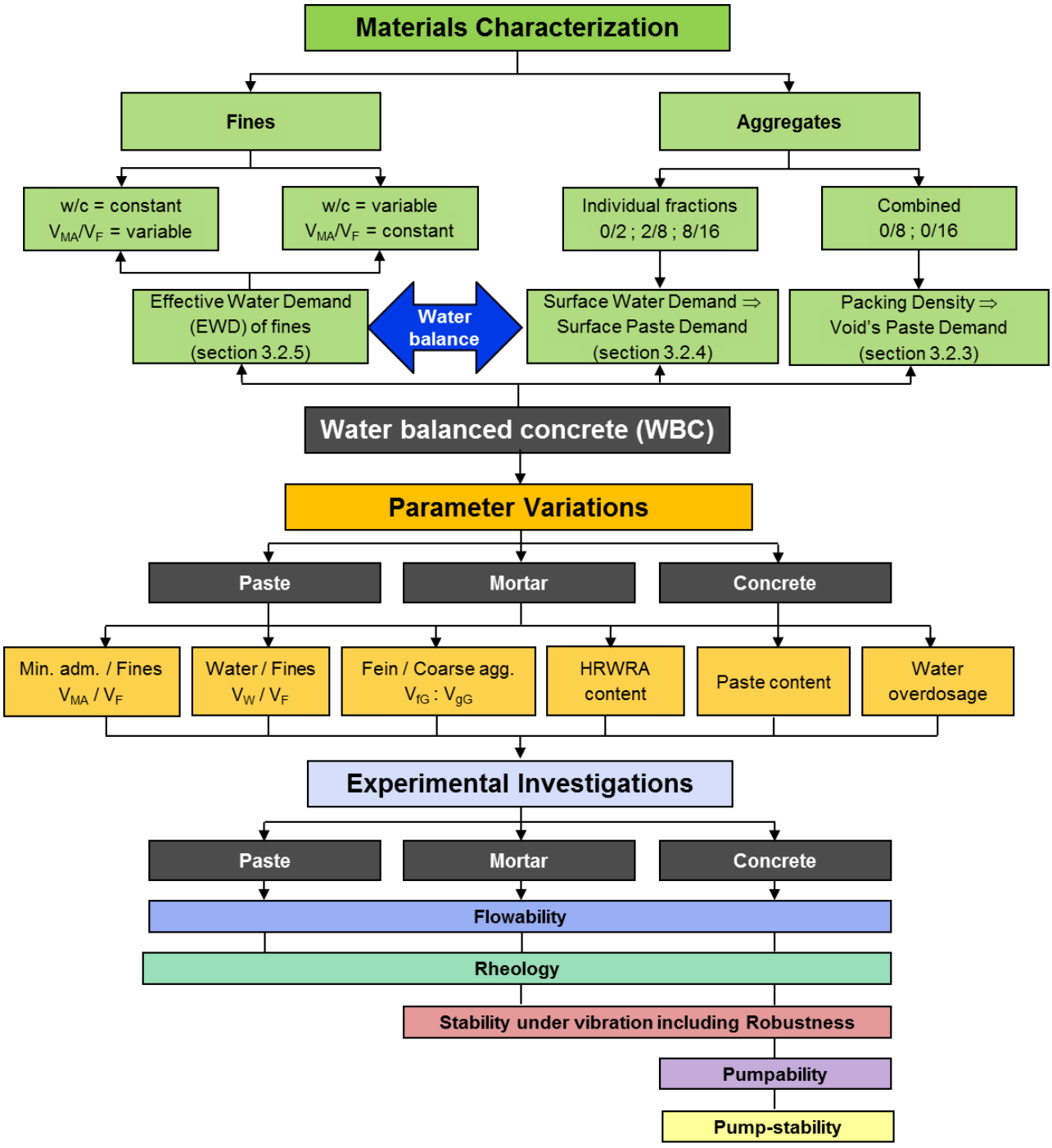

Figure 4.1: Schematic representation of the experimental conception

4.4 Preparation of mixtures

The mixing procedures for the concrete, mortar and paste compositions are summarized in Table 4.2.

Table 4.2: Mixing procedures for the concrete, mortar and paste

Duration [s]	Process	Intensity	Used Mixers
Concrete			
0 - 30	Dry mixing of solid materials	Constant	
30 - 60	Dosage of mixed water & SP		
60 - 210	Further mixing		
210 - 240	Pause		
240 - 420	Further mixing		
Mortar			
0 - 15	Dry mixing of solid materials	Low	
15 - 30	Dosage of mixed water & SP	Low	
30 - 90	Further mixing	Low	
90 - 120	Pause	-	
120 - 300	Further mixing	High	
Paste			
0 - 15	Dry mixing of solid materials	Low	
15 - 30	Dosage of mixed water & SP	Low	
30 - 90	Further mixing	Low	
90 - 120	Pause	-	
120 - 240	Further mixing	High	

4.5 Materials characterization

The material characterization is the basis from which the input parameters for the WBMD are determined. This involves determination of the effective water demand of the fines as well as determination of the packing density and water demand of the aggregates.

4.5.1 Effective water demand of fines

The effective water demand (β_E) of the fine compositions was determined on the basis of the method introduced in 3.3.6. The materials and parameters used for this investigation are shown in Table 4.3. The following factors were considered in order to investigate their effect on $\boldsymbol{\beta_E}$.

- Type of cement
- Type of mineral admixtures
- Composition of fines (V_{MA}/V_F)
- Type and amount of SP

Table 4.3: Parameters and material compositions for determining β_E

Parameter		**Fines Composition**		**SP**	
w/c	V_{MA}/V_F	Cement	Mineral Admixture	Type	Content [% M_W]*
0.6	variable	CEM I	FA WH	SP1	0%, 1.5%...7.5%
			FA SBF		
			FA HP		
			LS		
			TR		
		CEM I	FA SBF	SP2	
		CEM III	FA WH	SP1	
variable	0.2	CEM I	FA SBF	SP1	
	0.3				
	0.4				
	0.5				

* The SP content is calculated as a percentage of mass of water.

I. Effect of Type of Cement

The cement types used in the investigation seems to make not that much of a difference in $\boldsymbol{\beta_E}$, regardless of the mineral admixture that they are combined with as illustrated in Figure 4.2. In terms of the specific surface area, the CEM III particles (a = 3880 cm^2/g) should have a higher $\boldsymbol{\beta_E}$ than the CEM I (a = 3100 cm^2/g). The fact that $\boldsymbol{\beta_E}$ remains relatively the same could be attributed to the slag particles in the CEM III with their glassy texture and higher negative zeta-potential which is generally favourable for dispersion of the particles ultimately leading to a decreased water demand [151].

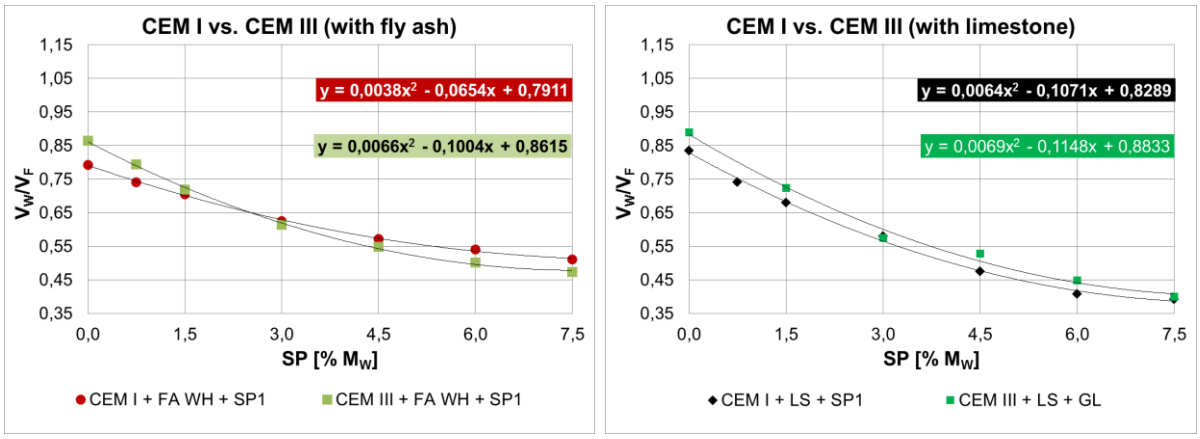

Figure 4.2: Effect of type of cement on β_E (w/c = 0.6, V_{MA}/V_F = variable)

II. Effect of Type of Mineral Admixture

Usage of different fly ashes does not seem to significantly influence $\boldsymbol{\beta_E}$ as can be seen in Figure 4.3, left, the reasons being the relatively similar fineness and probably shape of the fly ash particles. On the contrary, the combinations of CEM I with the fly ash, limestone and trass powders exhibit completely different $\boldsymbol{\beta_E}$; see Figure 4.3, right. The TR (a > 5000 cm^2/g) is significantly finer than the FA (a = 3120 cm^2/g) and as a result, its composition has considerably higher $\boldsymbol{\beta_E}$. The LS (a = 4140 cm^2/g) is also finer than the FA (a = 3120 cm^2/g).

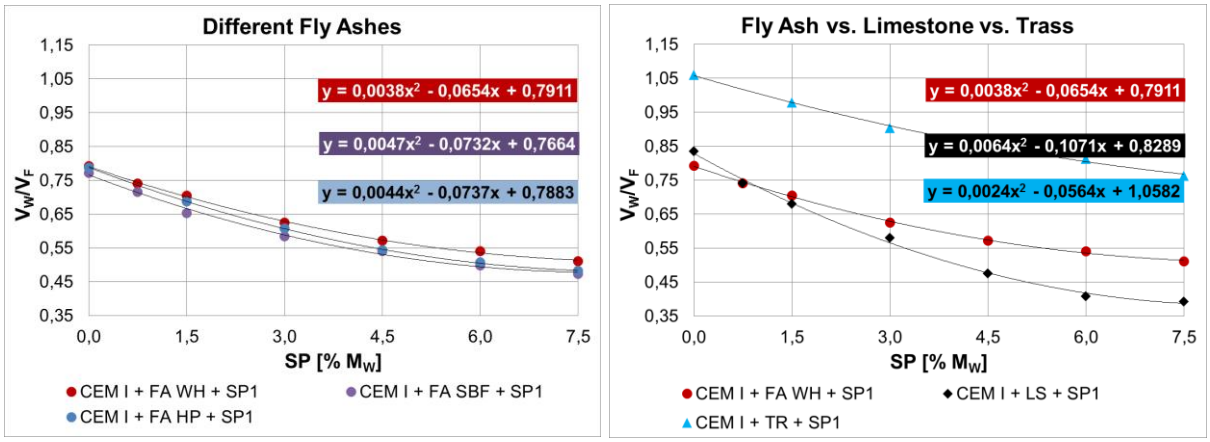

Figure 4.3: Effect of type of mineral admixtures on β_E (w/c = 0.6, V_{MA}/V_F = variable)

However, for the most part, the LS composition has a lower $\boldsymbol{\beta_E}$ when compared to the FA composition. This reveals that $\boldsymbol{\beta_E}$ is not always a function of the fineness or specific surface area but also of ϕ. The LS particles (D_{50} = 9 µm) are much smaller than the FA particles (D_{50} = 18.5 µm). Thus, when combined with the CEM I particles (D_{50} = 18.7 µm), the LS is able to fill the voids more effectively than the FA particles. The resulting higher packing density ultimately leads to a decreased $\boldsymbol{\beta_E}$.

III. Effect of Fines Composition

Changes in the fines composition also do not seem to have significant effect on $\boldsymbol{\beta_E}$ as illustrated in Figure 4.4. Here, while an increase in V_{MA}/V_F has generally led to a decreased $\boldsymbol{\beta_E}$, the difference is not as significant as the case for different types of admixtures. However, it should be noted that the fly ash (FA WH) used here have a relatively similar fineness and grain size distribution with the cement (CEM I) which might be the reason for the observed small differences.

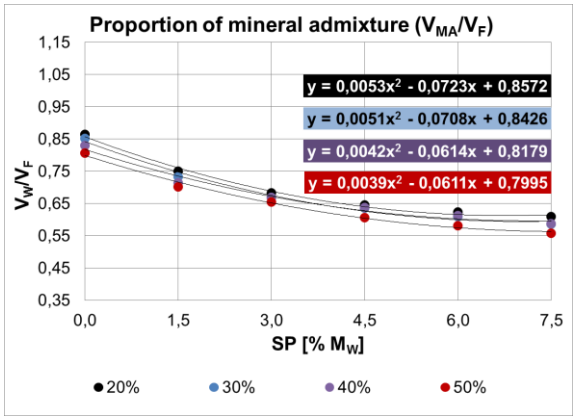

Figure 4.4: Effect of fines composition on the β_E (w/c = variable, V_{MA}/V_F = constant)

IV. Effect of type of SP

Depending on the performance of the type of SP, $\boldsymbol{\beta_E}$ could also differ significantly. As can be seen in Figure 4.5 , the high performance HRWRA (SP1) has led to a significant reduction in the $\boldsymbol{\beta_E}$ when compared to the WRA (SP2).

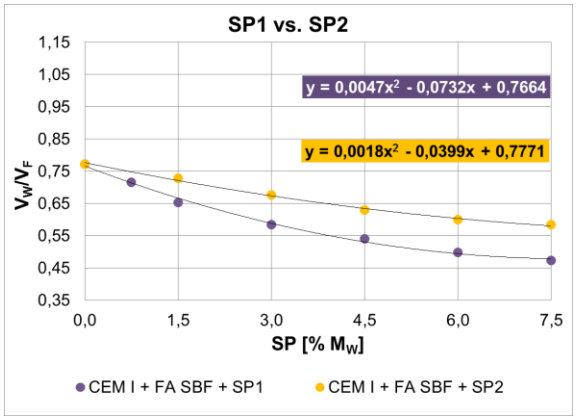

Figure 4.5: Effect of SP on the β_E (w/c = variable, V_{MA}/V_F = constant)

4.5.2 Determination of packing density (voids' paste demand) and water demand (surface paste demand) of aggregates

The effects of different aggregate compositions and properties on the packing density (ϕ) and the corresponding voids' paste demand as well as the water demand and the corresponding surface paste demand were investigated using the method as explained in section 3.3.3 and section 3.3.4 focusing on the following factors.

- Aggregate gradation: fine – coarse proportions
- Aggregate fractions: fine (0/2), intermediate (2/8), coarse (8/16)
- Maximum aggregate size and size range: 0/8 and 0/16 mm
- Type of aggregate: natural, crushed, round, flaky, irregular

Table 4.4: Composition of aggregates

Aggregate combination	**Exponent [q]**	**Mass proportions***				
		%				
	-	NS	RG1	RG2	FG	CG
NS	-	100	-	-	-	-
RG1	-	-	100	-	-	-
RG2	-	-	-	100	-	-
NS – RG1 (0/2 – 2/8)	0.3	70	30	-	-	-
	0.4	60	40	-	-	-
	0.5	50	50	-	-	-
	0.6	40	60	-	-	-
	0.8	30	70	-	-	-
	1.0	20	80	-	-	-
NS – RG1 – RG2 (0/2 – 2/8 – 8/16)	0.4	45	33	22	-	-
	0.5	35	38	27	-	-
	0.6	27	41	32	-	-
	0.7	21	42	37	-	-
NS – FG (0/2 – 2/8)	-	50	-	-	50	
NS – CG (0/2 – 2/8)	-	50	-		-	50

* The same natural sand (NS) is used for the aggregate combinations.

The reliability of the test method developed for the determination of ϕ was first checked by conducting a test series employing two different laboratory personnel. As

can be seen in Figure 4.6, the results calculated from the two test series for different NS – RG1 combinations are virtually the same confirming its reliability. The results are generated by conducting the test three times for each aggregate combination and taking the average values.

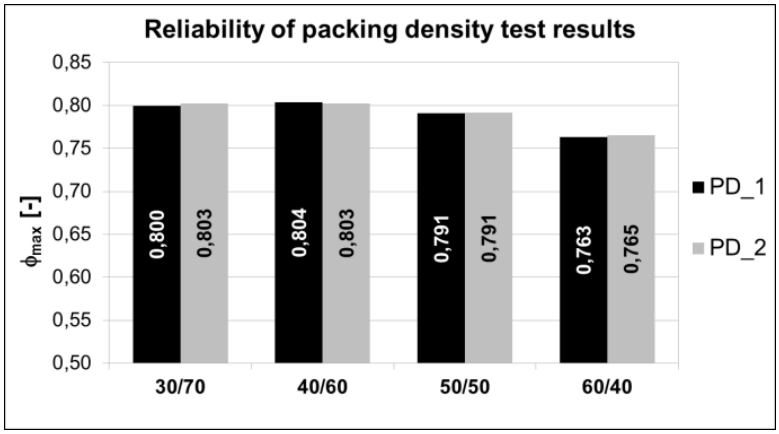

Figure 4.6: Proof of reliability of the packing density test method using two different lab personnel

I. Effect of aggregate gradation

Figure 4.7 illustrates the results of the investigations in relation to the effect of gradation using the natural sand – natural gravel compositions NS – RG1 (0/8) and NS – RG1 – RG2 (0/16) with different fine - coarse proportions. The aggregate combinations were determined by taking the effects of the changes that occur in the aggregate gradation due to different values of the gradation exponent **q**. Generally, a decrease in the exponent **q** leads to an increase in the 0/2 fractions and a simultaneous reduction in the 2/8 and 8/16 fractions, the reduction in the 8/16 fraction being relatively higher. However, for the purpose of comparison, the 0/16 aggregate combinations were composed in such a way that the 0/2 fractions increase, while the 2/8 fraction decrease with the 8/16 fraction remaining constant and vice versa. As can be seen from the diagrams in Figure 4.7, the packing density for the 0/8 compositions generally remain high for the fine – coarse proportions 30/70 – 50/50. The extreme fine - coarse proportions (20/80, 60/40 and 70/30), which lie well outside the favourable zone have led to a significant reduction in the packing density, thereby leading to a high voids' paste demand. The water demand and the corresponding surface paste demand increase almost linearly with an increase in the fine - coarse proportions. For the realistic aggregate proportions 30/70 – 50/50, the difference in the surface's paste demand is relatively higher than the voids' paste demand.

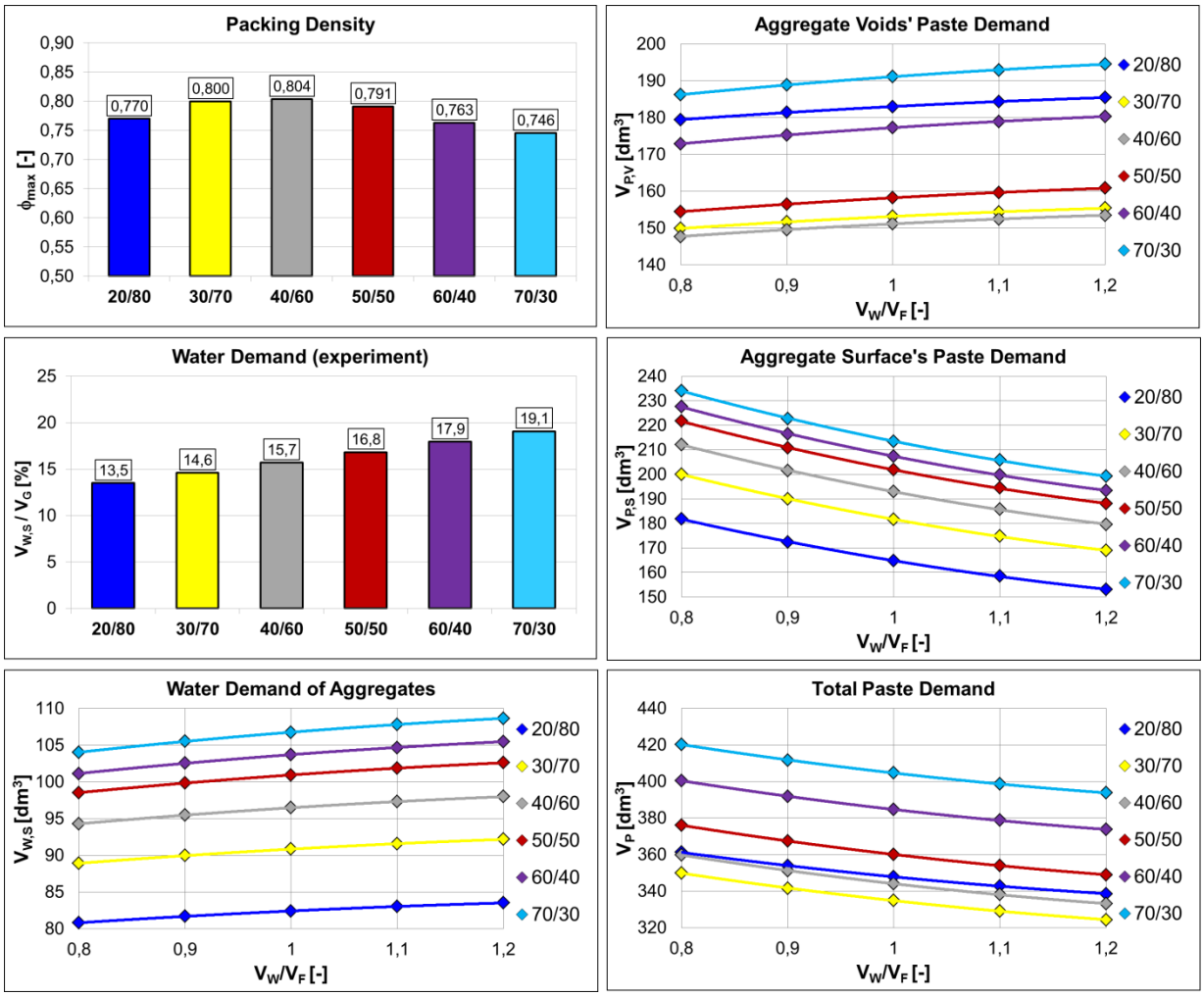

Figure 4.7: Effect of aggregate gradation: size range 0/8

Similarly, assuming a V_W/V_F = 1.0 for the 0/16 aggregate composition as shown in Figure 4.8, the gradation lines lying outside or on the periphery of the favorable zone with q = 0.4 (45/33/22) and q = 0.7 (21/42/37) are characterized by lower packing density / higher voids' paste demand. However, the total paste demand for the aggregate composition with q = 0.4 is much higher than for q = 0.7 as consequence of its higher surface paste demand. Generally, the water demand / surface paste demand increase with decreasing values of **q** or increasing fine - coarse proportions. These same trends were also observed for aggregate compositions with maximum size of 16 mm, where the 0/2 fraction increased with the 8/16 fraction decreasing while the 2/8 fraction remained constant.

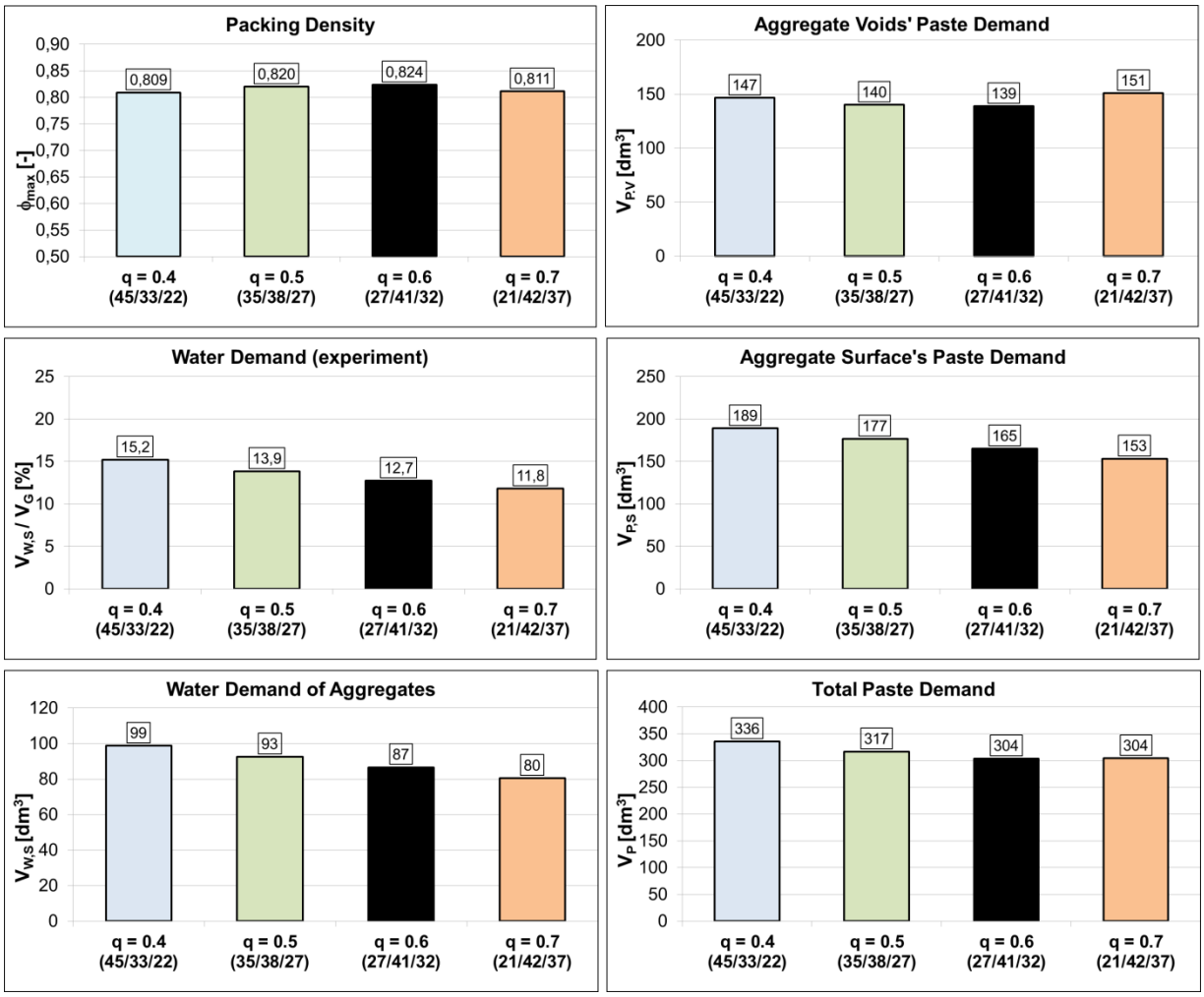

Figure 4.8: Effect of aggregate gradation: size range 0/16

Similar investigation results with regard to the effects of grain size and size range as well as the type of aggregates is documented in Appendix A-2.

4.6 Composing water balanced concretes

After the materials characterization, i.e. determining the effective water demand (β_E) of the fines and the surface water demand ($V_{W,S}$) as well as the total paste demand (V_P) of the optimized aggregate compositions, the next step is to apply them as input parameters for the production of a WBC. For this purpose, $\boldsymbol{\beta_E}$ for the CEM I + WH fine compositions and $\boldsymbol{V_P}$ of the NS – RG1 aggregate compositions with proportions of 50 : 50 corresponding to the Fuller exponent q = 0.5 shall be adopted.

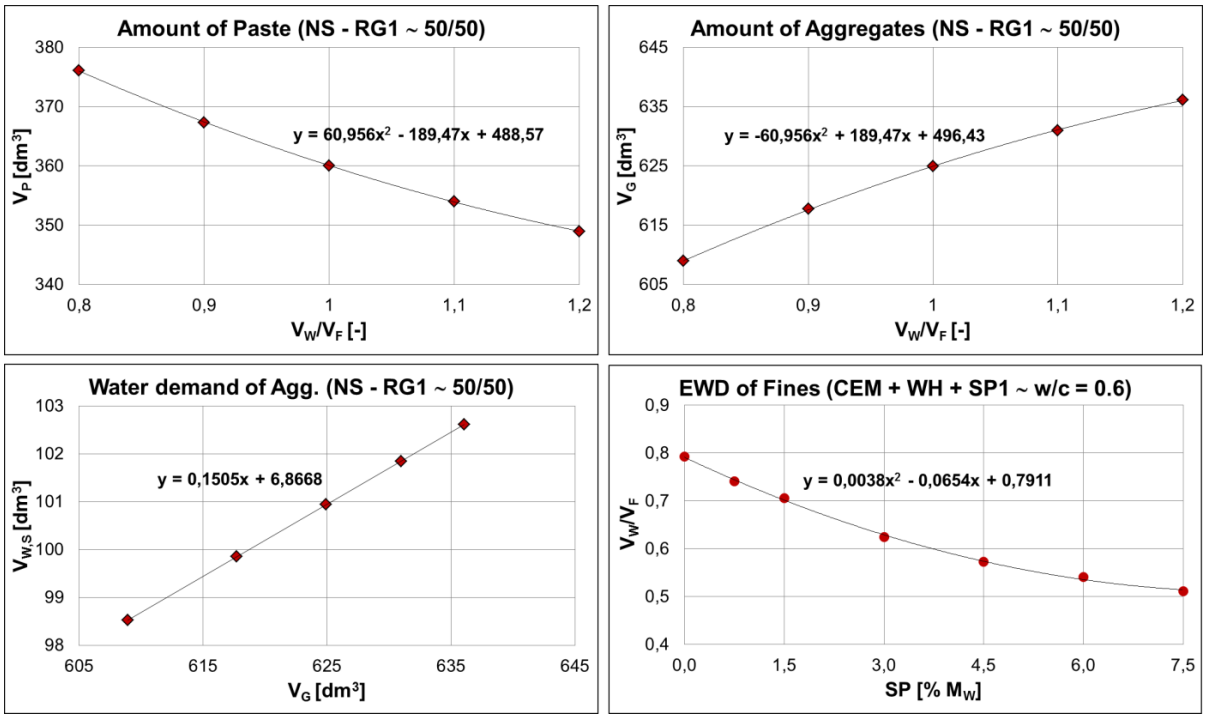

Figure 4.9: Input parameters for the WBMD

As a general rule, it is recommended to take a V_W/V_F value higher than the basic water demand (β_P), so that both the water demand of the fines as well as the aggregates could be satisfied. Since the fines have a $\beta_P = 0.8$, one could arbitrarily choose realistic V_W/V_F values up to 1.2, while maintaining the required w/c-ratio. For example, for a $V_W/V_F = 1.0$, the following basic components could be determined.

- Amount of paste, $V_P = 360$ dm^3
- Amount of Aggregate, $V_G = 625$ dm^3
- Assumed amount of air voids, $V_A = 15$ dm^3
- Surface water demand of aggregates, $V_{W,S} = 101$ dm^3

Now, the amount of unbound water in the paste composition without the addition of SP will be determined and compared with the surface water demand of the aggregates.

$$\Delta V_{W,P} = (V_W/V_F - \beta_P) \cdot V_F$$

The amount of water V_W and fines V_F in a paste composition with a certain $V_W/V_F = f$ could be determined using Equation (3.20).

$$V_W = V_P / (1+1/f) = 360 / (1+1/1.0) = 180 \text{ dm}^3$$

$$V_F = V_P / (1+f) = 360 / (1+1) = 180 \text{ dm}^3$$

$$\Delta V_{W,P} = (1.0 - 0.8) \cdot V_F = 0.2 \cdot 180 = 36 \text{ dm}^3 \ll V_{W,S} = 101 \text{ dm}^3$$

Since the amount of extra water (ΔV_W) in the paste is much smaller than the water demand ($V_{W,S}$) of the aggregates, the concrete will not exhibit adequate flowability. Hence, either a SP should be added or the V_W/V_F-value should be increased. For example, at SP = 5.4%.M_W, $\boldsymbol{\beta_E}$ has a value of 0.55. Now, the amount of unbound water for V_W/V_F = 1.0 and SP = 5.4% M_W is determined as:

$$\Delta V_{W,P} = (1.0 - 0.55) \cdot V_F = 0.45 \cdot 180 = 81 \text{ dm}^3 < V_{W,S} = 101 \text{ dm}^3$$

This is equivalent to water saving of about 45 lit revealing the remarkable effect of SP on the water demand. This could be a good starting point for the trial mix, even though $V_{W,S}$ is not yet completely satisfied. This is in line with the main goal of the WBMD, which is attaining good stability. This discrepancy from the optimum is advantageous and sometimes a prerequisite to account for the following unknown factors which occur during the concrete design and application processes.

i. The material characterizations, which provide the input parameters for the WBMD, are determined using relatively small samples of fines and aggregates. As such, a discrepancy from the whole batch, which is used in the concrete, is to be expected.
ii. Since different mixers were used for the paste investigations and for the concrete production, a direct transfer of the results of $\boldsymbol{\beta_E}$ of fines in the concrete design should be done with precaution. The paste phase in a concrete could be expected to be more dispersed as a result of the additional shear energy introduced by the aggregates. Because of the expected higher dispersion in the concrete mixer, more water could be set free which potentially increase the flowability and reduces the stability.
iii. Okamura's method generally gives higher water demand values when compared to other methods such as Puntke [174] or norm setting times [175] [176]. Thus, the water demand of the fines in reality could be smaller which results into additional unbound water in the paste which could negatively affect the stability of the concrete.
iv. Concrete production and delivery practices are not entirely immune to variations, especially in relation to water and SP overdosage. One good example is the existence of rest water in truck mixers which could potentially lead to significant loss of stability of concrete.

Of course, if the required flowability is not guaranteed, then a further addition of SP or increment of the V_W/V_F value is allowed, until the point is reached where $\Delta V_{W,P} = V_{W,S}$. However, the case where $\Delta V_{W,P} > V_{W,S}$ should absolutely be prohibited since that would trigger the availability of excessive unbound water in the concrete which would adversely affect the stability properties.

Moreover, for a chosen w/c-ratio, the amount of cement and mineral admixture could be determined as follows.

$$w/c = 0.6 \Rightarrow c = w / 0.6 = 180 / 0.6 = 300 \text{ kg}$$

Assuming a specific gravity of cement of ca. 3.0, the volume of cement and mineral admixtures could be determined as:

$$V_C = 300 / 3.0 = 100 \text{ dm}^3$$

$$V_{MA} = V_F - V_C = 180 – 100 = 80 \text{ dm}^3$$

4.7 Experimental investigation methods

The experimental investigations were conducted in order to characterize the relevant fresh concrete properties including flowability, pumpability, stability under vibration and pump-stability. Moreover, rheological investigations were conducted on the concrete, mortar and paste phases in order to give a fundamental description of the observed fresh properties. The methods used for the experimental investigations of each phase are schematically illustrated in Figure 4.10.

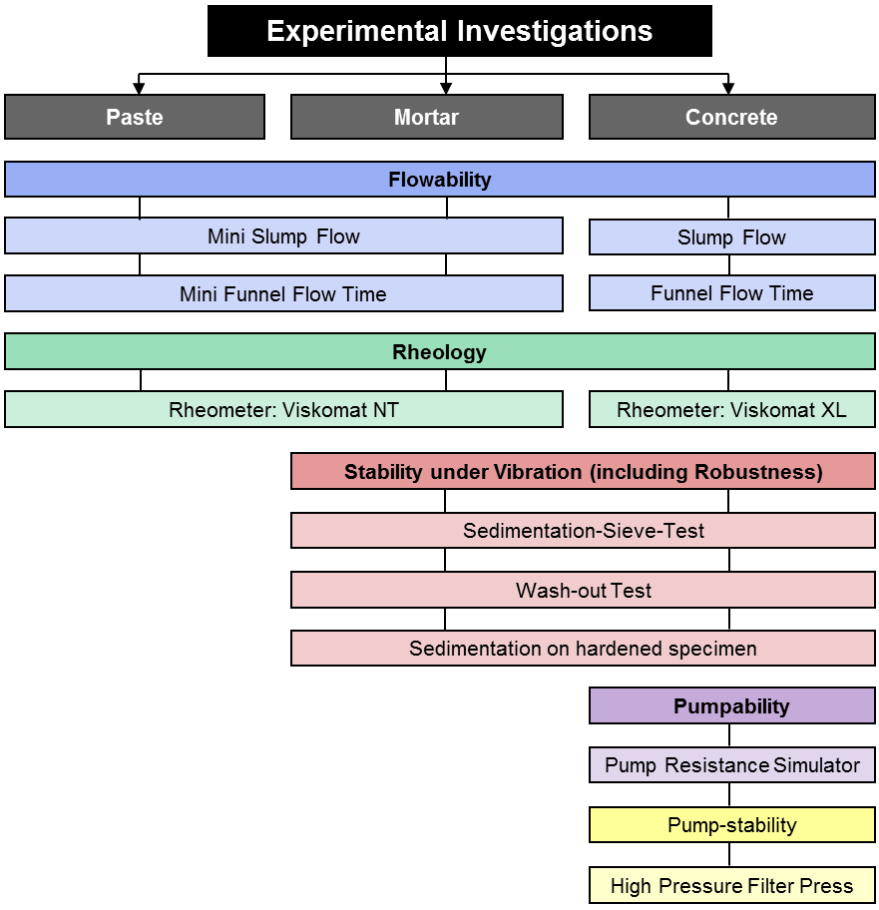

Figure 4.10: Investigation methods for concrete, mortar and paste compositions

4.7.1 Flowability investigation and evaluation methods

The flowability properties of the concretes were investigated using the following test methods.

- Flow table: slump flow diameter measurement after tapping 15 times according to DIN EN 12350-5
- Flow cone: measurement of flow time using a stop watch and slump flow diameter without tapping. The flow cone is built in order to determine the slump flow and flow time of SCC simultaneously. The results are comparable with the standard slump flow and V-funnel flow time of SCC [177]

The flowability properties of the paste and mortar compositions were investigated by modifying the methods developed for the design of SCC [171].

- Mini slump cone / Haegermann cone: mini slump flow measurement
- Mini V-funnel flow: determination of flow time using a stop watch

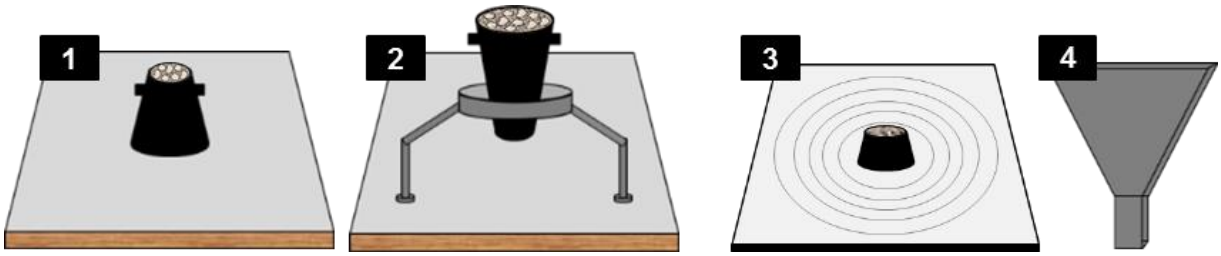

Figure 4.11: (1) Standard slump flow of concrete with tapping, (2) combined slump flow and flow time using flow cone, (3) slump flow of paste and mortar using mini slump cone and (4) flow time of mortar using mini V-funnel

4.7.2 Rheological investigation and evaluation methods

The rheological investigations on the concretes were conducted using a rotational viscometer Viskomat XL while the rheological properties of the paste and mortar compositions were quantified using Viskomat NT with different paddles.

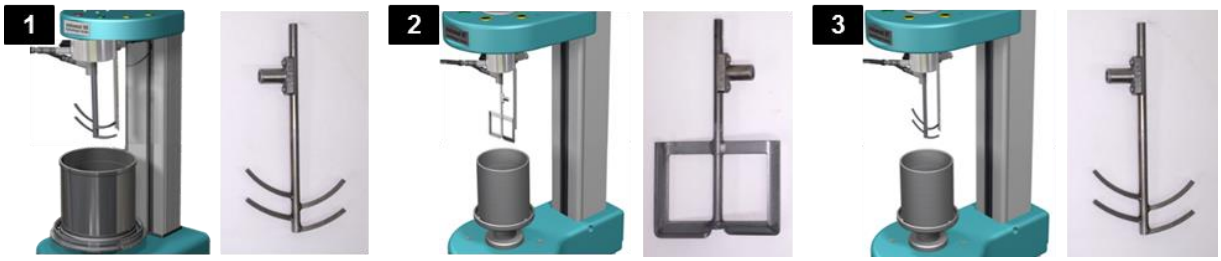

Figure 4.12: (1) Viskomat XL for concrete, (2) Viskomat NT for paste with paste paddle and (3) Viskomat NT for mortar with mortar paddle [Schleibinger]

The applied measurement profiles, which also considers the time and loading influences on the rheological properties, is shown in Figure 4.13. The first shear rates of 25 U/min for concrete and 150 U/min for paste and mortar are applied for ca. 3 minutes for the purpose of homogenizing the mixtures in order to start the measurements under similar conditions. The advantage with this measurement profile in comparison with the classic step or ramp profile is that in addition to the relative yield stress ($\tau_{o,r}$) and relative dynamic viscosity (η_r), which are determined in a steady state condition, the interparticle structural strength (A_S) could also be determined by quantifying the stress required to breakdown the interparticle structure and to bring the system to a steady state as illustrated in Figure 4.14. A comparison between the results of this measurement profile and the conventional step profile is shown in Appendix A-3.

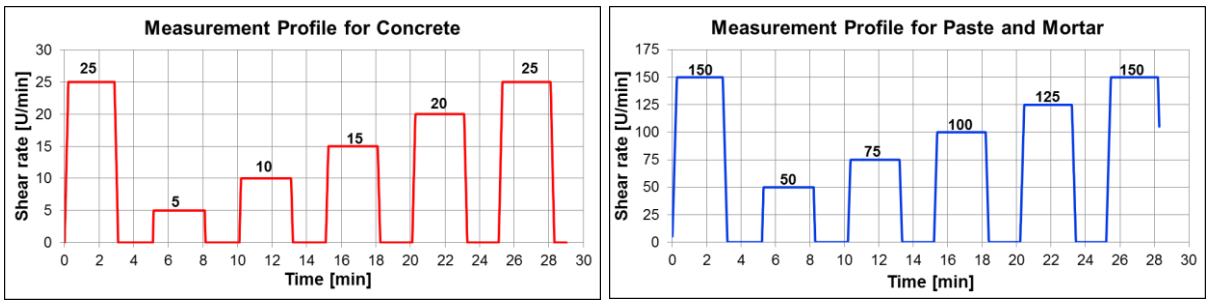

Figure 4.13: Measurement profiles for rheological investigation of concrete (left) and pastes or mortars (right)

The Herschel-Bulkley model was applied to determine the relative yield stress values $\tau_{o,r}$, since the classic Bingham model has at times led to negative values. These $\tau_{o,r}$ values are then integrated in the Bingham model in order to determine the relative dynamic viscosity (η_r); see Appendix A-4.

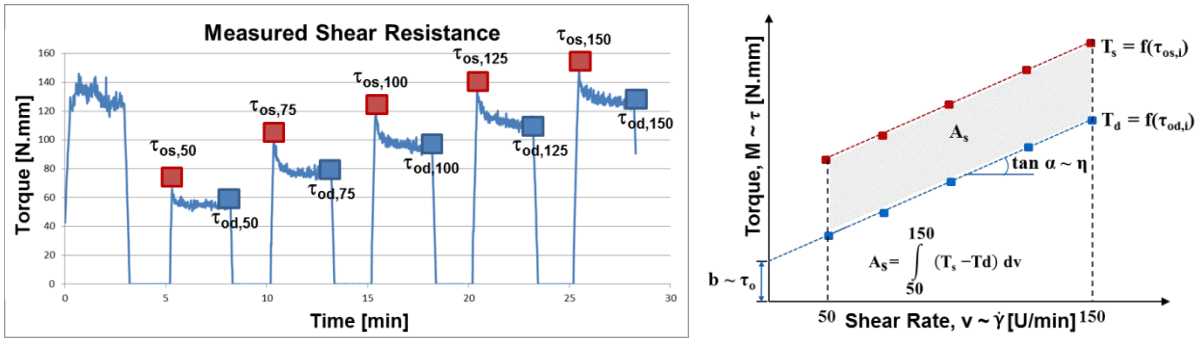

Figure 4.14: Measurement results (left) and evaluation method (right)

The Y-intercept (b) and the gradient (tan α) of the dynamic yield stress curve $T_d = f(\tau_{od,i})$ represent the relative yield stress ($\tau_{o,r}$) and relative dynamic viscosity (η_r) respectively. The area (A_S) between the two curves $T_s = f(\tau_{os,i})$ and $T_d = f(\tau_{od,i})$ as

determined using Equation (4.1) and (4.2) for concrete and paste or mortar respectively represents the interparticle structural strength of the mix.

$$A_{S,C} = \int_{5}^{25} (T_s - T_d)dv \tag{4.1}$$

$$A_{s,p} = \int_{50}^{150} (T_s - T_d)dv \tag{4.2}$$

4.7.3 Stability investigation and evaluation methods

The stability properties of the concrete or mortar compositions under the influence of vibration were investigated using the following test methods.

- Wash-out test (WT): determination of the sedimentation of coarse aggregates in concrete. Here, the test method developed for SCC [174] is modified by applying vibration of a high intensity (amplitude = 0.75 mm and Frequency = 100 Hz) to the tube (D = 150 mm and H = 600 mm) for 30 seconds. Afterwards, the concrete or mortar from each segment is washed out on a 4.0 mm or 0.25 mm sieves respectively.
- Sedimentation – Sieve – Test (SST): determination of the separation of the paste or mortar from the bulk concrete or paste from mortar under the influence of vibration. The concrete or mortar from each segment is sieved on a 4 mm and/or 0.25 mm sieves by applying vibration for 60 seconds. This test precedes the wash-out test.
- Sedimentation on hardened specimen: a visual assessment of the sedimentation of coarser particles on a sliced face of dried specimen (D = 100 mm and H = 500 mm), which are prepared under the application of vibration for 30 sec.

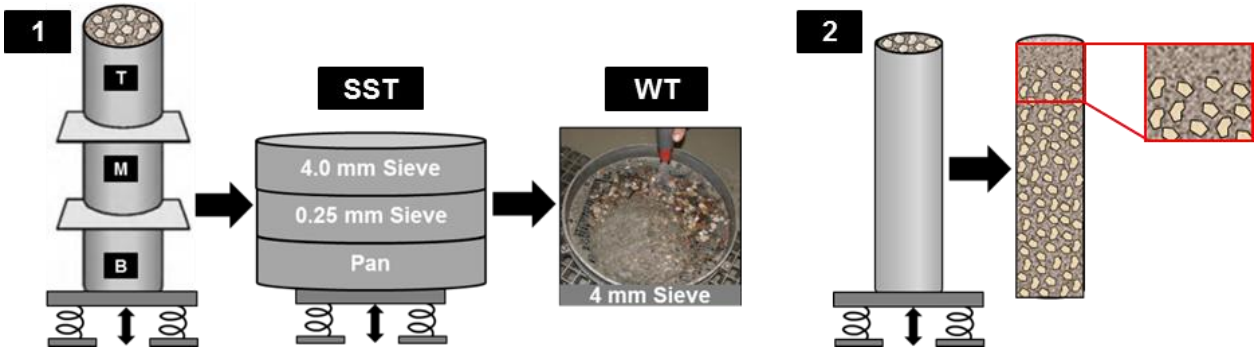

Figure 4.15: (1) Concrete under vibration → Sedimentation – Sieve – Test (SST) → Wash-out Test (WT) and (2) visual sedimentation evaluation on hardened specimen of vibrated concrete

The stability criterion for concretes under vibration is defined by modifying the criteria based on the wash-out test for SCC in accordance with the [174]. Here, similar to the method used in SCC, the average mass of retained aggregates (M_i) on the wash-out sieve is determined using Equation (4.3).

$$\overline{M} = \frac{M_T + M_M + M_B}{3} \tag{4.3}$$

A new adequate stability criterion, the so called stability index (SI), is introduced to evaluate the stability of vibrated concrete as discussed in section 5.1. To this end, the deviations from the top and bottom segments from the average as determined using Equation (4.3) are determined using Equation (4.4).

$$\Delta M_T = \left[\frac{M_T - \overline{M}}{\overline{M}}\right] \cdot 100 \text{ and } \Delta M_B = \left[\frac{M_B - \overline{M}}{\overline{M}}\right] \cdot 100 \tag{4.4}$$

The SI is then defined as the difference between the deviations of the bottom and top segments. Vibrated concretes with a SI ≤ 20% could be considered as stable under vibration.

$$SI = \Delta M_B - \Delta M_T \leq 20\% \tag{4.5}$$

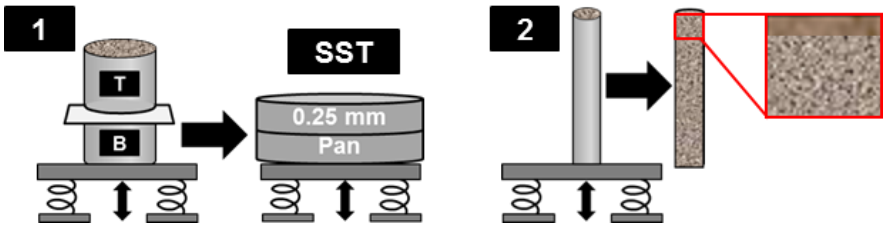

Figure 4.16: (1) Mortar under vibration → Sedimentation – Sieve – Test (SST) and (2) visual sedimentation evaluation on hardened specimen of vibrated mortar

The stability criterion for the mortars is defined on the basis of the combined sedimentation – sieve test by determining the volume of the sieved specimen < 0.25 mm from the top segment as a percentage of the total mortar volume. Mortar compositions with a sedimentation – sieve – index, SSI lower than 5% could be considered as stable.

$$SSI_M = \left[\frac{V_{M<0.125mm}}{V_M}\right] \cdot 100 \leq 5\% \tag{4.6}$$

Moreover, on the basis of the visual assessment on hardened specimen, a concrete or mortar is considered to be unstable when there is a clear accumulation of paste or fine mortar layer at the very top.

4.7.4 Pumpability investigation and evaluation methods

The pumpability properties were investigated using a pump resistance simulator (PuReSi), which was a modification of the sliding pipe rheometer [131]. The PuReSi is equipped with a pressure sensor and a cable actuated position sensor. The pipe rises up and falls down to a constant height of 500 mm. In addition to its own weight, three different weights of 20 kg, 40 kg and 60 kg are used in order to generate four different falling speeds. Since the pipe has a constant cross-sectional area ($A_P = \pi \cdot D^2$ with D = 125 mm), the four falling speeds (v_i) correspond to four different flow rates or discharges ($Q_i = v_i \cdot A_P$). In this way, a direct correlation between the discharge and pressure could be established for a concrete by assigning the discharge Q and the pressure P on the x-axis. The gradient of such a curve could be interpreted as a pumpability relevant viscosity while the ordinate at $Q_i = 0$ is the minimum pressure required to start movement of the concrete in the pipe, which represents the pumpability relevant yield stress, see Figure 2.47.

Figure 4.17: PuReSi (left), HPFP (middle) and BFP* (right)

* The BFP is used as a supplemental investigation method.

4.7.5 Pump-stability investigation and evaluation methods

The pump-stability is mainly investigated using a high pressure filter press (HPFP) with D = 150 mm and H = 300 mm. After setting up the HPFP in a compression machine, the applied force is increased linearly up to a maximum of 300 kN (ca. 170 bar) at a rate of 10 kN/min. Meanwhile, the amount of filtrate and the strain are measured continuously. The rate at which the filtrate is pressed out of the concrete as well as its total amount could be considered an indicator for the stability of concrete under the application of pressure.

4.8 Results of the flowability, stability (under vibration) and rheological investigations

On the basis of the WBMD, a wide ranging concrete mixtures with different the paste and aggregate compositions were composed in order to characterize the fresh concrete properties in terms of the flowability, pumpability, stability under vibration, pump-stability and robustness. These fresh concrete investigations were also accompanied by extensive investigations of the rheological properties of the concrete mixtures as well as the paste and mortar compositions extracted from them.

4.8.1 Concrete compositions

The basic component materials used for the main investigations are:

- Cement: CEM I 42.5 N
- Mineral admixtures: FA WH
- Aggregates: NS (0/2), RG1 (2/8) and RG2 (8/16)
- Chemical admixture: SP1

The following sets of test series were envisaged for the main investigation.

I. Effects of paste composition (different flowability)
   - Constants: w/c-ratio, paste amount and aggregate composition
   - Variables: V_W/V_F-values

II. Combined effects of paste composition and paste content (comparable flowability)
   - Constants: w/c-ratio and aggregate composition
   - Variable: V_W/V_F-values and paste amount

III. Combined effects of paste composition and paste content on the robustness against water overdosage based on series II

IV. Effects of aggregate composition (different flowability)
   - Constants: w/c-ratio, V_W/V_F-values and paste amount
   - Variable: Fuller exponent **q** (Sand / Coarse aggregate ratio)

V. Combined effects of aggregate composition and paste content (comparable flowability)
   - Constants: w/c-ratio and V_W/V_F-values
   - Variable: Fuller exponent **q** and paste amount

VI. Combined effects of aggregate composition and paste content on the robustness against water overdosage based on series V

The parameters used for the different concrete compositions are summarized in Table 4.5.

Table 4.5: Parameters used for the concrete compositions in the flowability, stability (under vibration) and rheological investigations

Test series	**w/c**	**V_W/V_F**			**q (0/8: NS - RG1) (0/16: NS - RG1 - RG2)**			**Max. Size**	**Paste content**	**Slump flow**
I	0.6	0.8	1.0	1.2	0.5 (50 - 50)			8	Constant	Variable
II								8	Variable	Constant
III	Water Overdosage of 10 lit and 20 lit based on series II									
IV	0.6	1.0			0.4 (60-40)	0.5 (50-50)	0.6 (40-60)	8	Constant	Variable
					0.4 (44-33-23)	0.5 (35-38-27)	0.6 (27-41-32)	16		
V					0.4 (60-40)	0.5 (50-50)	0.6 (40-60)	8	Variable	Constant
VI	Water Overdosage of 10 lit and 20 lit based on series V									

4.8.2 Series I: Effects of paste composition (different flowability)

For this investigation series, three paste compositions V_W/V_F values of 0.8, 1.0 and 1.2 were chosen. The paste amount in all three mixtures was maintained constant at 361 dm^3, which was determined for the reference WBC with V_W/V_F = 1.0 and q = 0.5 based on the approach as explained in section 4.6. However, results of the flowability tests has revealed that the mixture with V_W/V_F = 0.8 had shown no appreciable flowability and as a result, for the purpose of comparison, an additional concrete composition with V_W/V_F = 1.1 was incorporated in the series. The concrete compositions are shown in Table 4.6.

Table 4.6: Concrete compositions for test series I (paste compositions)

Materials	**V_W/V_F = 0.8**		**V_W/V_F = 1.0**		**V_W/V_F = 1.1**		**V_W/V_F = 1.2**	
	dm^3/m^3	kg	dm^3/m^3	kg	dm^3/m^3	kg	dm^3/m^3	kg
CEM I	85.1	267.4	95.7	300,8	100,3	315.2	104.5	328.2
FA WH	115.4	266.7	84.8	195,8	71,6	165.4	59.6	137.8
NS (0/2)	312.0	829.9	312.0	829,9	312,0	829.9	312.0	829.9
RG1 (2/8)	312.0	808.1	312.0	808,1	312,0	808.1	312.0	808.1
Water	160.4	160.4	180.5	180,5	189,1	189.1	196.9	196.9
SP1	5,41 [% M_W]							
WB	- 50		-19		-6,0		+6.0	
Key Parameters								
Paste content	dm^3/ m^3	361						
Aggregate content	dm^3/ m^3	624						
Air voids content	dm^3/ m^3	15						
w/c	-	0.6						
q	-	0.5						
Aggregate composition	Vol. %	NS – RG1 (50 – 50)						

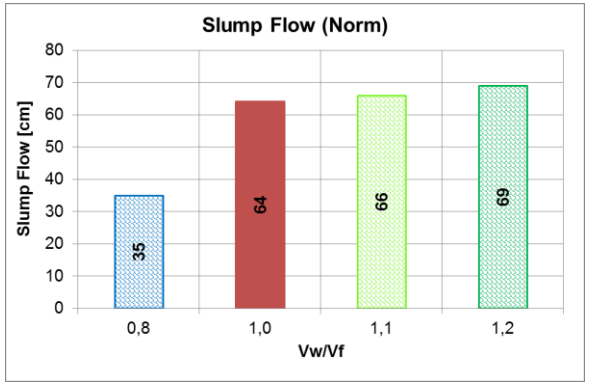

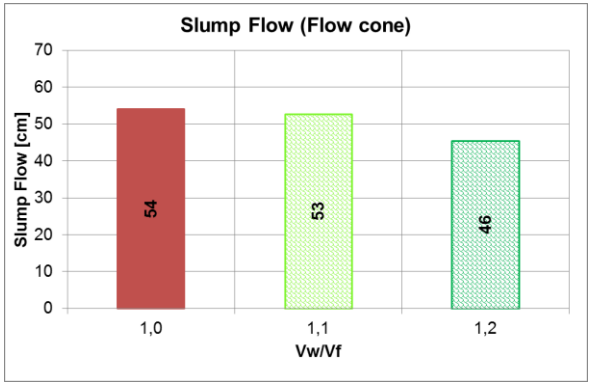

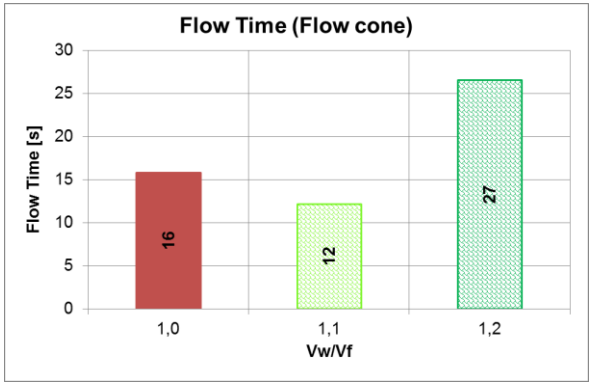

	Slump Flow (Norm)		
V_W/V_F = 0.8	V_W/V_F = 1.0	V_W/V_F = 1.1	V_W/V_F = 1.2
Ø = 35.0 cm	Ø = 64.0 cm	Ø = 66.0 cm	Ø = 69.0 cm
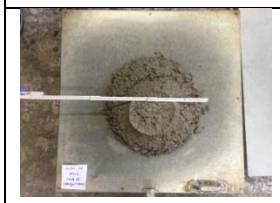	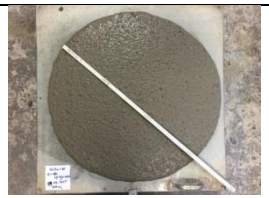	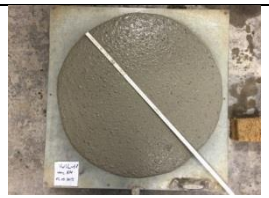	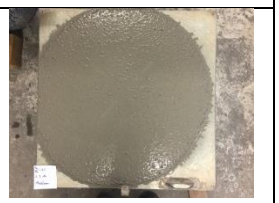
	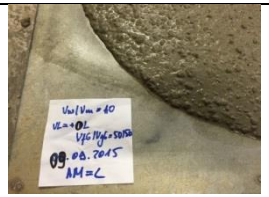		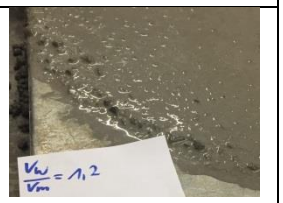

Slump Flow (Flow cone)			
V_W/V_F = 0.8	V_W/V_F = 1.0	V_W/V_F = 1.1	V_W/V_F = 1.2
Ø = -	Ø = 54.0 cm	Ø = 53.0 cm	Ø = 46.0 cm
Imossible to conduct	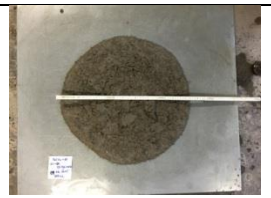	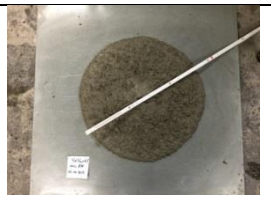	
		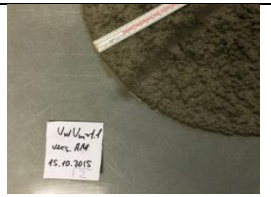	

Figure 4.18: Effects of paste composition (V_W/V_F) on the flowability (different flowability)

I. Flowability

As can be seen in Figure 4.18, the reference water balanced concrete (WBC) with V_W/V_F = 1.0 shows a very good flowability. A direct application of the paste amount determined specifically for the reference mixture with V_W/V_F = 1.0 to the other three compositions with V_W/V_F = 0.8, 1.0 and 1.2 results in a lower or higher flowability. The concrete with V_W/V_F = 0.8 exhibit no flowability, which could be attributed to the lack of adequate unbound water in the system to satisfy the water demand of the aggregates. Since the basic water demand for the CEM I and FA WH fine compositions has a value of β_P = 0.8, see Figure 4.2, the water demand for the aggregates could be satisfied only through the amount of water saved by the addition of SP, which is obviously not enough at SP content of 5.41% M_W. On the opposite end, the mixture with V_W/V_F = 1.2 shows a very high flowability but with a visually recognizable loss of stability. This could be attributed to the combined effects of the higher amount of paste and the V_W/V_F-value. Moreover, as a consequence of the extreme segregation, the friction and interlocking between the aggregates has led to an unexpectedly higher flow time than the one with V_W/V_F = 1.0. The supplementary mixture with V_W/V_F = 1.1, in which the WB criterion is maintained, also showed higher flowability but with no visible separation of the paste.

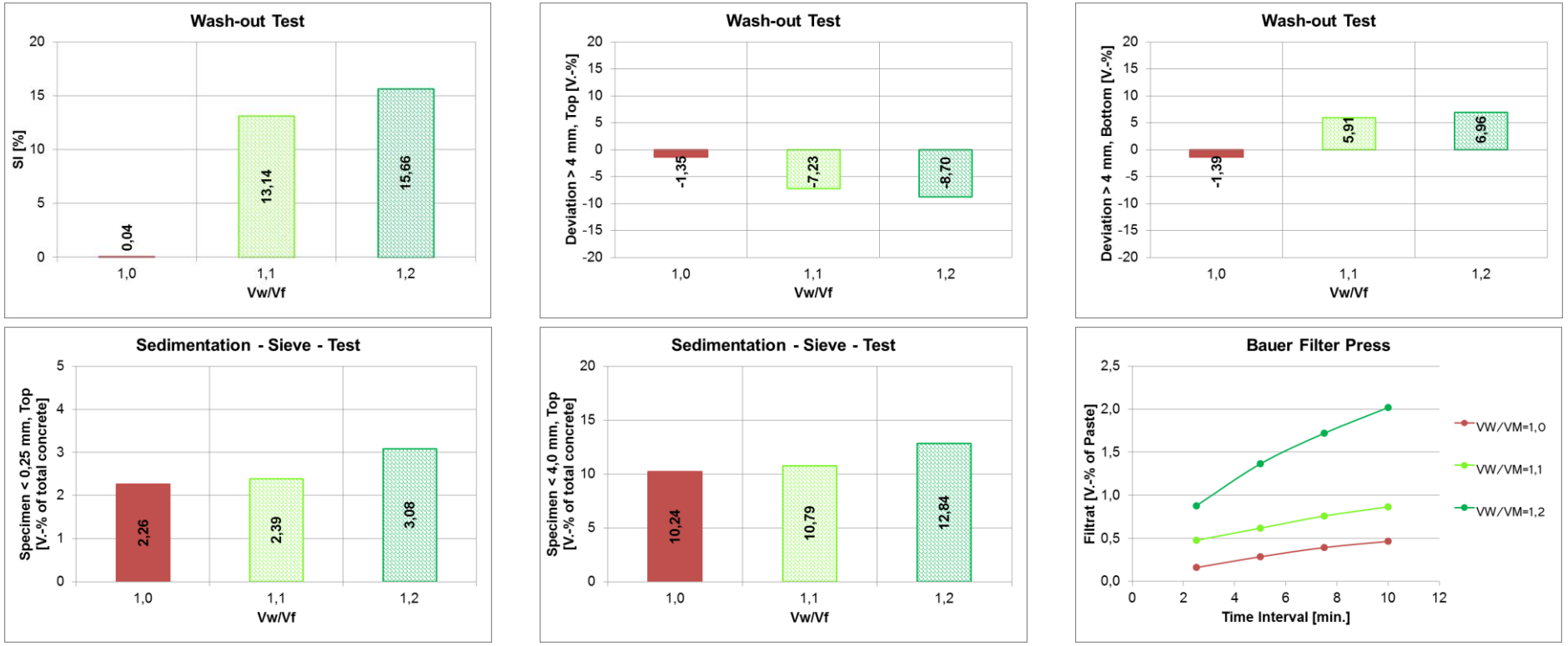

V_W/V_F = 0.8	V_W/V_F = 1.0	V_W/V_F = 1.1	V_W/V_F = 1.2
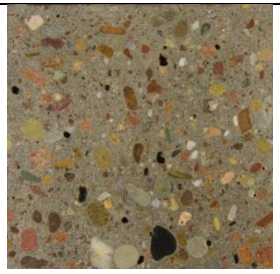	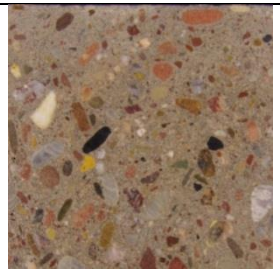	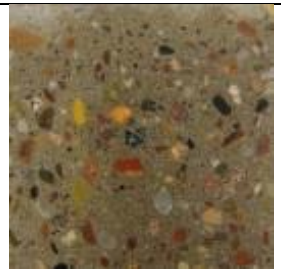	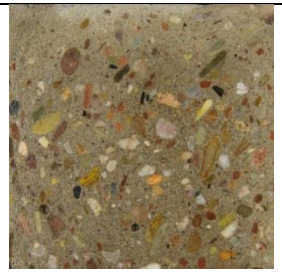

Figure 4.19: Effects of paste composition (V_W/V_F) on the stability (different flowability)

II. Stability

Irrespective of its high flowability, the reference WBC with $V_W/V_F = 1.0$ shows the best stability under the influence of vibration. The mixture with $V_W/V_F = 0.8$ obviously exhibit high stability since the chances for the sedimentation of the coarser particles is practically non-existent as there is no enough amount of paste through which they could settle. The stability, of course decreases, with increasing V_W/V_F values; the mixture with $V_W/V_F = 1.2$ exhibiting the poorest stability both under the influence of vibration and pressure as confirmed by the results of the WT, SST, the visual sedimentation evaluation as well as the BFP. This could be attributed to the availability of excessive unbound water in the mixture as confirmed by the water balance criteria (WB). Despite the higher paste volume, the mixture with $V_W/V_F = 1.1$ has shown good stability which could be attributed to the maintenance of WB criterion.

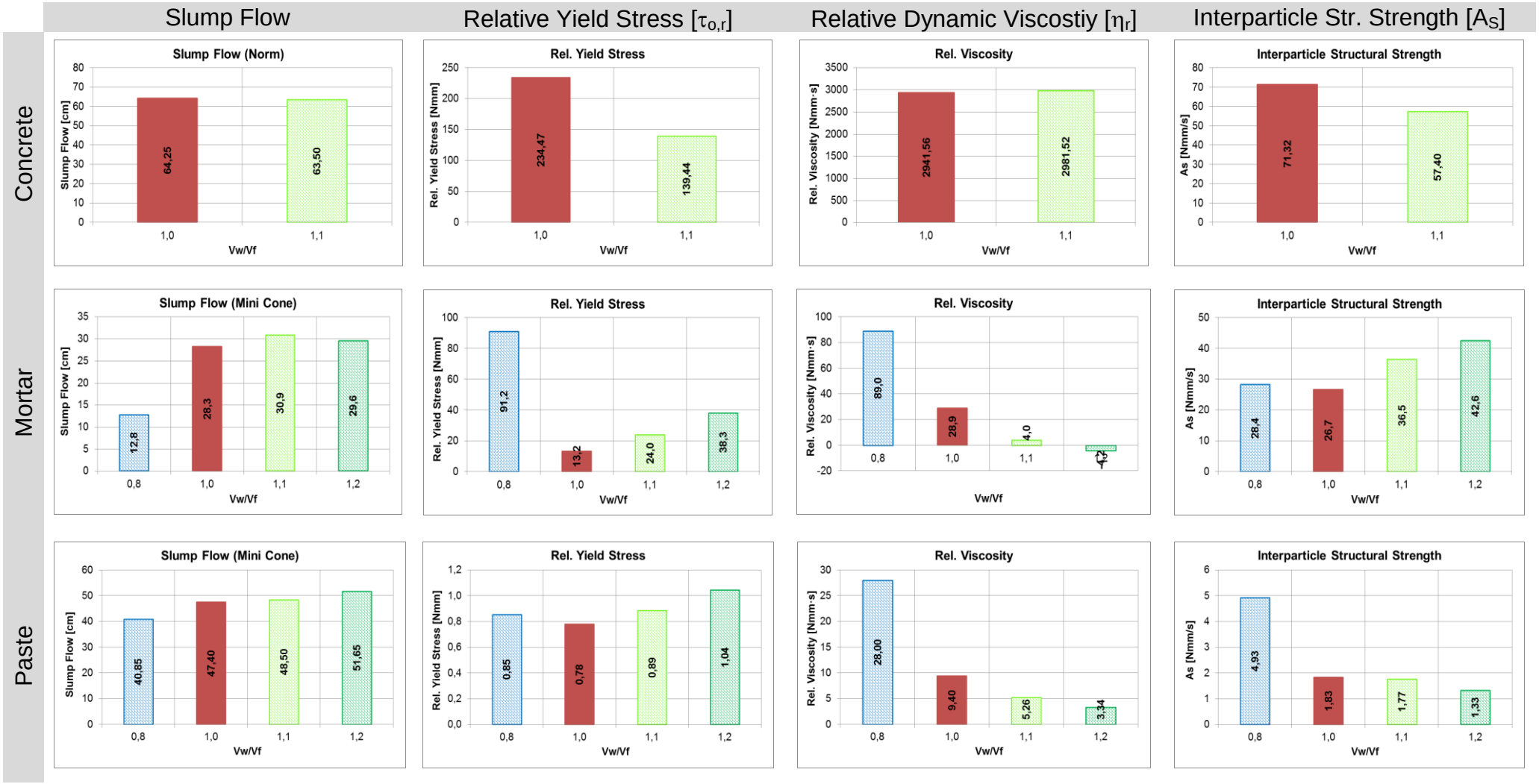

Figure 4.20: Effects of paste composition (V_W/V_F) on the rheological properties (different flowability)

III. Rheology

The results of the rheological investigations on the concrete mixtures as well as the mortar and paste compositions extracted from them are illustrated in Figure 4.20. The rheological comparison at the concrete level makes more sense if all the mixtures exhibit the same flowability. Nevertheless, the yield stress and the interparticle structural strength are higher for the mix with $V_W/V_F = 1.0$ in comparison with the one with $V_W/V_F = 1.1$. The relative viscosities of the two concrete mixtures remain almost the same. It was not possible to conduct the rheological tests on the concretes with $V_W/V_F = 0.8$ (due to its extreme stiffness) and $V_W/V_F = 1.2$ due to the extreme segregation of the mixture in the rheometer. The mortars are extracted from the mixtures just by neglecting the volume of the coarser fraction 2/8 from the concrete. This would obviously lead to the existence of an excess amount of unbound water in the mortar compositions which otherwise would have been bound by the coarser fractions. Consequently, the rheological investigations are prone to the occurrence of segregation of sand particles which has at times led to reversed trends with regard to the relative yield stress and interparticle structural strength and unrealistic negative values of the relative viscosity. The paste compositions are extracted from the concretes by neglecting the aggregate fraction 0/2 and 2/8. Contrary to the mortars, the rheological investigations on the paste compositions could be considered to be reliable since the chances for the occurrence of sedimentation of fines is relatively low, except at very high contents of water or SP. All the investigated paste compositions exhibit high flowability depicting a satisfactory dispersion of the fines as reflected by their comparable yield stress values. The viscosity and the interparticle structural strength, on the other hand, decrease with increasing V_W/V_F values. Increased V_W/V_F values bring about an increased water film thickness and greater distance between the individual particles which ultimately reduces the chances for the formation of colloidal flocculants as well as CSH bridges formed by products of early nucleation processes. Consequently, the resistance to flow (η_r) as well as the applied shear force required to break down the interparticle structure (A_S) decreases.

4.8.3 Series II: Combined effects of paste composition and paste amount (comparable flowability)

For this investigation series, three concrete mixtures with V_W/V_F values of 0.8, 1.0 and 1.2 were chosen. The paste amount for the reference mixture with $V_W/V_F = 1.0$ and $q = 0.5$ was determined to be around 361 dm^3 based on the WBMD. For the other two concrete mixtures with $V_W/V_F = 0.8$ and $V_W/V_F = 1.2$ (both with $q = 0.5$), the paste amount was also determined using the same technique, but with a slight adjustments to attain a comparable flowability as that of $V_W/V_F = 1.0$.

Table 4.7: Concrete compositions for test series II (paste composition and paste content)

Materials		**V_W/V_F = 0.8**		**V_W/V_F = 1.0**		**V_W/V_F = 1.2**	
		dm^3/m^3	kg	dm^3/m^3	kg	dm^3/m^3	kg
CEM I		98.1	308.1	95.7	300.8	101.6	319.1
FA WH		133.0	307.3	84.8	195.8	58.0	134.0
NS (0/2)		284.5	756.8	312.0	829.9	317.0	843.2
RG1 (2/8)		284.5	736.9	312.0	808.1	317.0	821.0
Water		184.9	184.9	180.5	180.5	191.5	191.5
SP1		5,41 [% M_W]					
WB		-34		-19		+2	
Key Parameters							
Paste content	dm^3/ m^3	416		361		351	
Aggregate content	dm^3/ m^3	569		624		634	
Air voids content	dm^3/ m^3	15					
w/c	-	0.6					
q	-	0.5					
Aggregate composition	Vol. %	NS – RG1 (50 – 50)					

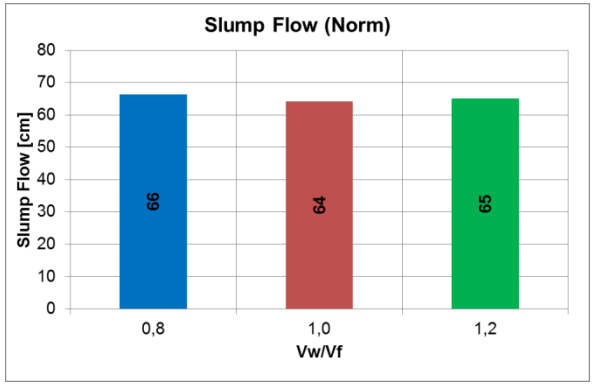

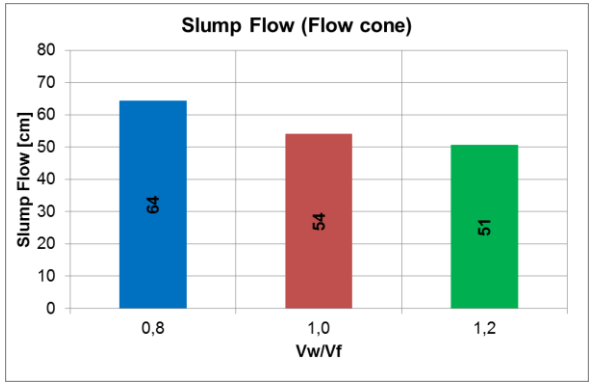

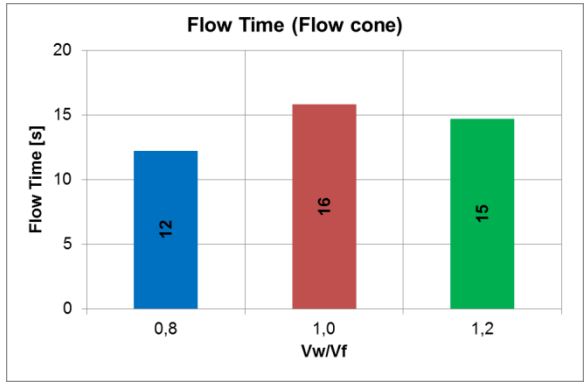

Slump Flow (Norm)		
V_W/V_F = 0.8	V_W/V_F = 1.0	V_W/V_F = 1.2
Ø = 66.0 cm	Ø = 64.0 cm	Ø = 65.0 cm
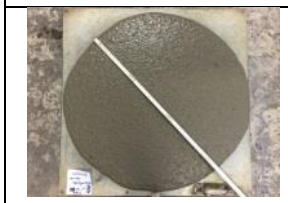	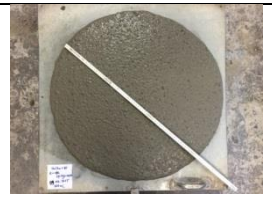	
	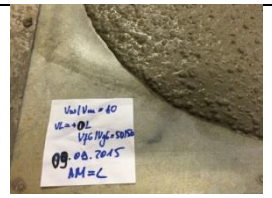	

Slump Flow (Flow cone)		
V_W/V_F = 0.8	V_W/V_F = 1.0	V_W/V_F = 1.2
Ø = 64.0 cm	Ø = 54.0 cm	Ø = 51.0 cm
	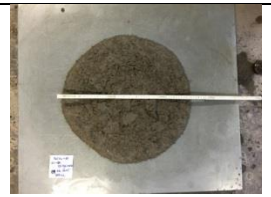	
		

Figure 4.21: Combined effects of paste composition (V_W/V_F) and paste content on the flowability (comparable flowability)

I. Flowability

In Figure 4.21, it could be observed that while all three mixtures possess comparable normative slump flow (with tapping), the flowability as determined using the slump cone (without tapping) decreases with increasing V_W/V_F values. The mixture with V_W/V_F = 0.8 flows almost to the same extent with or without tapping ($\Delta \approx 2$ cm) showing a similar behavior as that of SCC in terms of the self-leveling capacity. This mixture has required an additional paste amount of 55 lit to increase its flowability from 35 cm to 66 cm. In such paste dominated mixtures, the aggregates are engulfed in a highly viscous paste film, which reduces the friction between the aggregates making it possible to attain high flowability without a need for the application of external energy. This mixture also have the lowest flow time as a result of the high lubricating effect of the viscous paste film in comparison with the mixtures with V_W/V_F = 1.0 or 1.2. In contrast, the difference between the normative and flow cone slump flows is at its maximum for the mixture with V_W/V_F = 1.2 ($\Delta \approx 14$ cm). Here, the paste composition and / or amount are not adequate by themselves to attain the desired flowability without the application of external energy. Concrete compositions that tend to show extreme segregation and thus loss of homogeneity could exhibit a lower flowability even under the application of external energy, since this could also aggravate the separation of the liquid phase (paste) from the solid phase (aggregates).

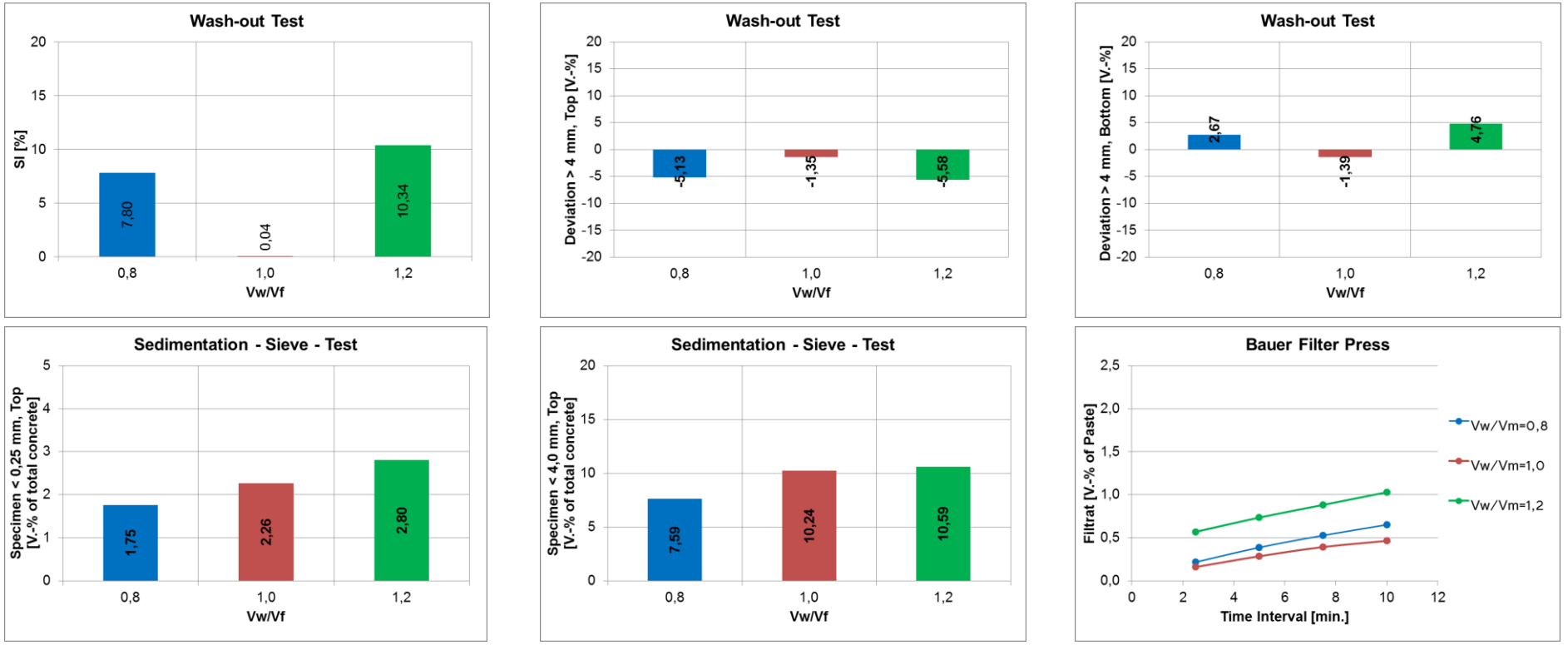

V_W/V_F = 0.8	V_W/V_F = 1.0	V_W/V_F = 1.2
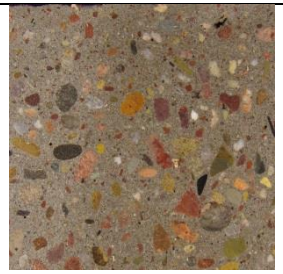	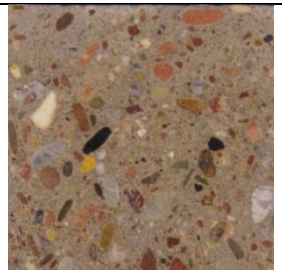	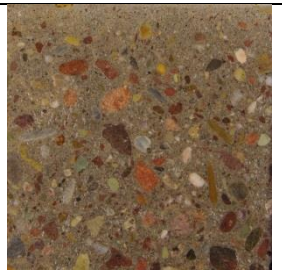

Figure 4.22: Combined effects of paste composition (V_W/V_F) and paste content on the stability (comparable flowability)

II. Stability

As can be seen in Figure 4.22, the ideal WBC with $V_W/V_F = 1.0$ here also shows the best stability under the influence of vibration and pressure when compared to those with $V_W/V_F = 0.8$ or $V_W/V_F = 1.2$ as confirmed by the results of the WT and the visual sedimentation evaluation as well as the BFP. The mixture with $V_W/V_F = 0.8$, despite its highly viscous paste composition, possesses a relatively lesser stability than the one with $V_W/V_F = 1.0$ which might be due to the high amount of paste used to achieve the desired flowability. Nevertheless, it has shown a satisfactory stability which could be attributed to the lattice effect of the optimized aggregate composition as well as the higher viscosity of the paste. In contrast, the mixture with $V_W/V_F = 1.2$ exhibit the poorest stability when compared to the other two mixtures with $V_W/V_F = 0.8$ and 1.0 despite the fact that it has the lowest amount of paste. The reason for this might be the relatively higher amount of excess unbound water in the concrete as determined using the WB criterion. However, even though the degree of stability differs from mixture to mixture, the overall stability of all three concrete compositors could be considered to be satisfactory, especially considering their high degree of flowability and the exposure to a high intensity vibration of 30 sec. A smaller V_W/V_F value or higher viscosity of paste seems to be advantageous in terms of reducing the potential separation of the liquid phase (paste or fine mortar) < 0.25 mm from the solid phase (aggregates) under the influence of vibration as confirmed by the results of the SST. The same trend was also observed in the test series I. This is in compliance with the results of the pump-stability investigations where the concrete mixtures with $V_W/V_F = 0.8$ has shown the best stability under the action of pressure; see section 4.9.2.

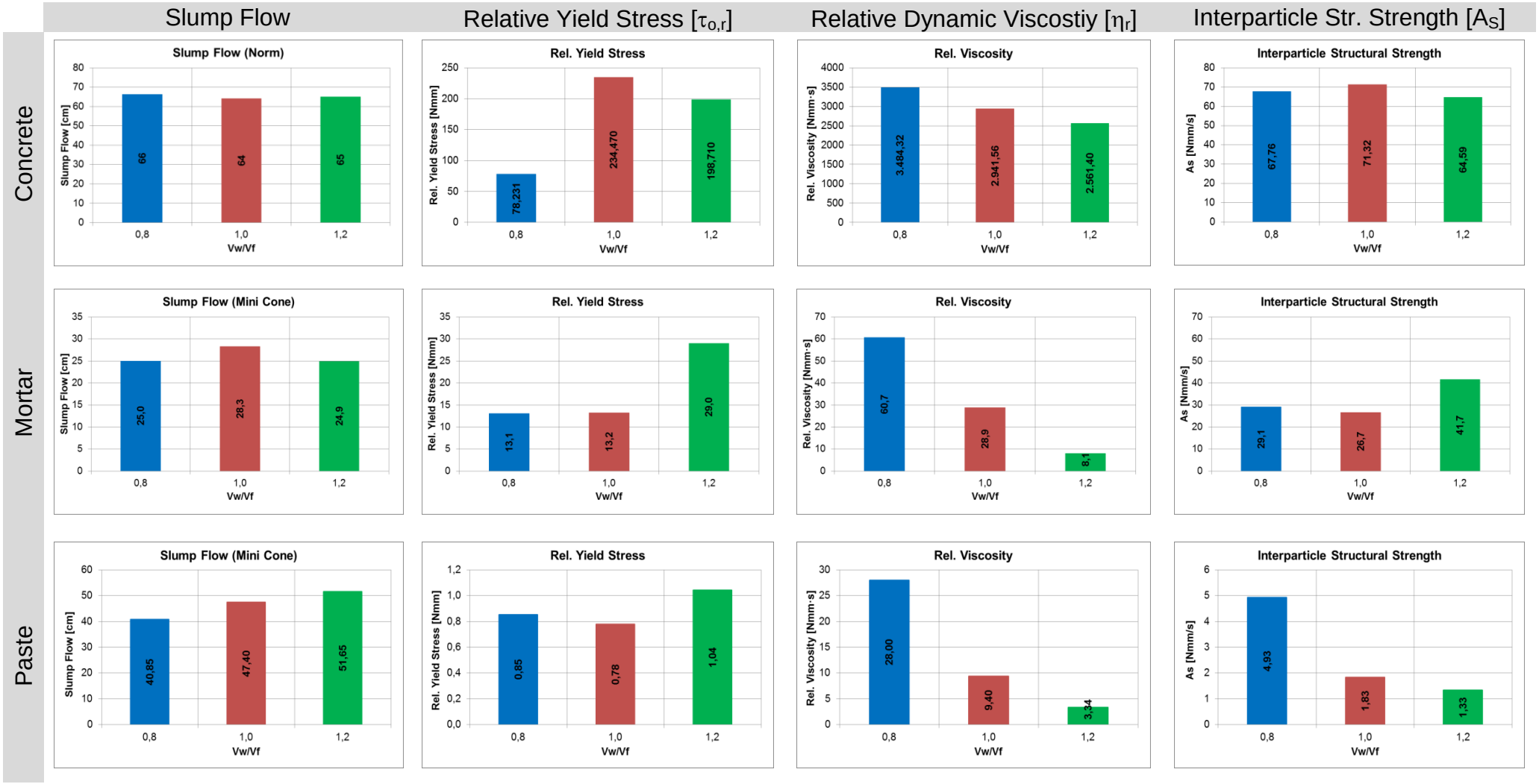

Figure 4.23: Combined effects of paste composition (V_W/V_F) and paste content on the rheological properties (comparable flowability)

III. Rheology

The results of the rheological investigations on the concrete mixtures as well as the mortar and paste compositions extracted from them are illustrated in Figure 4.23. The comparison at the concrete level makes here more sense as all mixtures exhibit the same flowability as determined using the normative slump flow test. Because of its higher amount of paste (55 lit more than the mixture with V_W/V_F = 1.0) and the resulting reduction in friction between the aggregates, $\tau_{o,r}$ of the concrete with V_W/V_F = 0.8 is significantly lower than the other two concrete mixtures. As long as the paste amount is not significantly different, as is the case between V_W/V_F = 1.2 and V_W/V_F = 1.0 with ΔV_P = 10 dm^3, $\tau_{o,r}$ decreases with increasing V_W/V_F values. The same trend was also observed in test series I. The value of A_S follows a similar trend as the yield stress, but with relatively smaller differences. The viscosity of the concrete mixtures has decreased with increasing V_W/V_F values, clearly indicating the dominant role played by the paste composition regardless of the paste volume. Here too, the results of the rheological investigations on the mortar compositions have shown no reliable trends, with the exception of the viscosity, pertaining to the fact that they are prone to the occurrence of sedimentation of the sand particles during the test. The analysis of the results of the rheological investigations on the paste compositions are already discussed in test series I. η_r and A_S decrease with increasing V_W/V_F values while the yield stress remains comparable. Based on the results of rheological investigation on the concrete mixtures, it could be argued that for concretes designed on the basis of the basic water demand β_P such as the one with V_W/V_F = 0.8 or generally SCC requiring high amount of paste, the initiation of flow which is related to $\tau_{o,r}$ is mainly governed by the amount of paste. However, after the flow initiation, the amount of stress that have to be applied to reach the steady state (A_S) or to keep the mixture flowing during steady state (η_r) depends primarily on the paste composition.

4.8.4 Series III: Combined effects of paste composition and paste amount on the robustness (comparable flowability)

For this investigation series, a water overdosage of 10 lit and 20 lit was applied to the WBC from test series II with V_W/V_F values of 0.8, 1.0 and 1.2 having comparable flowability, see 4.8.3. Here, the total volume of the concrete increases from 1000 dm^3 to 1010 dm^3 or 1020 dm^3 respectively for a 10 lit and 20 lit water overdosage. However, for the sake of consideration of a 1 m^3 of concrete, the amount of each component materials is adjusted proportionally to 1000 dm^3 as shown in Table 4.8.

Table 4.8: Concrete compositions for test series III (paste composition and paste content vs. robustness)

Materials		V_W/V_F = 0.8		V_W/V_F = 1.0		V_W/V_F = 1.2	
		Rob+10 L	**Rob+20 L**	**Rob+10 L**	**Rob+20 L**	**Rob+10 L**	**Rob+20 L**
		dm³/m³	dm³/m³	dm³/m³	dm³/m³	dm³/m³	dm³/m³
CEM I		97.1	96.2	94.8	93.9	100.6	99.6
FA WH		131.7	130.4	83.9	83.1	57.4	56.9
NS (0/2)		281.7	278.9	308.9	305.9	313.9	310.8
RG1 (2/8)		281.7	278.9	308.9	305.9	313.9	310.8
Water		193.0	200.8	186.6	196.6	199.5	207.3
SP1		5.41 [% M_W of Ref.]					
WB		-24	-14	-9	+1	+12	+22
Key Parameters							
Paste content	dm³/m³	422	427	367	373	357	363
Aggregate content	dm³/m³	563	558	618	612	628	622
Air voids content	dm³/m³	15					
q	-	0.5					

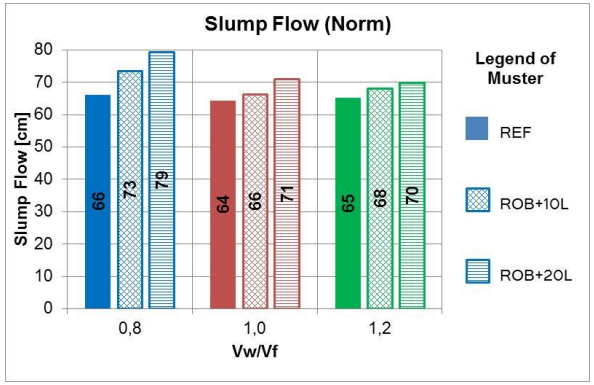

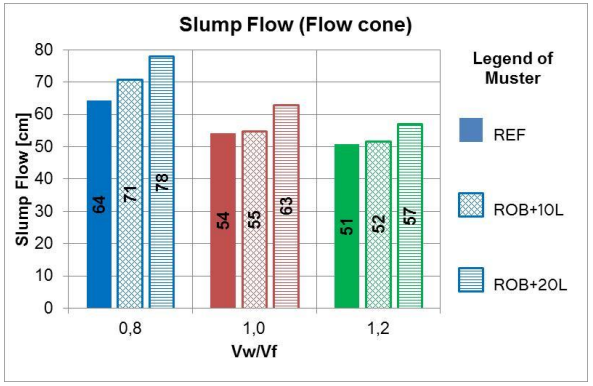

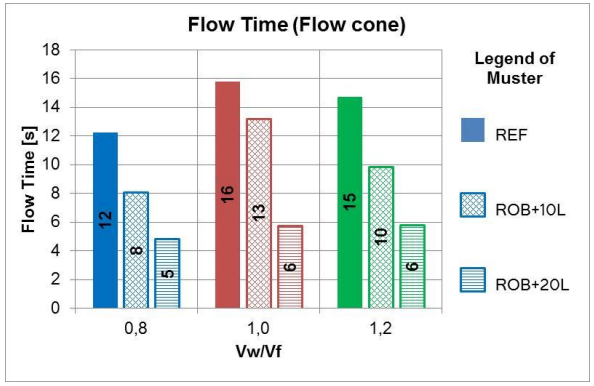

Slump Flow (Norm)								
V_W/V_F = 0.8			V_W/V_F = 1.0			V_W/V_F = 1.2		
Ref	Rob+10L	Rob+20L	Ref	Rob+10L	Rob+20L	Ref	Rob+10L	Rob+20L
Ø = 66.0 cm	Ø = 73.0 cm	Ø = 79.0 cm	Ø = 64.0 cm	Ø = 66.0 cm	Ø = 71.0 cm	Ø = 65.0 cm	Ø = 68.0 cm	Ø = 70 cm
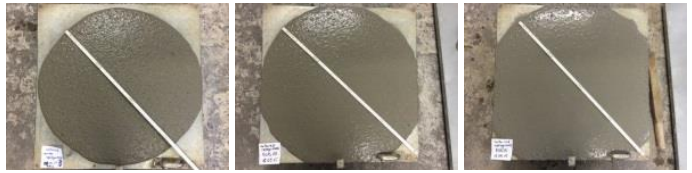								
								

Figure 4.24: Combined effects of paste composition and paste amount on the robustness of the flowability (comparable flowability)

I. Flowability

From Figure 4.24, it could be seen that the water overdosage has significantly affected the flowability of the mixture with V_W/V_F = 0.8 (ΔSF ≈ 7 cm and 13 cm) revealing the sensitivity of concrete mixtures with lower V_W/V_F values such as SCC to changes in water content. Such instances could be encountered in concrete construction, e.g., if there is rest water in truck mixers. On the contrary, the influence of water overdosage on the flowability properties is somewhat subdued in concretes with higher values of V_W/V_F as could be confirmed by the results of the mixture with V_W/V_F = 1.2 (ΔSF ≈ 3 cm and 5 cm). But, the separation of the paste from the bulk concrete should also be taken into consideration. The ideal WBC has shown a reliable robustness with tolerable changes in the flowability (ΔSF ≈ 2 cm and 6 cm). The flow time generally decreases with increasing water overdosage. Regardless of the paste composition, a water overdosage of 20 lit seems to affect the concrete mixtures to the same degree that they all assume a flow time of about 6 sec. The WBM with V_W/V_F = 1.0 has performed relatively well in terms of maintaining the flow time at water overdosage of 10 lit (ROB+10L) when compared to the other two mixtures.

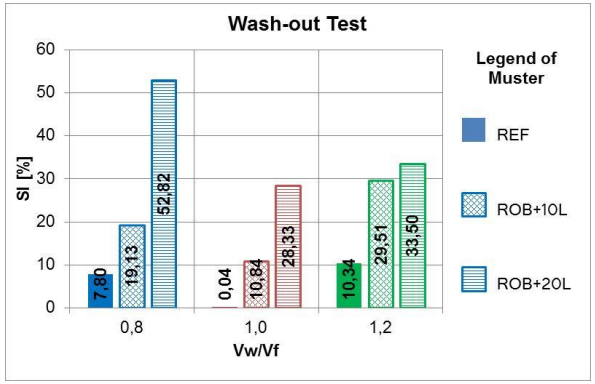

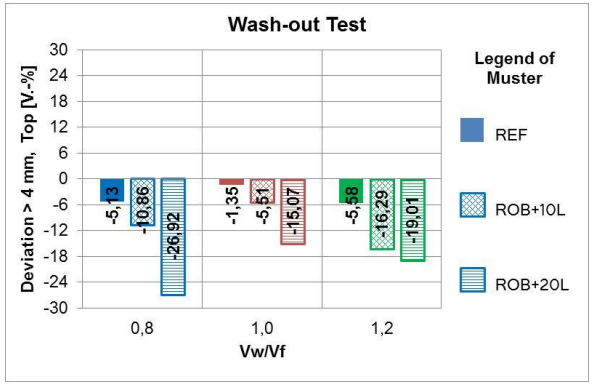

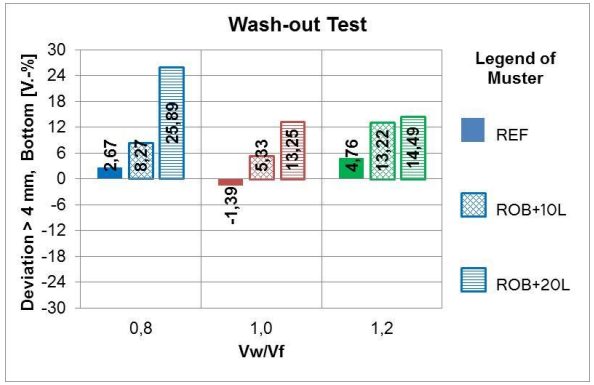

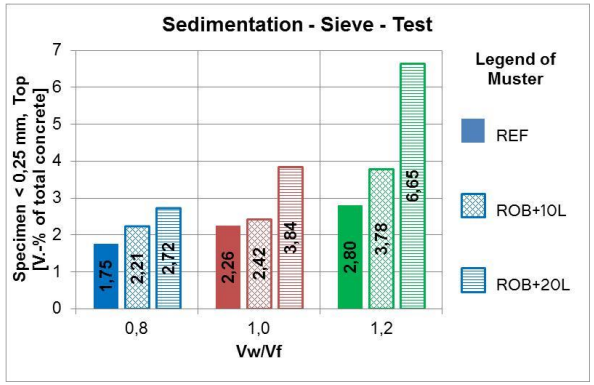

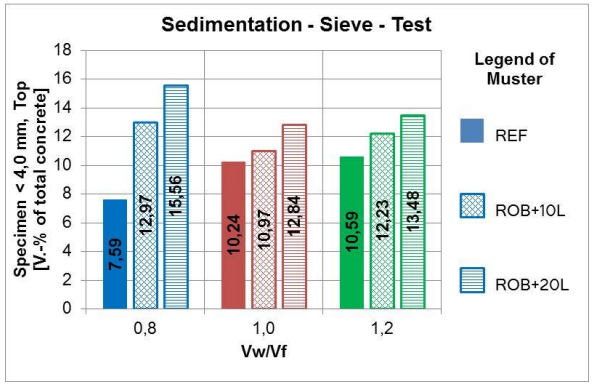

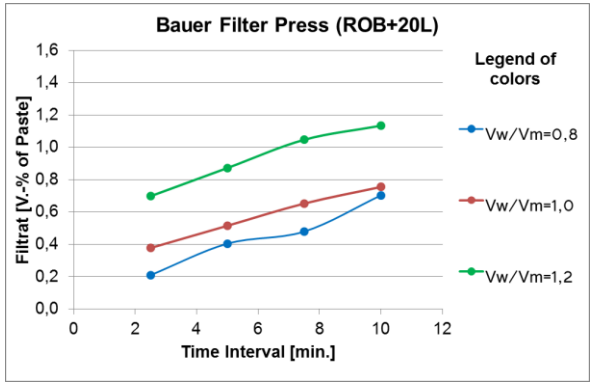

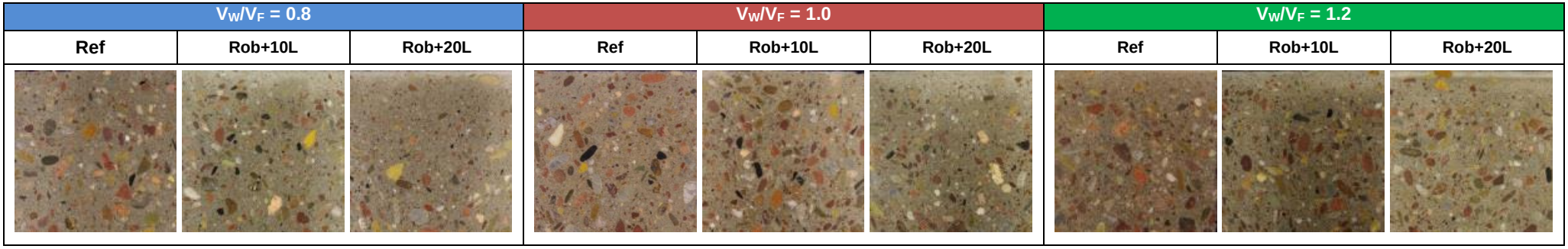

Figure 4.25: Combined effects of paste composition and paste amount on the robustness of the stability (comparable flowability)

II. Stability

Obviously, the stability of a concrete decreases with extra water overdosage as shown in Figure 4.25. The ideal WBC with V_W/V_F = 1.0 exhibit a much better robustness against water overdosage, when compared to the other two mixtures as confirmed by the WT and the visual sedimentation evaluation, especially at 10 lit water overdosage. While the visual evaluation of all mixtures indicates a significant sedimentation at a 20 lit water overdosage, the case for the mix with V_W/V_F = 0.8 is so extreme that almost no coarse aggregates lies in the top 70 mm of the hardened specimen. An exaggerated SI value is also determined for this mixture clearly indicating the risk associated with composing a concrete using a larger volume of highly viscous paste only with the aim of achieving high flowability. The mixture with V_W/V_F = 1.2, by virtue of the excessive unbound water in it, show a very poor robustness even at a 10 lit water overdosage. However, in terms of the robustness with regard to the separation of the fluid phase from the concrete, i.e. paste or fine mortar < 0.25 mm, concretes composed of highly viscous pastes (V_W/V_F = 0.8) performed much better than the other two as confirmed by the SST and the BFP results.

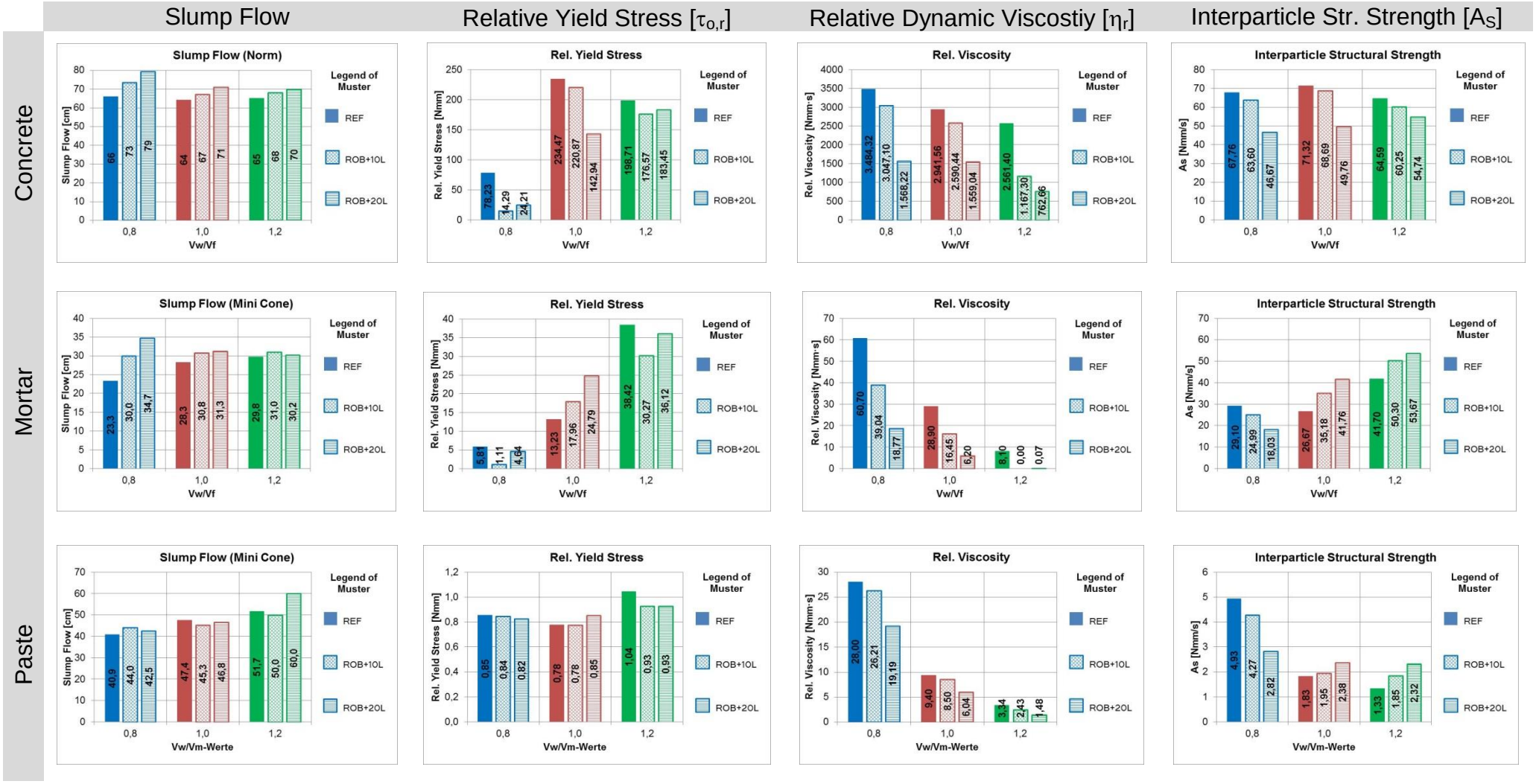

Figure 4.26: Combined effects of paste composition and paste amount on the robustness of the rheological properties (comparable flowability)

III. Rheology

The results of the rheological investigations on the concrete mixtures as well as the extracted mortar and paste compositions are illustrated in Figure 4.26. Generally, $\tau_{o,r}$, η_r and A_S of the concretes decrease with increasing water overdosage. As a result of the high amount of paste and the resulting reduced friction between the aggregates, $\tau_{o,r}$ of the overdosed mixture with $V_W/V_F = 0.8$ remains significantly lower than those of $V_W/V_F = 1.0$ and $V_W/V_F = 1.2$. The dominant role played by the paste composition is also reflected in the mixtures with water overdosage, since η_r decreases with increasing V_W/V_F values while the paste volume decreases simultaneously. Here too, due to the occurrence of sedimentation of the sand particles during the test, the results of the rheological investigations on the mortar compositions have shown no reliable trend, with the exception of the viscosity. The water overdosage does not seem to have significant influence on the yield stress $\tau_{o,r,P}$ of the paste compositions as the reference paste compositions themselves have very high slump flows. However, the viscosity $\eta_{r,P}$ clearly decreases with increasing water overdosage. The interparticle structural strength of the paste compositions also seems to be affected by the sedimentation of fines caused by the water overdosage for higher values of V_W/V_F. This is not the case for the viscous paste with $V_W/V_F = 0.8$.

4.8.5 Series IV: Effect of aggregate compositions (different flowability)

For this investigation series, different aggregate compositions with maximum grain sizes of 8 mm and 16 mm were considered. The gradation lines were optimized using the Andreasen and Andersen function with gradation exponent values of q = 0.4, 0.5 and 0.6 for both the 8 mm and 16 mm maximum grain sizes; see section 3.3.1. For the purpose of comparison, additional aggregate optimization was carried out using q = 0.8 for the maximum size of 8 mm. The paste composition with $V_W/V_F = 1.0$ was held constant for all mixtures while the respective paste amounts of 361 dm^3 and 325 dm^3 were applied for all mixtures with 8 mm and 16 mm maximum sizes.

Table 4.9: Concrete compositions for test series III for maximum grain size of 8 mm (aggregate compositions)

Materials	**q = 0.8 NS – RG1 (30% – 70%)**		**q = 0.6 NS – RG1 (40% – 60%)**		**q = 0.5 NS – RG1 (50% – 50%)**		**q = 0.4 NS – RG1 (60% – 40%)**	
	dm^3/m^3	kg	dm^3/m^3	kg	dm^3/m^3	kg	dm^3/m^3	kg
CEM I	95.7	300.8	95.7	300.8	95.7	300.8	95.7	300.8
FA WH	84.8	195.8	84.8	195.8	84.8	195.8	84.8	195.8
NS (0/2)	187.2	498.0	249.6	663.9	312,0	829.9	374.4	995.9
RG1 (2/8)	436.8	1131.3	374.4	969.7	312,0	808.1	249,6	646.5
Water	180.5	180.5	180.5	180.5	180.5	180.5	180.5	180.5
SP1	5,41 [% M_W]							
WB	-6.0		-13		-19		-26	
Key Parameters								
Paste content	dm^3/m^3	361						
Aggregate content	dm^3/m^3	624						
Air voids content	dm^3/m^3	15						
w/c	-	0.6						
V_W/V_F	-	1.0						
Mortar content	dm^3/m^3	548	611		673		735	
Paste in Mortar	dm^3/m^3	649	582		528		484	

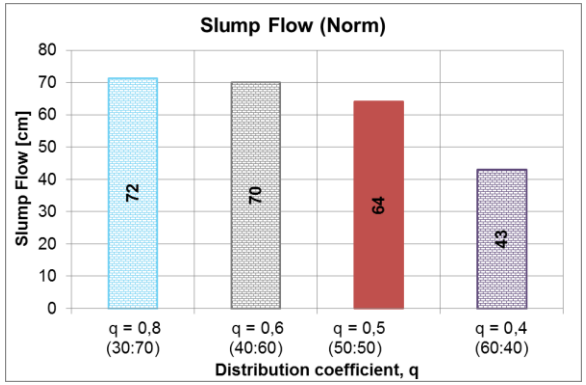

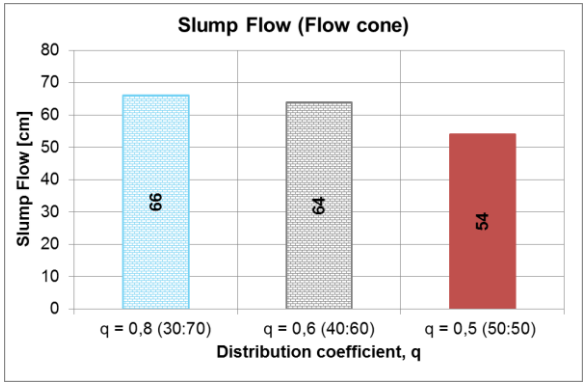

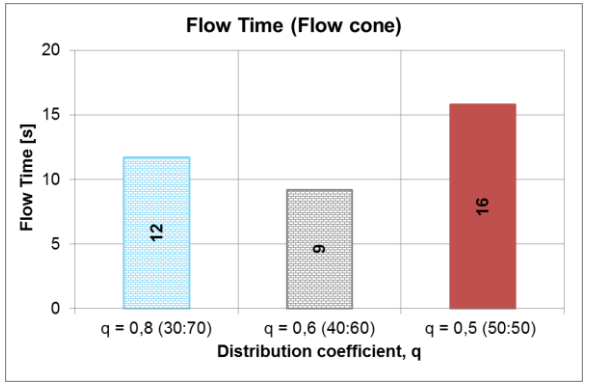

Slump Flow (Norm)			
q = 0.8 **NS – RG1** **(30% – 70%)**	**q = 0.6** **NS – RG1** **(40% – 60%)**	**q = 0.5** **NS – RG1** **(50% – 50%)**	**q = 0.4** **NS – RG1** **(60% – 40%)**
Ø = 72.0 cm	Ø = 70.0 cm	Ø = 64.0 cm	Ø = 43.0 cm
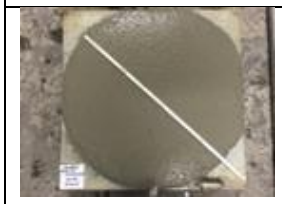	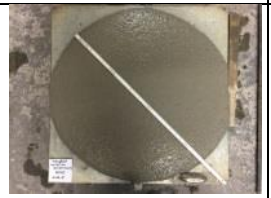	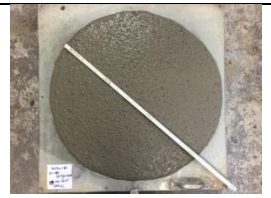	
		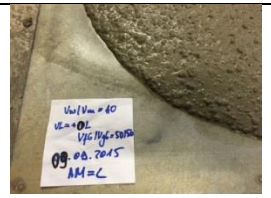	

Slump Flow (Flow cone)			
q = 0.8 **NS – RG1** **(30% – 70%)**	**q = 0.6** **NS – RG1** **(40% – 60%)**	**q = 0.5** **NS – RG1** **(50% – 50%)**	**q = 0.4** **NS – RG1** **(60% – 40%)**
Ø = 66.0 cm	Ø = 64.0 cm	Ø = 54.0 cm	Ø = -
	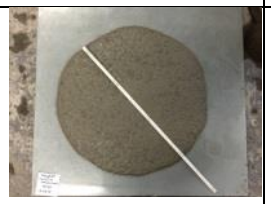	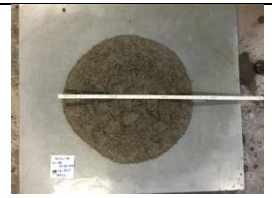	Impossible to conduct
			

Figure 4.27: Effects of aggregate composition (q) on the flowability – maximum size 8 mm (different flowability)

I. Flowability

In Figure 4.27, it could be seen that for a constant composition and volume of paste, which was actually determined for the ideal WBC with q = 0.5 (50 : 50), the slump flow decreases with decreasing values of **q** or increasing sand – coarse aggregate ratio. This is due to the combined effects of the decreasing packing density (higher voids' paste demand) and the increased surface paste demand of the aggregates, see section 4.5.2. The mixture with q = 0.4 (60 : 40) has a significantly lower packing density (higher voids' paste demand) and a relatively higher surface paste demand which has resulted into a relatively stiff consistency that it could not even flow through the flow cone. Provided that the mixtures remain homogeneous, the flow times tend to increase with decreasing values of **q** as a result of the reduction in the excess paste amount caused by the higher proportion of sand. Moreover, at very high values of **q,** the substantially small proportion of sand could lead to the occurrence of inhomogeneity or harshness of the concrete which ultimately causes the interlocking of the coarser aggregates. That might be the reason for the unexpectedly higher flow time measured for the mixture with q = 0.8 (30 : 70).

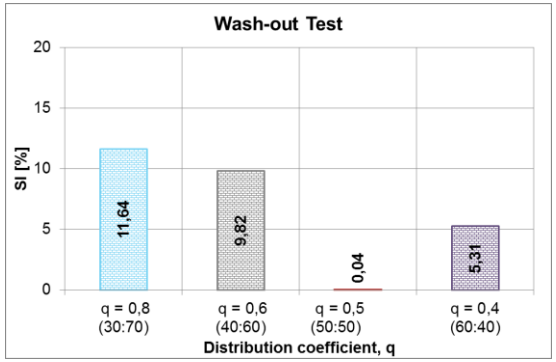

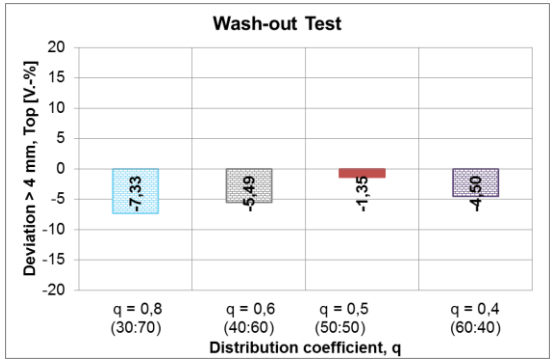

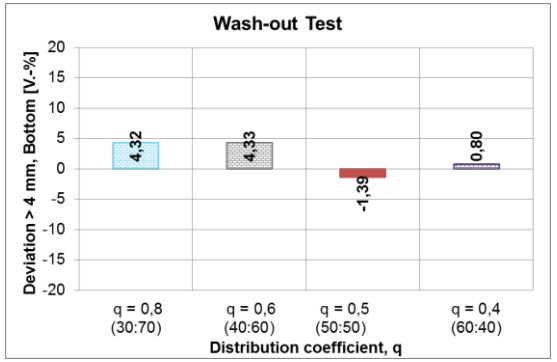

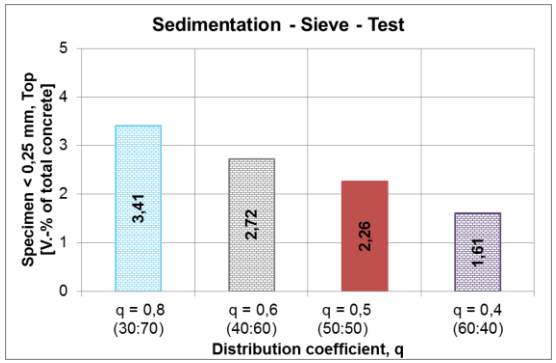

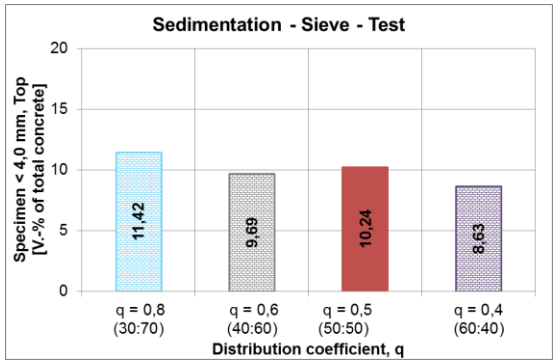

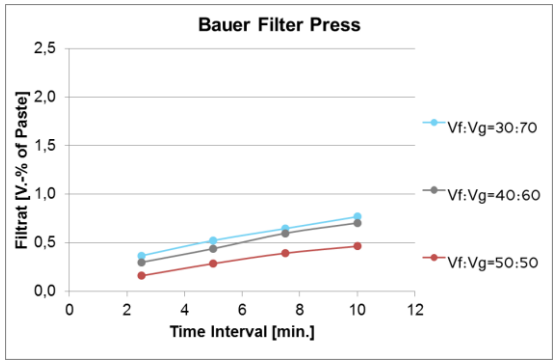

q = 0.8 (30% – 70%)	q = 0.6 (40% – 60%)	q = 0.5 (50% – 50%)	q = 0.4 (60% – 40%)
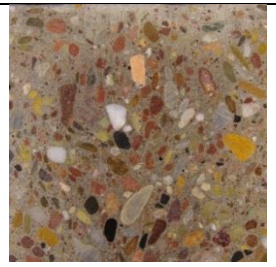	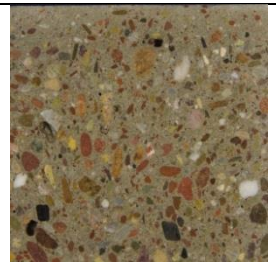	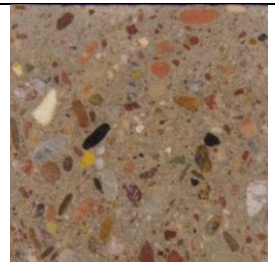	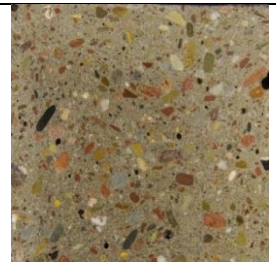

Figure 4.28: Effects of aggregate composition (q) on the stability – maximum size 8 mm (different flowability)

II. Stability

As can be seen in Figure 4.28, here also, the ideal WBC with the gradation exponent q = 0.5 shows the best stability under the influence of vibration and pressure when compared to those having higher or lower values of **q** as confirmed by the results the WT and the visual sedimentation evaluation as well as the BFP. Even so, the other three mixtures can also be considered as stable as no visible sedimentation of the aggregates could be observed. These mixtures have also satisfied the WB criterion which is responsible for ensuring the reliable stability despite the discrepancies in the paste content. The fact that no extreme sedimentation was observed for the mixture with q = 0.8 even though it showed some bleeding of paste in the slump flow test might be an indication as to the different stability phenomena during vibration in a confined space and casting where unrestricted movement of the mass takes place. The separation of the liquid phase (paste or mortar) from the bulk concrete under the influence of vibration decreases with increasing values of **q** as revealed by the results of the SST. As the paste amount applied in this series is determined for the aggregate composition with q = 0.5, a direct application of this paste amount to mixtures with higher values of **q** results into a higher amount of unbound paste which could lead to the increased separation of the phases.

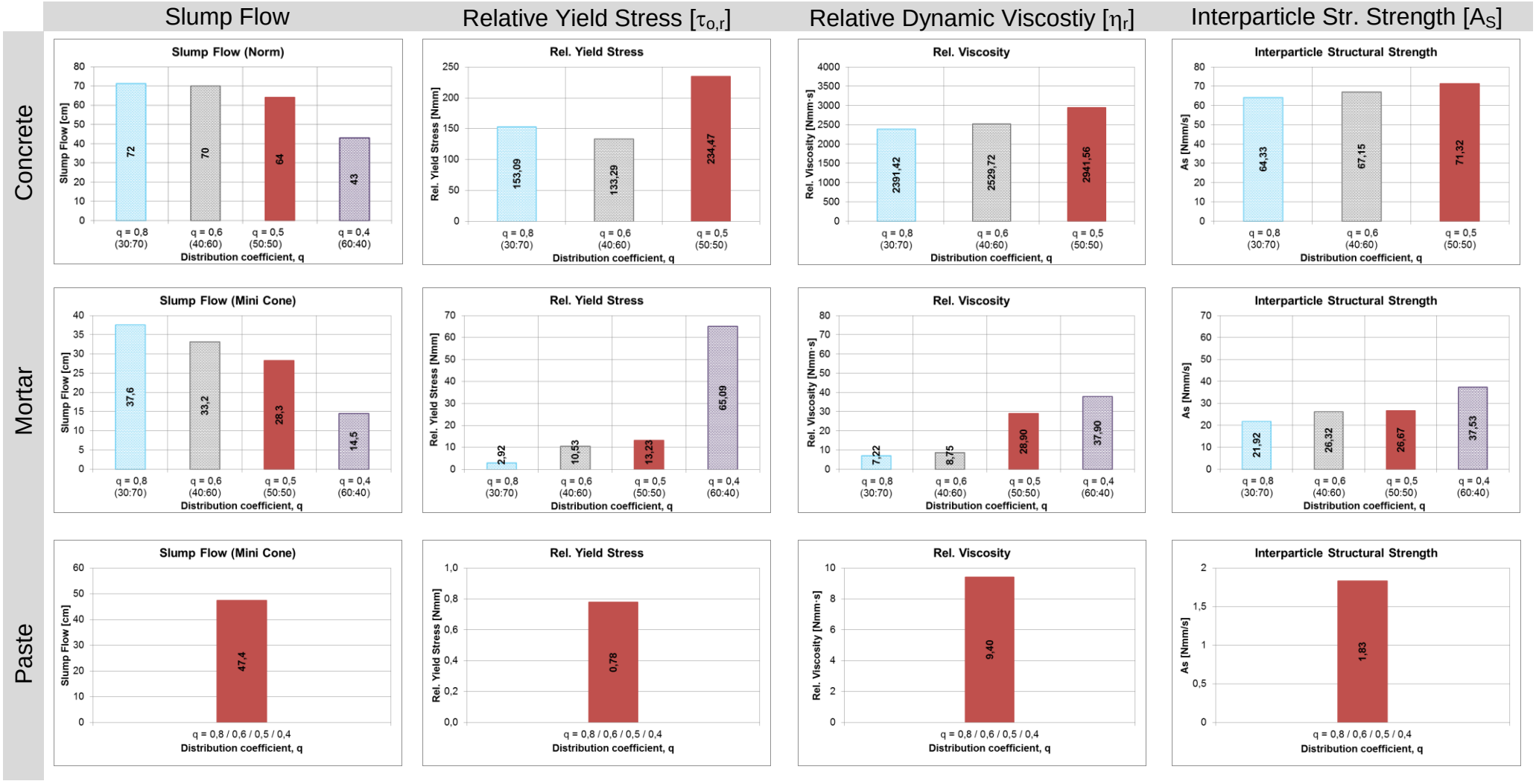

Figure 4.29: Effects of aggregate composition (q) on the rheological properties – maximum size 8 mm (different flowability)

III. Rheology

The results of the rheological investigations on the concrete mixtures as well as the extracted mortar and paste compositions are illustrated in Figure 4.29. The yield stress $\tau_{o,r}$ of the WBC q = 0.5 is significantly higher than the other two concrete mixtures with q = 0.6 and 0.8, both exhibiting relatively the same relative yield stress values. This confirms the finding in section 4.8.3 that in paste dominated concrete compositions, $\tau_{o,r}$ is more a function of the "unbound" paste volume. This is also in line with the slump flows; the ideal WBC mixture having a smaller slump flow than the other two mixtures. Both η_r and $\mathbf{A_S}$ increase with decreasing values of **q**. The general trend that $\tau_{o,r}$, η_r and $\mathbf{A_S}$ increase with decreasing values of **q** has to do with the amount of paste that is readily available to form a lubrication layer around the aggregates. In this series, the paste amount (determined for q = 0.5) and composition are kept constant and thus when applied to aggregate compositions with a lower paste demand as is the case with q = 0.6 and q = 0.8 with their respective total paste demands of ca. 345 and 335 dm^3, there remains an excess amount of paste which further enhances the lubrication effect decreasing the overall resistance of the concrete compositions against shearing effects as manifested by the decreasing values of $\tau_{o,r}$, η_r and $\mathbf{A_S}$. The same trend could also be observed with the rheological properties of the extracted mortar compositions.

Also investigated in this test series are the effects of different aggregate compositions with maximum grain size of 16 mm.

Table 4.10: Concrete compositions for test series III for maximum grain size of 16 mm (aggregate compositions)

Materials		**q = 0.4 NS – RG1 – RG2 (45% – 33% – 22%)**		**q = 0.5 NS – RG1 – RG2 (35% – 38% – 27%)**		**q = 0.6 NS – RG1 – RG2 (27% – 41% – 32%)**	
		dm³/ m³	dm³/ m³	dm³/ m³	dm³/ m³	dm³/ m³	kg
CEM I		86.2	270.8	86.2	270.8	86.2	270.8
FA WH		76.3	176.3	76.3	176.3	76.3	176.3
NS (0/2)		297.0	790.0	231.0	614.5	178.2	474.0
RG1 (2/8)		217.8	564.1	248.8	644.4	269.8	698.8
RG2 (8/16)		145.2	377.5	180.2	468.5	212.0	551.2
Water		162.5	162.5	162.5	162.5	162.5	162.5
SP1		5,41 [% M_W]					
WB		-22		-14		-7	
Paste content	dm³/m³	325					
Aggregate content	dm³/m³	660					
Air voids content	dm³/m³	15					
w/c	-	0.6					
V_W/V_F	-	1.0					
Mortar content	dm³/m³	622		556		503	
Paste in Mortar	dm³/m³	416		433		445	

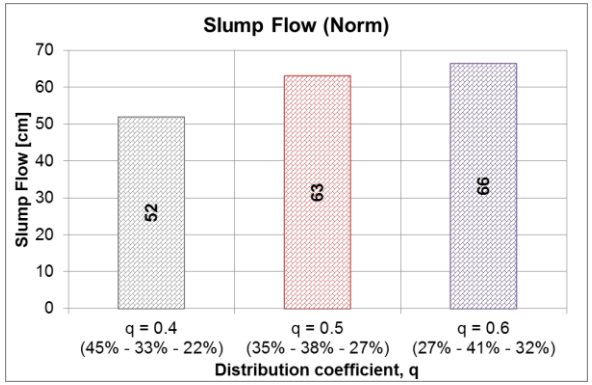

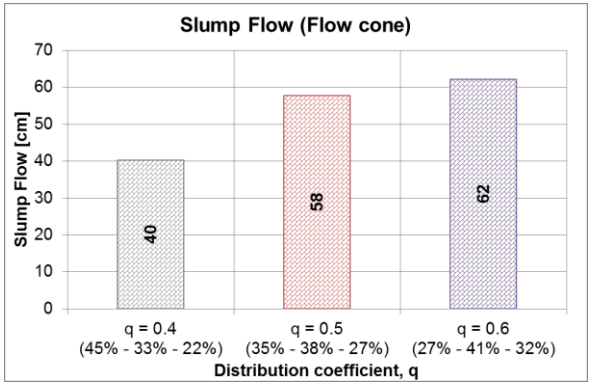

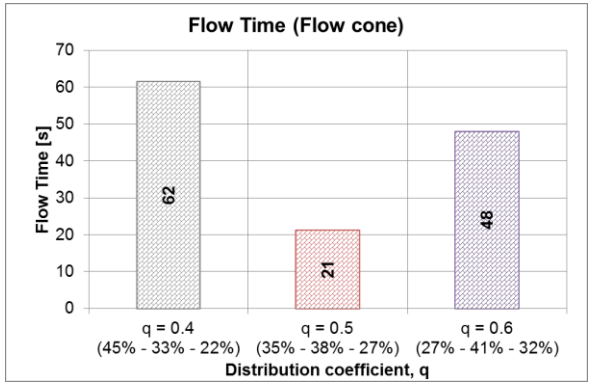

Slump Flow (Norm)		
q = 0.4 **NS – RG1 – RG2** **(45% – 33% – 22%)**	**q = 0.5** **NS – RG1 – RG2** **(35% – 38% – 27%)**	**q = 0.6** **NS – RG1 – RG2** **(27% – 41% – 32%)**
Ø = 52.0 cm	Ø = 63.0 cm	Ø = 66.0 cm
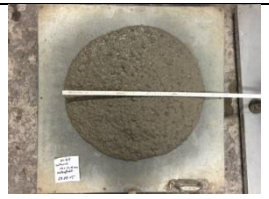	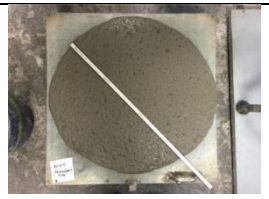	
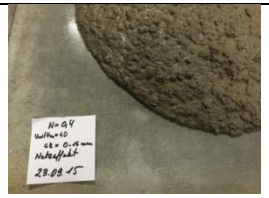		

Slump Flow (Flow cone)		
q = 0.4 **NS – RG1 – RG2** **(45% – 33% – 22%)**	**q = 0.5** **NS – RG1 – RG2** **(35% – 38% – 27%)**	**q = 0.6** **NS – RG1 – RG2** **(27% – 41% – 32%)**
Ø = 40.0 cm	Ø = 58.0 cm	Ø = 62.0 cm
	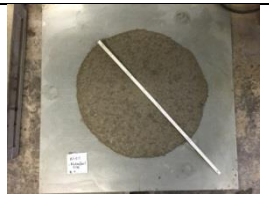	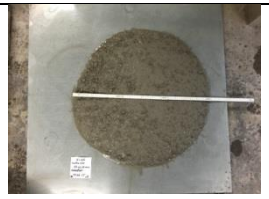
		

Figure 4.30: Effects of aggregate composition (q) on the flowability – maximum size 16 mm (different flowability)

I. Flowability

Similar to the observation made for the concrete compositions with 8 mm maximum grain size, the slump flow increases with increasing values of **q** or decreasing fine – coarse aggregate ratios as shown in Figure 4.30. This is due to the combined effects of the increased packing density (lower voids' paste demand) and the decreased surface paste demand of the aggregate compositions, see section 4.5.2. The mixture with q = 0.4 (45 : 33 : 22) has a lower packing density (higher voids' paste demand) and higher surface paste demand which has resulted into a relatively stiff consistency that it could not even flow through the slump cone. Provided that the mixtures remain homogeneous, the flow times tend to increase with decreasing values of q as a result of the reduction in the excess paste amount required for the separation of the aggregates. Here also, the loss of homogeneity might have led to the interlocking of the aggregates in the slump cone as revealed by the unrealistic flow time as is the case with q = 0.6 (27 : 41 : 32).

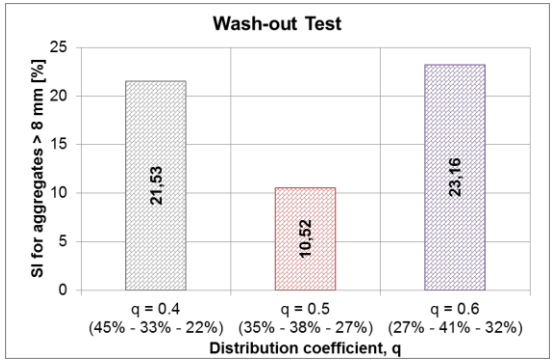

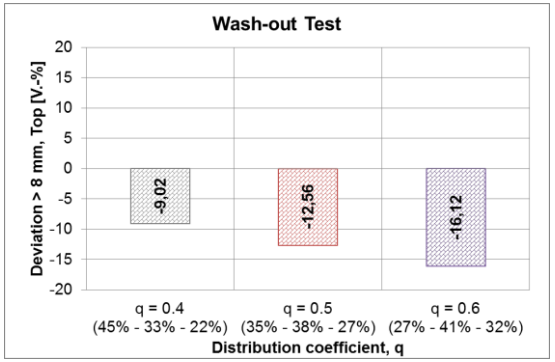

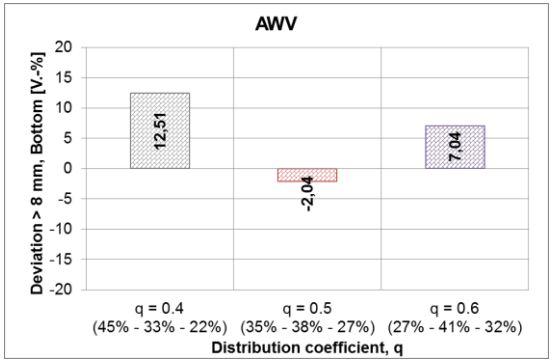

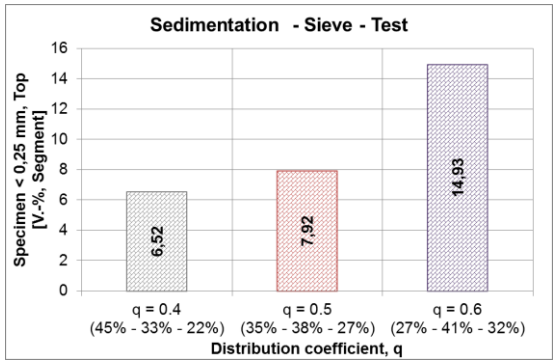

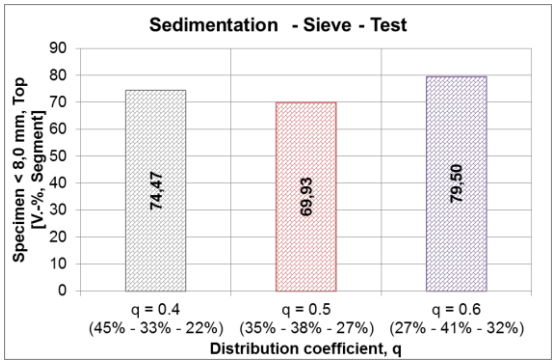

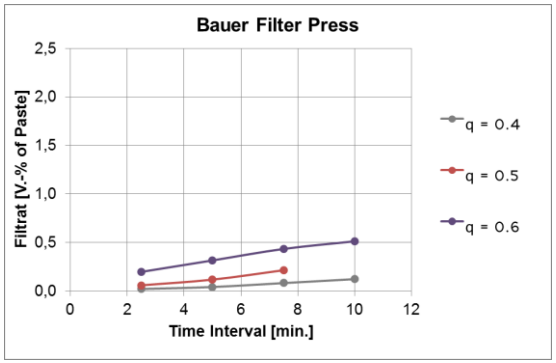

q = 0.4 (45% – 33% – 22%)	q = 0.5 (35% – 38% – 27%)	q = 0.6 (27% – 41% – 32%)
	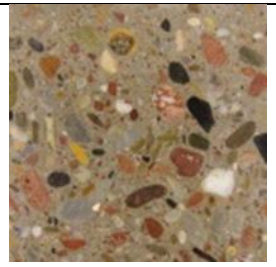	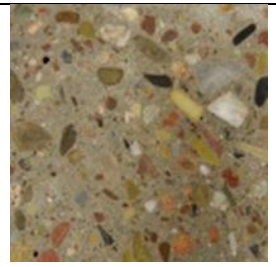

Figure 4.31: Effects of aggregate composition (q) on the stability – maximum size 16 mm (different flowability)

II. Stability

As can be seen in Figure 4.31 , the reference WBC with the gradation exponent q = 0.5 shows the best stability under the influence of vibration when compared to those having higher or lower values of **q** as confirmed by the results the WT and the visual sedimentation evaluation. However, the general stability of all the mixtures could be considered to be satisfactory on the ground that all of them have satisfied the WB criterion. The same observation is made as that of the mixture with q = 0.6 (maximum size of 8 mm) with regard to the different stability mechanisms of vibration in a confined space (WT) and casting where the concrete flows without restriction (slump flow). The separation of the liquid phase (paste or mortar) from the bulk concrete under the influence of vibration increases with increasing values of **q** as revealed by the results of the SST and the BFP. The paste amount applied in this series is approximately equal to the paste demand of the aggregate composition with q = 0.5. Consequently, a direct application of this paste amount to the other mixtures with different values of **q** is responsible for the relatively poor stability. This underscores the importance of determining the paste demand of aggregates depending on their composition.

III. Rheology

The rheological investigations could not be conducted for the concrete mixtures in this series, since their maximum size of 16 mm by far exceeds the maximum allowable grain size of 8 mm for the Viskomat XL rheometer.

4.8.6 Series V: Combined effects of aggregate composition and paste amount (comparable flowability)

For this investigation series, three gradation lines, which were optimized using the Andreasen and Andersen function with exponent values q = 0.4, 0.5 and 0.6 were chosen; see section 3.3.1. The paste composition with V_W/V_F = 1.0 remained constant for all three mixtures. For this paste composition, a paste amount ca. 361 dm^3 was determined for the reference mixture with q = 0.5 using the WBMD; see section 4.6. For the other concrete mixtures with q = 0.4 and q = 0.6 (both with V_W/V_F = 1.0), the paste amount was also determined using the WBMD with slight adjustments to attain a comparable flowability with that of the reference with q = 0.5. The concrete compositions are shown in Table 4.11.

Table 4.11: Concrete compositions for test series IV for maximum grain size of 8 mm (aggregate composition and paste content)

Materials		**q = 0.6** **NS – RG1** **(40% – 60%)**		**q = 0.5** **NS – RG1** **(50% – 50%)**		**q = 0.4** **NS – RG1** **(60% – 40%)**	
		dm³/m³	kg	dm³/m³	kg	dm³/m³	kg
CEM I		93.1	292.5	95.7	300.8	103.7	325.8
FA WH		82.4	190.4	84.8	195.8	91.8	212.1
NS (0/2)		253.6	674.6	312,0	829.9	356.4	948.0
RG1 (2/8)		380.4	985.2	312,0	808.1	237.6	615.4
Water		175.5	175.5	180.5	180.5	195.5	195.5
SP1		5,41 [% M_W]					
WB		-16		-19		-14	
Key Parameters							
Paste content	dm³/m³	351		361		391	
Aggregate content	dm³/m³	634		624		594	
Air voids content	dm³/m³	15					
w/c	-	0.6					
V_W/V_F	-	1.0					
Mortar content	dm³/m³	605		673		747	
Paste in Mortar	dm³/m³	572		528		515	

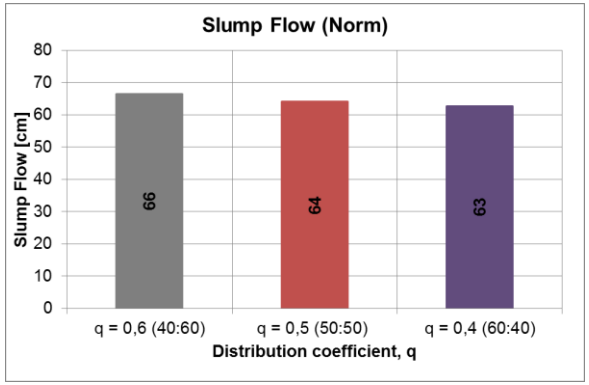

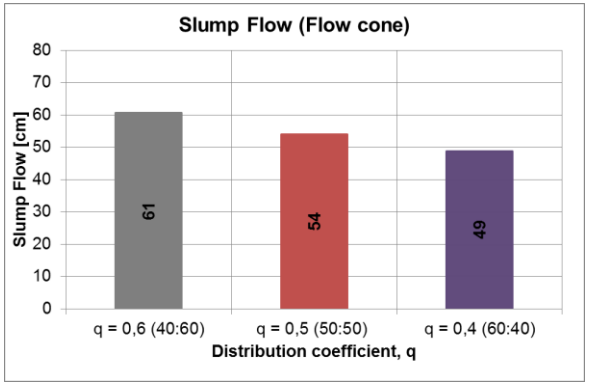

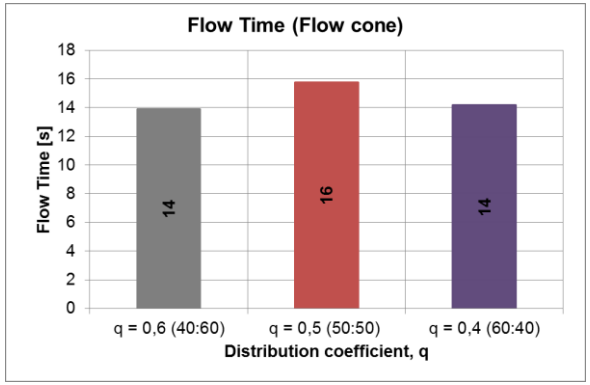

Slump Flow (Norm)		
q = 0.6 **NS – RG1** **(40% – 60%)**	**q = 0.5** **NS – RG1** **(50% – 50%)**	**q = 0.4** **NS – RG1** **(60% – 40%)**
Ø = 66.0 cm	Ø = 64.0 cm	Ø = 63.0 cm
	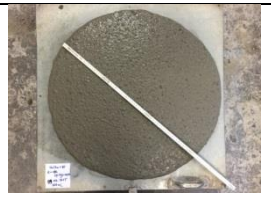	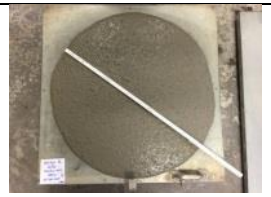
	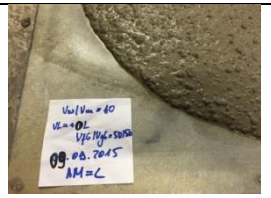	

Slump Flow (Flow cone)		
q = 0.6 **NS – RG1** **(40% – 60%)**	**q = 0.5** **NS – RG1** **(50% – 50%)**	**q = 0.4** **NS – RG1** **(60% – 40%)**
Ø = 61.0 cm	Ø = 54.0 cm	Ø = 49.0 cm
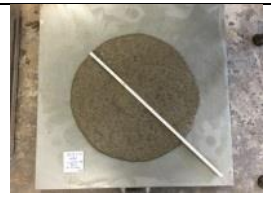	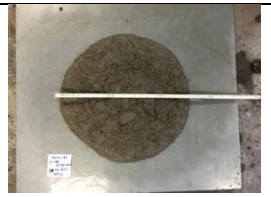	
	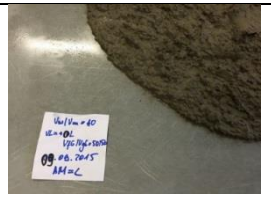	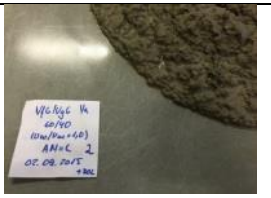

Figure 4.32: Combined effects of aggregate composition and paste amount on the flowability – max. size 8 mm (comp. flowability)

I. Flowability

In Figure 4.32, it could be seen that while all three mixtures possess comparable flowability as measured using the standard slump flow (with tapping), the flowability as determined using the flow cone (without tapping) decreases with decreasing values of gradation exponent **q** (increased fine – coarse aggregate ratios). This reveals the advantages associated with maximizing the packing density (for q = 0.6) or even the lattice effect (for q = 0.5) of aggregates in order to attain good flowability without the application of external energy. The flow time of the mixtures with q = 0.6 (40 : 60) is slightly lower than that of the mixture with q = 0.5 (50 : 50) which could be attributed to the positive effects of a thicker lubrication layer formed as a result of the lower paste demand of the aggregate composition with q = 0.6 (40 : 60), see also section 4.5.2. The mixture with q = 0.4 has a higher mortar / paste content in comparison with that of q = 0.5 which might be the reason why it has a slightly lower flow time.

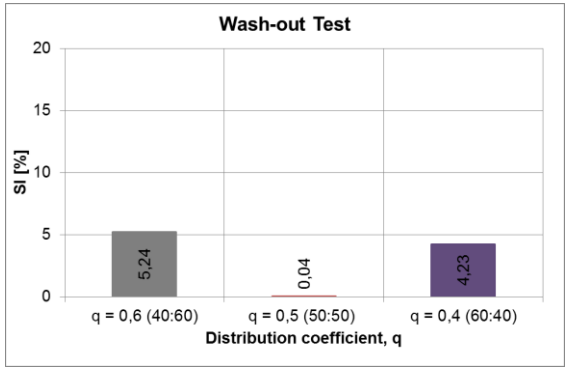

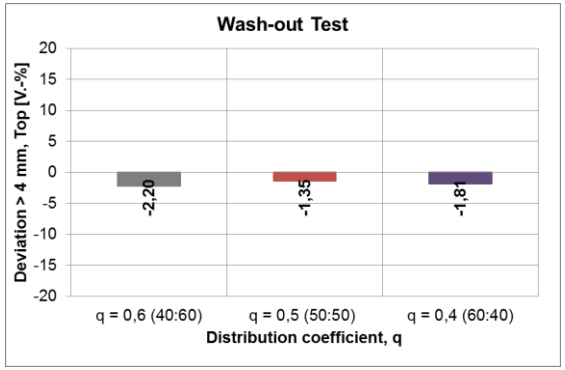

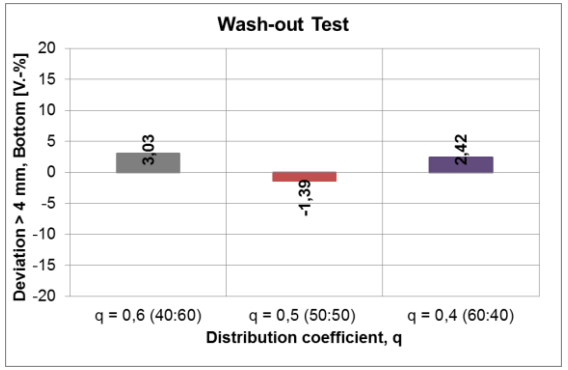

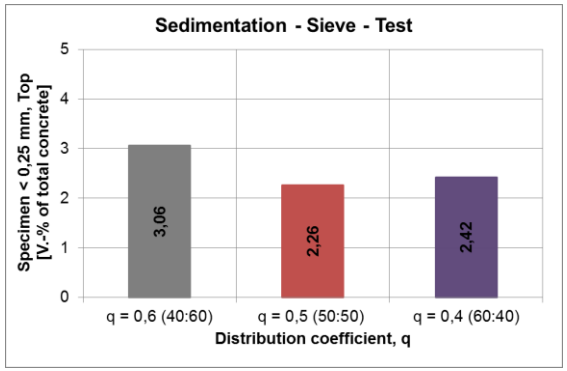

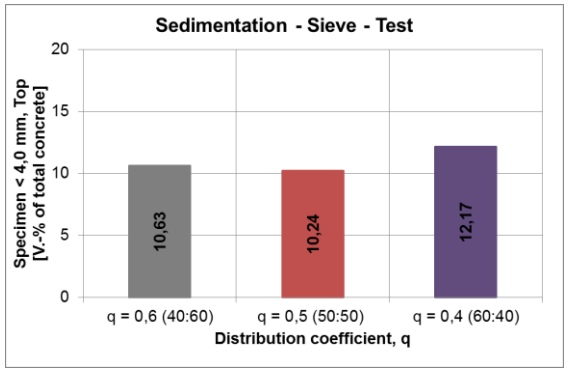

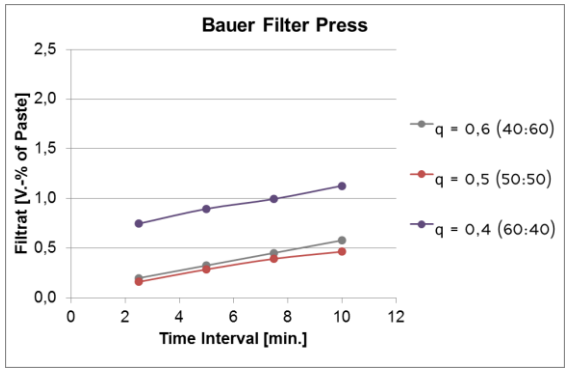

q = 0.6 (40% – 60%)	q = 0.5 (50% – 50%)	q = 0.4 (60% – 40%)
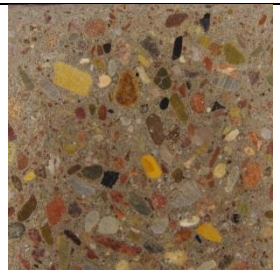	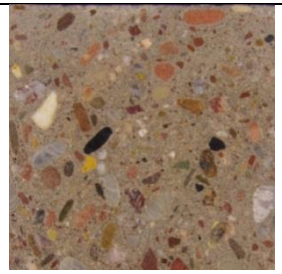	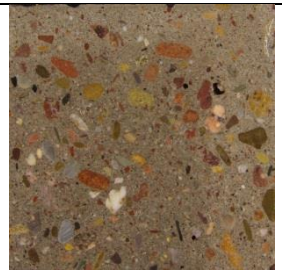

Figure 4.33: Combined effects of aggregate composition and paste amount on the stability – max. size 8 mm (comp. flowability)

II. Stability

Here also, the WBC with the gradation exponent q = 0.5 (50 : 50) shows the best stability under the influence of vibration and pressure when compared to those having higher or lower values of **q** as confirmed by the results the WT, SST, visual evaluation of the sedimentation as well as the BFP, see Figure 4.33. This is also in line with the results of the stability investigations in test series III, thereby confirming that aggregate optimization based on the gradation exponent q = 0.5 (50 : 50) does give a reliable lattice effect which plays a crucial role in terms of avoiding the sedimentation of coarser aggregates by creating a quasi-net formation in which the larger particles are buttressed by the smaller ones. Here also, the overall stability of all three mixtures could be considered to be satisfactory taking the facts into consideration that they have a high degree of flowability and are exposed to a high intensity vibration for 30 seconds. This confirms the importance of maintaining the WB in concrete for reliable stability.

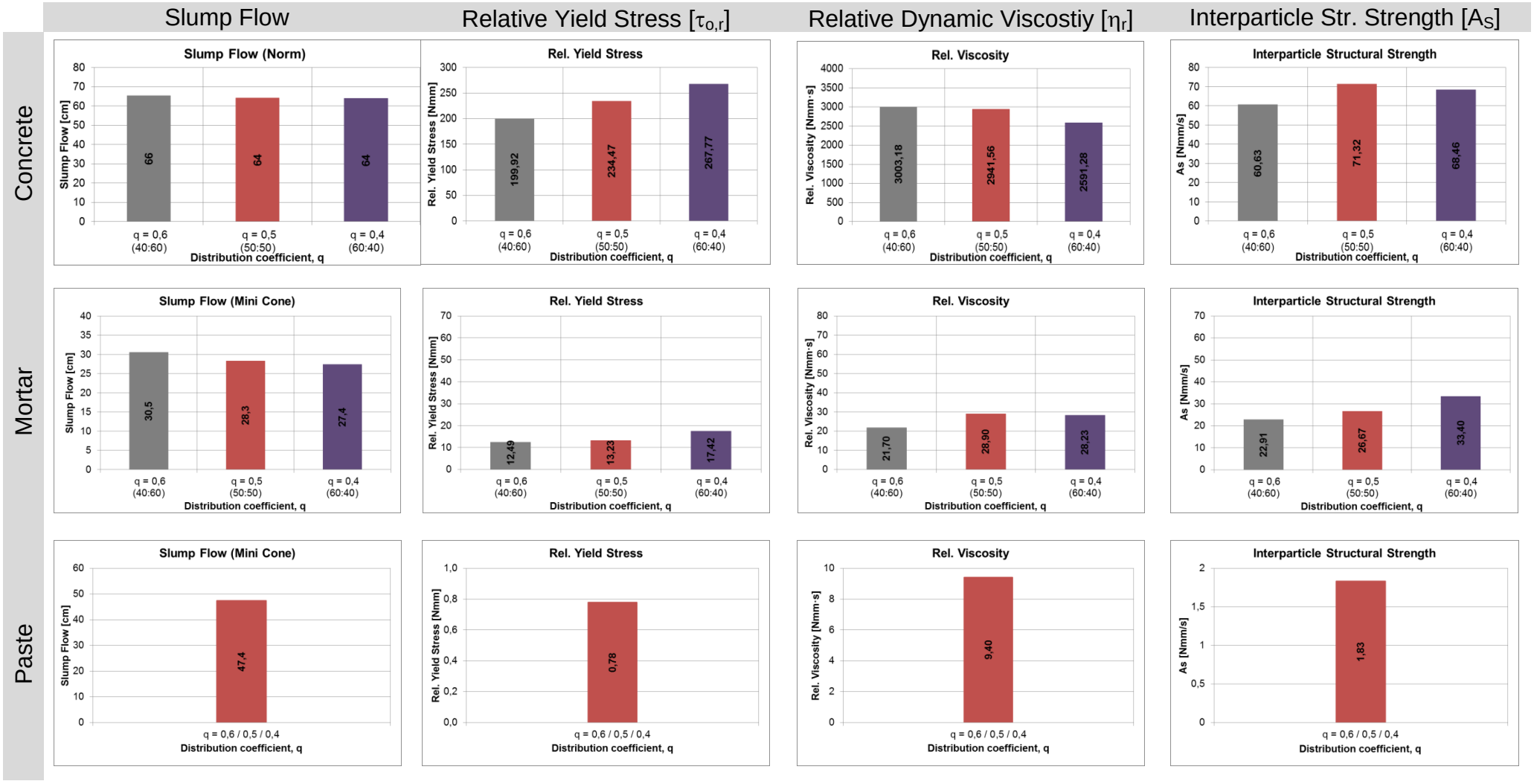

Figure 4.34: Combined effects of aggregate composition (q) and paste amount on the rheological properties – max. size 8 mm (comp. flowability)

III. Rheology

The results of the rheological investigations on the concrete mixtures as well as the mortar and paste compositions extracted from them are illustrated in Figure 4.34. The yield stress $\tau_{o,r}$ generally increases with decreasing values of **q**. The mixture with the highest packing density (q = 0.6 (40 : 60)) has the smallest $\tau_{o,r}$. The paste content of this mixture is only 10 dm^3 lower than that of the mixture with q = 0.5 (50 : 50). Thus, in combination with the maximum packing density, it could show some characteristics as that of a paste dominated mixture which might be the reason for the reduced value of $\tau_{o,r}$. As the paste domination decreases, the value $\tau_{o,r}$ increases as observed in the mixtures with q = 0.5 (50 : 50) and q = 0.6. (40 : 60) The mixture with q = 0.5 (50 : 50) exhibit relatively higher values of η_r and A_S which could be attributed to the optimal lattice effect of the aggregate composition. The results of the rheological investigations on the mortar compositions show generally increasing trend with regard to $\tau_{o,r}$, η_r and A_S with decreasing values of **q**.

4.8.7 Series VI: Combined effects of aggregate composition and paste amount on the robustness (comparable flowability)

For this investigation series, a water overdosage of 10 lit and 20 lit was applied to the reference concrete mixtures from test series V with **q** values of 0.4, 0.5 and 0.6 having constant slump flow, see 4.8.6. Here also, the increased total volume of concrete of 1010 dm^3 or 1020 dm^3 due to the water overdosage of 10 lit and 20 lit is converted to 1 m^3 of concrete by adjusting the amount of the component materials proportionally to 1000 dm^3 as shown in Table 4.12.

Table 4.12: Concrete compositions for test series VI (robustness vs. aggregates)

Materials		**q = 0.6 NS – RG1 (40% – 60%)**		**q = 0.5 NS – RG1 (50% – 50%)**		**q = 0.4 NS – RG1 (60% – 40%)**	
		Rob+10 L	**Rob+20 L**	**Rob+10 L**	**Rob+20 L**	**Rob+10 L**	**Rob+20 L**
		dm³/m³	dm³/m³	dm³/m³	dm³/m³	dm³/m³	dm³/m³
CEM I		92.2	91.3	94.8	93.9	102.7	101.7
FA WH		81.6	80.8	83.9	83.1	90.9	90.0
NS (0/2)		251.1	248.6	308.9	305.9	352.9	349.4
RG1 (2/8)		376.6	372.9	308.9	305.9	235.3	232.9
Water		183.7	191.7	186.6	196.6	203.5	211.3
SP1		5.41 [% M_W of Ref.]					
WB		-6	+4	-9	+1	-4	+6
Key Parameters							
Paste content	dm³/m³	357	364	367	373	397	403
Aggregate content	dm³/m³	628	621	618	612	588	582
Air voids content	dm³/m³	15					
V_W/V_F	-	1.0					

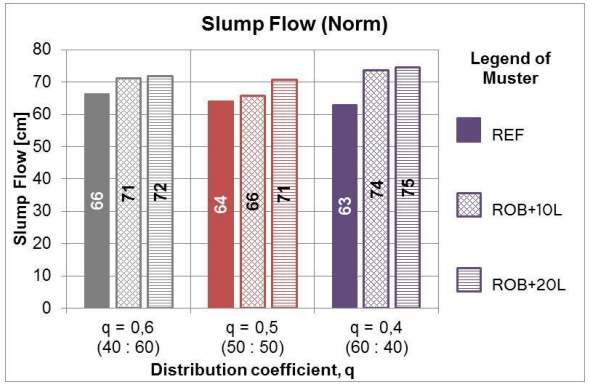

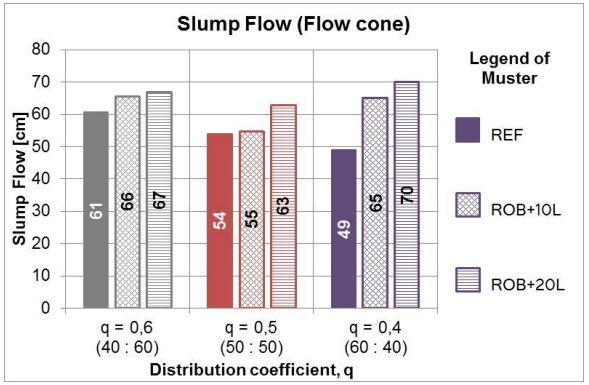

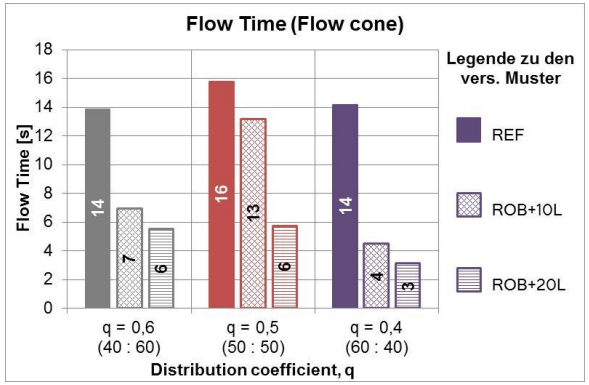

Slump Flow (Norm)								
q = 0.6 (40% – 60%)			q = 0.5 (50% – 50%)			q = 0.4 (60% – 40%)		
Ref	Rob+10L	Rob+20L	Ref	Rob+10L	Rob+20L	Ref	Rob+10L	Rob+20L
Ø = 66.0 cm	Ø = 71.0 cm	Ø = 72.0 cm	Ø = 64.0 cm	Ø = 66.0 cm	Ø = 71.0 cm	Ø = 63.0 cm	Ø = 74.0 cm	Ø = 75 cm
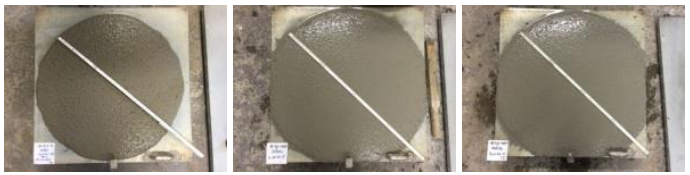								
								

Figure 4.35: Combined effects of aggregate composition (q) and paste amount the robustness of the flowability (comparable flowability)

I. Flowability

Obviously, the water overdosage has resulted into an increase in the flowability of all mixtures as can be seen in Figure 4.35. However, here too, the WBC possessing the optimized aggregate gradation with q = 0.5 (50 : 50) performs relatively very well, especially for a 10 lit water overdosage. The mixture with q = 0.6 (40 : 60), despite possessing the aggregate composition with the highest packing density (see section 4.5.2), has shown relatively poor robustness with regard to the flowability. Moreover, separation of paste could already be observed at the edges from the slump flow test even at a 10 lit water overdosage. Similarly, the flowability of the mixture with q = 0.4 (60 : 40), having the highest paste requirement, is also strongly affected by the water overdosage, even though no visible segregation could be observed at the edges. The flow times of the two mixtures q = 0.4 (60 : 40) and q = 0.6 (40 : 60) also changes drastically with the addition of extra water, while the one with q = 0,5 (50 : 50) remain at least for a 10 lit water overdosage reasonably tolerable. These facts demonstrate that aggregate optimization based on the method as introduced in the WBMD; see section 3.3.1 do also have positive contributions in terms of enhancing the robustness of the flowability properties of concrete mixtures against water overdosage.

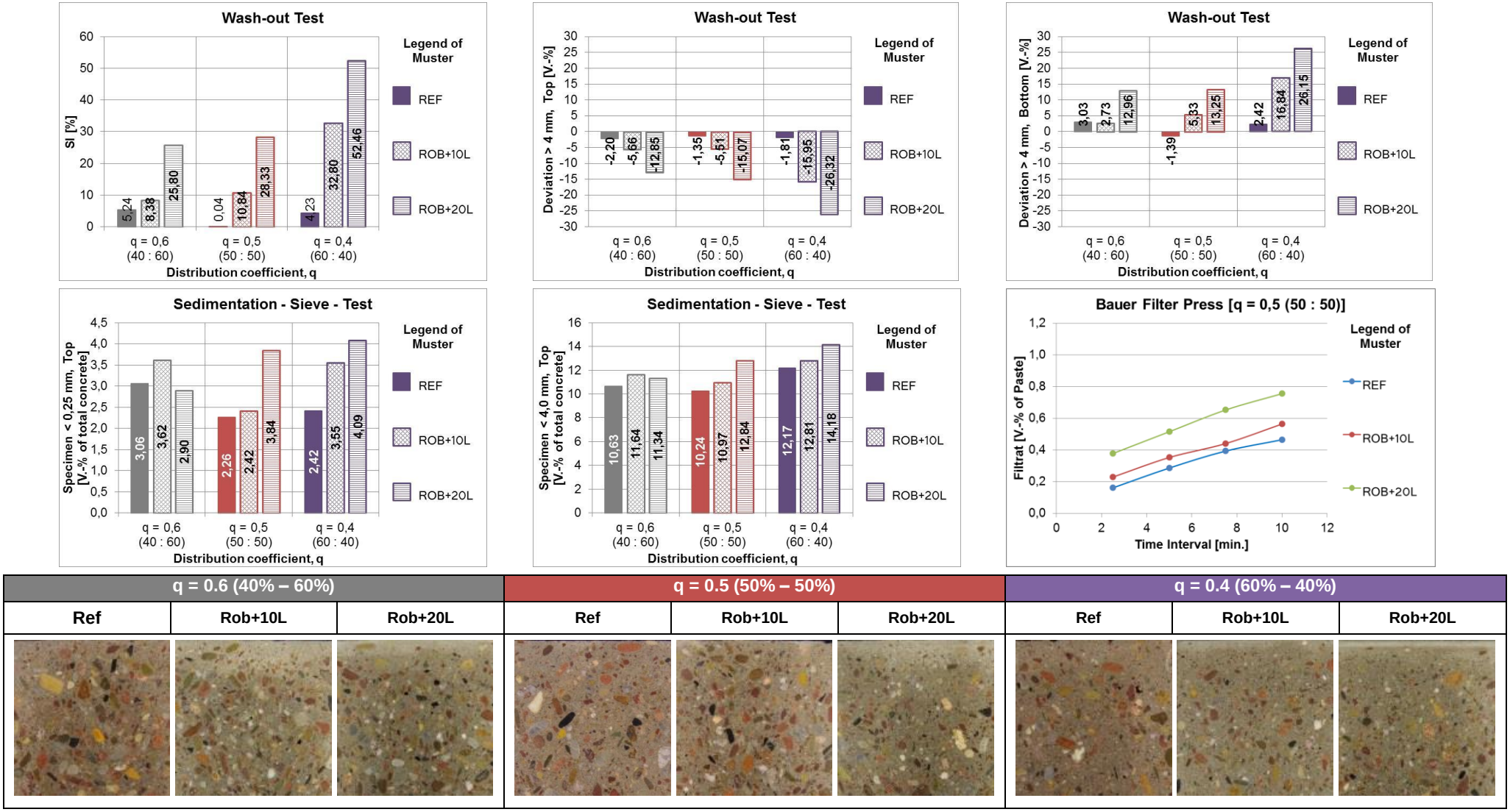

Figure 4.36: Combined effects of agg. composition (q) and paste amount on the robustness of the stability (comparable flowability)

II. Stability

The stability of the concrete mixtures is clearly affected by the water overdosage as confirmed by the WT, the SST, the visual sedimentation evaluation as well as the BFP; see Figure 4.36. However, the WBC composed using the optimized aggregate gradation with q = 0.5 (50 : 50) has shown reliable stability at a water overdosage of 10 lit (ROB+10L). This might be attributed to the positive effect of the enhancement of the lattice effect. Similarly, the mixture with the aggregate composition having the highest packing density q = 0.6 (40 : 60) has shown good stability at water overdosage of 10 lit (ROB+10L). This reveals the compensating effect of a maximum packing density and the resulting reduction in paste demand to a sub-optimal aggregate gradation in terms of enhancing the stability of a concrete. On the contrary, the mixture composed of aggregates with a sub-optimal gradation and the lowest packing density q = 0.4 (60 : 40) have exhibited the poorest robustness against water overdosage. Moreover, the fact that all the mixtures have shown strong sedimentation and segregation at a 20 lit water overdosage indicates that there is a limit to what a concrete mixture can tolerate in terms of maintaining the stability against water overdosage.

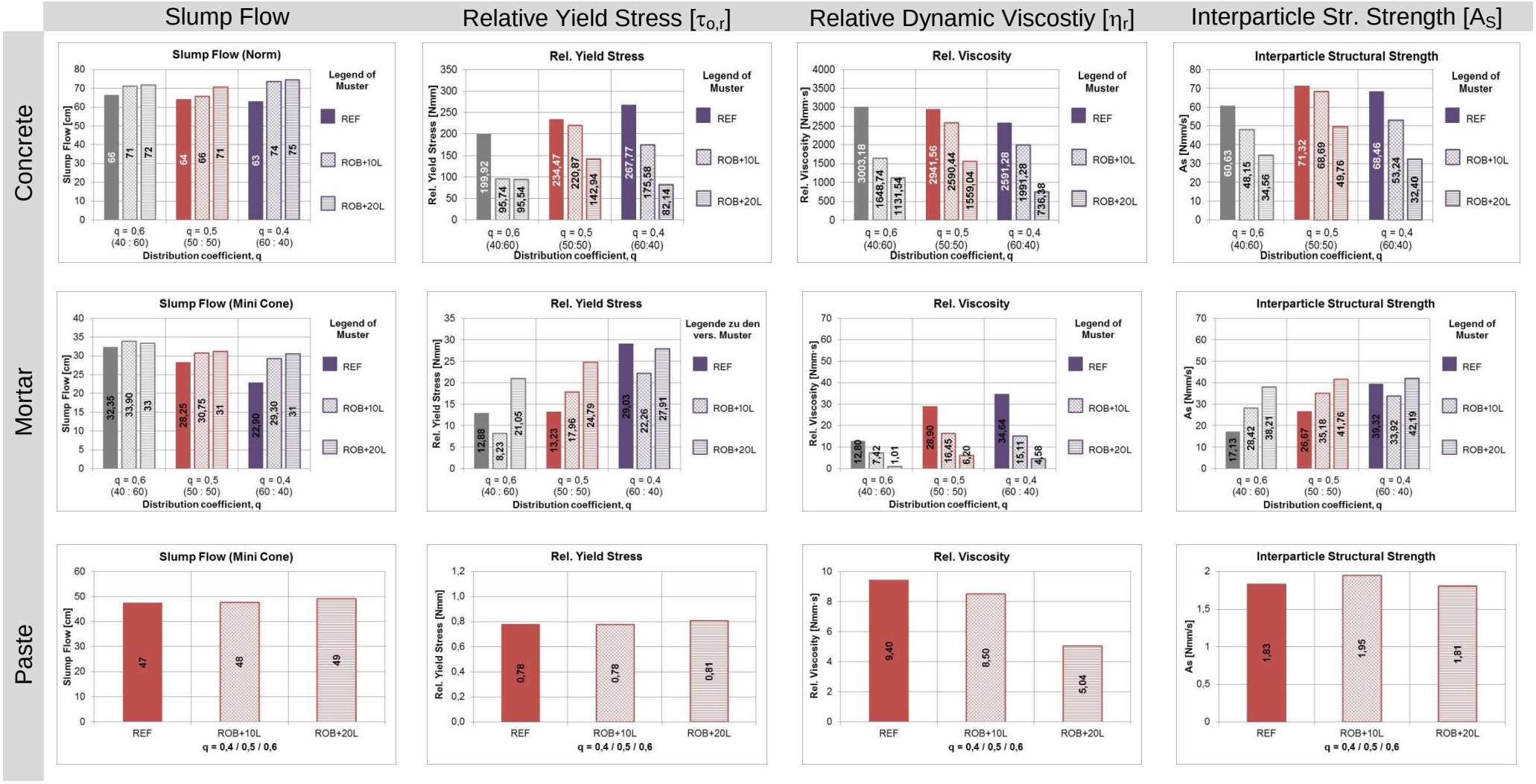

Figure 4.37: Combined effects of aggregate composition (q) and paste amount on the robustness of the rheological properties (comparable flowability)

III. Rheology

The results of the rheological investigations on the concrete mixtures as well as the extracted mortar and paste compositions are shown in Figure 4.37. Generally, $\tau_{o,r}$, η_r and A_S decrease with increasing water overdosage. Here too, the WBC with the optimized aggregation q = 0.5 (50 : 50) performs remarkably well in terms of maintaining the rheological properties at water overdosage of 10 lit (ROB+10L). Even at 20 lit water overdosage, it shows a better performance in comparison with the other two mixtures with q = 0.4 (60 : 40) and q = 0.6 (40 : 60). In compliance with the poor robustness observed with regard to the flowability properties, the mixture with q = 0.6 (40 : 60), despite possessing the aggregate composition with the highest packing density, has performed poorly in terms of maintaining the rheological properties. With the exception of viscosity $\eta_{r,M}$, no reliable trend could be observed with regard to the rheological investigations on the mortar compositions due to the occurrence of sedimentation of the sand particles during the test. $\tau_{o,r,P}$ and $A_{S,P}$ of the paste compositions do not seem to be significantly affected by the water overdosage as the reference paste composition itself has very high slump flow. However, the viscosity of the paste $\eta_{r,P}$ has clearly decreased with increasing water overdosage.

4.9 Results of the pumpability and pump-stability investigations

The pumpability and pump-stability investigations were conducted using the Pumping Resistance Simulator (PuReSi) and the high-pressure filter press (HPFP) as explained in sections 4.7.4 and 4.7.5 . The pumpability or the ease of pumping could be described in terms of the required pressure to pump a concrete at a certain flow rate or discharge. The pump-stability designates the ability of a concrete to maintain its homogeneity without significant separation of the solid and liquid phases under the action of pressure.

4.9.1 Concrete compositions

The investigations were conducted on the concrete compositions from test series II V and VI; see section 4.8.1. The parameters of the concrete compositions are shown in Table 4.13.

Table 4.13: Parameters used for the concrete compositions in pumpability and pump-stability investigations

Test series	w/c	V_W/V_F			q (NS - RG1)			Max. Size	Paste content	Slump flow
II	0.6	0.8	1.0	1.2	0.5 (50-50)			8	Variable	Constant
V		1.0			0.4 (60-40)	0.5 (50-50)	0.6 (40-60)			
VI	Water overdosage of 10 lit based on series V									

4.9.2 Series II: Combined effects of paste composition and paste amount (comparable flowability)

For a constant aggregate composition, the paste composition influences the pumpability and pump-stability properties of concrete more significantly than the paste amount. Increased values of V_W/V_F improve the pumpability properties of concrete as long as the homogeneity of the mixture is maintained through adjusting the paste amount; see Figure 4.38, left. The flow properties of concrete in a pipe could be characterized by a plug flow in which a lubrication layer, which is composed of paste or fine mortar, is formed along the pipe wall; see section 2.4.2. This lubrication layer is exposed to an extremely high level of shear stress in comparison with the bulk concrete. Thus, it could be argued that the shear resistance of the lubricating layer or the paste governs the pumpability properties of concrete. Generally, paste compositions with higher values of V_W/V_F have lower shear resistance and viscosity as confirmed by the results of the rheological investigations in section III. Thus, the pressure required for a constant discharge decreases with increasing values of V_W/V_F.

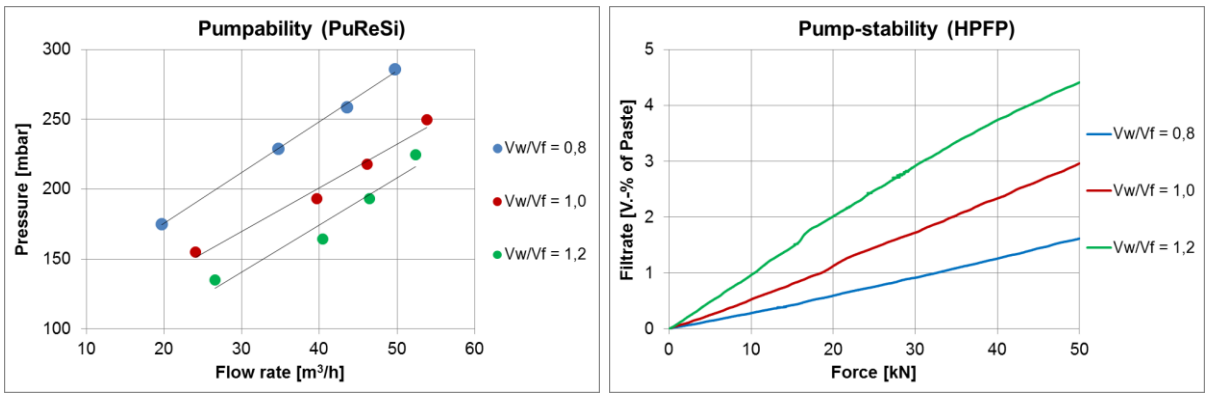

Figure 4.38: Effect of the paste composition on the pumpability and pump-stability

On the contrary, the pump-stability decreases with increasing values of V_W/V_F, even though the paste amount has decreased simultaneously. In a normal homogeneous plug flow, where there is enough paste content for the formation of a lubrication layer, the aggregates are transported within the bulk concrete as a unit. Under this assumption, the pump-stability depends mainly on the paste composition, which could be confirmed by the increased amount of filtrate with increasing values of V_W/V_F; see Figure 4.38, right.

4.9.3 Series V: Combined effects of aggregate composition and paste amount (comparable flowability)

For a certain paste composition, the pumpability of concrete depends to some extent on the aggregates composition and the required paste amount to attain good flowability. Generally, when shear loading is applied to a concrete, the aggregates tend to migrate from zones of high shear stress to zones of low shear stress. In the case of pumping, this migration takes place from the pipe wall to the center. When the migration occurs in a concrete mixtures that is already rich in paste or mortar, e.g. q = 0.4 (60 : 40), it leaves a relatively thick lubrication layer, which would favor the pumpability as can be seen in Figure 4.39, left. In contrast, the effects of the aggregate compositions on the pump-stability seem to be insignificant as long as the mixtures remains homogeneous, which was the case in this investigation. All three mixtures have shown remarkable stability even under the application of vibration; see section 4.8.6.

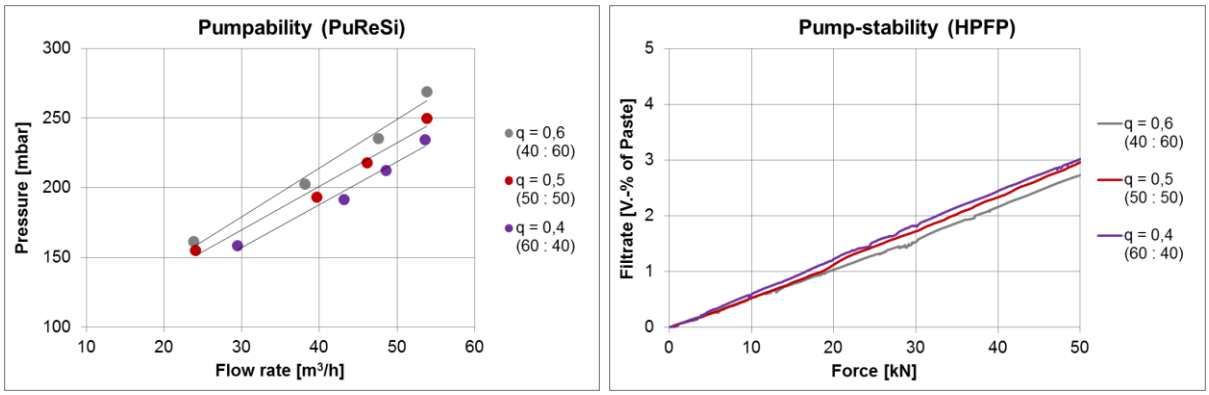

Figure 4.39: Effect of the aggregate composition on the pumpability and pump-stability

The mechanism of a homogeneous plug flow where the aggregates are transported in the bulk concrete is responsible for this phenomenon. This is also in line with the observation made in section 4.9.2 that the paste composition has a more pronounced role with regard to the pump-stability of concrete than the aggregates.

4.9.4 Series VI: Combined effects of aggregate composition and paste amount on the robustness (comparable flowability)

The robustness investigations with regard to the effect of water overdosage on the pumpability and pump-stability were carried out by applying water overdosage of 10 lit to the concrete mixtures q = 0.6 (40 : 60) featuring aggregate compositions with maximum packing density and q = 0.5 (50 : 50) with optimized aggregate gradation.

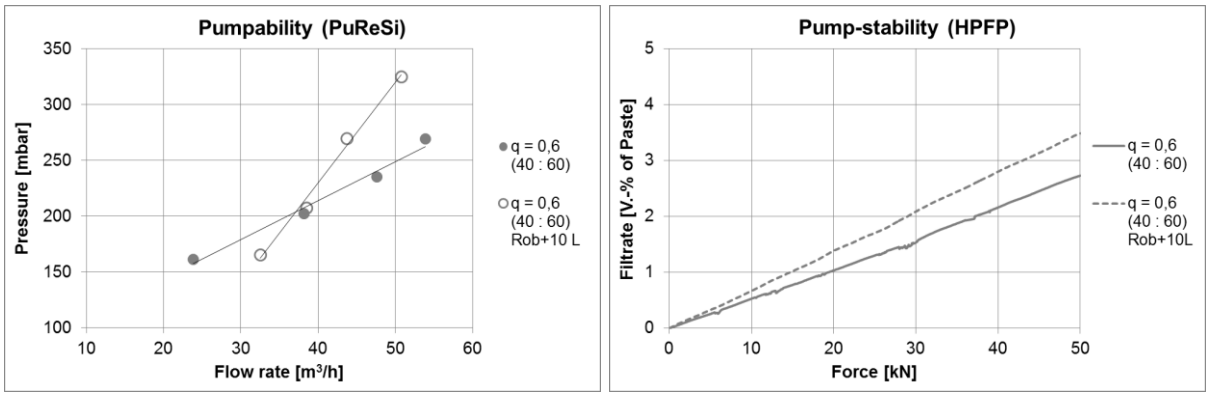

Figure 4.40: Effect of water-overdosage on the pumpability and pump-stability of a less robust concrete mixture

As can be seen in Figure 4.40, left, the water overdosage to the mix q = 0.6 (40 : 60) has at first led to a reduction in the required pumping pressure. At such lower discharge rates, it is possible that the concrete remains homogeneous in the pipe and the reduction in the viscosity of the lubrication layer as a result of the water overdosage could contribute positively to the pumpability. Secrieru et al. have also reported a reduced pumping pressure on concrete mixtures that tended to show instability [178]. However, at increased discharge rates, the risk for the separation of the phases increases dramatically as confirmed by the pump-stability investigation; see Figure 4.40, right. This would ultimately lead to interlocking of the aggregates and increased contact between the aggregates and the wall of the pipe. The resulting friction between the aggregates and the pipe wall as well as between the aggregates themselves would lead to a drastic increase in the required pumping pressure. The fact that there is a higher percentage of coarse aggregate in the mixture might have also aggravated the situation.

In contrast, the water overdosage to the mixture q = 0.5 (50 : 50) has resulted into a marginal reduction in pumping pressure at lower discharge rates followed by a slight increase at higher discharge rates. The robust nature of this mixture to water overdosage is responsible for maintaining its pumpability and pump-stability properties as can be seen in Figure 4.41.

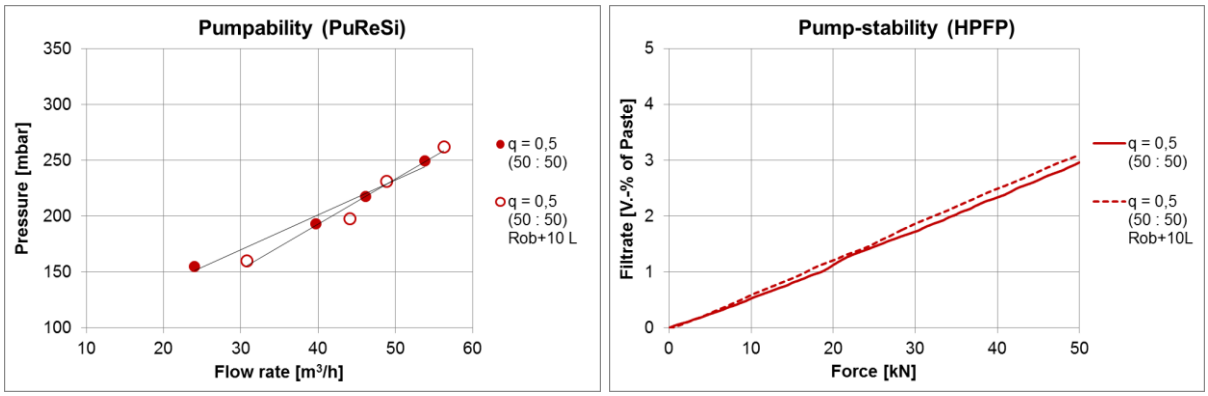

Figure 4.41: Effect of water-overdosage on the pumpability and pump-stability of a robust concrete mixture

The results of these investigations have clearly demonstrated that there is a certain point at which the positive effects of the “forced bleeding” on the pumpability could completely overturn and start to affect the pumpability in an adverse manner. The pump-stability investigation using the HPFP could also clearly detect the changes in the concrete composition. Now, in order to determine the extent to which the forced bleeding have a positive effect on pumpability and most importantly from which point on it starts to hamper the pumpability should be investigated in a more detail. Hopefully, the cooperative research project between LUH and TUD with regard to the pumpability and pump-stability of concrete would provide the answer in this regard.

4.10 Short summary

I. The effective water demand (β_E) functions were developed for different cements, mineral admixtures and SP compositions. Provided that the other constitute materials remain the same, it can be stated that:
   - β_E does not differ significantly due to changes in the type of cement (CEM I and CEM III). Here, CEM III has higher fineness than CEM I, but the slag particles in the CEM III have glassy texture and higher negative zeta-potential which compensate for its higher fineness in terms of β_E. However, CEM III has shown at times lesser compatibility to certain types of SP.
   - β_E does not differ significantly due to changes in the type fly ash (FA WH, FA HP and FA SBF) the reason being their comparable fineness.
   - β_E differ significantly depending on the type mineral admixtures (Fly ash, limestone powder and trass powder). This could be attributed to the difference in fineness between the mineral admixtures as well as the resulting packing density when they are combined with cement.

- β_E does not differ significantly due to substitution of cement with fly ash the reason being the comparable fineness and gradation of the cement and the fly ash.
- β_E differ significantly depending on the type SP. HRWRA (SP1) results into a significant reduction in β_E when compared to a WRA (SP2).

II. The packing density (ϕ) of different aggregate compositions was investigated by applying vibration and loading simultaneously in order to determine the voids' paste demand ($V_{P,V}$). Moreover, the water demand of the aggregates ($V_{W,S}$) was investigated by making use of filter press and water-jet pump ($V_{P,S}$).
    - Aggregate combinations with gradation lines well outside the favourable zone (between the standard gradation lines A and B) have significantly lower ϕ, thereby leading to a higher $V_{P,V}$.
    - ϕ increases with decreasing maximum size of the individual aggregate fractions (0/2 > 2/8 > 8/16) and broader size range of the combined aggregates (0/16 > 0/8).
    - ϕ of the individual aggregate fractions is significantly lower than combined aggregates (0/2, 2/8 or 8/16 < 0/16).
    - $V_{W,S}$ and the corresponding $V_{P,S}$ of aggregate compositions increase with an increase in the fine - coarse proportions.
    - The total paste demand ($V_P = V_{P,V} + V_{P,S}$) decreases with increasing size range (0/16 > 0/8).
    - Flaky and crushed gravels lead to smaller ϕ or higher $V_{P,V}$ than round ones.
    - Flaky gravel led to higher V_P than round and crushed aggregates.

III. Different standard and new test methods were applied to characterize the flowability, pumpability, stability (under vibration and pressure) and robustness (against water overdosage) of different concrete compositions.
    - Flowability: slump flow with tapping as well as combined determination of flow time and slump flow without tapping using a flow cone.
    - Pumpability: pumping resistance simulator (PuReSi) which helps to establish the pressure – discharge relationship.
    - Stability under vibration: wash-out test and visual evaluation of dried samples to evaluate the sedimentation tendency of the coarse aggregates as well as sedimentation – sieve – test for analyzing the separation of the paste or mortar from the bulk concrete.
    - Stability under pressure / pump-stability: high pressure filter press that quantifies the amount of filtrate pressed out of a concrete.
    - Robustness: analyzing the effect of water overdosage on the fresh concrete properties, especially with regard to the flowability, stability (under vibration and pressure) and pumpability.

IV. The flowability, pumpability, stability (under vibration and pressure) and robustness (against water overdosage) were investigated using different concrete compositions with a wide ranging paste compositions (V_W/V_F = 0.8 – 1.2) as well as aggregate compositions (q = 0.4 – 0.6).
    - Regardless of the difference in paste compositions as well as aggregate compositions, the reference WBC composed using the WBMD have generally shown very high flowability reaching consistency classes of F6 while maintaining a reliable stability even under the application of intensive vibration.
    - The WBC that are composed using lower values of V_W/V_F (high amount of fines) or lower values q (high amount of fine aggregates) require a relatively high amount of paste to achieve the desired flowability. As a consequence, these mixtures have shown poor robustness against water overdosage in terms of maintaining the desired flowability and stability of the reference mixtures.
    - The WBC that are composed using lower values of V_W/V_F (high amount of fines) or lower values q (high amount of fine aggregates) possess comparable features with SCC as confirmed by the flow spread (without tapping) and flow time determined using the flow cone.
    - The WBC that are composed using higher values of V_W/V_F also possess poor robustness against water overdosage in terms of the stability properties, since the risk for the occurrence of excessive unbound water in the mixture increases.
    - The ideal WBC that is designed by making use of the optimized aggregate gradation (q = 0.5) and the realistic $V_W/V_F \approx 1.3 \times \beta_P \approx 1.0$ have exhibited good flowability and pumpability as well as stability and robustness.
    - The pumpability and pump-stability are principally affected by the paste composition. The aggregate compositions play a minor role in this regard.
    - The pumpability gets enhanced with increasing values of V_W/V_F and decreasing paste content, while the pump-stability decreases. Thus, it might be stated that as long as the bulk concrete remains homogeneous in the pumping lines, the separation of the paste or water under pressure only enhances the formation of a less viscous lubrication layer and thus the pumpability.
    - Increased degree of separation of the liquid phase in combination with a higher proportion of coarse aggregates could potentially lead to an interlocking of the aggregates, which would ultimately increase the required pressure.

V. The rheological investigations were conducted on different concrete compositions (V_W/V_F = 0.8 – 1.2 and q = 0.4 – 0.6) as well as on extracted mortar and paste compositions by focusing on determining the relevant rheological parameters during the structural breakdown, e.g. due to vibration.
    - A newly developed “step and gap” measurement profile was applied that makes it possible to determine not only the classical rheological parameters such as yield stress (τ) and viscosity (η), but also the magnitude of interparticle structural strength (A_S), which quantifies the difference between the static yield stress (τ_s) and dynamic yield stress (τ_d).
    - A_S and η were found to be the relevant parameters to analyze the fresh concrete properties during the structural breakdown. A_S quantifies the overall shear resistance of the mixture until a steady state condition is reached and η represents the resistance of the mixture to flow after the steady state.
    - Paste compositions with lower V_W/V_F-values have higher value of $A_{S,P}$ by themselves, but their application in flowable concrete requires a high amount of paste leading to a reduced friction between the aggregates in the pre-steady state condition, thereby leading a reduced $A_{S,C}$ in concrete.
    - On the contrary, paste compositions with lower V_W/V_F-values have higher values of η_P which also results into higher values of η_C in concrete. In the post-steady state condition, the aggregates assume the “best possible” position and “swim” within the continuous paste phase. Consequently, the resistance of the concrete to flow, i.e. the viscosity, would be predominantly governed by the viscosity of the paste.
    - Deviation from the optimal aggregate gradation has led to a reduction in both A_S and η.
    - Unrealistically high or low V_W/V_F-values and also deviations from the optimum aggregate gradation had led to poor robustness against water overdosage as observed by the reductions in both A_S and η.

Chapter 5
Rheological Characterization of the Structural Breakdown in Relation to the Stability

5.1 Short introduction

This chapter deals with the rheological characterization and modeling of the structural breakdown process on a multiscale basis considering the subsequent paste, mortar and concrete phases as micro, meso, and macro scales. To this end, mathematical relationships are established in order to quantify the rheological parameters that have relevance to the structural breakdown at each scale on the basis of the chosen mix-design parameters. The interdependence between rheology and stability during the structural breakdown is also dealt with in great detail.

5.2 Rheological characterization of the structural breakdown

The application of intensive external stresses such as vibration to a concrete would cause a significant structural breakdown which would lead to a significant reduction in the yield stress of the suspending paste or mortar. Some researchers have argued that the changes could be so immense that the suspending medium transforms from a Bingham fluid into a Newtonian fluid [112] [114]. This would ultimately lead to the sedimentation of the coarser particles under the combined influence of vibration and gravitation. However, the extent of this segregation depends on the overall shear resistance and the viscosity of the concrete. The overall shear resistance of a concrete designated here as the interparticle structural strength (A_S) represents the total sum of the shear resistances of the colloidal forces and early CSH bridges at the paste level as well as the frictional forces between the aggregates until a steady state is reached. The relative dynamic viscosity (η_r) which is determined in a steady state condition depicts the resistance of the mixture to flow under the action of stress.

Clearly, both $\mathbf{A_S}$ and $\boldsymbol{\eta_r}$ of concrete depend on the combined effects of the paste and aggregate compositions. However, differentiating between the individual contributions of the frictional and the colloidal components is not straightforward.

Generally, paste compositions with lower V_W/V_F-values have relatively higher value of $\mathbf{A_{S,P}}$ by themselves [179] [180]; but their application in a concrete requires a high amount of paste which could lead to a reduced friction between the aggregates, thereby reducing the value of $\mathbf{A_{S,C}}$. On the contrary, paste compositions with higher V_W/V_F-values have lower value of $\mathbf{A_{S,P}}$, but applying them in a concrete with a reduced amount of paste could lead to higher values of $\mathbf{A_{S,C}}$ as a consequence of the increased friction between the aggregates; see Figure 5.1, left. Because of the extremely weak shear resistance, a paste composition which is exposed to high shear loading reaches the steady state in an instant making its contribution to the overall shear resistance of the concrete $\mathbf{A_{S,C}}$ negligible. Thus, the quantification of the structural breakdown process in concrete should necessarily consider the frictional resistance of the aggregates as the larger share of $\mathbf{A_{S,C}}$ emanates from it.

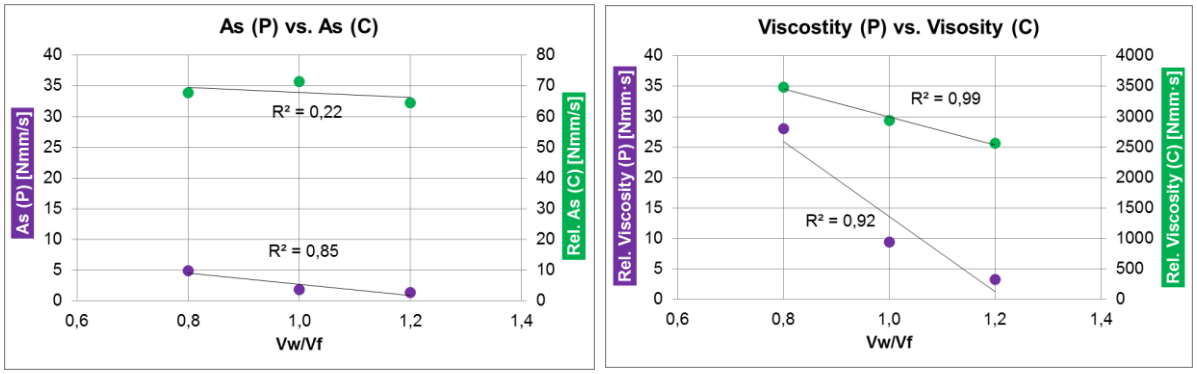

Figure 5.1: Effect of paste compositions (V_W/V_F) on the interparticle structural strength (A_S) and the dynamic viscosity (η_r) of concrete

The relative dynamic viscosity (η_r) decreases with increasing V_W/V_F-values in both the paste and concrete compositions as shown in Figure 5.1, right. As the viscosity is determined in a quasi-steady state condition, i.e. after the “completion” of the structural breakdown process, the aggregates could be assumed to be in a state where they have migrated from the high shear zone and “swim” within the paste phase. As a result, the resistance of the concrete to flow or its viscosity correlates strongly with the viscosity of the paste which is governed by its composition or V_W/V_F. With a simplified assumption that no colloidal interaction would take place between the fine particles, the viscosity of the paste mainly depends on its solid concentration (ϕ) [148] [150].

Extending the same assumption to a concrete where the aggregates are suspended in a continuous paste phase, the viscosity of the concrete would also depend on the concentration and the resulting physical interaction of the aggregates. According to Philips et al., the particle migration caused by the collision flux, which could be expected to increase with increasing concentration of the aggregates, leads to an

increase in the viscosity of the suspending medium [106]. Thus, as the larger share of the inter particle structural strength ($\mathbf{A_S}$) in concrete comes from the friction between the aggregates, a concrete exhibiting higher shear resistance until it reaches the steady state, could be expected to show a relatively higher resistance to flow during the steady state (η_r). This is confirmed by the results of the investigations as illustrated in Figure 5.2.

Accordingly, the rheological characterization of a concrete during the structural breakdown process could be done with the help of $\mathbf{A_S}$ and η_r. It could also be observed that $\mathbf{A_S}$ is more affected by the changes in the aggregate compositions (q) as shown in Figure 5.2 (right) when compared to the variations in the paste compositions (V_W/V_F) Figure 5.2 (left) confirming the dominant role the friction between the aggregates plays during structural breakdown process.

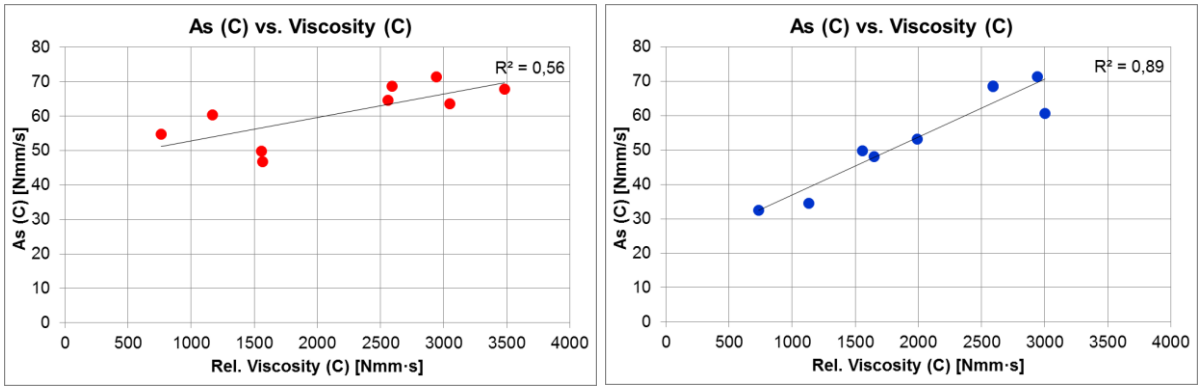

Figure 5.2: Relationship between A_S and η_r for concrete mixtures with different paste compositions (test series III, left) and aggregate compositions (test series VI, right)

5.3 Rheological modeling of the structural breakdown process

In order to develop a multiscale rheological model that helps to quantify the structural breakdown process, the interdependence between the rheological properties of the subsequent paste ↔ mortar and mortar ↔ concrete phases has to be studied first. Taking the original results of the investigations, it can clearly be observed that there is no reliable correlation between the phases regarding $\mathbf{A_S}$ as shown in Figure 5.3. Two reasons might have contributed to this. First, the inherently weak shear resistance of paste or even mortar compositions at higher shear rates makes it difficult to make a clear distinction between them. While the applied V_W/V_F- values ranging from 0.8 – 1.2 makes a huge difference at the concrete level, e.g. in terms of the required paste demand for a comparable flowability, their effect at the paste level with respect to the shear resistance is absolutely minimal.

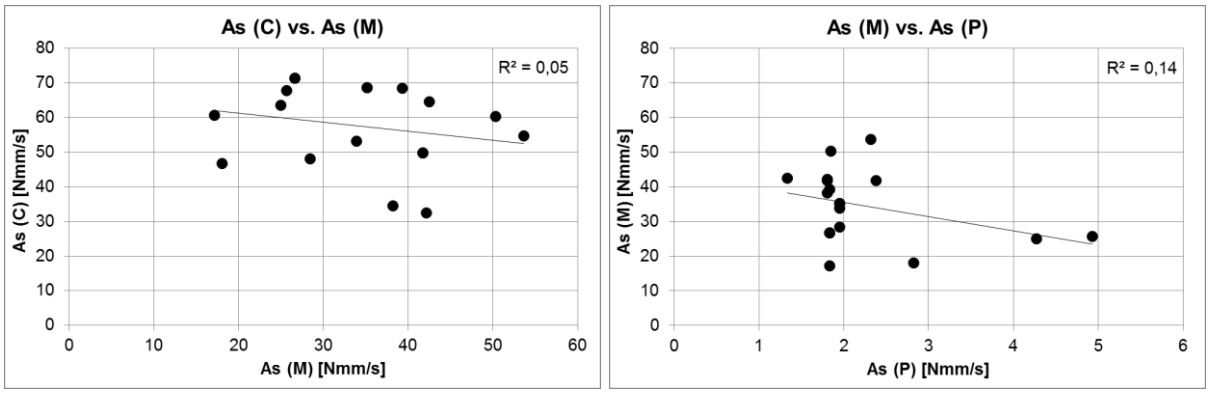

Figure 5.3: Relationship between A_S of the subsequent phases (mortar ↔ concrete and paste ↔ mortar) (test series III and VI)

Second, the paste and mortar extraction was done in such a way that the water that is supposed to be bound by the coarse aggregates still remains in these phases. While this approach has worked satisfactorily for the paste compositions, it has caused at times some segregation of the mortars in the Viskomat NT during the time interval when no shear loading was applied; see Figure 4.13. This might have led unrealistic values of the static shear stress ($\tau_{o,s}$). On the contrary, clear relationships could be observed with regard to $\boldsymbol{\eta_r}$ between the subsequent phases as shown in Figure 5.4. Overall, the results of the viscosity of all the phases show the expected trends. Since there is enough time for the mixtures to get homogenized until the steady state is reached, in case there was segregation during the pause, the measurements results become more reliable. Similarly, the results of the rheological instigations on the concrete compositions could be considered as reliable, since no segregation was observed during the investigations, which is confirmed by the expected trends. Thus, the multiscale model makes use of $\boldsymbol{\eta_r}$ for all phases and $\boldsymbol{A_S}$ for the concrete, which is in fact the ultimate goal of the rheological investigations.

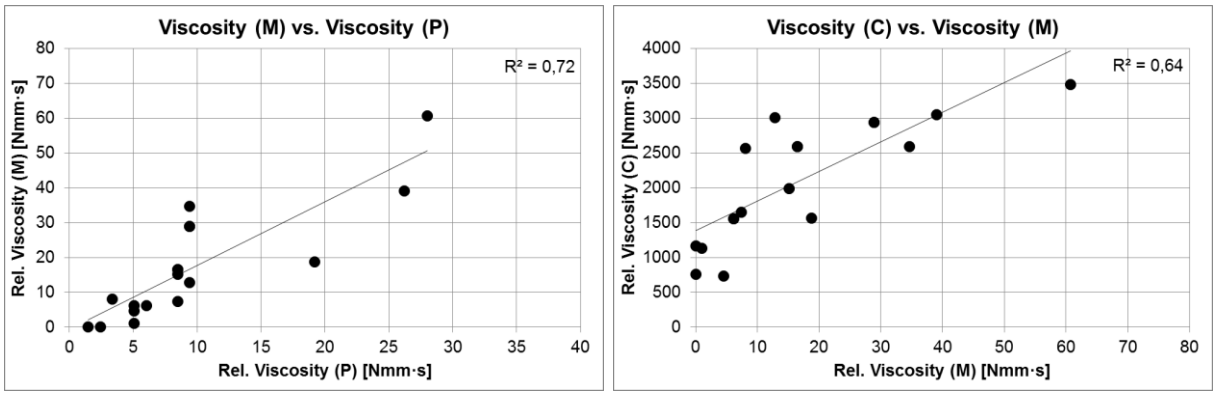

Figure 5.4: Relationship between η_r of the subsequent phases (mortar ↔ concrete and paste ↔ mortar) (test series III and VI)

Here, it should be noted that depending on the paste or aggregate compositions, the paste contents were adjusted in order to attain a comparable flowability. The discrepancy in paste content would surely affect the measured values of $\mathbf{A_S}$ and $\boldsymbol{\eta_r}$ of the different concrete compositions. Thus, for the purpose of comparison, a simplified assumption is made that the effect of the different paste contents on $\mathbf{A_S}$ and $\boldsymbol{\eta_r}$ is proportional to the surface paste demand of the aggregates ($V_{P,S}$ in dm^3/m^3). The viscosity of the paste $\boldsymbol{\eta_{r,P}}$ depends solely on its composition while the viscosity of the mortar is $\boldsymbol{\eta_{r,M}}$ depends on both the paste composition and the paste amount. Thus, viscosity of the mortar $\boldsymbol{\eta_{r,M}}$ could be adjusted by considering the surface paste demand of the fine aggregates ($V_{P,S}$ 0/2) in the mortar; see Figure 5.5.

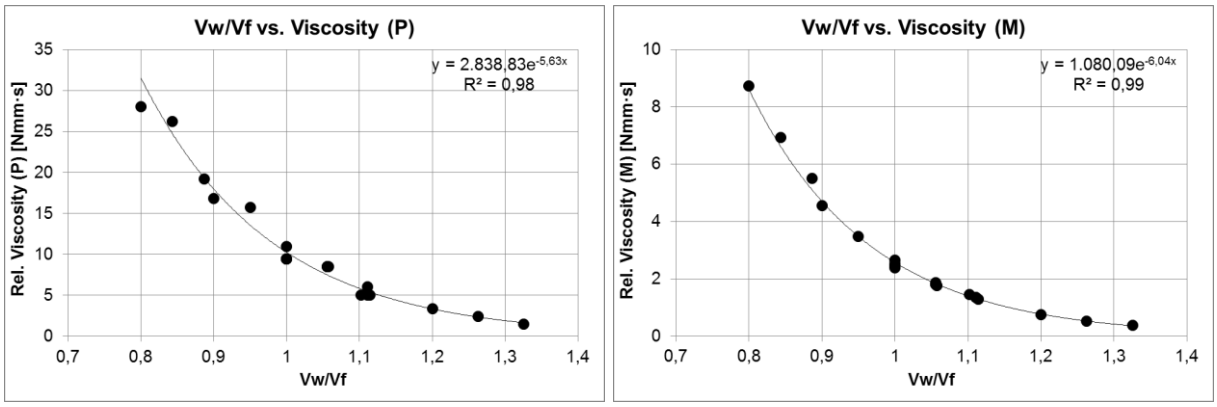

Figure 5.5: Quantification of the viscosity of paste (left) and mortar (right) as a function of the paste composition (V_W/V_F) (test series III and VI)

The relationships between $\boldsymbol{\eta_{r,P}}$ and $\boldsymbol{\eta_{r,M}}$ as a function of the paste composition (V_W/V_F) are presented in Equations (5.1) and (5.2).

$$\eta_{r,P} = X_P \cdot e^{Y_P \cdot \frac{V_W}{V_F}} \tag{5.1}$$

$$\eta_{r,M} = \frac{\left[X_M \cdot e^{Y_M \cdot \frac{V_W}{V_F}}\right]}{V_{P,S\,(0/2)}} \cdot 1000 \tag{5.2}$$

Where: X_P = 2,838.83; Y_P = -5.63 and X_M = 1,080.09; Y_M = -6.04

The diagrams in Figure 5.5 also reveal that $\boldsymbol{\eta_{r,P}}$ and $\boldsymbol{\eta_{r,M}}$ show no sizable difference after V_W/V_F = 1.1. This value is in agreement with the recommendation of the WBMD where the chosen V_W/V_F should lie between 1.2 x β_P – 1.4 x β_P; see section 3.3.7. The fine compositions used in this investigation have a β_P = 0.8 which corresponds to a maximum recommended V_W/V_F = 1.4 x 0.8 ≈ 1.1. As discussed earlier, the changes in paste compositions directly affect the viscosity of the concrete. Hence, mathematical functions based on the adjusted values of $\boldsymbol{\eta_r}$ could also be developed

for the subsequent paste ↔ mortar and mortar ↔ concrete phases as shown in Figure 5.6. The paste ↔ mortar and mortar ↔ concrete viscosity functions are presented in Equation (5.3) and (5.4).

$$\eta_{r,M} = \frac{[P_P \cdot \eta_{r,P} + Q_P]}{V_{P,S\,(0/2)}} \cdot 1000 \tag{5.3}$$

$$\eta_{r,C} = \frac{[M_P \cdot \eta_{r,M} + N_P]}{V_{P,S\,(0/8)}} \cdot 1000 \tag{5.4}$$

Where: $\eta_{r,P}$, $\eta_{r,M}$ and $\eta_{r,C}$ = rel. dynamic viscosity of paste, mortar and concrete; $V_{P,S}$ = surface paste demand of agg.; P_P = 0.28; Q_P = -0.20; M_P = 9.96; N_P = 275.48

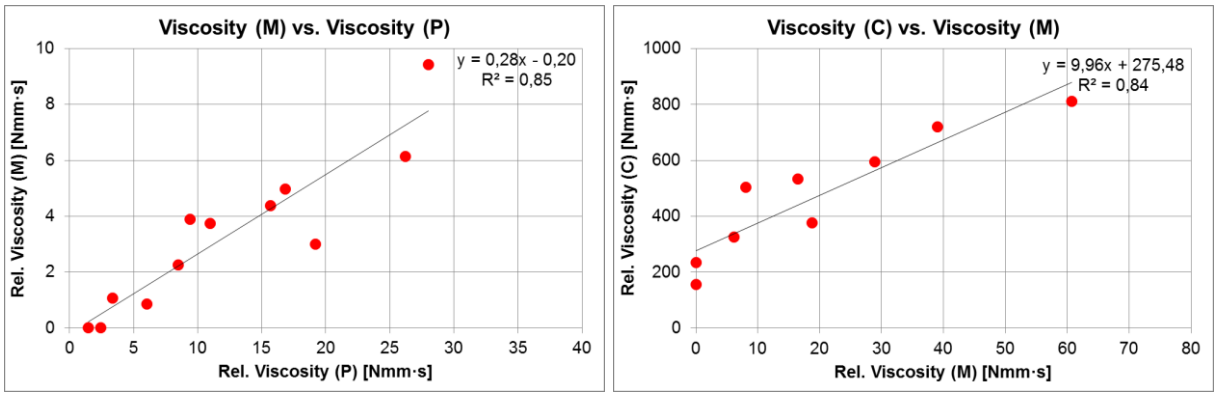

Figure 5.6: Relationship between η_r of the subsequent phases in concrete mixtures with different paste compositions (test series III)

The relationship between $\mathbf{A_S}$ and $\boldsymbol{\eta_r}$ on the basis of the adjusted values could also be determined based on Figure 5.7. If only the paste composition is altered while the aggregate composition remains constant, the value of $\mathbf{A_S}$ could be estimated using Equation (5.5).

$$A_{S,C} = \frac{[C_P \cdot \eta_{r,C} + D_P]}{V_{P,S\,(0/8)}} \cdot 1000 \tag{5.5}$$

Similarly, the effects of changes in the aggregate composition for a constant paste composition could be quantified using Equation (5.6).

$$A_{S,C} = \frac{[C_G \cdot \eta_{r,C} + D_G]}{V_{P,S\,(0/8)}} \cdot 1000 \tag{5.6}$$

Where: $\boldsymbol{A_{S,C}}$ = interp. structural strength of concrete; $\boldsymbol{\eta_{r,C}}$ = rel. dynamic viscosity of concrete; $\boldsymbol{V_{P,S}}$ = surface paste demand of agg.; C_P = 0.01; D_P = 9.24; C_G = 0.02 and D_G = 4.19

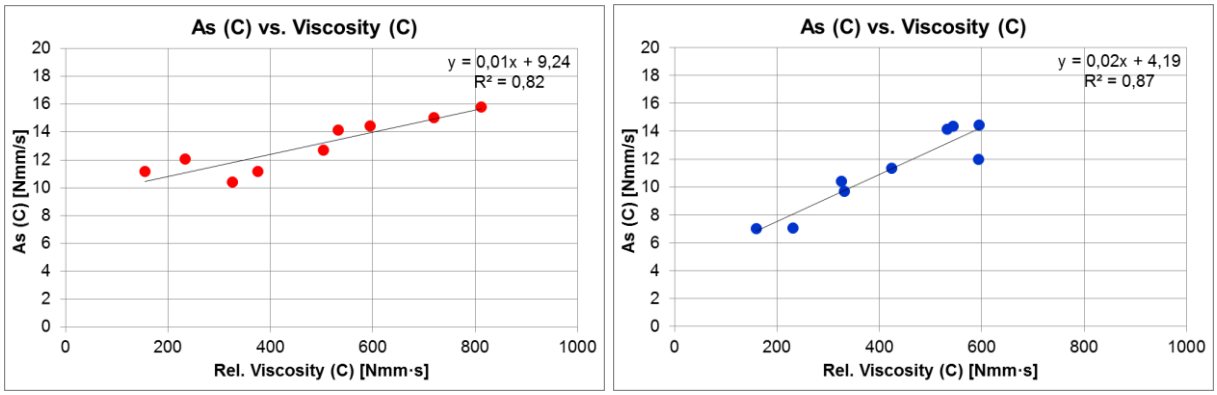

Figure 5.7: Effect of paste composition (test series III, left) and aggregate composition (test series VI, right) on A_S and the η_r of concrete considering the effects of the surface paste volume

Therefore, the pure effects of the paste or aggregate compositions during the structural breakdown process could be determined by applying this approach. Accordingly, the value of $\eta_{r,C}$ could be determined on the basis of $\eta_{r,M}$ as shown in Equation (5.4). If the change occurs only in the paste composition, the value of $\eta_{r,M}$ could be estimated as a function of $\eta_{r,P}$ using Equation (5.3). If the changes occur in the aggregate composition, it is recommended to determine the value of $\eta_{r,M}$ experimentally, since the content of fine aggregates in the mortar also changes. But it can also be roughly estimated using Equation (5.3) since the changes caused by the fine aggregates could indirectly be considered by determining their surface paste demand. On the basis of this extensive analysis, a multiscale rheological model is developed for the structural breakdown process that considers the interdependence between the subsequent paste, mortar and concrete phases; see Figure 5.8. The data used for the rheological model are tabulated in Appendix A-5.

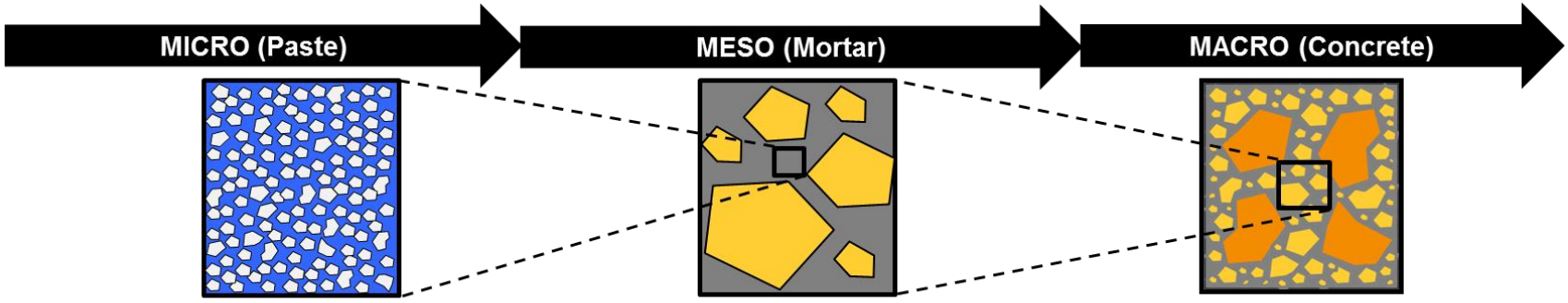

	Viskomat NT				Viskomat XL	
Parameter Variation						
Paste Composition (V_W/V_F)	$\eta_{r,P=} X_P \cdot \mathrm{Exp}\left[Y_P \cdot \frac{V_W}{V_F}\right]$ ...Eq. 5.1		$\eta_{r,M=} \frac{X_M \cdot \mathrm{Exp}\left[Y_M \cdot \frac{V_W}{V_F}\right]}{V_{P,S\,(0/2)}} \cdot 1000$ ...Eq. 5.2 or $\eta_{r,M=} \frac{[P_P \cdot \eta_{r,P} + Q_P]}{V_{P,S\,(0/2)}} \cdot 1000$ ...Eq. 5.3		$\eta_{r,C} = \frac{[M_P \cdot \eta_{r,M} + N_P]}{V_{P,S\,(0/8)}} \cdot 1000$ ...Eq. 5.4 $A_{S,C} = \frac{[C_P \cdot \eta_{r,C} + D_P]}{V_{P,S\,(0/8)}} \cdot 1000$ ...Eq. 5.5	
Aggregate Composition (q)	–		▪ $\eta_{r,M}$ to be determined experimentally or rough estimation using Eq. 5.3		▪ $\eta_{r,C}$ to be determined experimentally or rough estimation using Eq. 5.4 $A_{S,C} = \frac{[C_G \cdot \eta_{r,C} + D_G]}{V_{P,S\,(0/8)}} \cdot 1000$ ...Eq. 5.6	

Figure 5.8: Multiscale rheological model of the structural breakdown process

The adequacy of this approach, namely the proportional deduction depending on the surface paste demand of the aggregates, is confirmed by the strong relationships between the estimated and the measured values of the relevant rheological parameters of the subsequent phases as illustrated in Figure 5.9.

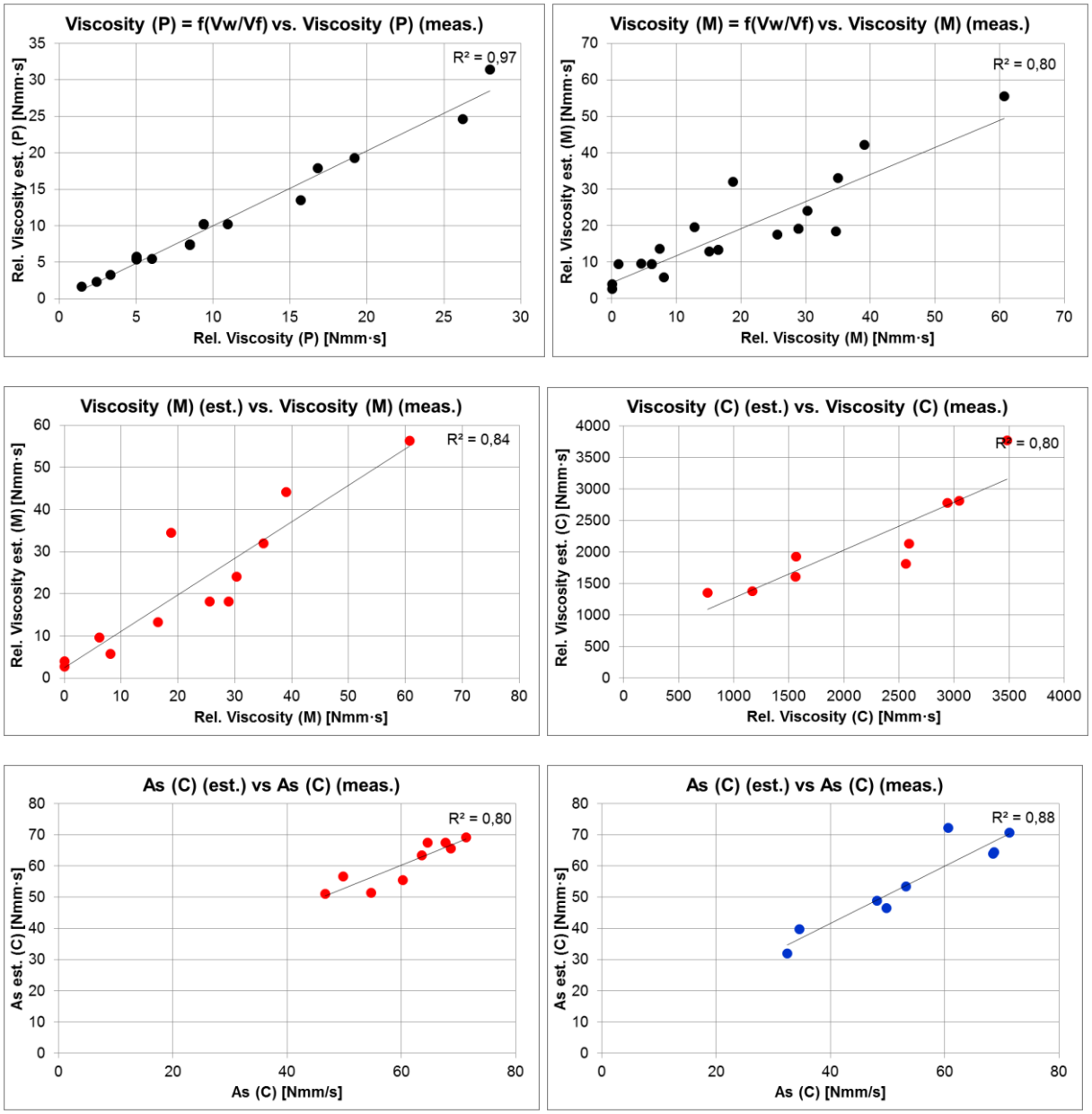

Figure 5.9: Comparison between the estimated and measured values of A_S and η_r of the subsequent phases [Left to right from top to bottom Equation 5.1 – 5.6]

5.4 Rheological characterization of the stability during the structural breakdown

As discussed in section 2.3.5 and 2.3.6 the static as well as dynamic stability properties of cement based mixtures are governed by the rheological properties. On the one hand, the static stability, which is relevant to the segregation process in a state of rest such as the sedimentation of coarse aggregates after casting of self-compacting concrete (SCC), depends first and foremost on the yield stress. At rest, no segregation of coarse aggregates would take place as long as the yield stress of the suspending medium (τ_o) remains higher than a certain critical yield stress ($\tau_{o,c}$), i.e. $\tau_o > \tau_{o,c}$. However, the sedimentation of the coarse aggregates would be inevitable if $\tau_o < \tau_{o,c}$, which is the case most of the time during mixing, transporting and casting processes [98].

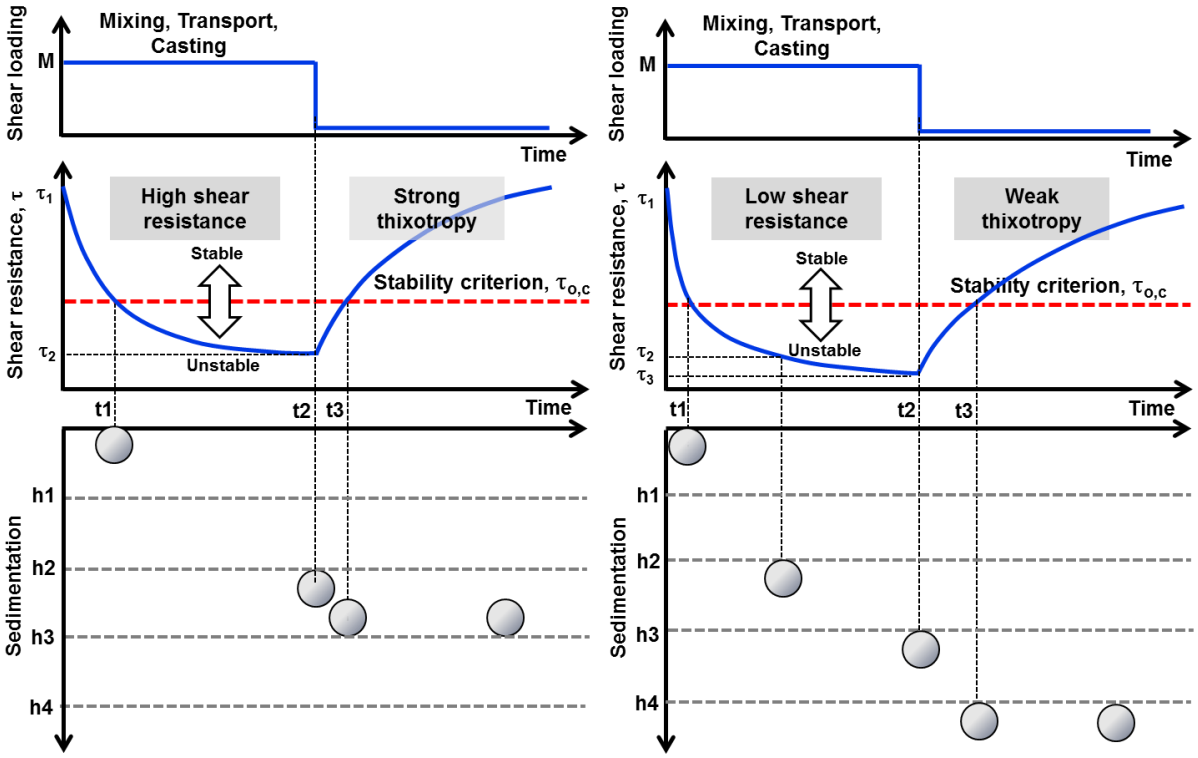

Figure 5.10: Effects of the shear resistance and thixotropy on the segregation

The dynamic segregation or particularly the sedimentation of coarse aggregates during this period depends on the interparticle structural strength of the concrete. As shown in Figure 5.10, the sedimentation reaches hypothetical depths of h2 and h3 for concrete mixtures with strong and weak interparticle structural strength respectively. The extent of segregation after the casting process depends on the rate at which the interparticle structures get re-built after the structural breakdown, i.e. thixotropy. A

SCC with a strong thixotropic behavior rebuilds its interparticle structures in a relatively short time, thereby increasing its viscosity and yield stress which ultimately limits the extent of segregation. Comparison of the hypothetical sedimentation depth between the two cases in Figure 5.10 reveals that the mixture with a strong thixotropic behavior is able to exceed the critical yield stress ($\tau_{o,c}$) in a relatively short time span (t2 – t3), thereby limiting further sedimentation (h < h3). The other mixture with lower interparticle structural strength and thereby weak thixotropic behavior needs a relatively longer time span (t2 – t3) to exceed the critical yield stress ($\tau_{o,c}$), during which a relatively high level of sedimentation could take place (position h4). Further sedimentation of the coarse aggregates would not take place after the critical yield stress ($\tau_{o,c}$) is exceeded.

The application of vibration would, however, change the response of the system and consequently the segregation phenomena significantly. The shear loading applied to a concrete during the mixing, transportation and casting processes acts predominantly at a “global” level in that the concrete gets sheared and undergoes a deformation as a mass and in a relatively unconstrained condition, since it can move sideways or flow in a certain direction. Due to the higher shear resistance of the mass and the unconstrained deformation, the chances for the separation of phases, e.g. sedimentation of aggregates, would remain relatively lower. On the contrary, vibration is a concerted loading action which takes place at a “local” level and in a relatively constrained condition. Consequently, the low resistance provided by the small shear zone would not be adequate to withstand the shear loading. This in combination with the limited possibility for a free deformation could lead to a substantial separation of the phases, which is why sedimentation under the effects of vibration is very critical, see Figure 5.11.

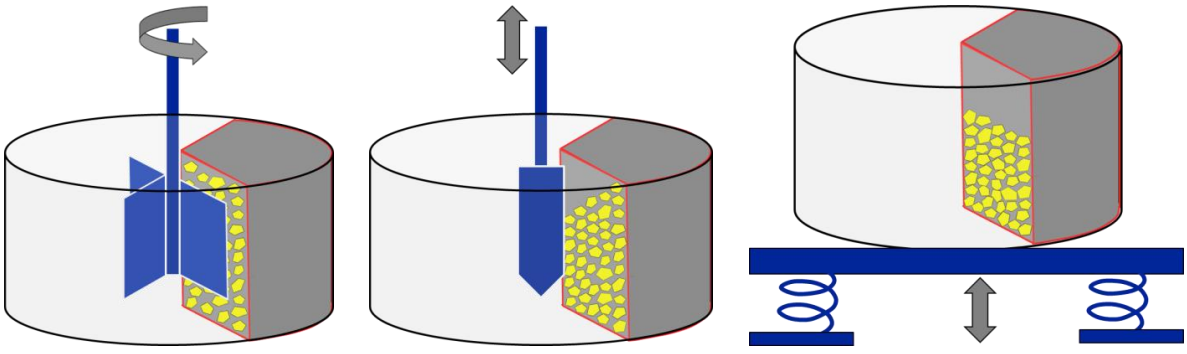

Figure 5.11: Comparison of the effects of mixing (left) and poker vibration (middle) and table vibration (right) on the segregation of coarse aggregates

The changes in the rheological properties of the concrete and the extent of segregation of course depend on the magnitude of the applied vibration energy. But it could be argued that, even if the structure build up process would take place after the

application of vibration, the damage caused by the highly intensive shear stress is as such that it causes significant sedimentation of the coarse aggregates making the structural build up or thixotropy more or less irrelevant. Thus, due to the high level of shear stress during vibration which causes a significant reduction in yield stress (τ_o), the stability criteria based on the critical yield stress $\tau_o < \tau_{o,c}$ does not hold anymore; see Figure 5.12 . The application of vibration to the concrete not only interrupts the structure build up process but also the shear resistance of the concrete plunges to such a low level that the sedimentation increases drastically (h3 → h6).

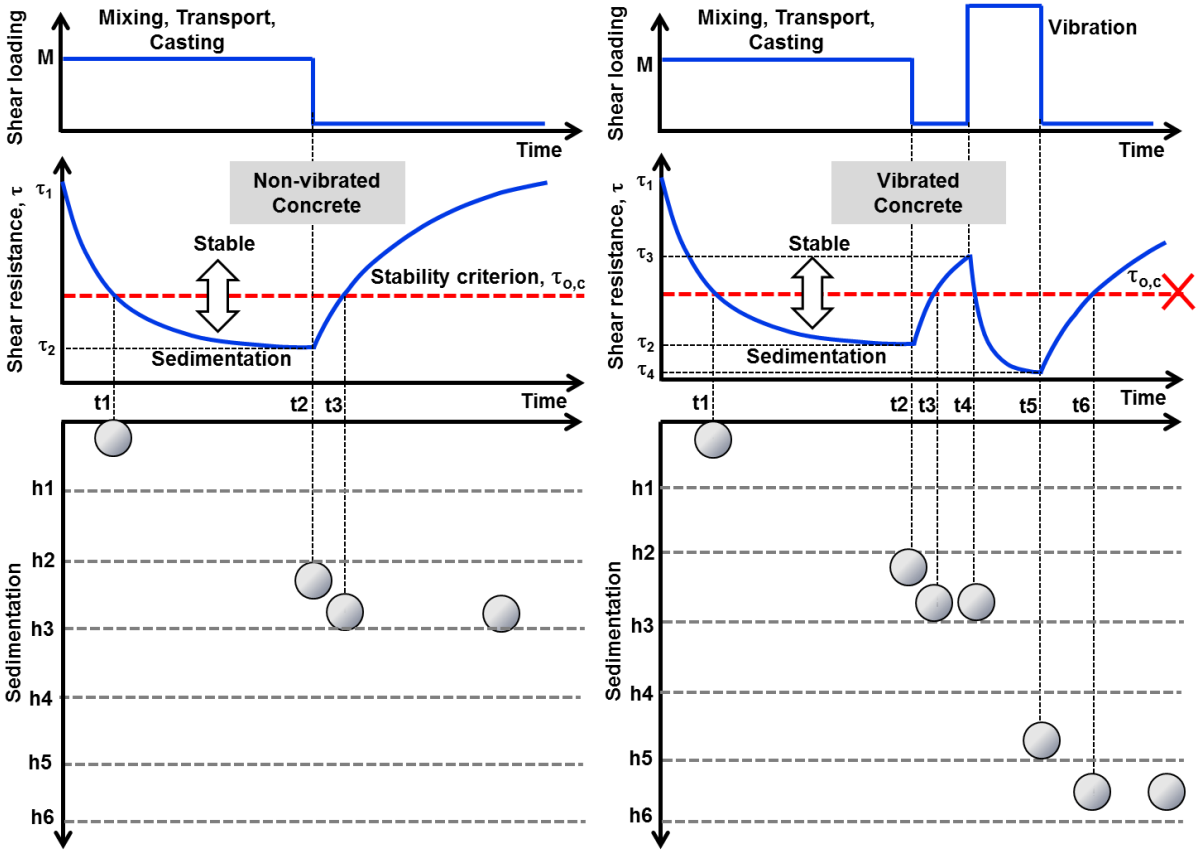

Figure 5.12: Comparison between the segregation phenomena with and without vibration in relation with the shear resistance

Hence, the rheological characterization of concrete under vibration should solely focus on the structural breakdown process. In this regard, the shear resistance due to the interparticle structural strength (A_S) would play the dominant role until the steady state condition is reached. Afterwards, the viscosity (η_r) determines the velocity of segregation of the aggregates. Thus, it could be postulated that there is a critical interparticle structural strength ($A_{S,crit}$) or viscosity ($\eta_{r,crit}$), in compliance with the critical yield stress ($\tau_{o,c}$) as applied to SCC, which guarantees the stability of concrete under vibration. Similarly, applying the same logic as that of the thixotropic

behavior of SCC, the extent of segregation caused by vibration could be expected to depend on the magnitude of $\mathbf{A_S}$ and $\boldsymbol{\eta}$. For a certain time period and constant loading, a mixture with higher $\mathbf{A_S}$ and $\boldsymbol{\eta_r}$ undergoes lower sedimentation by virtue of the fact that its shear resistance remains relatively higher limiting the effects of vibration. The reverse is true if the mixture has lower values of $\mathbf{A_S}$ and $\boldsymbol{\eta_r}$; see Figure 5.13.

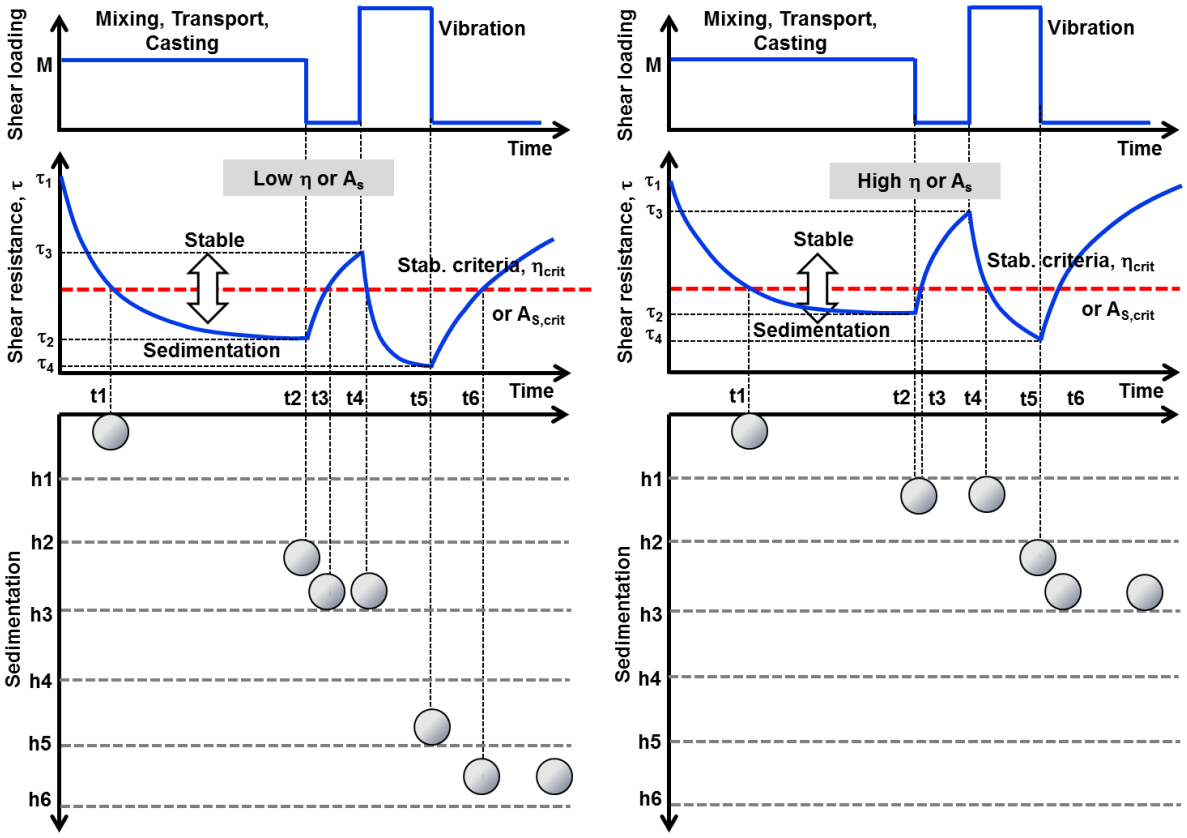

Figure 5.13: Stability criteria for vibrated concrete based on critical A_S and η_r

The results of the investigations as discussed in Chapter 6 have revealed the existence of strong relationships between the stability properties of concrete under vibration and the viscosity (η_r) as well as the interparticle strength (A_S). This also holds true for mortar compositions [179] [180] [181]. The discussions as to the application of the rheological model for the definition of the critical values of $\boldsymbol{\eta_r}$ and $\mathbf{A_S}$ are also presented there.

5.5 Short summary

I. The static stability such as the case in SCC at rest depends on the yield stress (τ_o) and the thixotropy (A_{thix}). The dynamic stability such as the case of

sedimentation of aggregates during vibration of concrete depends on the interparticle structural strength (A_S) and the dynamic viscosity (η).

II. The structural breakdown due to vibration causes a significant reduction in τ_o which is accompanied by a severe sedimentation of the coarse aggregates making A_{thix} irrelevant.

III. Vibration is a concerted loading action which takes place at a “local” level and in a relatively constrained condition (small shear zone) while mixing, transport and casting processes act predominantly at a “global” level where the concrete gets sheared and undergoes a deformation as a mass (large shear zone). Therefore, the effect of vibration on the structural breakdown and sedimentation is much more pronounced.

IV. A new multiscale rheological model is developed for the structural breakdown process by considering the paste, mortar and concrete respectively as micro, meso and macro scales.

V. The multiscale rheological model enables the quantification of η for all phases (paste, mortar, concrete) and A_S for a concrete by considering the interdependence between the rheological properties of the subsequent phases. To do so, the viscosity (η) of the suspending medium (paste) and the paste demand of the aggregate particles ($V_{P,S}$) are used as input parameters.

VI. The resistance to dynamic segregation as well as the flow time increases with increasing A_S or η.

VII. There is a strong relationship between A_S and η. However, their relevance to describe a certain stress related fresh concrete property may not be of equal importance. For example, the pumpability and pump-stability properties correlate more strongly with η rather than A_S.

Chapter 6
Performance Evaluation Criteria Based on Experimental Investigations

6.1 Short introduction

In this chapter, new performance evaluation criteria for flowable concretes exposed to vibration are introduced. These criteria are defined on the basis of the rheological, stability and flowability parameters. Moreover, a preliminary performance criterion for pump-stability of flowable concrete is also introduced. Also illustrated is an overview of the sequential performance evaluation that integrates the rheological performance criteria of the subsequent phases with the stability and flowability performance criteria of concrete and mortar.

6.2 Stability criteria based on stability parameters

One of the challenges with regard to guaranteeing the quality of flowable concrete casted through the application of vibration is the lack of performance criteria upon which the stability properties could be evaluated. There is of course a stability criterion defined for SCC on the basis of the wash-out test in accordance with the DAfStb guideline [174]. Since this criterion has been proven to work successfully for SCC, it would be advisable to adopt the same approach also for vibrated concrete.

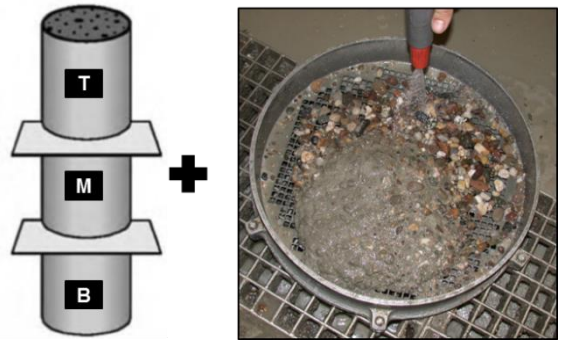

Figure 6.1: Wash-out Test for SCC

The chosen sieve sizes for the wash-out should have mesh sizes equivalent to half of the maximum aggregate size, e.g. 8 mm sieve for a 16 mm maximum grain size. The

average mass of the retained aggregates (M_i) from each segment is determined using Equation (6.1).

$$\overline{M} = \frac{M_T + M_M + M_B}{3} \tag{6.1}$$

The stability criterion is defined on the basis of the deviations of the mass of retained aggregates from that of the average value. SCC is considered to be stable when the deviations from each section are not higher than 20%.

$$\Delta M_i = \left[\frac{M_i - \overline{M}}{\overline{M}}\right] \cdot 100 \leq 20\% \tag{6.2}$$

However, this criterion was found to be too lenient to quantify the stability behavior of concretes that are exposed to vibration as illustrated with the following examples based on test series VI – combined effects of aggregate composition and paste amount on the robustness, see section 4.8.7.

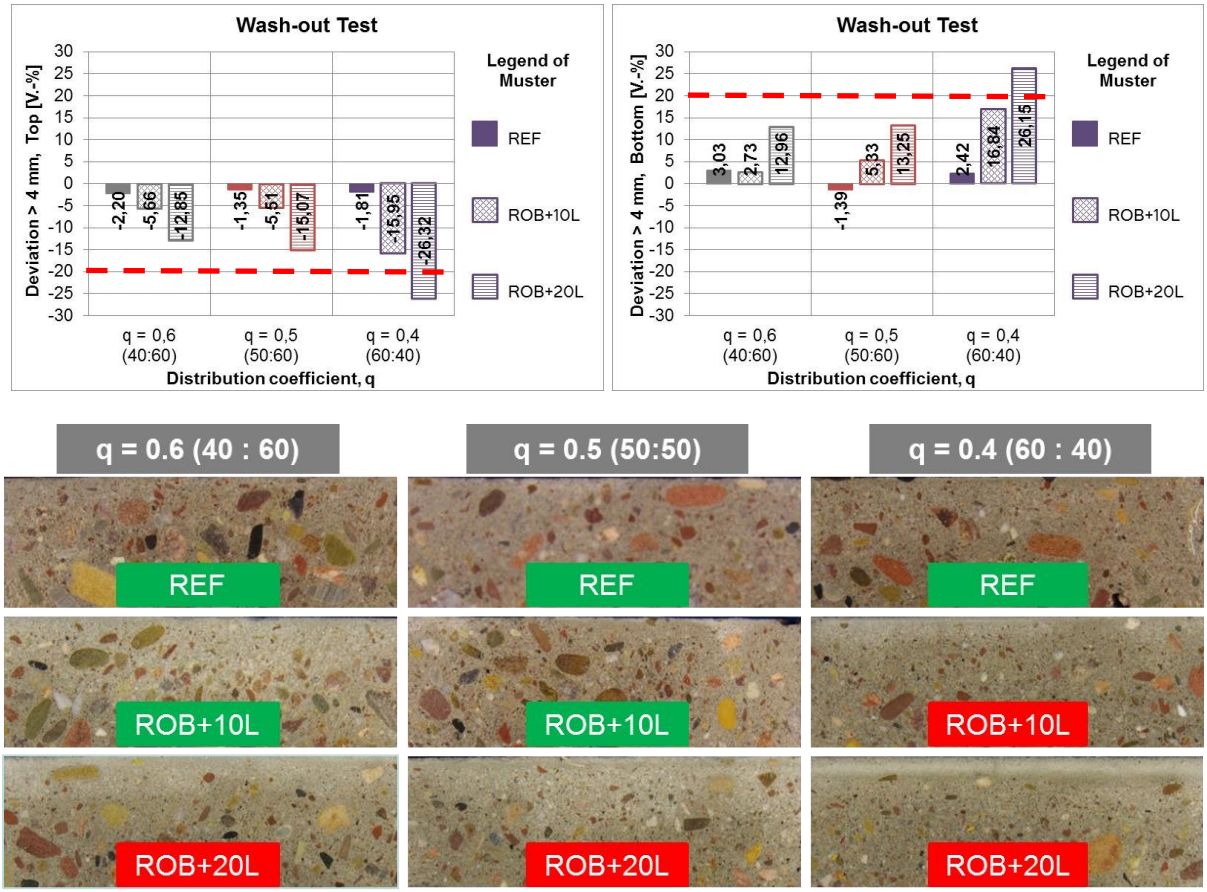

Figure 6.2: Comparison of the stability criterion of SCC with sedimentation under vibration for different aggregate compositions (test series VI)

As can be seen in Figure 6.2, based on the stability criterial of SCC ΔMi ≤ ± 20% depicted by the red lines, only the concrete with q = 0.4 (60 : 40) could be considered to be unstable. However, this does not reflect the real sedimentation behavior observed on the dry specimen of some of the other concrete compositions. Those concrete specimens indicated in red do also show significant accumulation of paste or fine mortar at the top even though this is not reflected by the stability criteria. Therefore, a new strict stability criterion, the so called stability index (SI), is introduced with which the stability of concretes exposed to vibration could be assessed. For this purpose, the average mass of retained aggregates (M_i) from each segment is determined using Equation (6.1) and then the deviations from the top and bottom segments are determined using Equation (6.3).

$$\Delta M_T = \left[\frac{M_T - \overline{M}}{\overline{M}}\right] \cdot 100 \text{ and } \Delta M_B = \left[\frac{M_B - \overline{M}}{\overline{M}}\right] \cdot 100 \tag{6.3}$$

The SI is then defined as the difference between the deviations of the bottom and top segments from the average. As such, vibrated concretes with a SI values less than 20% could be considered as stable.

$$SI = |\Delta M_B - \Delta M_T| \leq 20\% \tag{6.4}$$

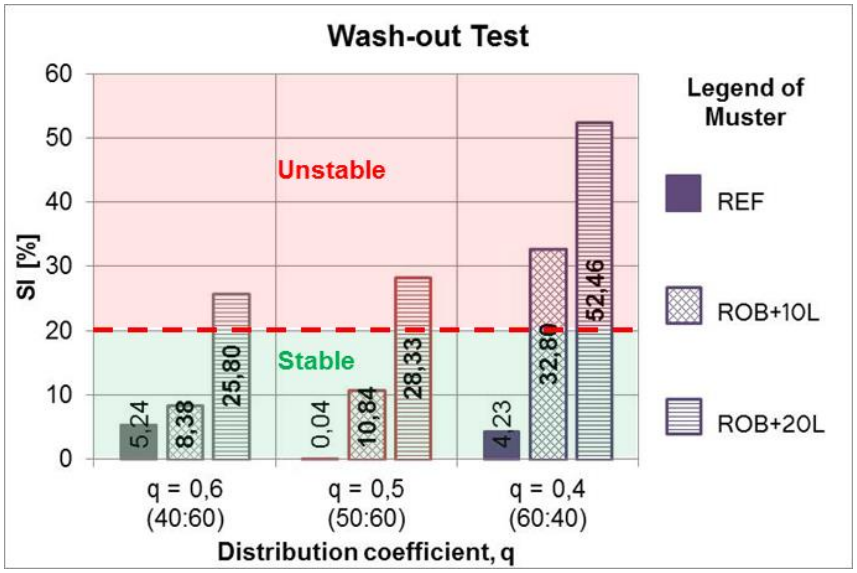

Figure 6.3: Comparison of the stability index with sedimentation under vibration for different aggregate compositions (test series VI)

Comparison between the wash-out test based on the SI and the sedimentation behavior on the dried specimen in Figure 6.2 clearly shows the adequacy of this stability criterion since all the concretes lying in the stable zone (SI ≤ 20%) have shown good stability against sedimentation under vibration. On the contrary, the

concrete specimens showing significant sedimentation lie in the unstable zone (SI > 20%), also confirming the suitability of the SI as a reliable stability criterion for vibrated concrete. The same conclusion could also be reached based on the results of the investigations in test series III as illustrated in Figure 6.4.

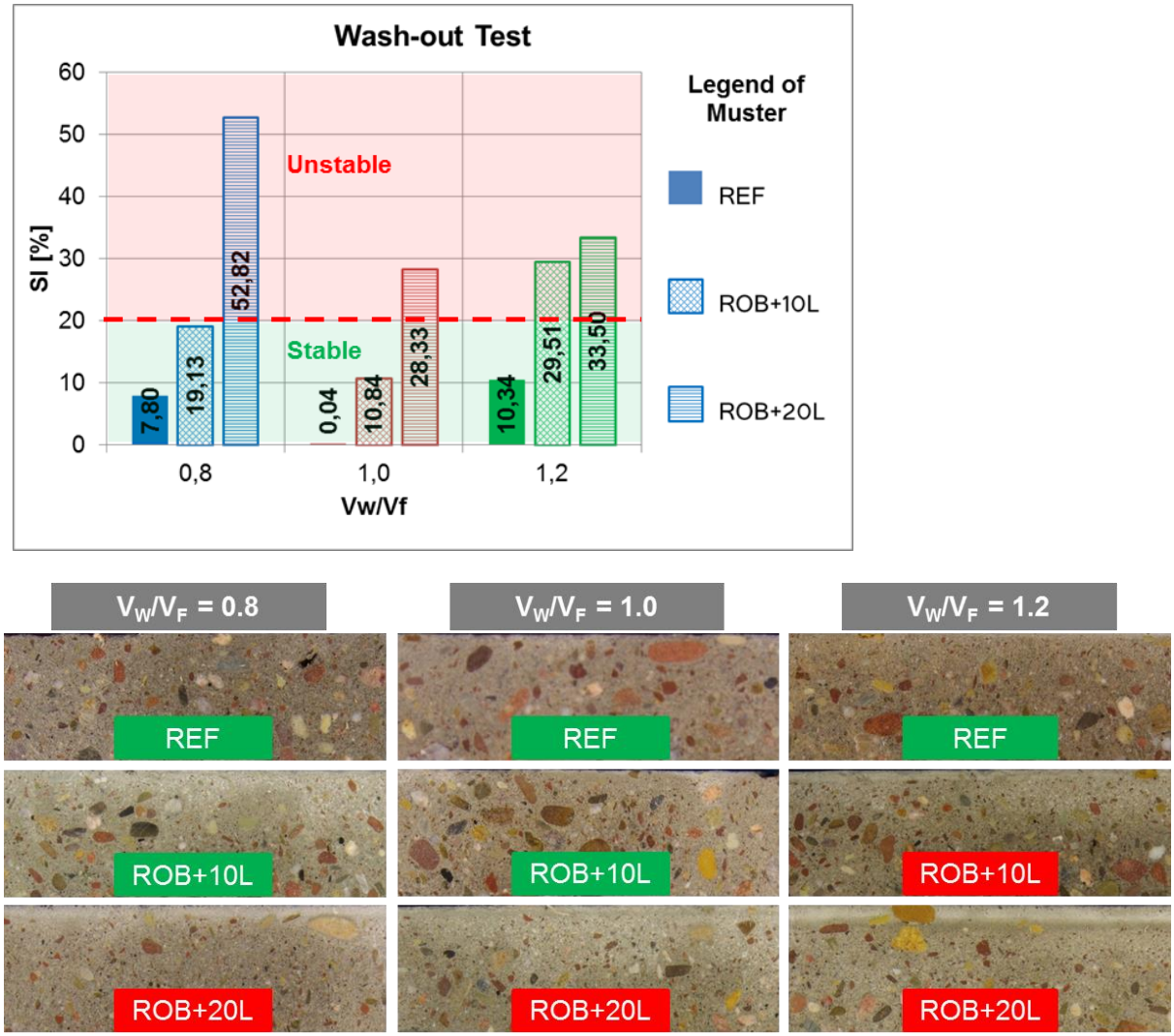

Figure 6.4: Comparison of the stability index with sedimentation under vibration for different paste compositions (test series III)

6.3 Stability criteria based on the rheological model

For the purpose of defining a rheology based stability criteria for vibrated concrete, the trends and correlations between the results of the stability, rheological and flowability investigations were analyzed.

- Stability investigations:
  - Stability index (SI) from wash-out test
  - Visual sedimentation evaluation

- Rheological investigations:
  - Relative dynamic viscosity (η_r)
  - Interparticle structural strength (A_S)
- Flowability investigations:
  - Flow time (FT) of flow cone

The analysis was carried out based on the results of the investigations of test series III (effects of paste compositions on the robustness against water overdosage) and test series VI (effects of aggregate compositions on the robustness against water overdosage); see section 4.8.1.

6.3.1 Stability criteria based on interparticle structural strength (A_S)

The values of $\mathbf{A_S}$ determined using the mathematical correlation of the rheological model for the structural breakdown (see section 5.3) are correlated with the stability index SI from the wash-out test as shown in Figure 6.5. A relatively strong correlation could be observed between the both parameters; the loss of stability increasing with decreasing value of $\mathbf{A_S}$. Based on the stability criteria SI ≤ 20% for concretes exposed to vibration, the corresponding critical value of the interparticle structural strength $A_{S,crit} \approx 60$ N·mm/s could be determined. Accordingly, three zones of stability could be delineated for flowable concrete by making use of the critical parameters. Concrete mixtures in the green zone satisfying both the rheological and the stability criteria could be deemed as necessarily stable. Those lying in the red zone could be categorized as unstable. Those in the yellow zone might require some other measures such as the addition of VMA in order to satisfy the rheological criteria.

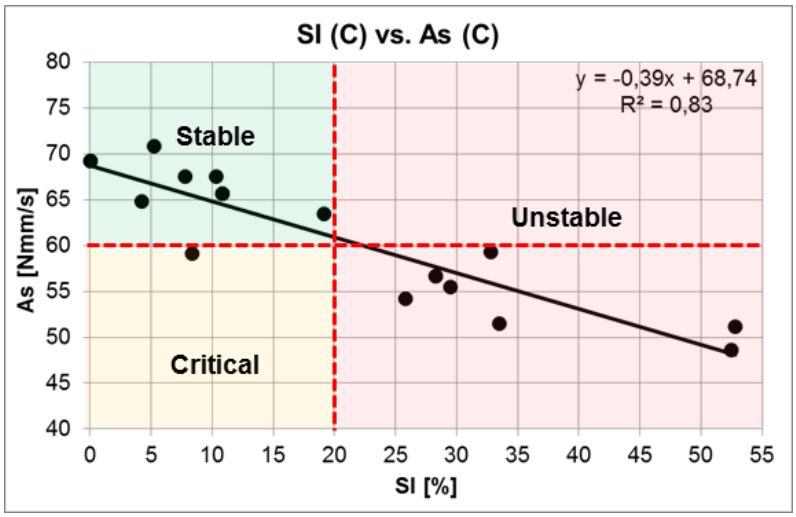

Figure 6.5: Stability criteria based on the interparticle structural strength (A_S)

The adequacy of $A_{S,CRIT}$ to be used as a rheological based stability criteria is checked by comparing it with the stability properties of the different concrete compositions from test series III and VI. As can be seen in Figure 6.6, 90 % of the concrete compositions from both test series that were classified as stable on the basis of the SI ≤ 20% and the visual sedimentation evaluation have values of $\mathbf{A_S} \geq 60$ N·mm/s. Furthermore, all of the unstable concretes have $\mathbf{A_S}$ values smaller than that. Thus, for the chosen rheological measurement techniques, $A_{S,crit}$ = 60 N·mm/s could be adopted as a reasonable rheological evaluation criterion for the stability of concretes under vibration.

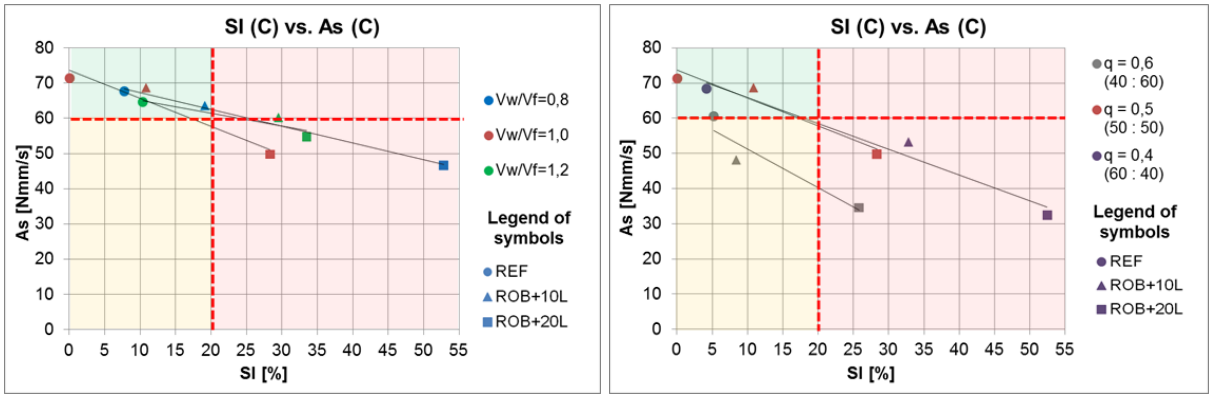

Figure 6.6: Conformity of A_S as a rheological stability criterion (test series III and VI)

A clear distinction between the points lying above and below the boundary line for the test series VI indicates the more pronounced effect of aggregate compositions on $\mathbf{A_S}$ in comparison with paste compositions. This is in agreement with the suggestion by Banfill that the aggregates offer the major share of shear resistance in a concrete when compared to the paste [141].

6.3.2 Stability criteria based on dynamic viscosity (η_r)

Similarly, the values $\boldsymbol{\eta_r}$ determined on the basis of the rheological model are correlated with the SI from the wash-out test as shown in Figure 6.7. The loss of stability also increases with decreasing value of $\boldsymbol{\eta_r}$. The critical relative dynamic viscosity which corresponds to the stability index SI ≤ 20% has a value of $\eta_{r,crit} \approx 2500$ N·mm·s. The zonal definition of the stability is shown in Figure 6.7.

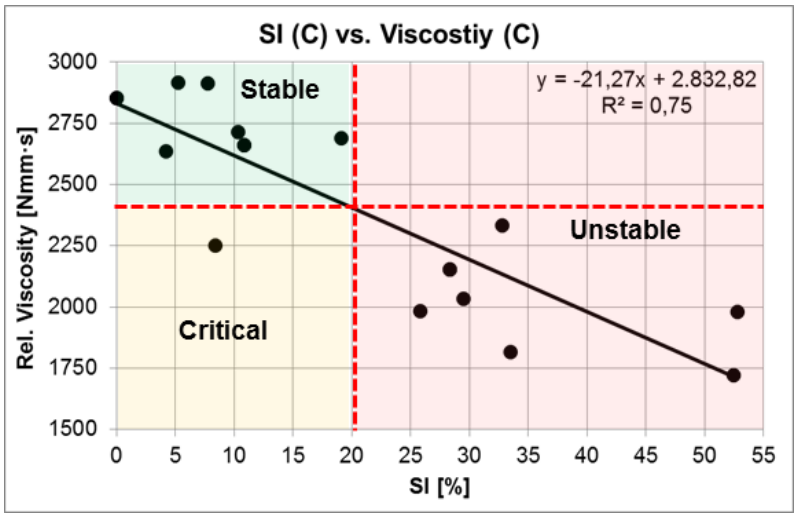

Figure 6.7: Stability criteria based on the relative dynamic viscosity (η_r)

The gap between the stable and unstable concrete compositions is more distinct when η_r is applied as a rheological stability criterion. Here too, 90 % of the concrete compositions from test series III and VI, which were deemed to be stable based on the criteria SI ≤ 20% and the visual sedimentation evaluation have values of $\eta_{r,C} \geq$ 2500 N·mm·s. Those concretes that were deemed unstable have lower η_r values. Hence, adding some safety factor, for the applied rheological measurement techniques, $\eta_{r,C} \geq$ 2500 N·mm·s could be adopted as a reliable rheological stability criterion for concretes exposed to vibration. Moreover, unlike A_S, which is mainly governed by the frictional resistance of the aggregates, η_r is influenced by both the paste and the aggregate compositions see Figure 6.8.

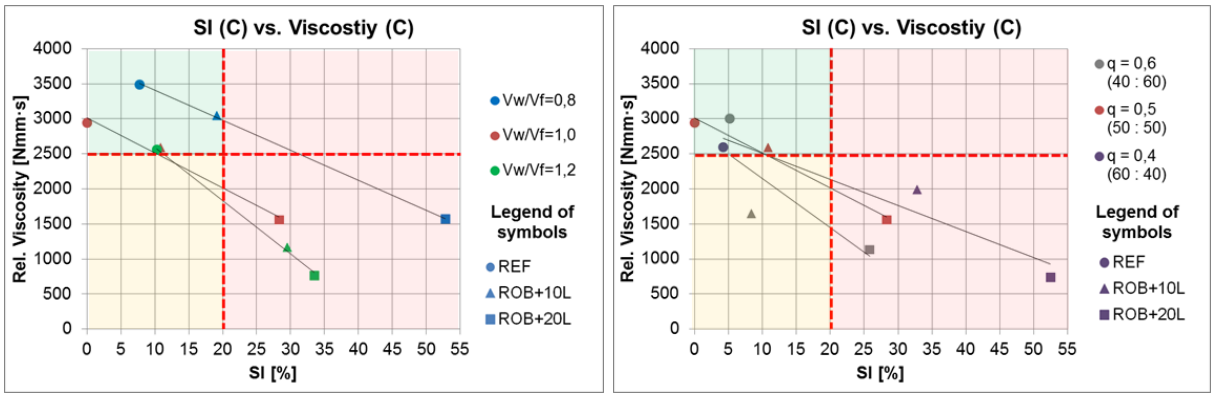

Figure 6.8: Conformity of η_r as a rheological stability criterion (test series III and VI)

6.3.3 Stability criteria based on rheological parameters of extracted paste and mortar

Evaluation of the stability of concrete based on the rheological properties of the paste or mortar compositions determined using the rheological model does not give a clear picture as can be seen in Figure 6.9. There is virtually no correlation between the stability of concrete and the rheological properties of the extracted paste and mortar.

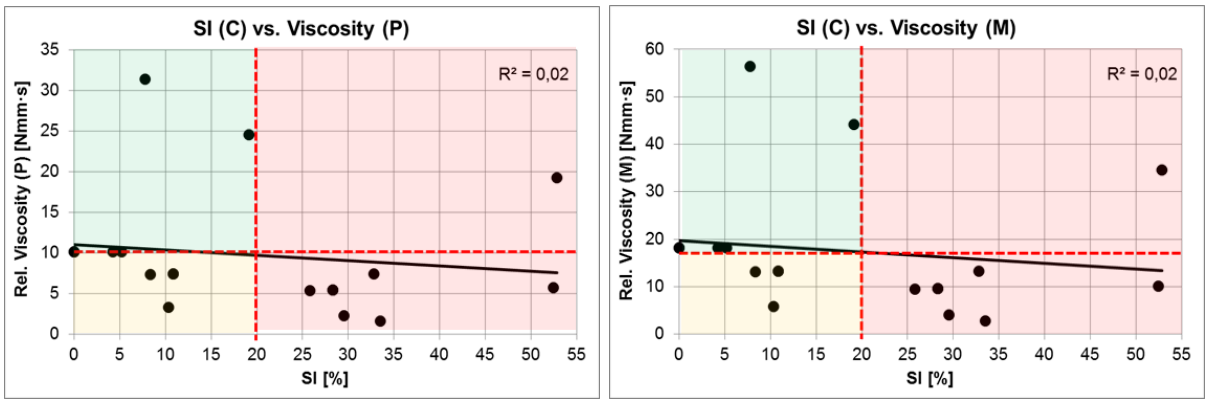

Figure 6.9: Stability criteria based on η_r of extracted paste and mortar compositions

While relatively strong relationships could be established between the rheological properties of the subsequent paste ↔ mortar and mortar ↔ concrete phases, transferring these for the purpose of assessing the stability of concrete is not straightforward. At times, it was observed that the paste compositions extracted from stable and unstable concrete compositions lie above the theoretical stability threshold (the red line) making the differentiation in terms of their influence on the stability difficult. Conversely, most of the paste compositions extracted from stable concrete compositions do not pass this threshold.

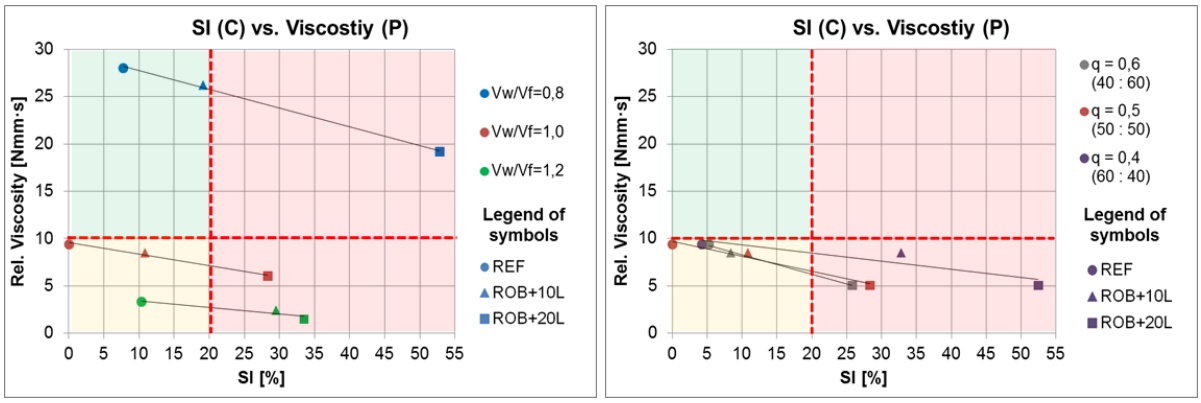

Figure 6.10: Non-conformity of $\eta_{r,P}$ as a rheological stability criterion (test series III and VI)

This is a further proof that the stability of concrete under vibration is immensely influenced by the frictional resistance of the aggregates, which in turn depends on the aggregate composition and the paste content. The extent of the structural breakdown in pastes during vibration is as such that their contribution to the overall shear resistance of the concrete is absolutely minimal. Thus, it could be argued that while the rheological properties of the paste certainly have a role in determining the rheological properties of the concrete, its relevance to the stability during vibration is negligible.

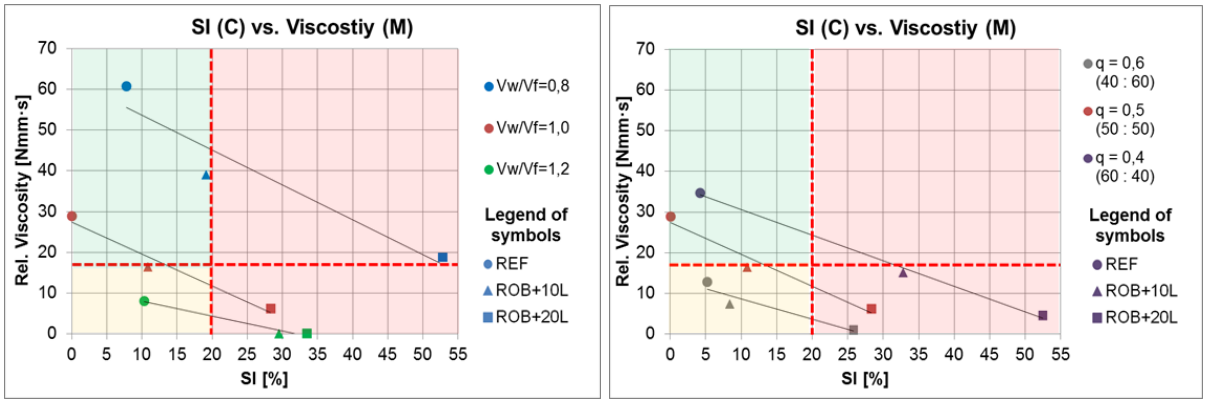

Figure 6.11: Conformity of $\eta_{r,M}$ as a rheological stability criterion (series III and VI)

The stability evaluation based on the rheological properties of mortar gets somewhat better. Here, almost 80% of the concrete compositions that were deemed stable are composed of mortar compositions with $\eta_{r,M} \geq 18$ N·mm·s, while 90% of the mortars from the unstable concretes have values lower than that. Provided that the mortars have adequate flowability and $\eta_{r,M} \geq 20$ N·mm·s based on the applied measurement technique, the chances for composing a stable and flowable concrete should be promising.

6.3.4 Stability criteria based on flowability parameters

The flow time (FT), which was determined on the basis of the flow cone test and has a direct relevance to η_r and A_S as shown in Figure 6.12, could also be used as an indicator as to whether a certain concrete composition remains stable under the influence of vibration.

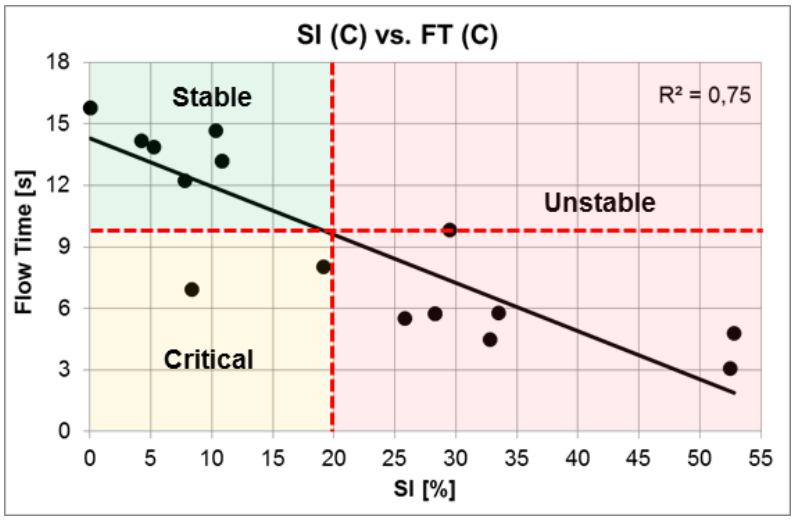

Figure 6.12: Relationship between the flow time and A_S (left) as well as η_r (right)

In this regard, 80% of the concretes from both test series III and VI that were deemed as stable have a minimum FT of ca. 10 s, while all of the unstable concrete mixtures have values lesser than that. However, considering the error-prone nature of this test method, a FT ≥ 12 s could be considered as a good starting point to compose a flowable concrete that would later show good stability against under the influence of vibration. Here too, the stability of concrete decreases with decreasing flow time. The adequacy of this criterion for the evaluation of the stability is shown in

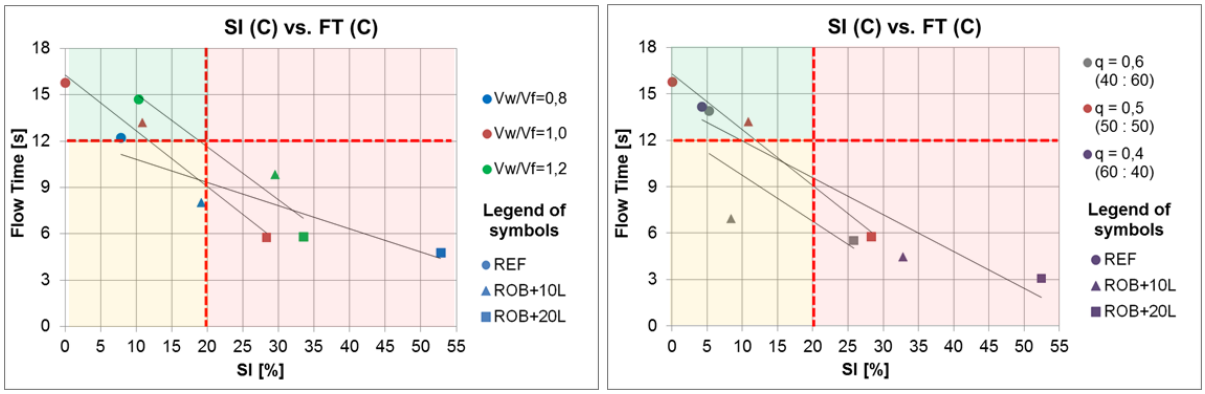

Figure 6.13: Conformity of the flow time (FT) stability criterion (series III and VI)

6.4 Sequential performance evaluation

An overview of the sequential performance evaluation for the stability (under vibration and pressure) of flowable concrete that were defined on the basis of the flowability, stability and rheological parameters as applied to the paste, mortar and concrete phases is shown in Figure 6.14.

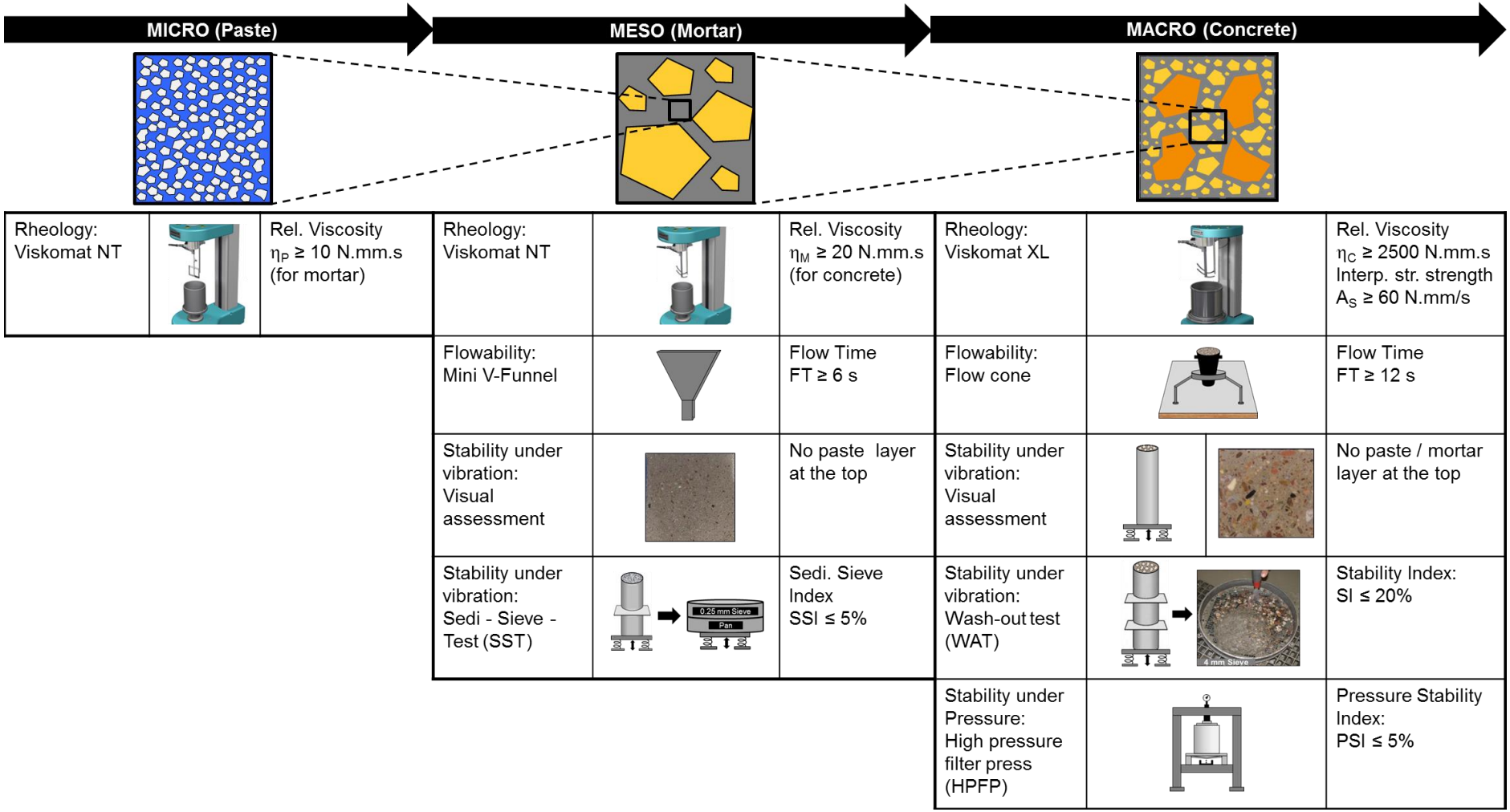

Figure 6.14: Overview of the sequential performance evaluation criteria for flowable and stable concrete

6.5 Short summary

I. Strong relationships exist between the stability and the relevant rheological parameters of the structural breakdown process, namely the dynamic viscosity (η) and interparticle structural strength (A_S).

II. There is a critical dynamic viscosity (η_{crit}) as well as a critical interparticle structural strength ($A_{S,crit}$) that guarantees the stability of concrete or mortar under vibration. This is in contrast to SCC where the critical yield stress ($\tau_{o,c}$) is the relevant stability criteria.

III. Accordingly, a set of performance criteria, which guarantee the stability of flowable concrete compositions under the influence of vibration and pressure, are defined on the basis of the stability (under vibration and pressure), rheological and flowability investigations. The same also applies to mortars exposed to vibration.

- Stability criteria of concrete under vibration based on stability tests:
  - Stability index, SI ≤ 20%: the difference in aggregate distribution between the top and bottom segments in a wash-out test.
  - No noticeable accumulation of paste / mortar at the top of a hardened specimen after vibration.
- Stability criteria of concrete under pressure based on pump-stability tests:
  - Pump-stability index, PSI ≤ 5%: the water retaining capacity of a concrete expressed in filtrate amount as a percentage of the paste content determined using the high pressure filter test.
- Stability criteria of concrete under vibration based on rheological tests:
  - Relative interparticle structural strength of concrete $A_S \geq 60$ N·mm/s.
  - Relative dynamic viscosity of concrete $\eta_{r,C} \geq 2500$ N·mm·s.
  - Relative dynamic viscosity of mortar $\eta_{r,M} \geq 20$ N·mm·s.
- Stability criteria of concrete under vibration based on flowability tests:
  - Flow time; FT ≥ 12 s as determined using the flow cone.
- Stability criteria of mortar under vibration based on stability:
  - Sieve stability index, SSI ≤ 5%: separation of paste under vibration in a sieve – sedimentation – test on a 0.25 mm sieve.
- Stability criteria of mortar under vibration based on rheological tests:
  - Relative dynamic viscosity of paste $\eta_{r,P} \geq 10$ N·mm·s.
- Stability criteria of mortar under vibration based on flowability tests:
  - Flow time; FT ≥ 6 s as determined using the mini V-funnel.

Chapter 7
Rheological Characterization of Pumpability and Pump-stability

7.1 Short introduction

In this chapter, the pumpability and pump-stability are characterized in relation to the rheological properties. The interdependence between the two is also illustrated.

7.2 Rheological characterization of the pumpability

The analysis with regard to the effects of rheological parameters on the pumpability and pump-stability is conducted solely based on the dynamic viscosity (η) as it is dominant rheological parameter that has relevance to the effects of pumping on concrete. A concrete replenished with enough amount of paste would be able to form a lubrication layer around the pipe wall, which ensures a quasi-laminar flow where the bulk concrete flows as a plug; see section 2.4.2. In such cases, the shear stress induced by the friction along the pipe wall predominantly affects the lubrication layer, which is composed of paste or fine mortar. For different concrete compositions possessing adequate amount of paste for the formation of a lubrication layer, the required pumping pressure primarily depends on the rheological properties of the paste, which in turn depends on the paste composition. The aggregate composition, on the contrary, plays somewhat a marginal role, as could be seen in Figure 7.1.

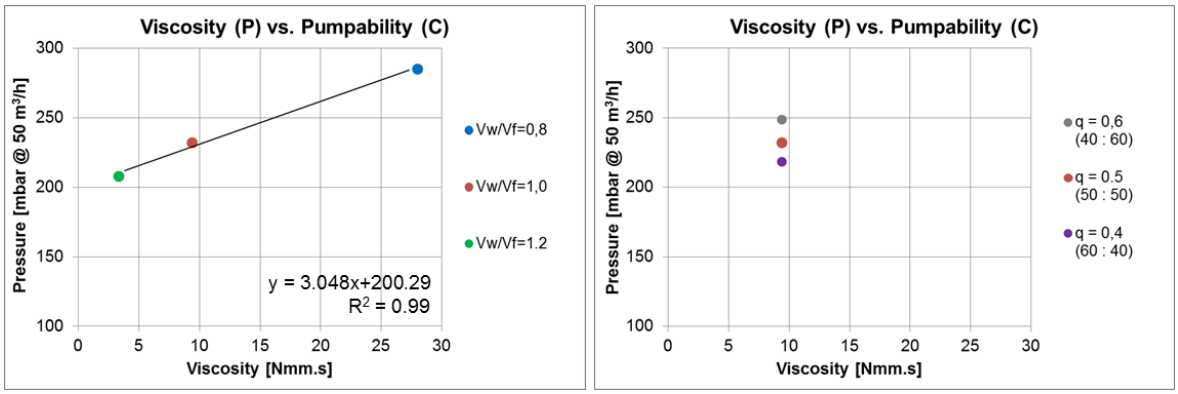

Figure 7.1: Effect of the viscosity of extracted paste compositions on the pumpability

Accordingly, a correlation could be established for determining the required pumping pressure for a certain discharge based on the viscosity the concrete or the extracted paste composition. For a constant flow rate (Q), the effect of the paste viscosity on the required pressure can be quantified as:

$$P = b_P \cdot \eta_{r,P} + P_{0,P} \quad (7.1)$$

Where: P = the required pressure, $b_{p,}$ = pressure gradient as a function of paste viscosity, $\eta_{r,P}$ = dynamic viscosity of paste, $P_{0,P}$ = reference pressure @ $\eta_{r,P} \approx 0$

With increasing values of q, the portion of coarse aggregates in the concrete also increases. Consequently, even though there is enough amount of paste for the formation of a lubrication layer, a relatively higher internal friction between the coarse aggregates could be expected. Generally, solid particles tend to migrate from zones of higher shear stress to lower shear stress. Accordingly, if the local internal friction between the aggregates in the bulk concrete is higher than the shear stress at the pipe wall, there is a chance that the aggregates could migrate towards the pipe wall which ultimately increases the required pressure. In fact, if this process continues for a long time, the formation of a local aggregate cluster would be inevitable which could potentially lead to complete blockage of the pipe.

The reverse is true when the value of q decreases. Here, the concrete is rich in mortar which increases the distance between the coarser aggregates, thereby reducing the internal friction. This might also be advantageous with regard to the formation of a thicker lubrication layer which prevents the coarser aggregates from coming into contact with the pipe wall. Thus, for a concrete composed of a certain paste composition, the marginal effects of the aggregates on the pumpability (P_G) could be integrated for the determination of the required pressure as:

$$P = b_P \cdot \eta_{r,P} + P_{0,P} \pm P_G \quad (7.2)$$

As far as the theoretical models for conventional concrete are concerned, the shear stress caused by pumping acts only on the lubrication layer. However, for highly flowable concrete possessing low yield stress, the effect of the shearing could propagate towards the bulk concrete. This could also happen if the acting shear stress is higher than the yield stress of the conventional concrete; see section 2.4.2.

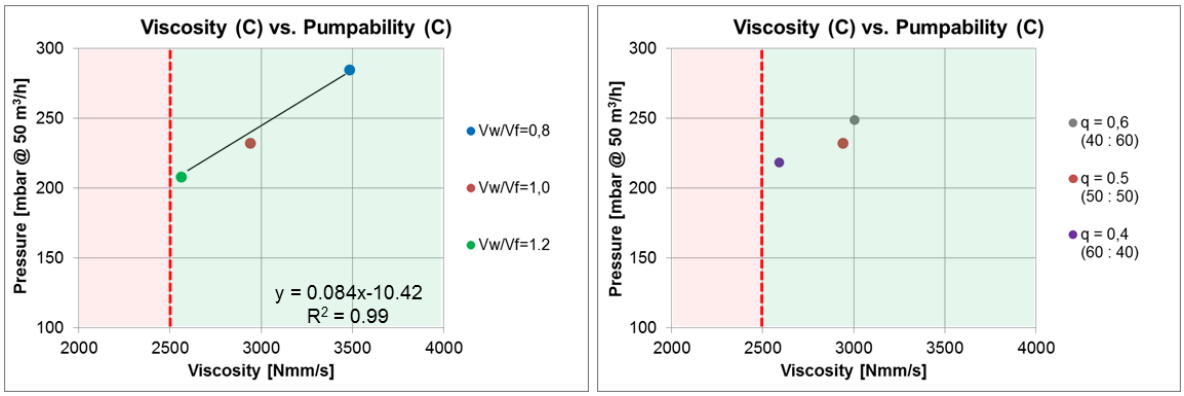

Figure 7.2: Effect of the viscosity of concrete on the pumpability

In such cases, the required pressure for a certain constant flow rate could also be estimated depending on the viscosity of the concrete (η_C) as:

$$P = b_C \cdot \eta_{r,C} + P_{0,C} \pm P_G \qquad (7.3)$$

Where: b_c = pressure gradient as a function of concrete viscosity, $\eta_{r,C}$ = dynamic viscosity of concrete, $P_{0,C}$ = reference pressure @ $\eta_{r,C} \approx 0$

It should be noted that η_r cannot realistically assume a value of zero. But the correlation generally applies for characterization of the pumpability of concrete for mixtures satisfying the rheological stability criteria for vibrated concrete $\eta_{r,c} \geq 2500$ N.mm.s. Generally, an increase in η_r tend to increase the required pressure for a constant discharge, the effect being more pronounced in relation to changes in paste compositions (V_W/V_F-values) rather than aggregate compositions (q-values).

However, both the viscosity and the required pressure are also slightly influenced by the aggregate composition. For a constant paste volume and composition, the aggregate packing which takes place in the pipe due to the migration process could be expected to increase with increasing packing density of the original aggregate compositions. This leaves a relatively thick lubrication layer which is advantageous for the pumping process as is the case with the concrete mixture with q = 0.6, which is composed of a fine – coarse aggregate proportion of 40 : 60 resulting into maximum packing density; see Figure 7.3, left. The maximum packing density has also led to a decrease in viscosity which could also be attributed to the increased thickness of the paste layer around the aggregates which reduces the friction between the coarser aggregates during the rheological measurements.

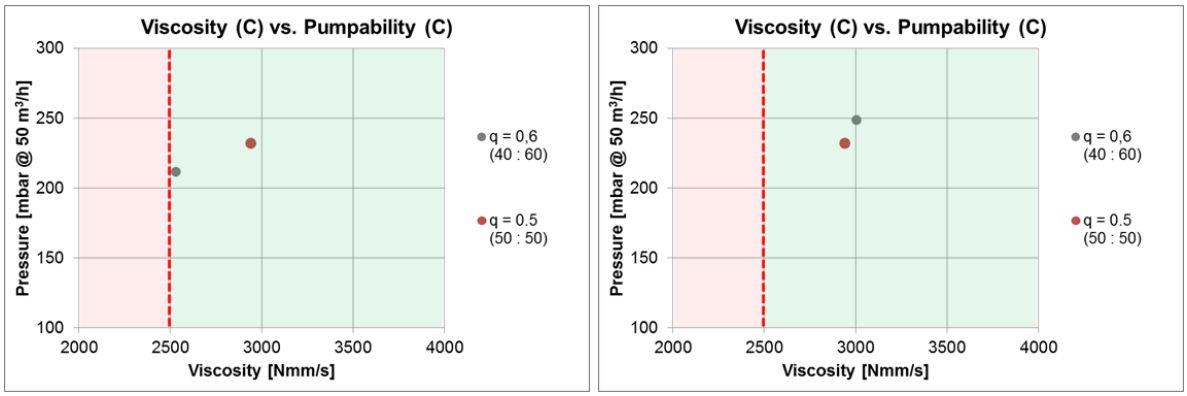

Figure 7.3: Effect of the aggregate composition with constant paste volume (left) and adjusted paste volume (right) on the pumpability

The reverse is true when the paste volume is adjusted for a constant slump flow as could be seen in Figure 7.3, right. A reduction in paste content of 10 lit for the mixture q = 0.6 (40 : 60) has led to a major increase in the required pumping pressure and viscosity of the concrete of about 17% and 19% respectively. The same logical tendency was also observed for the mixture q = 0.4 (60 : 40). Here, an increase in paste volume of about 30 lit has resulted into a ca. 9% reduction in the required pumping pressure. The relatively higher volume of mortar due to the combined higher proportions of fine aggregates and paste is also advantageous in terms of building a thick lubrication layer. Unfortunately, no quantifiable comparison could be made with regard to the viscosity as the mixture with the constant paste volume was too stiff to conduct the rheological measurements, see section III. Nevertheless, the viscosity could be expected to decrease with increasing paste volume due to the reduced friction between the coarse aggregates as a consequence of the increased mortar layer around them.

7.3 Rheological characterization of the pump-stability

If the application of pressure on a concrete causes the separation of the paste from the bulk concrete, the same argument could be extended to suggest that application of pressure also causes separation of water from the paste. Under this assumption, the water retention capacity of a concrete, which is investigated using the high pressure filter press (HPFP) could be considered as a good indicator for the stability of the concrete under pressure, i.e. pump-stability. Here also, the relationship between the pump-stability and the rheological properties was analyzed by making use of the dynamic viscosity (η_r), which is the most relevant rheological parameter to pumping.

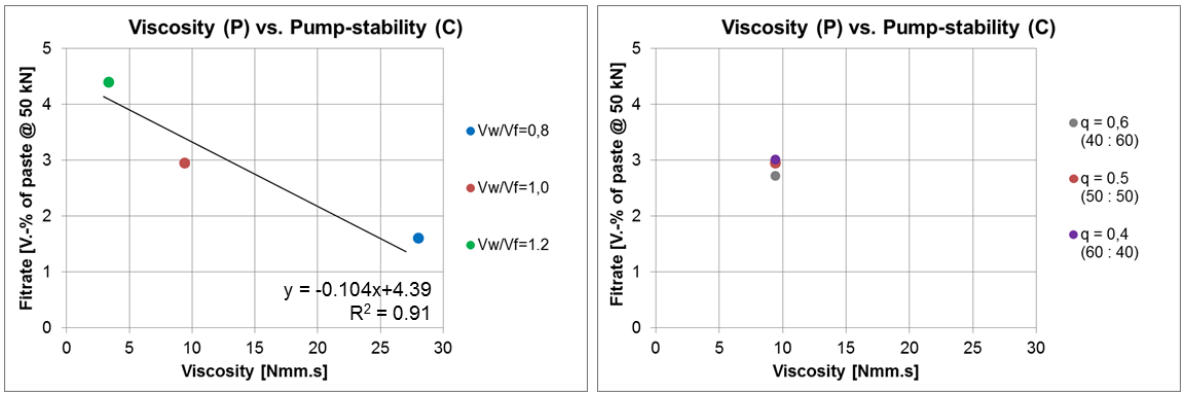

Figure 7.4: Effect of the viscosity of extracted paste compositions on the pump-stability

For a constant pressure (P), the effect of the paste viscosity on the pump-stability can be quantified as:

$$F = d_P \cdot \eta_{r,P} + F_{0,P} \pm F_G \tag{7.4}$$

Where: d_P = filtrate gradient as a function of paste viscosity, $\eta_{r,P}$ = rel. dynamic viscosity of paste, $F_{0,P}$ = reference filtrate @ $\eta_{r,P} \approx 0$

The same relationship for determining the pump-stability could also be established on the basis of the rheological parameters of the concrete compositions as shown in Figure 7.5.

$$F = d_C \cdot \eta_{r,C} + F_{0,C} \pm F_G \tag{7.5}$$

Where: d_C = filtrate gradient as a function of concrete viscosity, $\eta_{r,C}$ = rel. dynamic viscosity of concrete, $F_{0,C}$ = reference filtrate @ $\eta_{r,C} \approx 0$

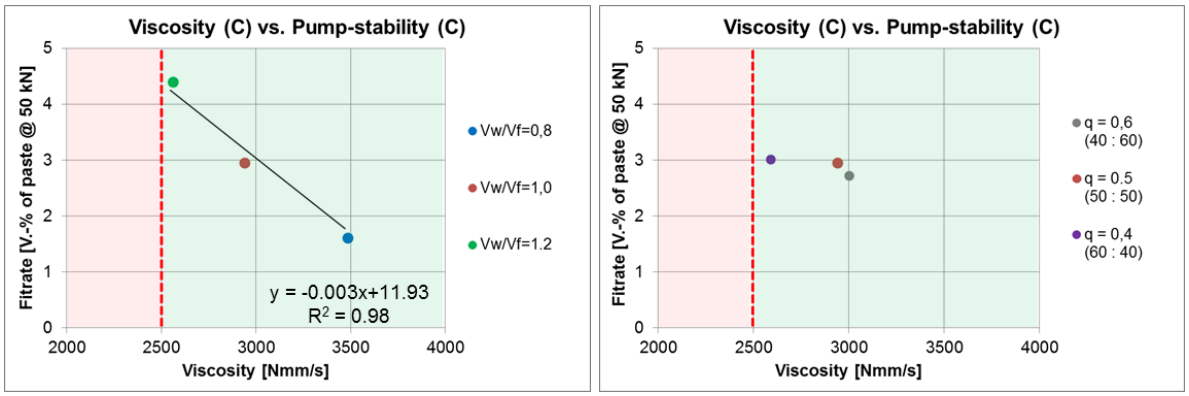

Figure 7.5: Effect of the viscosity of concrete on the pump-stability

The results of the investigations have revealed that the pump-stability is directly related to the dynamic viscosity of the concrete or extracted paste compositions. The

pump-stability generally increases with increasing η-values. However, the changes in the viscosity of concrete caused by alterations in the paste composition have a more pronounced effect on the pump-stability than the aggregate compositions. This is in agreement with the findings of the analysis with regard to the pumpability. Moreover, a new preliminary pump-stability criterion could be defined by adopting the rheological stability criteria $\eta_{r,C} \geq 2500$ N·mm·s corresponding to a stability index SI ≤ 20% for vibrated concrete as introduced in section 6.3.2. This, of course, requires further labor investigations on concrete compositions with different parameters as well as actual in-situ pumping tests. However, a pump-stability index **PSI ≤ 5 %** of filtrate as a percentage of paste @ 50 kN loading or pressure of ca. 30 bar seems to be a good starting point. This is in agreement with the results of the pump-stability investigations conducted within the scope of a research project regarding the development of adequate investigation methods for characterization of the pump-stability of concrete [182]. The adequacy of this criterion shall further be verified within a scope of a cooperative research project between the Leibniz Universität Hannover (LUH) and Technische Universität Dresden (TUD) involving field pumping using a 150 m long pipe. To this end, an onsite HPFP developed by the author will come into use for the in-situ pump-stability investigations.

7.4 Effect of pump-stability on the pumpability

Migration of the paste from the bulk concrete to the pipe wall is an inevitable phenomenon during pumping. As long as the plug flow in the pipe remains homogeneous and stable, the “forced bleeding” caused by the application of pressure could enhance the pumpability of concrete as a result of the decreased viscosity of the lubrication layer, which ultimately leads to a reduction in the required pumping pressure; see section 5.7. This is most probably the case for the concrete mixtures considered in this investigation as they have shown a remarkable stability even under the application of intensive vibration.

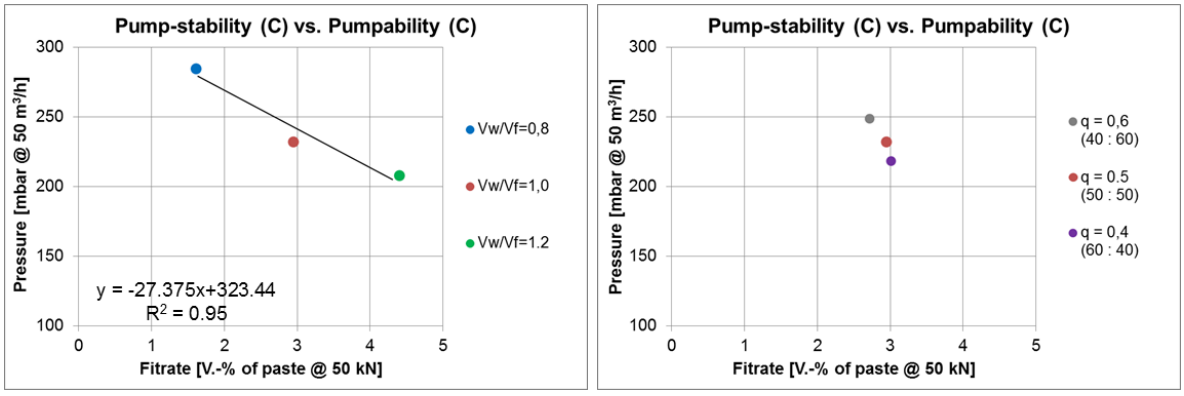

Figure 7.6: Effect of the pump-stability on the pumpability of concrete

Assuming that satisfying the pump-stability criterion PSI ≤ 5 % ensures a homogeneous and stable flow in the pipe, the pump-stability expressed in terms of the amount of filtrate could also be considered as an input parameter to determine the required pumping pressure.

$$P = h \cdot F_C + P_{0,F} \pm P_G \tag{7.6}$$

Where: P = required pressure, h = pressure gradient as a function of filtrate, F_C = amount of filtrate from HPFP, $P_{0,F}$ = reference pressure @ $F_C \approx 0$

The results of the investigations have revealed that both the pumpability and pump-stability are primarily influenced by the paste compositions when the slump flow of the mixtures is maintained constant through adjusting the paste content. On the contrary, the aggregate compositions have somewhat a subdued effect, especially with respect to the pump-stability. The most important aspect with regard to the relationship between pumpability and pump-stability is finding out the equilibrium at which the “forced bleeding” would adversely affect the pumpability. As illustrated in Figure 4.40, unforeseen in-situ factors such as water overdosage due to rest water in truck mixers could directly affect the pump-stability, which would in turn affect the pumpability. Thus, the pump-stability could be considered as a key parameter upon which, in an ideal case, a prediction about the pumpability of concrete could be made by establishing correlations such as Equation (7.6). But, this approach could at least be devised for quality control in concrete production and delivery processes by testing the pump-stability properties of new batches of concrete and comparing the results with a reference pumpable concrete. The approach with respect to the quantification of the pumpability based on the pump-stability shall also be verified within the scope of a cooperative research project between LUH and TUD.

7.5 Short summary

I. The dynamic viscosity (η) is the most relevant rheological parameter that governs the pumpability and pump-stability of concrete.
II. A concrete replenished with enough amount of paste would be able to form a lubrication layer that facilitates a quasi-laminar flow where the bulk concrete flows as a plug. Accordingly, the dynamic viscosity the lubricating paste layer (η_P) governs the pumpability and pump-stability.
III. If cases where the shearing is not limited to the lubrication layer, but propagates towards the bulk concrete, the pumpability and pump-stability depend on the dynamic viscosity of the concrete (η_C).

IV. The pumpability and pump-stability are primarily influenced by the paste compositions, while the aggregate compositions have only a minor effect, especially if the concrete is composed with adequate amount of paste.

V. For a constant paste volume and composition, aggregate compositions with a lower total paste demand (maximum packing density and / or lower surface paste demand) enhance the pumpability due to the formation of thicker lubrication layer.

VI. In a quasi-laminar flow condition where the concrete maintains its homogeneity in the pipe, the pumpability is indirectly correlated with the pump-stability. The required pumping pressure could thus be quantified using the amount of filtrate from the pump-stability investigation as an input parameter.

VII. In a quasi-laminar and homogeneous flow condition, the pumpability could in fact be enhanced by the “forced bleeding” which entails the formation of a less viscous lubrication layer and thus a decrease in the required pumping pressure.

VIII. The most important aspect regarding the relationship between the pumpability and pump-stability is finding out the equilibrium at which the “forced bleeding” would adversely affect the pumpability.

Chapter 8
Performance Evaluation based on the Water Balance

8.1 Short introduction

An analysis regarding the effect of water balance on the rheological, stability (under vibration and pressure) and pumpability properties of concretes is presented in this chapter. The adequacy of the water balance criterion (WB ≤ 0) for performance evaluation is also assessed in correlation with the experimental performance criteria.

8.2 Effect of water balance on the rheological properties

As can be seen in Figure 8.1, the strong relationship between the WB and η_r indicates that the viscosity is more affected by the WB than A_S. This is due to the fact that the relative increase in extra "unbound" water in the concrete affects first and foremost the viscosity of the paste and thereby that of the concrete. Even so, the value of $\eta_r \approx 1750$ N·mm·s which corresponds to WB = 0 is lower than the critical viscosity $\eta_{r,crit}$ = 2500 N·mm·s required to ensure the stability of concrete under vibration. But, it should be noted that all the reference WBC are designed in such a way that the WB lie between -15 and -35 dm^3, with the exception of the mixture with V_W/V_F = 1.2. This, in fact, validates the recommended precautions stipulated in section 4.6 when devising the WBMD to not go all the way to the critical WB = 0.

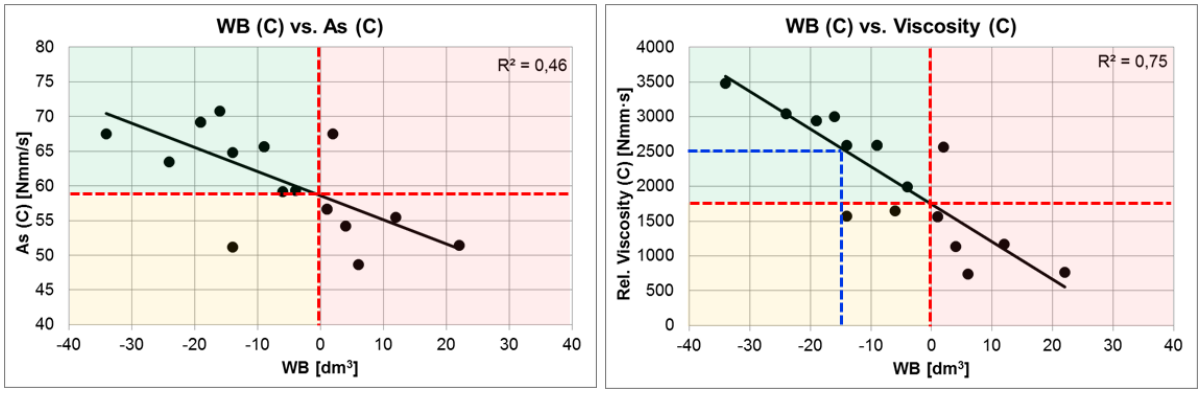

Figure 8.1: Relationship between the WB and A_S (left) and η_r (right)

The WB could be used as a first indicator for the stability of concrete as proven by the comparison with the rheological stability criteria $\mathbf{A_S}$ and $\boldsymbol{\eta_r}$ as shown in Figure 8.2. Here, almost 90% of the concrete compositions from test series III and VI which satisfy the rheological stability criteria $A_S \geq 60$ N·mm/s and $\eta_r \geq 2500$ N·mm·s also fulfill the WB criterion. From the diagrams, it could be observed that a WB ≤ 10 dm^3 seem to be a good control value when applying the WBMD.

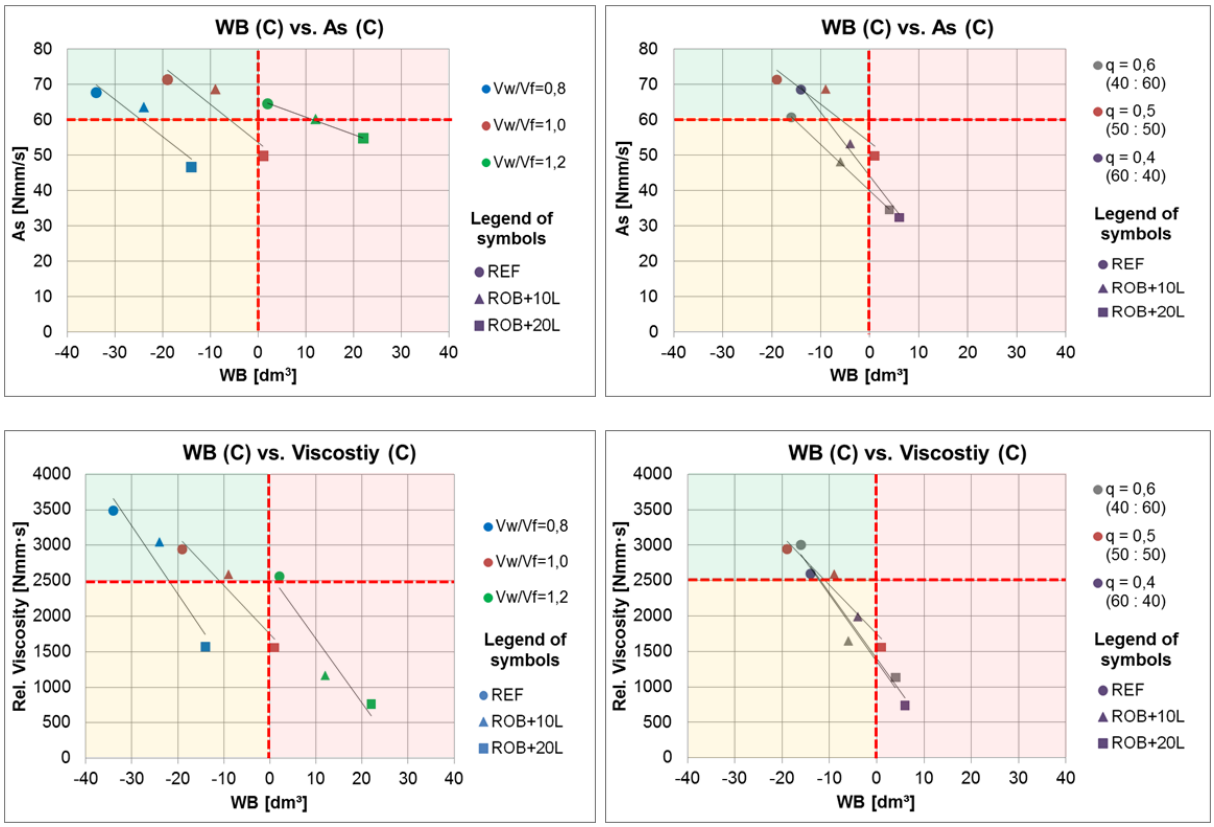

Figure 8.2: WB as stability criteria based on A_S and η_r

8.3 Effect of water balance on the stability under vibration

The main aim of the WBMD is the avoidance of excessive unbound water in the concrete so that the risk for bleeding and sedimentation of flowable concrete could be minimized. Accordingly, 90% of the concrete compositions from test series III and VI which satisfy the water balance criterion WB ≤ 0 also meet the stability criteria SI ≤ 20% as illustrated in Figure 8.3.

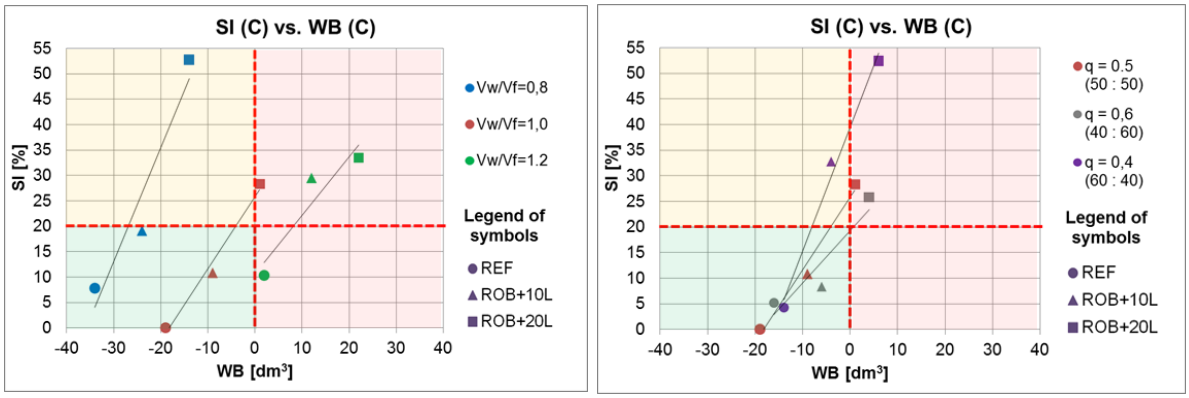

Figure 8.3: WB as stability criteria based on the stability index (SI)

Generally, the stability decreases when the relative unbound water in the concrete increase. The fact that the stability of different concrete mixtures, which are composed using a wide range of mix design parameters (paste compositions with V_W/V_F = 0.8 – 1.2 and aggregate compositions with q = 0.4 – 0.6), could be guaranteed through the application of this criterion reveals the reliability and flexibility of the WBMD. It could also be argued that concrete compositions designed using the same parameters but having lower consistency, e.g. due to reduced SP or paste content, would definitely fulfill the stability criterion SI ≤ 20%.

8.4 Effect of water balance on the pumpability

As can be seen in Figure 8.4, left, the relative increment of unbound water in a concrete as indicated by the WB getting close or exceeding zero, would result into a reduction in the required pressure for a constant discharge. This was the case for the concrete mixtures composed of different paste compositions (V_W/V_F values). Concrete mixtures characterized by relatively smaller differences in the WB as is the case with those possessing different aggregate compositions (q-values), require comparable pressure for a constant discharge; see Figure 8.4, right.

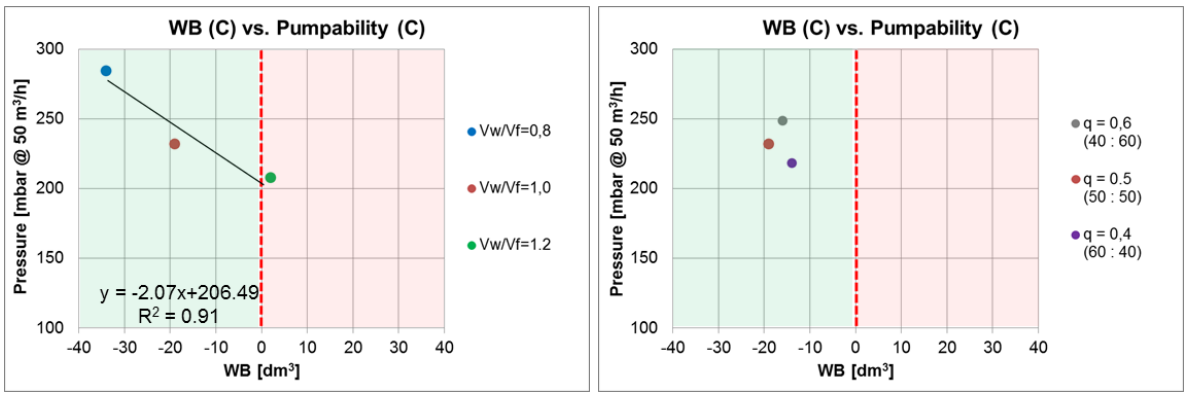

Figure 8.4: Effect of the WB on the pumpability

8.5 Effect of water balance on the pump-stability

Similarly, the WB in the concrete seems to have a direct influence on the pump-stability. A relative increment of unbound water in a concrete would cause a reduction in the pump-stability as indicted by the increased amount of filtrate.

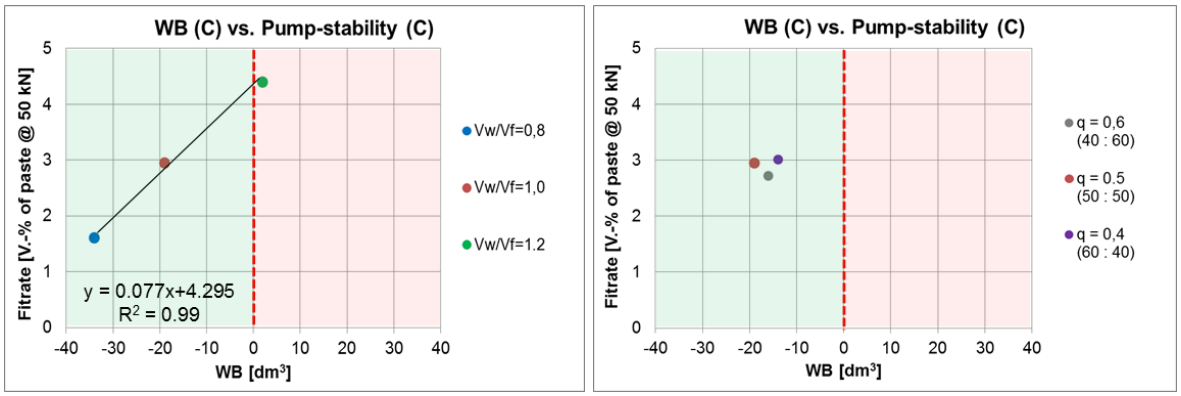

Figure 8.5: Effect of WB on the pump-stability

The concrete mixtures exhibiting higher differences in the WB as is the case with those composed of different paste compositions (V_W/V_F-values) also show significant differences in pump-stability; see Figure 8.5, left. In contrast, the pump-stability remains relatively the same as long as the WB remains comparable; see Figure 8.5, right. At least on the basis of these findings, it could be argued that there is a direct relationship between the pumpability and pump-stability properties and the WB of concrete. Consequently, the WBMD could be used as an important tool for the design and optimization of concrete mixtures that exhibit good pumpability and pump-stability characteristics.

8.6 Short summary

I. Maintaining the water balance criterion (WB ≤ 0) at the mix-design level is a satisfactory approach to guarantee a reliable performance of flowable concretes, especially with regard to the stability under vibration or pressure.
II. The concretes satisfying the experimental performance criteria based on the stability indices as applied to vibration (SI) or pressure (PSI) or the rheological stability criteria (η_C or A_S) also satisfy the water balance criteria WB ≤ 0.
III. An increment in the relative unbound water in concrete as controlled by the WBMD leads to a reduction in η which in turn results into loss of the dynamic stability (under vibration and pressure).
IV. Concrete mixtures exhibiting higher differences in the WB also show significant differences in the pumpability and pump-stability characteristics.

Chapter 9
Essence of the Dissertation

A successful application of flowable concrete would require first and foremost a comprehensive and tailored mix-design method which is dictated by the properties of the readily available construction materials and the interaction between them. The concrete designed in such a way should ultimately satisfy the relevant performance requirements in the fresh state including the flowability, pumpability, stability, and robustness as well as in the hardened state such as the strength and durability. The **water balance mix-design (WBMD)** addresses these objectives by integrating the following main components.

- **Aggregate optimization** ensures good homogeneity and stability through maximizing the lattice effect. Any type and size of aggregates could be optimized to meet the normative requirements by applying a non-linear algorithm based on ideal particle size distribution functions; see section 3.3.1
- The **effective water demand of fines (β_E)** could be determined by considering the effect of SP on the saturation point of paste suspensions and their flowability characteristics. The classical **β_P** method developed by Okamura was modified and applied for determining the **β_E**; see section 3.3.6.
- A **minimum amount of paste** that is required to ensure adequate flowability and stability could be determined for the optimized aggregate composition. This depends on the chosen paste composition (V_W/V_F-values), the packing density (voids' paste demand) and the water demand (surface paste demand) of the aggregates. The packing density was determined by applying vibration and additional loading while the water demand was determined using a filter press and water-jet pump; see section 3.3.3 and 3.3.4.
- Maintaining the overall **water balance (WB)** in a concrete is a crucial design requirement that guarantees a reliable stability of flowable concrete mixtures, see section 3.3.7.

The WBMD aims at guaranteeing the flowability and stability of concrete, through a systematic characterization, optimization and integration of the basic components in a concrete including the aggregates, fines, water and SP. It also provides a controlling mechanism at the design level, namely the WB ≤ 0, with which the

functioning of the systematic integration of these individual components could be ensured. This is achieved by maintaining the equilibrium between the unbound water in a paste, which results from the difference between the chosen V_W/V_F-values and β_E, and the water demand of the aggregates.

The actual performances of the concretes designed using the WBMD were evaluated with respect to their flowability, stability (under vibration and pressure), robustness (against water overdosage) and the pumpability characteristics. To this end, different standard and new test methods were applied.

- **Flowability**: characterized using a slump flow with tapping as well as combined determination of flow time and slump flow without tapping using a flow cone; see section 4.7.1.
- **Pumpability**: characterized using the pumping resistance simulator (PuReSi) which helps determine the pressure – discharge relationship of concrete compositions; see 4.7.4.
- **Stability under vibration**: the sedimentation tendency of the coarse aggregates was quantified using a wash-out test and visual evaluation on hardened specimen. Moreover, separation of the paste or mortar from the bulk concrete was quantified using sedimentation – sieve – test; see section 4.7.3.
- **Stability under pressure / pump-stability**: analyzed by quantifying the amount of filtrate pressed out of a concrete using a high pressure filter press; see section 4.7.5.
- **Robustness**: analyzed the effect of water overdosage on the behavior of fresh concrete, especially with regard to the flowability, stability (under vibration and pressure) and pumpability properties.

The extensive characterization of the fresh concrete properties was accompanied by rheological studies in order to provide a fundamental clarification with regard to the influence of the basic component materials and design parameters on the performance of the corresponding concrete compositions. The rheological characterizations were conducted at the concrete, mortar and paste levels in order to observe the changes occurring at these different phases. This is of great importance to understand the interdependence between each phase and how this ultimately affects the performance characteristics of the concrete. The applied rheological method, which makes use of a newly developed **step and gap measurement profile**, was conceptualized in such a way that not only the classical rheological parameters such as yield stress (τ) and viscosity (η), but also the magnitude of interparticle structural strength (A_S) could be quantified indirectly from the difference between the static yield stress (τ_s) and dynamic yield stress (τ_d); see section 4.7.2.

The scope of this dissertation mainly deals with flowable concrete that show reliable stability even under the application of extreme external stresses such as vibration and pumping pressure. Accordingly, a relatively high level of shear loading was applied for the rheological investigation in order to quantify the relevant changes that occur during the structural breakdown process. This is in stark contrast with rheological studies conducted to quantify the thixotropic or structural build up process that are mostly relevant to SCC which makes use of a very low level of shear loading. By making use of the relevant rheological parameters that help quantify the structural breakdown process at the subsequent paste, mortar and concrete phases, **a new multiscale rheological model** is introduced that makes it possible to determine these parameters on the basis of the concrete technological parameters.

On the basis of the results of the extensive investigations of the fresh concrete properties, a set of **performance evaluation criteria** could be defined that guarantee the stability of flowable concrete against sedimentation of coarse aggregates under vibration and separation of phases under pressure.

- Stability criteria against sedimentation under vibration: no noticeable accumulation of paste / mortar at the top of a hardened vibrated specimen and stability index **SI ≤ 20%** which designates the difference in aggregate distribution between the top and bottom segments in a wash-out test; see section 6.2.
- Stability criteria against separation under pressure: pump-stability index **PSI ≤ 5%** which indicates the water retaining capacity of concrete by quantifying the amount of filtrate as a percentage of the paste content; see section 7.3.

Moreover, a number of rheological stability criteria were defined based on the rheological parameters. These criteria could be defined by making use of either the rheological parameters of the phase at hand, e.g. rheological stability criteria of concrete based on rheological parameters of concrete, or the rheological properties of the suspending medium, e.g. rheological stability criteria of concrete based on the rheological parameters of the suspending mortar. The same holds true when the rheological stability criteria are defined for mortar with the paste considered as the suspending medium. The results of the investigations have clearly shown that during the application of intensive external stresses which lead to a significant reduction in yield stress (τ_o), the extent of the interparticle structural strength (A_S) as well as the dynamic viscosity (η) assume the major role in determining the stability properties of a concrete. Based on these considerations, the following sets of rheological stability criteria are introduced based on rheological parameters of the phases in question or the suspending mediums.

- Rheological stability criteria of concrete under vibration:
  - Relative interparticle structural strength of concrete $\mathbf{A_S \geq 60\ N{\cdot}mm/s}$; see section 6.3.1.
  - Relative dynamic viscosity of concrete $\mathbf{\eta_{r,C} \geq 2500\ N{\cdot}mm{\cdot}s}$; see section 6.3.2.
  - Relative dynamic viscosity of mortar $\mathbf{\eta_{r,M} \geq 20\ N{\cdot}mm{\cdot}s}$; see section 6.3.3.
- Rheological stability criteria of mortar under vibration:
  - Relative dynamic viscosity of paste $\mathbf{\eta_{r,P} \geq 10\ N{\cdot}mm{\cdot}s}$; see section 6.3.3.

Moreover, based on the results of the flowability investigations, it could be confirmed that the stable concrete mixtures satisfying the above rheological stability criteria had flow time **FT ≥ 12 s** as measured by the flow cone. Similarly, a **FT ≥ 6 s** was determined for the stable mortar compositions using a mini V-funnel flow apparatus.

The adequacy of the WB design criterion to predict the performance of flowable concrete, especially with regard to the stability against sedimentation due to vibration or separation of phases due to applied pressure, has been proven successfully. The concretes satisfying the performance criteria based on the stability indices (SI or PSI) or rheological criteria (η_C or A_S) had also satisfied the water balance criteria **WB ≤ 0**.

In summary, it could be argued that the systematic approach adopted within the scope of this dissertation has provided a comprehensive strategy which guarantees a reliable performance and application of flowable concrete through:

- Introduction of a new design concept (WBMD) which makes it possible to guarantee the flowability and stability of concrete from the get-go.
- Application of new and standard test methods to characterize and quantify the most important fresh concrete properties (flowability, stability under vibration, stability under pressure, pumpability and robustness).
- Introduction of a new rheological test and evaluation methods as well as a multiscale rheological model to quantify the behavior of cementitious based compositions during the structural breakdown process.
- Introduction of new performance criteria on the basis of mix design (WB), the fresh concrete properties (FT, SI and PSI) as well as rheological parameters (η_C and A_S) that guarantee the stability and robustness of concrete even under the application of intensive external stress.

An overview incorporating the main components of the design, characterization and performance evaluation of flowable and stable concrete is illustrated in Figure 9.1.

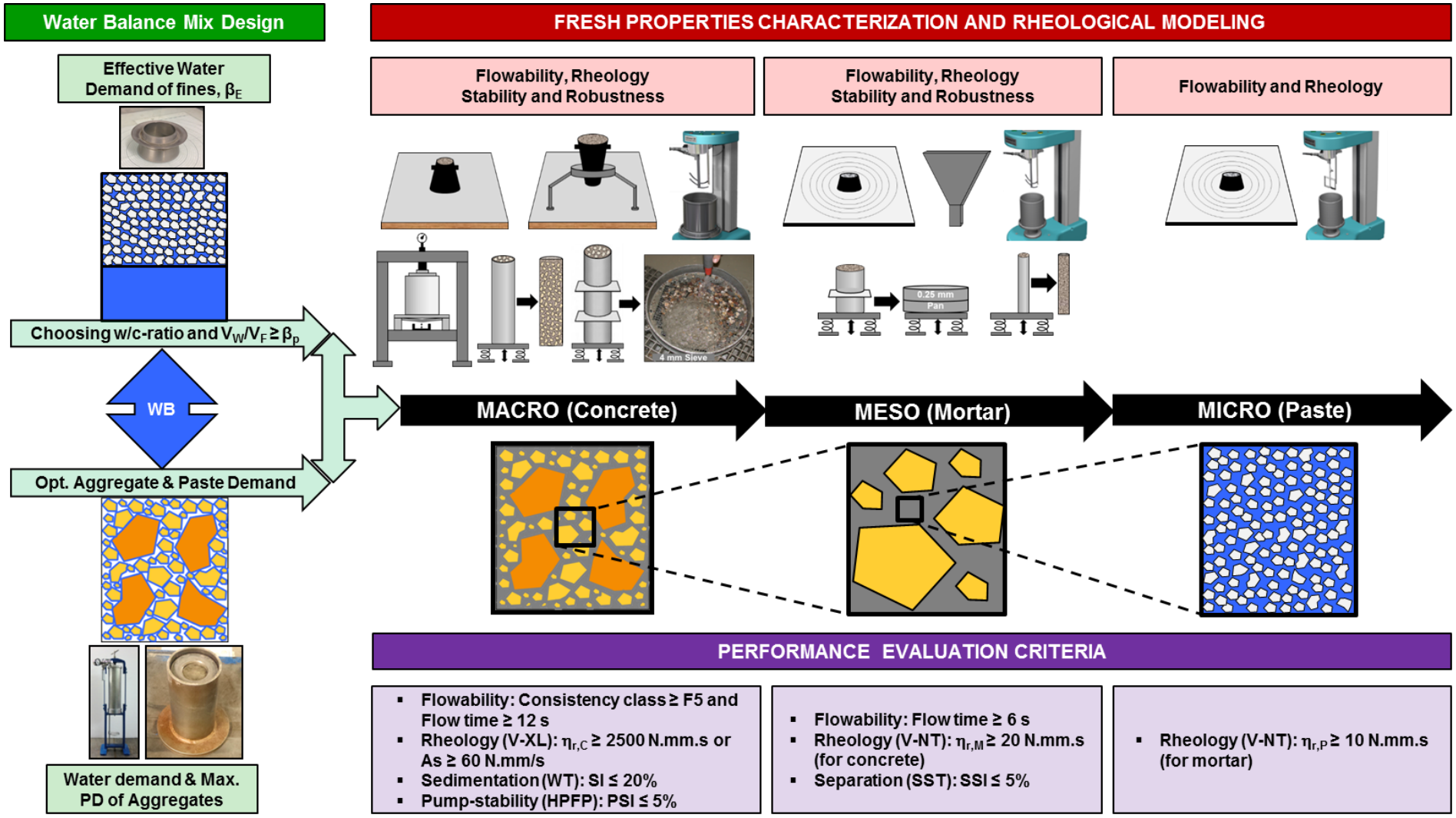

Figure 9.1: Overview of the design, characterization and performance evaluation of flowable and stable concrete

Chapter 10
Conclusions and Recommendations

10.1 Conclusions

The ever increasing dimension and geometrical complexity of today's modern structures require a highly workable concrete that is pumpable, flowable, deformable and passable through tight spacing. At the same time, such a concrete is expected to have reliable stability and robustness properties as these are decisive criteria upon which the quality of the fresh concrete and ultimately the construction elements depend. While self-compacting concrete (SCC) adequately satisfies most of the workability requirements, some critical challenges remain with regard the stability and robustness aspects. Furthermore, the higher costs associated with the raw materials and the intensive quality control mechanisms required by SCC have been a great obstacle to its wider application. The prohibition regarding the application of vibration energy in SCC also leaves no room for ad-hoc measures, especially in cases where flow stagnation occurs. The usage of conventional concretes (CC) in such challenging casting conditions is also not a feasible solution, since they usually do not satisfy the workability requirements such as filling and passing ability.

Thus, the only solution for the realization of such projects is the usage of highly flowable concrete that has the attributes of SCC in terms of the workability properties and CC with regard to the stability under external stresses. Such a concrete should also exhibit a high level of robustness to fluctuations in the quality of the raw materials and the environmental conditions. However, there are some hurdles that have to be overcome in order to realize these objectives. First, there are no adequate mix-design methods that are specifically developed for such concretes, especially in relation to the stability aspects. Second, the behavior of such concrete are not yet thoroughly investigated. Here, the lack of the proper investigation and evaluation methods for the characterization of the stability and rheological properties under the influence of vibration and pressure are definitely contributing factors. Third, there are neither concrete technological nor rheological performance evaluation criteria upon which the quality of such concretes could be assessed in terms of ensuring the workability and stability requirements. Thus, within the scope of this dissertation, three main aspects that are absolutely crucial for application of flowable and stable

concrete are addressed – the mix-design, characterization and performance evaluation.

The newly developed Water Balance Mix-Design method (WBMD) guarantees not only the flowability but also the stability of concrete even under the application of extreme vibration and pumping pressure. The WBMD stipulates that the availability of excessive water paste in concrete is the main reason for the occurrence of bleeding, sedimentation and segregation. Superplasticizers, by virtue of their function as dispersing agents, facilitate the release of the water that is trapped within the fines agglomerates. Hence, their effect on the stability cannot be neglected. The WBMD incorporates this effect through the determination of the effective water demand of the fines by considering the superplasticizer as part and parcel of the liquid phase in the paste. Excessive amount of paste or imbalanced aggregate compositions are also contributing factors to the instability. Thus, the WBMD makes use of a mathematical algorithm for aggregate optimization so that the lattice effect could be enhanced. The minimum required paste amount for the optimized aggregate composition is then determined based on the maximum packing density (voids paste demand) and the surface water demand (surface paste demand) of the aggregates. The minimum paste amount is also mathematically correlated with the paste composition based on the water - fines ratio (V_W/V_F). The higher the value of V_W/V_F, the lower the paste demand. Ultimately, the avoidance of unbound water and the enhancement of the lattice effect of the aggregates in combination with the usage of the right amount of paste are the mechanisms with which the WBMD guarantees the flowability, pumpability, stability (under vibration and pressure), and robustness of concrete. This makes the WBMD a tailor made mix-design method in which all the component materials are interdependently integrated so that the conflicting fresh concrete requirements could be satisfied.

The reference Water-Balanced Concrete mixtures (WBC) were composed using a wide ranging paste and aggregate compositions. Regardless of the chosen paste compositions, aggregate compositions or aggregate size, the WBC have generally shown high flowability reaching consistency class of F6 based on the standard flow table test (with tapping). The mixtures with lower the V_W/V_F-values tend to show the characteristics of SCC as confirmed by the smaller difference between the slump flows determined using the flow table (with tapping) and the flow cone (without tapping). However, with regard to the robustness against water overdosage, the mixtures with lower V_W/V_F-values show the highest change in the slump flow both with the flow table and the flow cone. The flow time tendencially decreases with lower V_W/V_F-values mainly due to the relatively high amount of paste required to attain the desired flowability. As to the effects of aggregate compositions, the difference

between the slump flows with the flow table and the flow cone increases with increasing content of fine aggregates. The flow time is not significantly affected by the changes in the aggregate composition. Moreover, the robustness against water overdosage with respect to both the slump flow and flow time declines when deviances from the optimized aggregate gradation occur; the changes being more pronounced with increasing content of fine aggregates. Using an excessive amount of paste as a consequence of choosing a smaller V_W/V_F-values or higher content of fine aggregates also leads to poor robustness in terms of the flowability properties. The ideal WBC shows the best flowability properties, especially in terms of maintaining the slump flow and the flow time against water overdosage.

The WBC have also shown reliable stability under the action of vibration regardless of the wide ranging paste or aggregate compositions as confirmed by the wash-out test (WT) and the visual evaluation of the sedimentation behavior on hardened concrete specimen. However, in terms of the robustness against water overdosage, the usage of high amount of paste as a result of lower values V_W/V_F or higher amount of sand makes the concrete mixtures more susceptible to sedimentation. The same is also true for concrete mixtures with higher values of V_W/V_F, since the chances for the occurrence of excessive amount of unbound water increases drastically. When it comes to the effects of the aggregates composition, the mixture with the optimized aggregate gradation has shown the best stability against sedimentation. The separation of the paste or fine mortar with grain sizes ≤ 0.25 mm under vibration as investigated using the sedimentation – sieve – test (SST) increases with increasing values of V_W/V_F. Overall, the deviation from the optimized aggregate combination leads to a higher degree of sedimentation of the coarse aggregates and separation of the fine mortar. Here too, the ideal WBC has shown the best stability and robustness under the actions of vibration.

The pumpability and pump-stability as investigated using the pumping resistance simulator (PuReSi) and the high pressure filter press (HPFP) respectively are principally affected by the paste composition. The aggregate compositions play a minimal role in this regard. A strong indirect relationship was observed between the two properties. With increasing values of V_W/V_F and decreasing paste content, the pumpability increases while the pump-stability decreases. Thus, it could be assumed that as long as the bulk concrete remains relatively homogeneous in the pumping lines, the separation of the paste or water under pressure would enhance the formation of a lubrication layer. As a consequence, the required pressure for a certain discharge decreases. However, this strongly depends on the intricate balance between the paste and aggregate compositions. Increased degree of separation of the liquid phase in combination with a higher proportion of coarse aggregates could

also lead to an interlocking of the aggregates, which would ultimately increase the required pressure.

The characterization of the fresh concrete properties was accompanied by comprehensive rheological investigations that were conducted on the concrete mixtures as well as mortar and paste compositions extracted from them. This is of great importance for a better analysis of the rheological interdependence between each phase and how this ultimately affects the fresh concrete properties. Here, the focus lies in the quantification of the relevant rheological properties in relation to the application of intensive external stresses such as vibration which usually causes a structural breakdown in concrete. To this end, a high level of shear loading was applied in order to determine the classical rheological parameters of relative yield stress (τ_r) and relative dynamic viscosity (η_r) as well as a new term, the so called interparticle structural strength (A_S) which depicts the shear resistance of the mixture.

The shear resistance of a concrete constitutes the colloidal forces and early CSH bridges at the paste level and the frictional forces acting between the aggregates. The results of the investigations have revealed that $\mathbf{A_S}$ and $\boldsymbol{\eta_r}$ are the most relevant parameters for analyzing the fresh concrete properties during the application of shear stress. In this context, $\mathbf{A_S}$ quantifies the overall shear resistance of the mixture during the structural breakdown process, until a steady state condition is reached while $\boldsymbol{\eta_r}$ represents the resistance of the mixture to flow after the steady state is reached. Based on these considerations, a multiscale rheological model is proposed for the quantification of the structural breakdown process in the subsequent phases of paste, mortar and concrete. The model, which treats the paste, mortar and concrete respectively as micro, meso and macro scales, not only describes the interdependence between the rheological properties of the subsequent phases, but also makes it possible to determine the values $\boldsymbol{\eta_r}$ for all phases and $\mathbf{A_S}$ in particular for the concrete.

The rheological studies have revealed that even though paste compositions with lower V_W/V_F-values have higher value of $\mathbf{A_{S,P}}$ by themselves, their application in a concrete requires a high amount of paste leading to a reduced friction between the aggregates and thereby reduced value of $\mathbf{A_{S,C}}$ in concrete. The reverse is true for higher V_W/V_F-values with reduced amount of paste. The viscosity (η) decreases with increasing V_W/V_F-values in both the paste and concrete compositions. This might be attributed to the fact that in the steady state condition, the aggregates assume the “best possible” position and “swim” within the continuous paste phase and as a result, the resistance to the flow would be predominantly governed by the viscosity of the paste which in turn depends on its composition (V_W/V_F). With regard to the

influence of the aggregate compositions, deviating from the optimal aggregate composition has led to a reduction in both $\mathbf{A_S}$ and $\boldsymbol{\eta_r}$. In terms of the robustness against water overdosage, the reductions in both $\mathbf{A_S}$ and $\boldsymbol{\eta_r}$ are more pronounced in cases where unrealistically high or low V_W/V_F-values were used or when there is a deviation from the optimum aggregate gradation, i.e. deviation from the ideal WBC.

A comprehensive analysis of the investigation results has revealed strong relationships between the rheological characteristics and the relevant fresh concrete properties. In this regard, an increase in $\mathbf{A_S}$ and $\boldsymbol{\eta_r}$ increases the resistance of the mixture to dynamic segregation. Similarly, an increase in $\mathbf{A_S}$ and $\boldsymbol{\eta_r}$ would lead to an increase in flow time. The pumpability and pump-stability properties correlate more strongly with $\boldsymbol{\eta_r}$. Accordingly, depending on where the shearing takes place in a pipe – it could be limited to the lubrication layer or it could propagate towards the bulk concrete – the required pressure could theoretically be quantified using the viscosity of the paste or the concrete. Likewise, the pump-stability could also be estimated based on the viscosity of the paste or concrete. Furthermore, an increment of the relative unbound water in concrete as controlled by the WBMD leads to a reduction in $\boldsymbol{\eta_r}$ which in turn results into loss of the dynamic stability (under vibration and pressure) and an improvement in the pumpability. It is to be noted that even though a strong relationship exists between $\mathbf{A_S}$ and $\boldsymbol{\eta_r}$, they might not be equally relevant for describing a certain fresh concrete property. All in all, it could be stated that the design strategies devised in the WBMD – enhanced lattice effect of the aggregates in combination with the right amount of paste and a reasonable paste composition – would makes it possible to produce a concrete that has high flowability, good pumpability, reliable dynamic stability and robustness.

To this end, a set of concrete technological and rheological performance criteria could be defined, which guarantee the stability of flowable concrete under vibration and most probably under pressure. Accordingly, concrete mixtures that are deemed to be stable under vibration have a stability index SI ≤ 20% (WT), pump-stability index PSI ≤ 5% (HPFP), internal structural strength $A_{s,C}$ ≥ 60 N·mm/s or a relative viscosity $\eta_{r,C}$ ≥ 2500 N·mm·s (Viskomat XL) and a flow time FT ≥ 12 s (Flow cone). The mortars extracted from these stable concrete mixtures have $\eta_{r,M}$ ≥ 20 N·mm·s (Viskomat NT). Similarly, the mortars that have shown reliable stability have a SSI ≤ 5% (SST), flow time FT ≥ 6 s (V-funnel) and were composed of pastes with $\eta_{r,P}$ ≥ 10 N·mm·s. Evaluation of the stability of concrete based on the rheological parameters of the paste compositions extracted from it is not conclusive. Concrete compositions that satisfy these criteria could be expected to have good pumpability as they possess enough amount of paste for the formation of the lubrication layer. Finally, a

comprehensive engineering model for flowable and stable concrete is introduced, which encompasses the WBMD, the relevant characterization methods and the stipulated concrete technological and rheological performance evaluation criteria.

10.2 Recommendations

The design, characterization and performance evaluation of flowable and stable concrete presented in this dissertation provide a basis upon which further research areas of interest could be derived from. Starting with the WBMD, the mixture with lower V_W/V_F-values has shown somewhat a similar flowability behavior as that of SCC with respect to the self-leveling capacity while satisfying the stipulated performance criteria of SI ≤ 20% under intensive vibration. In fact, these concretes show combined characteristics of SF1 and SF2 based on the slump flow (550 mm – 650 mm) and the flow time (9 s – 25 s) in accordance with the consistency classification of SCC as shown in Table 2.2. Thus, the potential of the WBMD to design a new type of SCC where even vibration could be applied could be valuable in terms of alleviating problems in the application of SCC such as stagnation. Without the application of vibration, the new type of SCC could be expected to show reliable stability and robustness.

On the other side, the WBC with higher V_W/V_F-values has shown a higher tendency to segregate which could be attributed to the availability of excessive unbound water in concrete. From an economical point of view, however, these concretes are advantageous since they contain smaller amount of fines. Thus, other options for enhancing the stability such as the addition of VMA should be tested and evaluated in relation to the stipulated performance requirements. Even though the WBC possess higher flowability with relatively higher compressive strength; see Appendix A-3, it is still possible to apply the WBMD for concretes of lower consistency by reducing the paste amount or the SP content or both. Such a concrete could be expected to show reliable stability. Thus, the prospective investigations in this regard should focus on developing a systematic approach to reach the desired flowability while ensuring the hardened concrete properties of strength and durability.

The performance evaluation criteria are mainly derived from concrete compositions that are composed of aggregates with maximum size of 8 mm the reason being the limitation imposed by the Viskomat XL rheometer. While the adequacy of the performance evaluation criteria is exemplarily tested on concrete mixtures with maximum aggregate size of 16 mm, additional tests might be required to make a conclusive determination. Furthermore, the rheological model for the structural breakdown process is more precise in determining the relevant rheological parameters of the subsequent phases of paste, mortar and concrete when the

changes occur in the paste composition. Nevertheless, there is still some room for improving its accuracy with the help of additional investigations constituting different aggregate compositions. Moreover, the performance criteria with regard to the pump-stability and the established relationships between the rheological properties and the pumpability as well as pump-stability need to be confirmed in full scale pumping tests. In doing so, the ultimate objective should be oriented towards providing a fundamental rheological explanation and preferably a holistic model that also incorporates the pump-stability characteristics as an input parameter. In this regard, the cooperation research project between TUD and LUH provides a good platform.

References

[1] ERMCO, "Ready-Mixed Concrete Industry Statistics - Year 2013," 2014.

[2] T. Hammer, "Nordic network for RTD on Self Compacting Concrete," 2006.

[3] W. Brameshuber, Selbstverdichtender Beton, Beton: Schriftenreihe Spezialbetone ed., vol. 5, Bau+Technik, 2004.

[4] M. Höppner and J. Malcherek, "Entwicklung des Selbstverdichtenden Betons für das Spezial Science Center Wolfsburg und Umsetzung in dieTransportbetonpraxis," *Beton-Information,* no. 3, pp. 17-21, 2002.

[5] ACI Committee 304, "Guide for Measuring, Mixing, Transporting, and Placing Concrete," 2000.

[6] Deutscher Beton- und Bautechnikverein (DBV), "Betonierbarkeit von Bauteilen aus Beton und Stahlbeton," Berlin, 2004.

[7] Institut für Baustoffe, Lebiniz Universität Hannover, "Lecture Materials".

[8] Verein Deutscher Zementwerke e.V. (VDZ), "Bereiten und Verarbeiten von Beton," 2013.

[9] ASTM, "ASTM C143 / C143M-05: Standard Test Method for Slump of Hydraulic Cement Concrete," 2005.

[10] EN, "EN 206-1: Concrete – Part 1: Specification, performance, production and conformity," 2000.

[11] G. Tattersall, Workability and Quality Control of Concrete, 1st ed., London: E & FN Spon, 1991.

[12] EN, "EN 206-9: Additional rules for self-compacting concrete (SCC)," 2010.

[13] C. Kennedy, "The design of concrete mixes," in *Proceedings of the ACI, 36*, 1940.

[14] T. Powers, The properties of fresh concrete, New York: John Wiley and Sons, 1968.

[15] L. Li and A. Kwan, "Concrete mix design based on water film thickness and paste film," *Cement & Concrete Composites, Vol. 39,* pp. 33-42, 2013.

[16] N. Su and B. Miao, "A new method for the mix design of medium strength flowing concrete with low cement content," *Cement & Concrete Composites 25,* pp. 215-222, 2013.

[17] T. Neumann, "Einflüsse auf die Pumpbarkeit von Beton," *Beton 5,* p. 166 – 171, 2012.

[18] EFNARC, "Specification and Guidelines for Self-Compacting Concrete," Farnham. UK, 2002.

[19] E. Koehler and D. Fowler, "Aggregates in self-consolidating concrete," The University of Texas at Austin, 2007.

[20] A. Kwan and H. Wong, "Packing density of cementitious materials: part 2 - packing and flow of OPC + PFA + CSF," *Materials and Structures 41(4),* p. 773–784, 2008.

[21] P. Nanthagopalan, M. Haist, M. Santhanam and H. Müller, "Investigation on the influence of granular packing on the flow properties of cementitious suspensions," *Cement & Concrete Composites 30,* p. 763–768, 2008.

[22] C. Artelt and E. Garcia, "Impact of superplasticizer concentration and of ultra-fine particles on the rheological behaviour of dense mortar suspensions," *Cement and Concrete Research 38,* pp. 633-642, 2008.

[23] A. Papo, L. Piani and R. Ricceri, "Rheological Properties of Very High-Strength Portland Cement Pastes: Influence of Very Effective Superplasticizers," *International Journal of Chemical Engineering,* 2010.

[24] L. Lohaus and T. Gläser, "Improving the Workability of Concrete - Additions of Fly Ash and Use of Small Maximum Grain Size," in *Proceedings pro077 : International RILEM Conference on Material Science - AdIPoC - Additions Improving Properties of Concrete - Theme 3*, Aachen, Germany, 2010.

[25] A. Kwan, W. Fung and H. Wong, "Water film thickness, flowability and rheology of cement-sand mortar," *Advances in Cement Research, 22, No. 1,* p. 3–14, 2010.

[26] S. Hanehara and K. Yamada, "Interaction between cement and chemical admixture from the point of cement hydration, absorption behaviour of admixture, and paste rheology," *Cement and Concrete Research 29,* pp. 1159 - 1165, 1999.

[27] H. Uchikawa, S. Hanehara and D. Sawaki, "The role of steric repulsive force in the dispersion of cement particles in fresh paste prepared with organic admixture," *Cement and Concrete Research, Vol. 27,* pp. 37-50, January 1997.

[28] K. Yoshioka, E. Sakai, M. Daimon and A. Kitahara, "Role of Steric Hindrance in the Performance of Superplasticizers for Concrete," *Journal of the American Ceramic Society, 80,* p. 2667–2671, 1997.

[29] W. Schmidt, Design concepts for the robustness improvement of self-compacting concrete, PhD Thesis, Netherlands: Eindhoven University of Technology, 2014.

[30] C. Jolicouer, F. Perreault, M. Simard and A. Nuyt, "The Chemistry of Concrete Superplasticizers, Rheology and Hydration kinetics of Portland Cement Pastes Containing Mixture of Naphthalene and Melamine Based Superplasticizers," Ottawa, Canada, 1993.

[31] S. Hanehara and K. Yamada, "Rheology and early age properties of cement systems," *Cement and Concrete Research, Vol. 21,* pp. 175-195, 2008.

[32] P. Ramge and L. Lohaus, "Robustness by Mix Design – A New Approach for Mixture," in *Design, Production and Placement of Self-Consolidating: Vol. 1*, Netherlands, Springer Netherlands, 2010, pp. 37-49.

[33] Y. Abebe and L. Lohaus, "Effects of the composition and amount of paste on the pumpability and pump-stability of flowable concretes," in *Proceedings of the XXII Nordic Concrete Research Symposium*, Reykjavik, Iceland, 2014.

[34] K. Khayat and A. Ghezal, "Effect of viscosity-modifying admixture-superplasticizer combination on flow properties of SCC equivalent motar," in *3rd International RILEM Symposium on Self-Compacting Concrete*, Reykjavik, Iceland, 2003.

[35] A. Leemann and F. Winnefeld, "The effect of viscosity modifying agents on mortar and concrete," *Cement & Concrete Composites, Vol. 29,* pp. 341-349, 2007.

[36] W. Schmidt and H. Kühne, "Einfluss der Verarbeitungstemperatur auf die Eigenschaften von SVB bei Verwendung von Fließmittel und weiteren Zusatzmitteln (in German)," *Betonwerk + Fertigteil-Technik,* pp. 40-49, 2007.

[37] M. Sonebi, "Rheological properties of grouts with viscosity modifying agents as diutan gum and welan gum incorporating pulverised fly ash," *Cement and Concrete Research, Vol. 36,* pp. 1609-1618, 2006.

[38] K. Khayat, "Viscosity-enhancing admixtures for cement-based materials - An overview," *Cement and Concrete Composites, Vol. 20,* pp. 171-188, 1998.

[39] M. Lachemia, K. Hossain, V. Lambrosa, Nkinamubanzib, P.-C. and N. Bouzoubaa, "Performance of new viscosity modifying admixtures in enhancing the rheological properties of cement paste," *Cement and Concrete Research, Vol. 34,* pp. 185-193, 2004.

[40] W. Schmidt, H. Brouwers, H.-C. Kühne and B. Meng, "The Working Mechanism of Starch and Diutan Gum in Cementitious and Limestone Dispersions in Presence of Polycarboxylate Ether Superplasticizers," *Applied Rheology, Vol. 23,* 2013.

[41] J. Galloway, "Grading, Shape and Surface Properties," Philadelphia, 1994.

[42] P. Nel Quiroga and F. D.W., "The effects of aggregates characteristics on the performance of portland cement concrete," The University of Texas at Austin, Austin, Texas, 2003.

[43] C. Mora and A. Kwan, "Sphericity, shape factor, and convexity measurement of coarse aggregate for concrete using digital image processing," *Cement and Concrete Research, Vol. 30,* pp. 351-358, 2000.

[44] M. Powers, "A new roundness scale for sedimentary particles," *Journal of Sedimentary Petrology, Vol. 23, No. 2,* pp. 117-119, 1953.

[45] N. Ahn, An experimental study on the guidelines for using higher contents of aggregate mircrofines in portland cement concrete, Ph.D. Dissertation, Texas: University of Texas at Austin, 2000.

[46] W. Krumbein and L. Sloss, Stratigraphy and Sedimentation, vol. 2nd Edition, San Francisco, 1963.

[47] E. Masad, T. Al-Rousan, J. Button, D. Little and E. Tutumluer, "Test methods for characterizing aggregate shape, texture and angularity," 2007.

[48] J. Wilson, L. Klotz and C. Nagaraj, "Automated measurement of aggregate indices of shape," 1995.

[49] A. Huss, Mischungsentwurf und Fließeigenschaften von Selbstverdichtendem Beton (SVB) vom Mehlkorntyp unter Berücksichtigung der granulometrischen Eigenschaften der Gesteinskörnung, Ph.D. Dissertation (in German), Materialprüfungsanstalt Universität Stuttgart, 2010.

[50] H. Kim, C. Haas, A. Rauch and C. Browne, "Development of a laser-based system for testing construction aggregate," in *18th Inernational Symposium on Automation and Robotics in Construction*, 2001.

[51] J. Anochi-Boateng, J. Komba and G. Mvelase, "Three-dimensional laser scanning technique to quantify aggregate and ballast shape properties," Pretoria, South Africa, 2013.

[52] E. Garboczi, N. Martys, H. Saleh and R. Livingston, "Acquiring, analysing and using complete three-dimensional aggregate shape information," in *International Center for Aggregate Research,9th Annual Symposium - Aggregates: Concrete, Bases, and Fines*, Austin, Texas, 2001.

[53] M. Alexander and S. Mindess, Aggregates in concrete, Abingdon, England: Taylor & Francis, 2005.

[54] J. Shilstone, "Concrete mixture optimization," *Concrete International, Vol. 12,* pp. 33-39, 1990.

[55] R. Wendhorst, Baustoffkunde (in German), 26. überarbeitete Auflage ed., D. Vollenschar, Ed., Hannover, Germany: Vieweg+Teubner, 2004.

[56] M. Kaplan, "The effects of the properties of coarse aggregates on the workability of concrete," *Magazine of Concrete Research, Vol. 10,* pp. 63-74, 1958.

[57] S. Bloomer, Futher development of the two-point test for the measurement of the worability of concrete, University of Sheffield, 1979.

[58] ACI Committee E-701, "Aggregates for Concrete," 2007.

[59] M. Rixom and N. Mailvaganam, Chemical Admixtures for Concrete, 2nd ed., London: E & F.N. Spon, 1986.

[60] V. Bui and D. Montgomery, "Mixture proportioning method for self-compacting high performance concrete with minimum paste volume," in *Proceedings of the First International RILEM Symposium on Self-Compacting Concrete*, Stockholm, Sweden, 1999.

[61] S. Oh, T. Noguchi and F. Tomosawa, "Toward mix design for rheology of self-compacting concrete," in *Proceedings of the First International RILEM Symposium on Self-Compacting Concrete*, Stockholm, Sweden, 1999.

[62] T. Wüstholz, Experimentelle und theoretische Untersuchungen der Frischbetoneigenschaften von Selbstverdichtendem Beton, Institut für Werkstoffe im Bauwesen der Universität Stuttgart, 2005.

[63] H. Wong and A. Kwan, "Packing Density: A Key Concept for Mix Design of High Performance Concrete," in *Proceedings of the Materials Science and Technology in Engineering Conference, HKIE Materials Division*, Hong Kong, 2005.

[64] A. Kwan and L. Li, "Combined effects of water film, paste film and mortar film thicknesses on fresh properties of concrete," *Construction and Building Materials, Vol. 50,* pp. 598-608, 2014.

[65] H. Wong and A. Kwan, "Packing density of cementitious materials: part 1 - Measurement using a wet packing method," *Materials and Structures 41 (4),* p. 689–701, 2008.

[66] T. Midorikawa, I. Galia and C. Joost, "Application of" The Water Layer Model" to self-compacting mortar with different size distributions of fine aggregate," *HERON, Vol. 54, No. 2/3.,* pp. 73-100, 2009.

[67] ACI Committee 309, "Behavior of Fresh Concrete During Vibration," 1998.

[68] Y. Peng and S. Jacobsen, "Influence of water/cement ratio, admixtures and filler on sedimentation and bleeding of cement paste," *Cement and Concrete Research, Vol. 54,* pp. 133-142, 2013.

[69] T. Tan, T. Wee, S. Tan, C. Tam and S. Lee, "A consolidation model for bleeding of cement paste," *Advanced Cement Research, Vol. 1,* pp. 18-26, 1987.

[70] P. Schiessl and R. Schmidt, "Bleeding of Concrete," in *Proceedings of the 10th RILEM Colloquium: Properties of fresh concrete*, Hanover, 1990.

[71] L. Josserand and F. De Larrard, "A method for concrete bleeding measurement," *Materials adn Structures, Vol. 37,* pp. 666-670, 2004.

[72] Y. Ji, Z. Sun, X. Yang, C. Li and X. Tang, "Assessment and mechanism study of bleeding process in cement paste by 1H low-field NMR," *Construction and Building Materials Vol. 100,* p. 255–261, 2015.

[73] C. Loh, T. Tan, K. Yong and T. Wee, "An experimental study on bleeding and channeling of cement paste and mortar," *Advances in Cement Research, Vol.10,* pp. 1-16, 1998.

[74] T. Tan, C. Loh, K. Yong and T. Wee, "Modelling of bleeding of cement paste and mortar," *Advances in Cement Research, Vol. 9, No. 34,* pp. 75-91, 1997.

[75] H. Yim, J. Kim, H. Kwak and J. Kim, "Evaluation of internal bleeding in concrete using a self-weight bleeding test," *Cement and Concrete Research, Vol. 53,* pp. 18-24, 2013.

[76] T. Soshiroda, "Effects of bleeding and segregation on the inernal structure of hardened concrete," in *Proceedings of the 10th RILEM Colloquium: Properties of Fresh Concrete*, Hanover, 1990.

[77] AiF, "Zielsichere Herstellung von Industrieböden für Frei- und Hallenflächen," 2012.

[78] H. Steinour, "Further studies of the bleeding of portland cement paste," *Portland Cement Association Research Bulletin, No. 4,* 1945.

[79] K. Siewert, D. Hornung, P. Fitzenreiter, W. Kranert and B. Hochhausen, "Neubau des Lobdeburg-Tunnels bei Jena," 2010.

[80] G. Spanka, H. Grube and G. Thielen, "Operative mechanism of plasticizing concrete admixtures," VBT, 1998.

[81] Z. Zakka and R. Carrasquillo, "Effects of high range water reducers on the properties of fresh and hardened concrete," Texas, 1989.

[82] V. Ramachandran and V. Malhotra, "Superplasticizers," in *Concrete Admixtures Handbook: Properties, Science and Technology*, 2nd Edition ed., New Jersey, USA, np, 1996.

[83] EFNARC, "Guidelines for Viscosity Modifying Admixtures for Concrete," 2006.

[84] K. Khayat and Z. Guizani, "Use of Viscosity-Modifying Admixture to Enhance Stability of Fluid Concrete," *Materials Journal, Vol. 94, Issue 4,* pp. 332-340, 1997.

[85] M. Vahdani, I. Mehdipour and S. Yousefi, "Effect of viskosity modifying admixtures on the rheological properties and stability of self consolidating cementious materials," in *35th Conference on "OUR WORLD IN CONCRETE & STRUCTURES"*, Singapore, 2010.

[86] W. Dolch, "Air Entraining Admixtures," in *Concrete Admixtures Handbook: Property, Science and Technology*, New Jersey, USA, np, 1984.

[87] ACI Committee E-701, "Cementitious Materials for Concrete," 2001.

[88] K. Khayat, A. Yahia and M. Sayed, "Effect of supplementary cementitious materials on rheological properties, bleeding, and strength of structural grout," *ACI Materials Journal, Vol. 105,* pp. 585-593, 2008.

[89] P. Mehta, "Natural Pozzolans," in *Supplementary Cementing Materials for Concrete*, V. Malhotra, Ed., Ottawa, Canada, 1987.

[90] M. Thomas, "Optimizing the use of fly ash in concrete," Skokie, IL, 2007.

[91] ACI Committee 232, "Use of Fly Ash in Concrete," 1996.

[92] G. Carette and V. Malhotra, "Characterization of Canadian fly ashes and their relative performance in concrete," Ottawa, Canada, 1987.

[93] P. Mehta, "High-performance, high-volume fly ash concrete for sustainable development," in *Proceedings of the international workshop on sustainable development and concrete technology*, Beijing, China, 2004.

[94] V. Malhotra, "Properties of fresh and hardened concrete incorporating ground, granulated, blast-furnace slag," in *Supplementary Cementing Materials for Concrete*, V. Malhotra, Ed., Ottawa, Canada, 1987.

[95] E. Sellenvold and T. Nilsen, "Condensed silica fume in concrete: a world review," in *Supplementary Cementing Materials for Concrete*, V. Malhotra, Ed., Ottawa, Canada, 1987.

[96] ACI Committee 233, "Ground Granulated Blast-Furnace Slag as a Cementitious Constituent in Concrete," 2000.

[97] ACI Committee 234, "Guide for the Use of Silica Fume in Concrete," 2000.

[98] D. Lowke, Sedimentationsverhalten und Robustheit Selbstveredichtender Betone - Optimierung auf Basis der Modellierung der interpartikulären Wechselwirkungen in zementbasierten Suspensionen, Ph.D. Thesis, TU München, Germany, 2013.

[99] A. Beris, J. Tsamopoulos, R. Armstrong and R. Brown, "Creeping motion of a sphere through a Bingham plastic," *Journal of Fluid Mechanics, Vol. 158,* pp. 219-244, 1985.

[100] M. Petrou, B. Wan, F. Gadala-Maria, V. Kolli and K. Harries, "Influence of mortar rheology on aggregate settlement," *ACI Materials Journal, Vol. 97, No. 4,* pp. 479-485, 2000.

[101] N. Roussel, "A theoretical frame to study stability of fresh concrete," *Materials and Structures, Vol. 39,* pp. 81-91, 2006.

[102] S. Bethmont, L. Schwartzentrube, C. Stefani, J. Tailhan and P. Rossi, "Contribution of granular interactions to self compacting concrete stability : Development of a new device," *Cement and Concrete Research, Vol. 39,* pp. 30-35, 2009.

[103] S. Yang, G. Leal and Y. Kim, "Hydrodynamic interaction between spheres coated with deformable thin liquid films," *Journal of Colloid and Interface Science, Vol. 250,* pp. 457-465, 2002.

[104] J. Spangenberg, N. Roussel, J. Hattel, H. Stang, J. Skocek and M. Geiker, "Flow induced particle migration in fresh concrete: Theoretical frame, numerical simulations and experimental results on model fluids," *Cement and Concrete Research, Vol. 42,* 2012.

[105] D. Leighton and A. Acrivos, "The shear-induced migration of particles in concentrated suspensions," *Journal of Fluid Mechanics, Vol. 181,* pp. 415-439, 1987.

[106] R. Phillips, R. Armstrong, R. Brown, A. Graham and J. Abbott, "A constitutive equation for concentrated suspensions that accounts for shear-induced particle migration," *Physyics of Fluids A 4,* pp. 30-40, 1992.

[107] T. Dbouk, Rheology of concentrated suspensions and shear-induced migration, Ph.D. Thesis, Nice Sophia Antipolis University, 2011.

[108] G. Onoda and E. Liniger, "Random loose packings of uniform spheres and the dilatancy onset," *Physical Review Letters, Vol. 64, Iss. 25,* 1990.

[109] J. Spangenberg, N. Roussel, J. Hattel, E. Sarmiento, G. Zirgulis and M. Geiker, "Patterns of gravity induced aggregate migration during casting of fluid concretes," *Cement and Concrete Research, Vol. 42,* pp. 1571-1578, 2012.

[110] L. Shen, H. Jovein, Z. Sun, Q. Wang and W. Li, "Testing dynamic segregation of self-consolidating concrete," *Construction and Building Materials, Vol. 75,* pp. 465-471, 2015.

[111] P. Bartos, Fresh Concrete: Properties and Tests, Amsterdam, The Netherlands: Elsevier , 1992.

[112] G. Tattersall and P. Baker, "The effect of vibration on the rheological properties of fresh concrete," *Magazine of Concrete Research, Vol. 40, No. 143,* pp. 79-89, 1988.

[113] G. Tattersall and P. Baker, "An investigation on the effect of vibration on the workability of fresh concrete using a vertical pipe apparatus," *Magazine of Concrete Research, Vol. 41, No. 146,* pp. 3-9, 1989.

[114] P. Banfill, X. Yongmo and P. Domone, "Relationship between the rheology of unvibrated fresh concrete and its flow under vibration in a fresh concrete and its flow under vibration in a vertical pipe apparatus," *Magazine of Concrete Research, Vol. 51, No: 3,* pp. 181-190, 1999.

[115] P. Banfill, M. Teixeira and R. Craik, "Rheology and vibration of fresh concrete: Predicting the radius of action of poker vibrators from wave propagation," *Cement and Concrete Research, Vol. 41,* pp. 932-941, 2011.

[116] M. Petrou, K. Harries, F. Gadala-Maria and V. Kolli, "A unique experimental method for monitoring aggregate settlement in concrete," *Cement and Concrete Research, Vol. 30,* pp. 809-816, 2000.

[117] S. Juradin and P. Krstulovic, "The vibration rheometer: the effect of vibration on fresh concrete and similar materials," *Materialwissenschaft und Werkstofftechnik, Vol. 43, No. 8,* pp. 733-742, 2012.

[118] O. Olateju, "Laboratory evaluation of the response of reinforced concrete to internal vibration," Indianapolis, Indiana, 1973.

[119] G. Pigman, F. Hornibrook and J. Rogers, "A portable apparatus for measuring vibration in fresh concrete," *Journal of Research of the National Bureau of Standards, Vol. 20,* pp. 707-721, 1938.

[120] L. Forssblad, "Investigations of Internal Vibration of Concrete," *Acta Polytechnica Scandinavica, VII, 29,* 1965.

[121] S. Venkatramaiah, "Measurement of the work done in compacting a known weight of concrete by vibration," *Magazine of Concrete Research, Vol. 2, Issue 5,* pp. 89-96, 1951.

[122] R. Paiovici, S. Bucuresti and S. Ionescu, "About concrete consolidation and vibration," *The annals of "Dunarea de Jos",* pp. 71-76, 2004.

[123] M. Safawi, I. Iwaki and T. Miura, "The segregation tendency in the vibration of high fluidity concrete," *Cement and Concrete Research, Vol. 34,* pp. 219-226, 2004.

[124] H. Olbert and K. Moses, "Entmischng von Beton durch Überverdichtung (in German)," *Tec 21, Band 130, Vol. 44,* pp. 13-16, 2004.

[125] ACI Committee 304, "Placing Concrete by Pumping Methods," 1996.

[126] M. Jolin, F. Chapdelaine, F. Gagnon and B. D., "Pumping concrete: A Fundamental and Practical Approach," in *Proceedings of the 10th International Conference on Shotcrete for Underground Support*, Whister, Britisch Columbia, 2006.

[127] Nübling, "Die Rorhförderung von Frischbeton durch Rohre," 1971.

[128] R. Tobin, "Hydraulic Theory of Concrete Pumping," *ACI Journal,* pp. 505-512, 1972.

[129] Tanigawa, "Theoretical Study on Pumping of fresh Concrerte," 1991.

[130] D. Kaplan, Pompage des bétons, Ph.D. Dissertation, Paris, 2001.

[131] K. Kasten, Gleitrohr-Rheometer - Ein Verfahren zur Bestimmung der Fließeigenschaften von Dickstoffen in Rohrleitungen, Ph.D. Thesis, TU Dresden: Shaker Verlag, 2010.

[132] D. Feys, K. Khayat, A. Perez-Schell and R. Khatib, "Prediction of pumping pressure by means of new tribometer for highly-workable concrete," *Cement & Concrete Composites, Vol. 57,* pp. 102-115, 2015.

[133] R. Weber, "Rohrförderung von Beton," 2 ed., Beton-Verlag, 1963.

[134] Putzmeister, "Betontechnologie für Betonpumpen," rr medien gmbH, Riederich, 2004.

[135] R. Browne and P. Bamforth, "Tests to Establish Concrete Pumpability," *ACI Journal,* pp. 193-203, May 1977.

[136] D. Kaplan, F. de Larrard and T. Sedran, "Avoidance of Blockages in Concrete Pumping Process," *ACI Material Journal,* pp. 183 - 191, May 2005.

[137] V. Mechtcherine, V. Nerella and K. Kasten, "Testing pumpability of concrete using Sliding Pipe Rheometer," *Construction and Building Materials, Vol. 53,* pp. 312-323, 2014.

[138] Y. Abebe and L. Lohaus, "Optimization and design strategies for pumpable, flowable and stable concretes," in *Proceedings of the 10th International PhD Symposium in Civil Engineering*, Québec, 2014.

[139] T. Neumann and M. Lietzmann, "Pumpfähigkeit von Betonen: Beurteilung der Pumpfähigkeit von Betonen im Labor und in der Praxis," *Die SCHWENK Bauberatung informiert,* pp. 8-13, 2011.

[140] G. Tattersall and P. Banfill, The Rheology of Fresh Concrete, London: Pitman, 1983.

[141] P. Banfill, "The rheology of fresh cement and concrete - A review," in *Proceedings of the 11th International Cement Chemistry Congress*, Durban, 2003.

[142] J. Wallevik, "Rheological properties of cement paste: Thixotropic behavior and structural breakdown," *Cement and Concrete Research, Vol. 39,* pp. 14-29, 2009.

[143] N. Roussel, G. Ovarlez, S. Garrault and C. Brumaud, "The origins of thixotropy of fresh cement pastes," *Cement and Concrete Research, Vol. 42,* pp. 148-157, 2012.

[144] Z. Toutou and N. Roussel, "Multi scale experimental study of concrete rheology: From water scale to gravel scale," *Materials and Structures, Vol. 39,* pp. 189-199, 2006.

[145] P. Banfill, "A viscometric study of cement pastes containing superplasticizers with a note on experimental techniques," *Magazine of Concrete Research, Vol. 33, Issue 114,* pp. 37-47, 1981.

[146] O. Wallevik and J. Wallevik, "Rheology as a tool in concrete science: The use of rheographs and workability boxes," *Cement and Concrete Research, Vol. 41,* pp. 1279-1288, 2011.

[147] P. Banfill, "Rheology of fresh cement and concrete," in *Rheology Reviews* , T. B. S. o. Rheology, Ed., 2006, pp. 61-130.

[148] P. Coussot, "Introduction to the rheology of complex fluids," in *Understanding the Rheology of Concrete*, N. Roussel, Ed., Cambridge, UK, WP, 2012.

[149] J. Assaad and K. Khayat, "Assessment of thixotropy of self-consolidating concrete and concrete-equivalent-mortar: Effect of binder composition and content," *ACI Materials Journal, Vol. 101, No 5,* pp. 400-408, 2004.

[150] P. Billberg, "The structural behaviour of SCC at rest," in *36th Conference on Our World in Concrete & Structures*, Singapore, 2011.

[151] P. Billberg, "Influence of superplasticizers and slag blended cement on the rheology of fine mortar part of concrete," *Nordic Concrete Research Publications, Vol. 24,* pp. 25-34, 2000.

[152] K. Khayat and J. Assaad, "Effect of w/cm and high-range water-reducing admixture on formwork pressure and thixotropy of self consolidating concrete," *ACI Materials Journal, Vol. 103, No. 3,* pp. 186-193, 2006.

[153] L. Schwartzentruber, R. Roy and J. Cordin, "Rheological behaviour of fresh cement pastes formulated from a Self Compacting Concrete (SCC)," *Cement and Concrete Research, Vol. 36,* pp. 1203-1213, 2006.

[154] R. Ferron, A. Gregori and Z. a. S. S. Sun, "Rheological Method to Evaluate Structural Buildup in Self-Consolidating Concrete Cement Pastes," *ACI Materials Journal, Vol. 104,* 2007.

[155] K. Khayat and J. Assaad, "Relationship between washout resistance and rheological properties of high-performance underwater concrete," *ACI Materials Journal,* pp. 185-193, 2003.

[156] J. Assaad and K. Khayat, "Effect of viscosity-enhancing admixtures on formwork pressure and thixotropy of self-consolidating concrete," *ACI Materials Journal, Vol. 103, Issue 4,* pp. 280-287, 2006.

[157] R. Bouras, M. Chaouche and S. Kaci, "Influence of viscosity modiying admixtures on the thixotropic behaviou of cement pastes," *Applied Rheologie, Vol. 18, Issue 4,* 2008.

[158] R. Lohtia and R. Joshi, "Mineral Admixtures," in *Concrete Admixtures Handbook: Properties, Science and Technology*, 2nd Edition ed., R. V., Ed., np, 1996.

[159] BS 812-2:1995, "Testing aggregates. Methods for determination of density," 1995.

[160] H. Wong and A. Kwan, "Packing density of cementitious materials: part 1 - Measurement using a wet packing method," *Materials and Structures 41 (4),* p. 689–701, 2008.

[161] A. Kwan and H. Wong, "Packing density of cementitious materials: part 2 - packing and flow of OPC + PFA + CSF," *Materials and Structures 41(4),* p. 773–784, 2008.

[162] J. Chen and A. Kwan, "Superfine cement for improving packing density, rheology and strength of cement paste," *Cement & Concrete Composites 34,* pp. 1-10, 2012.

[163] F. De Larrard and T. Sedran, "Mixture-proportioning of high-performance concrete," *Cement and Concrete Research, Vol. 32,* pp. 1699-1706, 2002.

[164] A. Hummel, Das Beton ABC - 12. überarbeitete und erweitete Auflage, Berlin: Ernst & Sohn, 1959.

[165] Y. Abebe and L. Lohaus, "The Influence of Aggregate Composition on the Packing Density and Paste Demand of flowable Concretes," in *Proceedings of the 4th International Symposium on Ultra-High Performance Concrete and High Performance Construction Materials*, Kassel, 2016.

[166] W. Fuller and S. Thompson, "The laws of proportioning concrete," *ASCE Journal of Transport Engineering , Vol. 59,* 1907.

[167] A. Andreasen and J. Andersen, "Über die Beziehung zwischen Kornabstufung and Zwischenraum in Produkten aus losen Körnern (mit einigen Experimenten)," *Kolloid Zeitschrift, Vol. 50,* pp. 217-228, 1930.

[168] J. Funk and D. Dinger, Predictive Process Control of Crowded Particulate Suspension, Applied to Ceramic Manufacturing, Kluwer Academic Press, 1994.

[169] U. Stark and A. Mueller, "Optimization of packing density of aggregates," in *Proc. 2nd International Symposium on Ultra High Performance Concrete*, Kassel, 2008.

[170] R. Flatt, "Towards a prediction of superplasticized concrete rheology," *Materials and Structures, Vol. 37,* pp. 289-300, 2004.

[171] H. Okamura and M. Ouchi, "Self-Compacting Concrete," *Journal of Advanced Concrete Technology, Vol. 1, No. 1,* pp. 5-15, 2003.

[172] S. Kordts and H. Grube, "Steuerung der Verarbeitbarkeitseigenschaften von Selbstverdichtendem Beton als Transportbeton," *Beton, Vol. 52, Heft 4,* pp. 217-223, 2002.

[173] L. Lohaus and P. Ramge, "Robustness of UHPC – A New Approach for Mixture Proportioning," in *2nd International Symposium on Ultra-High Performance Concrete*, Kassel, 2008.

[174] DAfStb, "SVB Richtlinie," 2012.

[175] DIN EN 196-3, "Bestimmung der Erstarrungszeiten und der Raumbeständigkeit," 2009-02.

[176] H. Höveling, Robustheit von selbstverdichtendem Beton, Ph.D. Thesis, Leibniz Universität Hannover, Germany, 2006.

[177] S. Kordts and W. Breit, "Combined test method for assessing the workability of SCC - Flow cone," in *Concrete Technology Reports 2004-2006*, D. r. n. M. Schneider, Ed., Düsseldorf, Bau+Technik GmbH, 2007.

[178] E. Secrieru, M. Butler and V. Mechtcherine, "Prüfen der Pumpbarkeit von Beton – Vom Labor in die Praxis," *Bautechnik, Vol. 91,* 2014.

[179] Y. Abebe and L. Lohaus, "Application of Rheology to Characterize the Stability of Mortar Compositions under Vibration," in *Tagungsband zum 25. Workshop und Kolloquium: Rheologische Messungen an Baustoffen*, Regensburg, 2016.

[180] Y. Abebe and L. Lohaus, "Rheological characterization of the structural breakdown process to analyze the stability of flowable mortars under vibration," *Construction and Building Materials, Vol. 131,* pp. 517-525, 2017.

[181] L. Lohaus, D. Cotardo and Y. Abebe, "Methoden zur Quantifizierung last- und zeitabhängiger rheologischer Eigenschaften von Leimen mittels Rotationsviskosimeter," in *Tagungsband der 19. Internationale Baustofftagung (ibausil), Band 1*, Weimar, 2015.

[182] L. Lohaus, Y. Abebe and D. Cotardo, "Pumpstabilität von Beton - Prüfverfahren zur Mischungsstabilität unter hohem Druck (in German)," Leibniz Universität Hannover, 2015.

List of Figures

List of Tables

Appendix

A-1 Aggregate Optimization

A-1.1 Flaky agg. / Max. size 8 mm and 16 mm / q = 0.5

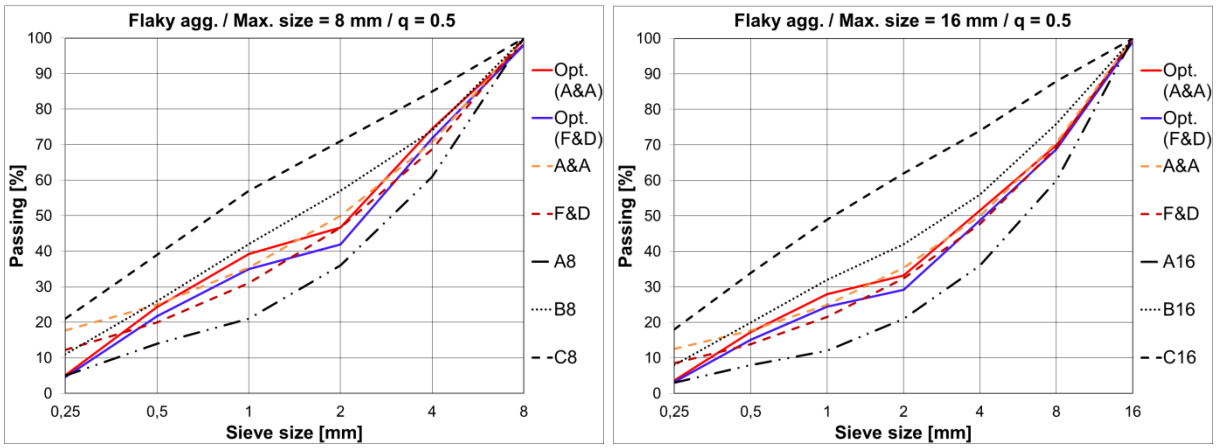

Figure A-1.1: Optimization of flaky aggregates with q = 0.5

A-1.2 Crushed agg. / Max. size 8 mm and 16 mm / q = 0.5

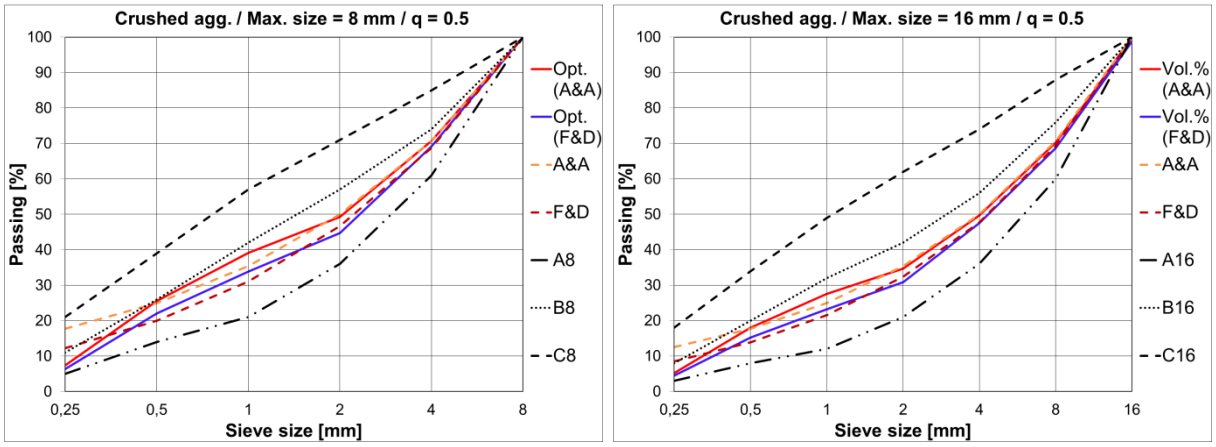

Figure A-1.2: Optimization of crushed aggregates with q = 0.5

A-1.3 Normal agg. / Max. size 8 mm / q = 0.4 and 0.6

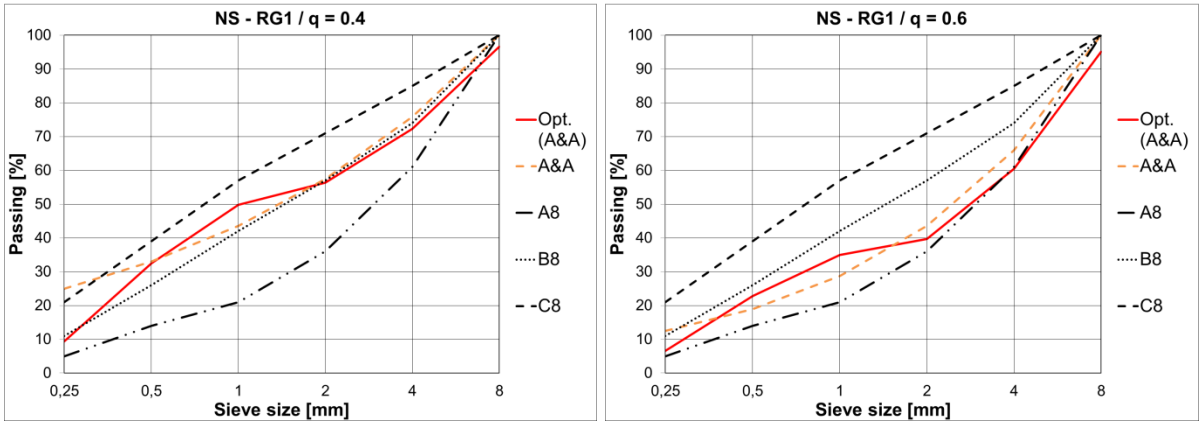

Figure A-1.3: Optimization of normal aggregate (max. size 8 mm) with q = 0.4 (left) and q = 0.6 (right)

A-1.4 Normal agg. / Max. size 16 mm / q = 0.4 and 0.6

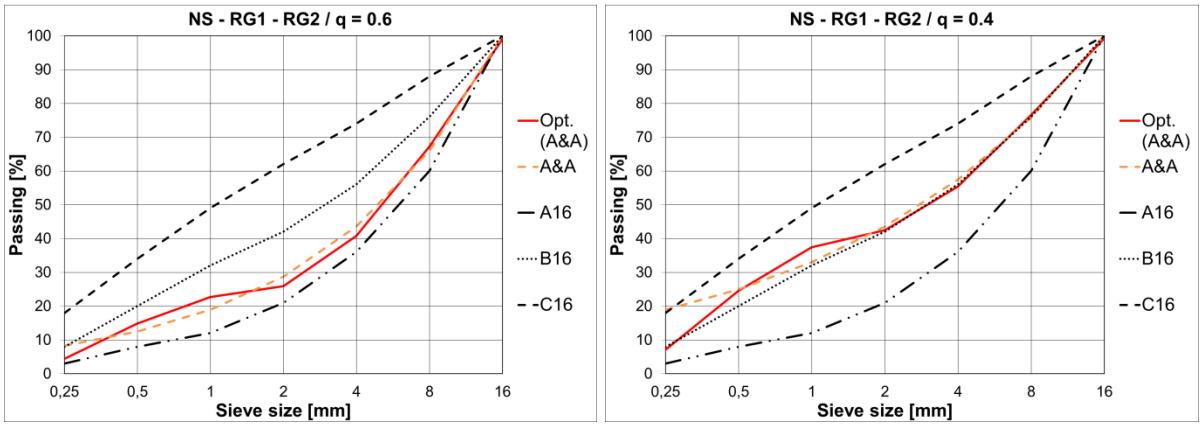

Figure A-1.4: Optimization of normal aggregate (max. size 16 mm) with q = 0.4 (left) and q = 0.6 (right)

A-2 Effect of Aggregate Size, Range and Type on the Paste Demand

A-2.1 Effect of grain size and size range

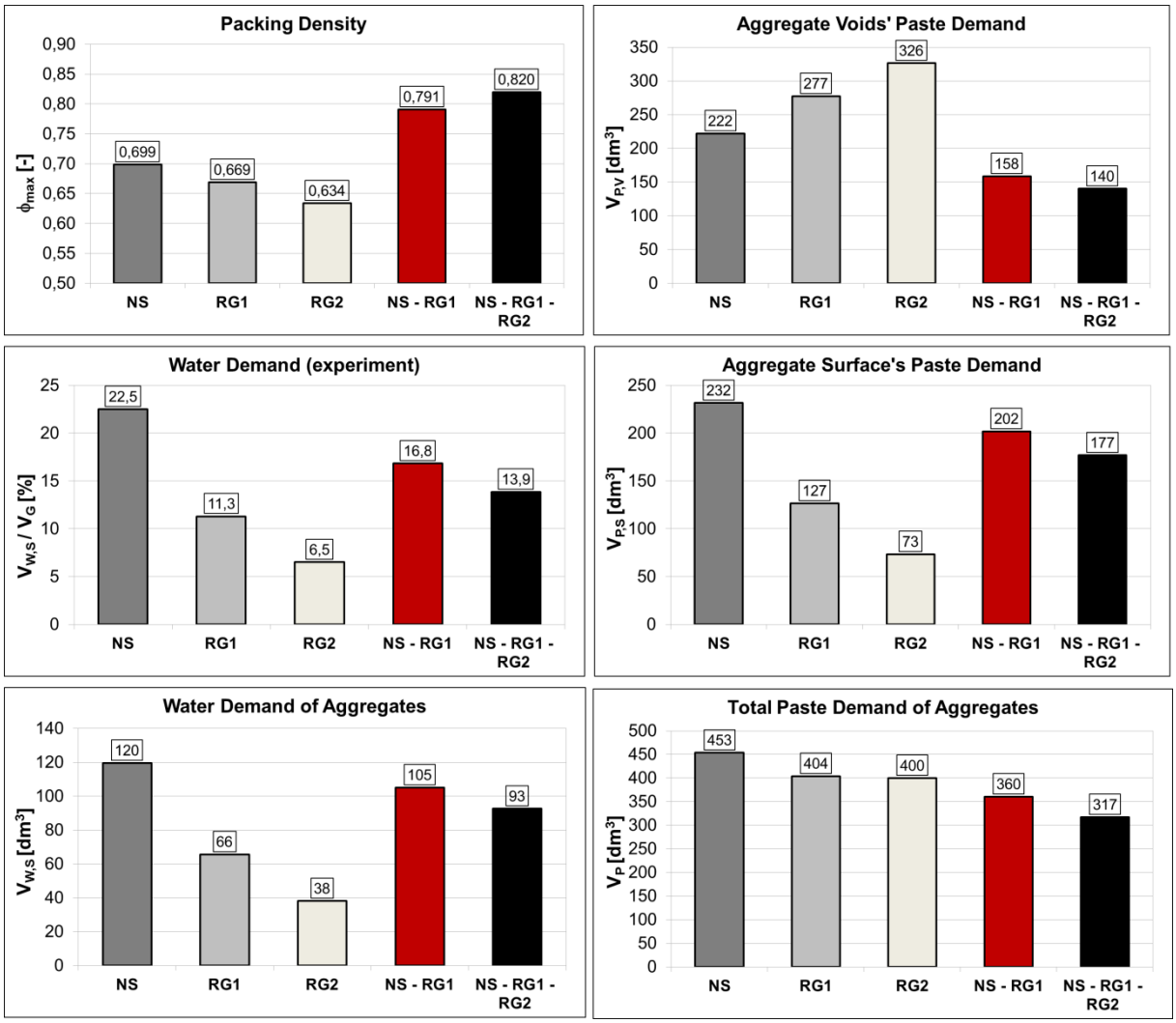

Figure A-2.1: Effect of type of aggregate Effect of grain size and size range

- ϕ increases and with decreasing maximum size of the individual aggregate fractions.
- ϕ_{Max} for the individual aggregate fractions is significantly lower than combined aggregates.
- ϕ increases with broader size range of the combined aggregates; 0/16 > 0/8.

- $V_{P,V}$ decreases with decreasing grain size of individual aggregate fractions or increasing size range of combined aggregates.
- $V_{W,S}$ and $V_{P,S}$ increase with smaller fractions or narrow size ranges; 0/8 > 0/16.
- A significant reduction in V_P with increased size ranges; 0/16 > 0/8.

A-2.2 Effect of type of aggregate

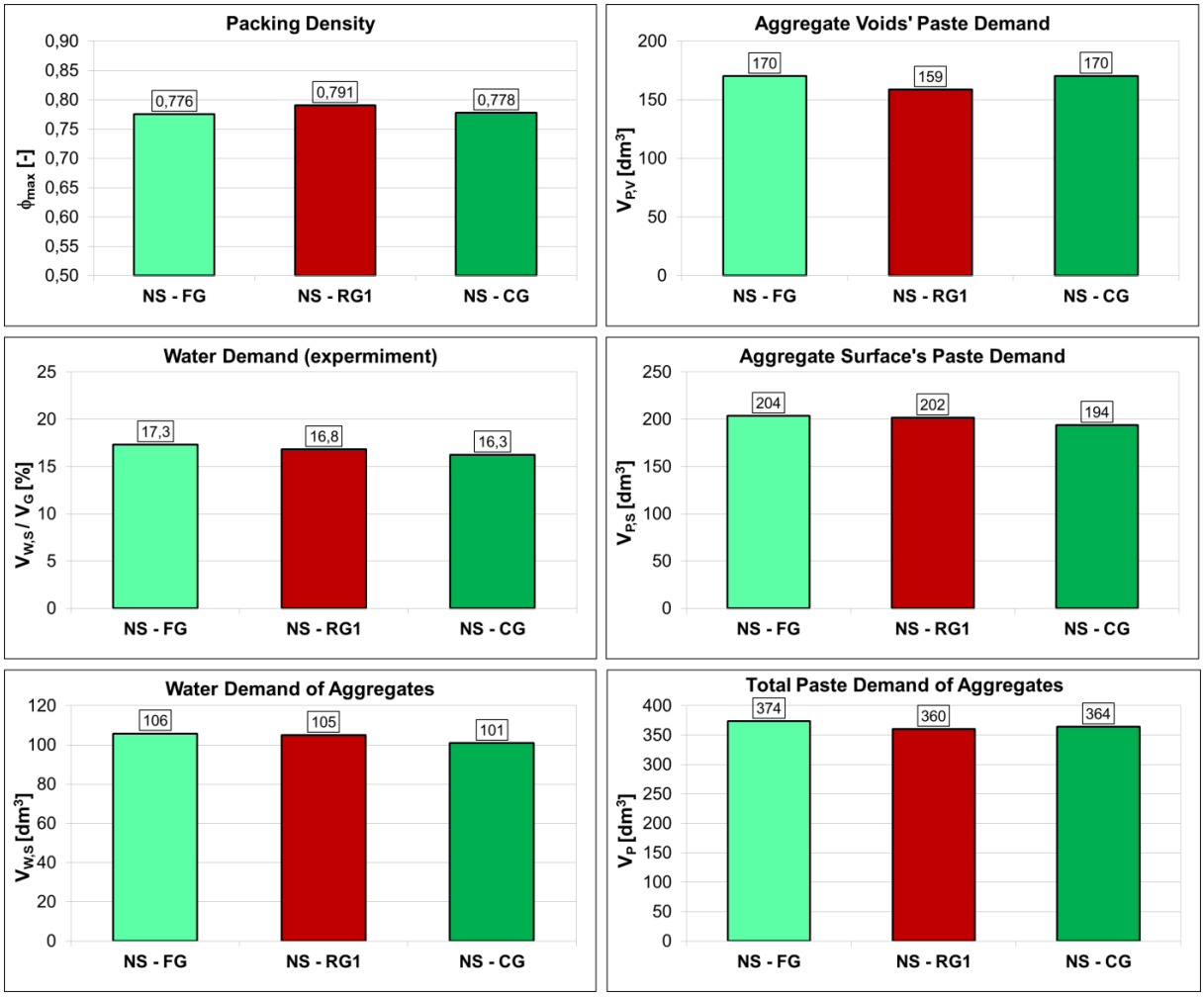

Figure A-2.2: Effect of type of aggregate

- Flaky and crushed gravels lead to smaller ϕ or higher $V_{P,V}$ than round gravels.
- Crushed gravels led to slightly lesser $V_{W,S}$ or $V_{P,S}$ than normal gravels due to their higher portion of the size fraction 2/4.
- Flaky gravel led to higher V_P than round and crushed aggregates.

A-3 Comparison of Rheological Measurement Profiles

The measurement results of the step profile and the step and gap profile are basically the same with regard to the relative viscosity (η_r) and relative yield stress ($\tau_{o,r}$). However, the step and gap profile has an advantage in that the interparticle structural strength (A_s) could also be determined.

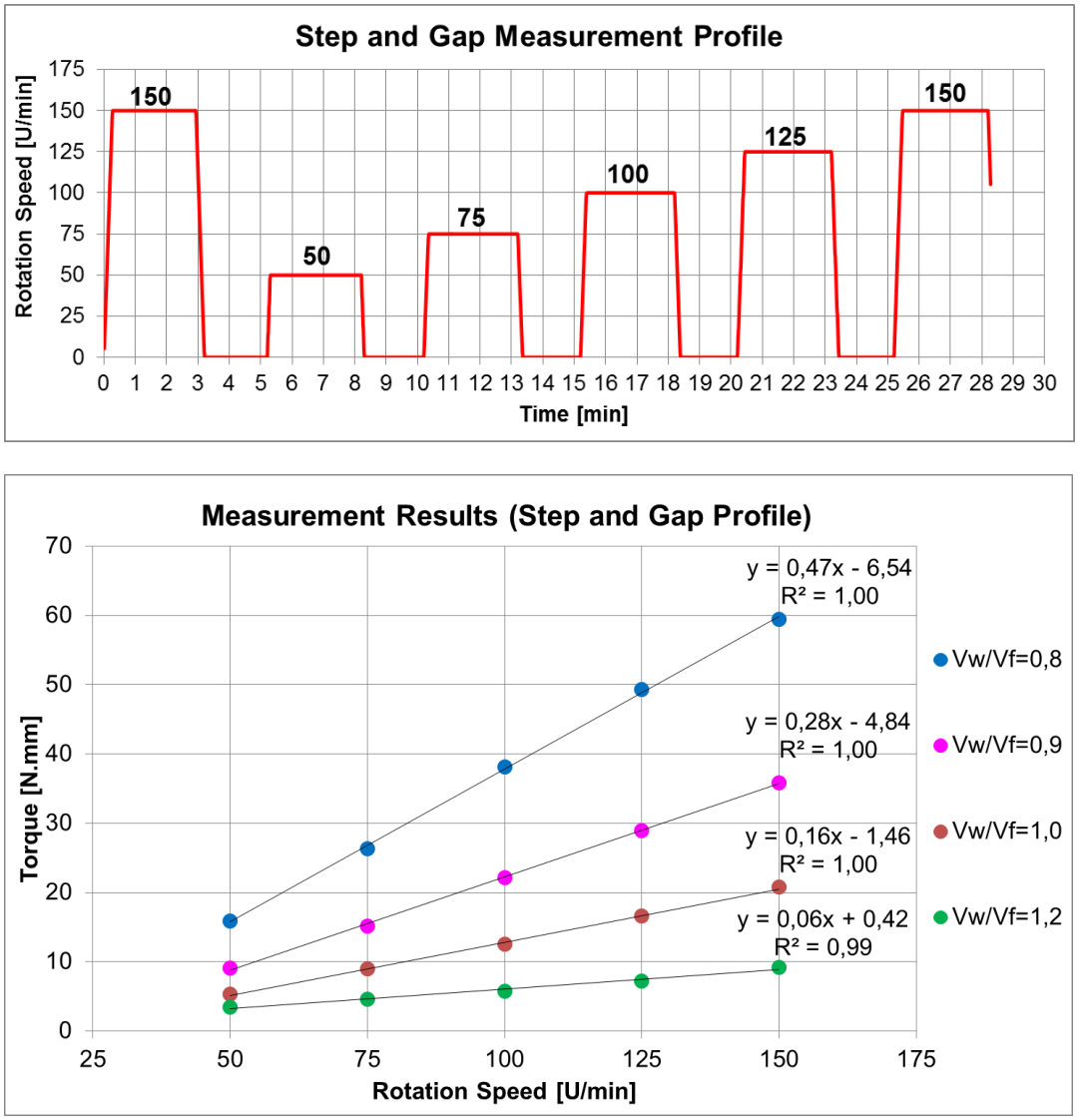

Figure A-3.1: Measurement results based on the step and gap profile

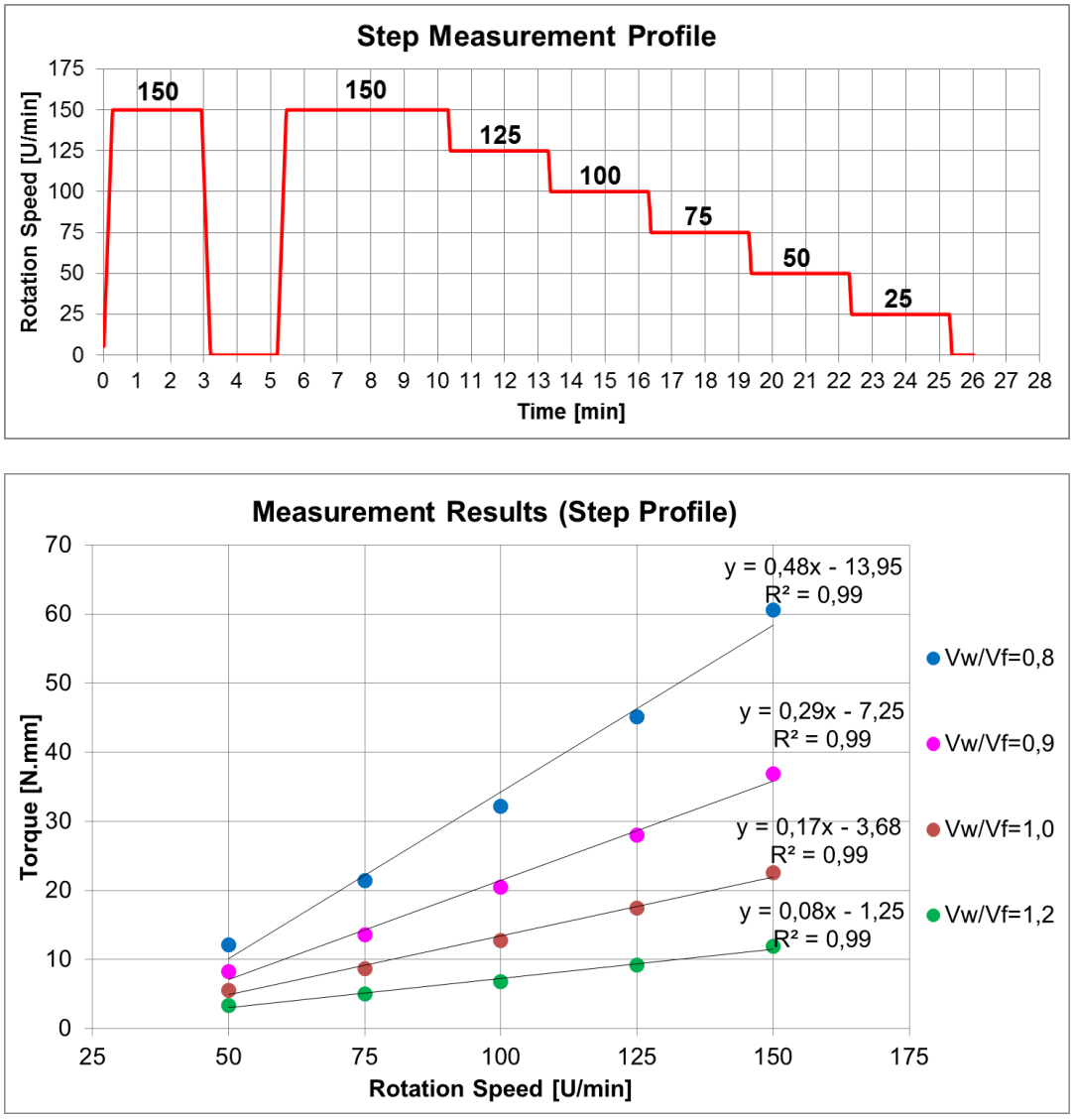

Figure A-3.2: Measurement results based on the step profile

A-4 Application of the Herschel-Bulkley Model

The least square method is applied on the basis of the Herschel-Bulkley model in order to determine the relative yield stress values ($\tau_{o,r}$), since the classic Bingham model has at times led to negative values.

$$\tau_{o,r} = \tau_o + n \,.\, \dot{\gamma}^{\,k} \Rightarrow M = b + n \,.\, v^{\,k}$$

These $\tau_{o,r}$ values are then integrated in the Bingham model in order to determine the relative dynamic viscosity (η_r).

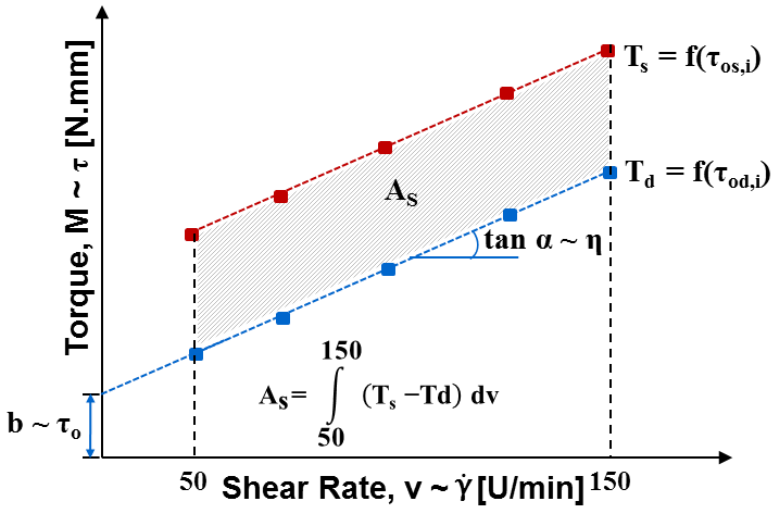

Figure A-4.1: Determination of the rheological parameters ($\tau_{o,r}$; η_r and A_S)

The sum of the squares to be minimized could be calculated as:

$$S = \sum_{i=1}^{n} [M_i - b_i]^2$$

Here, '$\mathbf{b_i}$' and 'M_i' represent the observed and fitted data points respectively while '**n**' and '**k**' are the adjustable cells. The calculated values for the paste compositions are shown in the following table as an example.

Mixture	V_i	50	75	100	125	150	$S = \Sigma[M_i - b_i]^2$	n	k
$V_W/V_F = 0.8$	$b_{(0.8)}$	16.90	27.66	40.19	52.26	63.37	2.10	1.22	0.14
	$M_{(0.8)}$	17.47	28.07	39.47	51.51	64.09			
	$[M_{(0.8)} - b_{(0.8)}]^2$	0.33	0.17	0.52	0.56	0.52			
	$\tau_{r,0.8}$	24.19	35.86	47.52	59.19	70.86	$\Rightarrow \tau_{r(0.8)} = 0.47 \cdot v_i + 0.85$		
$V_W/V_F = 0.9$	$b_{(0.9)}$	9.29	15.73	23.00	30.32	37.47	0.53	1.29	0.06
	$M_{(0.9)}$	9.73	15.86	22.64	29.95	37.71			
	$[M_{(0.9)} - b_{(0.9)}]^2$	0.19	0.02	0.12	0.14	0.06			
	$\tau_{r,0.9}$	14.88	21.88	28.89	35.90	42.91	$\Rightarrow \tau_{r(0.8)} = 0.28 \cdot v_i + 0.86$		
$V_W/V_F = 1.0$	$b_{(1.0)}$	6.04	9.91	13.93	18.50	22.97	1.12	1.19	0.05
	$M_{(1.0)}$	6.58	10.18	14.01	18.04	22.23			
	$[M_{(1.0)} - b_{(1.0)}]^2$	0.29	0.07	0.01	0.21	0.55			
	$\tau_{r,1.0}$	8.61	12.53	16.45	20.37	24.28	$\Rightarrow \tau_{r(0.8)} = 0.16 \cdot v_i + 0.78$		
$V_W/V_F = 1.2$	$b_{(1.2)}$	2.87	4.58	6.33	8.23	10.54	3.01	0.97	0.06
	$M_{(1.2)}$	3.95	5.35	6.74	8.13	9.51			
	$[M_{(1.2)} - b_{(1.2)}]^2$	1.16	0.60	0.18	0.01	1.07			
	$\tau_{r,1.2}$	3.82	5.21	6.60	7.99	9.38	$\Rightarrow \tau_{r(0.8)} = 0.06 \cdot v_i + 1.04$		

Table A-4.2: Adjusting the measurement results with Hershey-Bulkley model

The adjusted rheological functions based on the corrected values of the relative yield stress ($\tau_{o,r}$,) for the diagram shown in Figure A-3.1 are shown in Figure A-4.3.

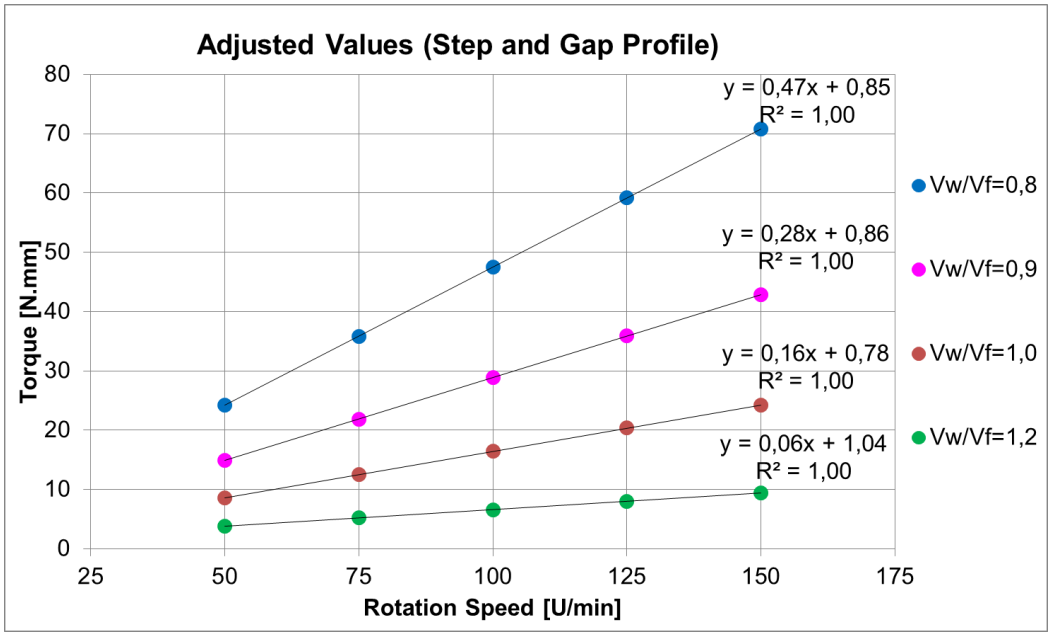

Figure A-4.3: Adjusted rheological functions based on Hershel-Bulkley model

A-5 Data for the Multiscale Rheological Model

Mixture	Mix. Id.	V_W/V_F	Aggregates' Surface Paste Demand		WB	Flowability	Stability	Rheology (measured)						Rheology (adjusted for $V_{P,S}$)			
								Concrete		Mortar		Paste		Concrete		Mortar	Paste
			$V_{P,S}$ (0/8)	$V_{P,S}$ (0/2)		Flow Time	SI	$A_{S,C}$	$\eta_{r,C}$	$A_{S,M}$	$\eta_{r,M}$	$A_{S,P}$	$\eta_{r,P}$	$A_{S,C}$	$\eta_{r,C}$	$\eta_{r,M}$	$\eta_{r,P}$
		[-]	[dm^3/m^3]	[dm^3/m^3]	[dm^3]	[s]	[%]	[N.mm/s]	[N.mm.s]	[N.mm/s]	[N.mm.s]	[N.mm/s]	[N.mm.s]	[N.mm/s]	[N.mm.s]		
V_W/V_F = 0.8	Ref	0.8	233	155	-34	12	7.80	67.76	3484.32	25.66	60.70	4.93	28.00	67.52	812.04	8.74	31.41
	Rob + 10L	0.843	236	157	-24	8	19.13	63.60	3047.1	24.99	39.04	4.27	26.21	63.48	720.02	6.94	24.62
	Rob + 20L	0.887	239	159	-14	5	52.82	46.67	1568.22	18.03	18.77	2.82	19.19	51.13	375.54	5.51	19.30
V_W/V_F = 1.0	Ref	1.0	202	135	-19	16	0.04	71.32	2941.56	26.67	28.90	1.83	9.40	69.22	594.91	2.44	10.19
	Rob + 10L	1.055	206	137	-9	13	10.84	68.69	2590.44	35.18	16.45	1.95	8.50	65.62	533.08	1.81	7.46
	Rob + 20L	1.111	209	139	1	6	28.33	49.76	1559.04	41.76	6.19	2.38	6.04	56.63	326.25	1.34	5.46
V_W/V_F = 1.2	Ref	1.2	197	131	2	15	10.34	64.59	2561.4	42.48	8.1	1.33	3.34	67.48	503.68	0.75	3.30
	Rob + 10L	1.263	200	133	12	10	29.51	60.25	1167.3	50.30	0.06	1.85	2.43	55.48	233.74	0.53	2.32
	Rob + 20L	1.325	204	136	22	6	33.50	54.74	762.66	53.67	0.07	2.32	1.48	51.45	155.41	0.37	1.63
q = 0.6 (40 : 60)	Ref	1.0	198	131	-16	14	5.24	60.63	3003.18	17.13	12.80	1.83	9.40	70.81	593.19	2.39	10.19
	Rob + 10L	1.057	201	134	-6	7	8.38	48.15	1648.74	28.42	7.42	1.95	8.50	59.13	331.62	1.76	7.39
	Rob + 20L	1.114	205	136	4	6	25.80	34.56	1131.54	38.21	1.01	1.81	5.04	54.20	231.60	1.29	5.36
q = 0.5 (50 : 50)	Ref	1.0	202	135	-19	16	0.04	71.32	2941.56	26.67	28.90	1.83	9.40	69.22	594.91	2.44	10.19
	Rob + 10L	1.055	206	137	-9	13	10.84	68.69	2590.44	35.18	16.45	1.95	8.50	65.62	533.08	1.81	7.46
	Rob + 20L	1.111	209	139	1	6	28.33	49.76	1559.04	41.76	6.20	1.81	5.04	56.63	326.25	1.34	5.46
q = 0.4 (60 : 40)	Ref	1.0	210	140	-14	14	4.23	68.46	2591.28	39.32	34.64	1.83	9.40	64.78	543.58	2.53	10.19
	Rob + 10L	1.055	213	142	-4	4	32.80	53.24	1991.28	33.92	15.11	1.95	8.50	59.31	424.16	1.88	7.46
	Rob + 20L	1.102	216	144	6	3	52.46	32.40	736.38	42.19	4.58	1.81	5.04	48.63	159.19	1.46	5.73
V_W/V_F = 0.9	Ref	0.9	-	142	-	-	-	-	-	34.23	34.99	2.86	16.82	-	-	4.55	17.89
	Rob + 10L	0.95	-	144	-	-	-	-	-	22.77	30.28	2.26	15.70	-	-	3.48	13.50
	Rob + 20L	1.0	-	147	-	-	-	-	-	24.97	25.59	2.48	10.97	-	-	2.66	10.19

A-6 Compressive Strength

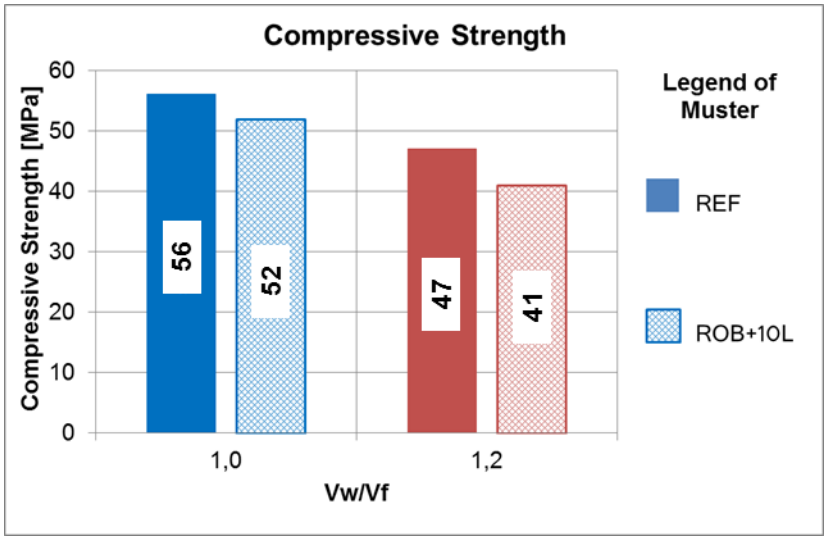

Figure A-6.1: Compressive strength of selected reference and water-overdosed WBC

Lebenslauf

Name :	Yared Assefa Abebe
Schulausbildung :	1984 - 1992: Grundschule Kidane Meheret Elementary School in Addis Abeba
	1992 - 1997: Gymnasium Kokebe Tsibah High School in Addis Abeba
Studium:	1997 - 2002: Bauingenieurwesen, Bachelorstudium Arbaminch University in Arbaminch, Äthiopien
	2007 - 2010: Geotechnik und Infrastruktur, Masterstudium Leibniz Universität Hannover
Berufliche Tätigkeit:	2003 - 2007: Baustoffingenieur und stellvertretender Laborleiter Transport Construction Design Share Co. in Addis Abeba
	2011 - 2016: Wissenschaftlicher Mitarbeiter und Doktorand Leibniz Universität Hannover

Curriculum Vitae

Name :	Yared Assefa Abebe
School Education:	1984 - 1992: Elementary School Kidane Meheret Elementary School, Addis Ababa
	1992 - 1997: High School Kokebe Tsibah High School, Addis Ababa
Higher Education:	1997 - 2002: Civil Engineering, B.Sc. Arbaminch University, Arbaminch, Ethiopia
	2007 - 2010: Geotechnique and Infrastructure, M.Sc. Leibniz Universität Hannover, Hannover, Germany
Work Experience:	2003 - 2007: Construction Materials Engineer and Acting Head of Laboratory Transport Construction Design Share Co., Addis Ababa
	2011 - 2016: Research Assistant and Doctoral Candidate Leibniz Universität Hannover, Hannover, Germany

Berichte aus dem Institut für Baustoffe

Bisher in dieser Reihe erschienene Hefte:

Heft 1: Thomas Freimann: „Einfluß von Steinkohlenflugaschen auf das rheologische Verhalten von Zementleimen und –mörteln“, 2002.

Heft 2: Susanne Thoke-Weidlich: „Alkaliionendiffusion in carbonatisierte und nicht carbonatisierte Betone“, 2002

Heft 3: Lasse Petersen: „Einfluss baustofflicher Schädigungsprozesse auf das Tragverhalten von Stahlbetonbauteilen“, 2003

Heft 4: Holger Höveling: „Robustheit von Selbstverdichtendem Beton (SVB)“, 2006

Heft 5: Jens Uwe Pott: „Entwicklungsstrategien für zementgebundene Schäume“, 2006

Heft 6: Steffen Anders: „Betontechnologische Einflüsse auf das Tragverhalten von Grouted Joints“, 2008

Heft 7: Maik Wefer: „Materialverhalten und Bemessungswerte von ultrahochfestem Beton unter einaxialer Ermüdungsbeanspruchung“, 2010

Heft 8: Fongjan Jirasit: „Chemical, Mechanical and Microstructural Properties of Alkali-Activated Cement“, 2010

Sonderheft: 2. Betonfachtagung Nord – Sichtbeton, 2010

Heft 9: Ludger Lohaus und Thomas Steinborn: „Fortschritte in der Baustofftechnik“, 2011

Sonderheft: 4. Betonfachtagung Nord – WU Konstruktionen als Regel- und Sonderbauweise, 2012

Heft 10: Nick Lindschulte: „Drucktragverhalten von Rohren aus Ultrahochfestem Beton mit Stahlblechummantelung“, 2013

Heft 11: Karen Fischer: „Betontechnische Einflüsse auf das Erscheinungsbild von Sichtbetonflächen bei Zementleimleckagen“, 2014

Heft 12: Thomas Steinborn (Hrsg.): „Festschrift Ludger Lohaus zur Vollendung des sechzigsten Lebensjahres“, 2014

Heft 13: Nadja Oneschkow: „Analyse des Ermüdungsverhaltens von Beton anhand der Dehnungsentwicklung“, 2014

Heft 14: Yared Assefa Abebe: „Flowable and Stable Concrete: Design, Characterization and Performance Evaluation“, 2017

Mitteilungen des Instituts für Baustoffkunde und Materialprüfung

Die Hefte der bis 1995 laufenden Schriftenreihe „Mitteilungen des Instituts für Baustoffkunde und Materialprüfung“ können ebenfalls über das Institut für Baustoffe der Leibniz Universität Hannover bezogen werden.

Institut für Baustoffe
Leibniz Universität Hannover
Appelstraße 9A
30167 Hannover
Tel.: 0511/762-3722
Fax: 0511/762-4736
http://www.baustoff.uni-hannover.de